Chemical synthesis of membrane-associated peptides: A model study on influenza virus B protein BM2(1-51)

TECHNISCHE UNIVERSITÄT DARMSTADT

Vom Fachbereich Chemie
der Technischen Universität Darmstadt

zur Erlangung des Grades
Doctor rerum naturalium
(Dr. rer. nat.)

Dissertation
von Andreas Christopher Baumruck

Erstgutachterin:	Associate Senior Lecturer (Asst. Prof.) Dr. Alesia Tietze
Zweitgutachter:	Prof. Dr. Harald Kolmar

Darmstadt 2020

Tag der Einreichung: 04. Februar 2020

Tag der mündlichen Prüfung: 09. April 2020

Baumruck, Andreas: Chemical synthesis of membrane-associated peptides: A model study on influenza virus B protein BM2(1-51)
Darmstadt, Technische Universität Darmstadt
Jahr der Veröffentlichung der Dissertation auf TUprints: 2020
URN: urn:nbn:de:tuda-tuprints-117312
Tag der mündlichen Prüfung: 09.04.2020

Wir können den Wind nicht ändern, aber die Segel anders setzen.

Aristoteles, griechischer Philosoph und Schüler Platons.[A]

Danksagung

Mein herzlicher Dank geht an erster Stelle an Frau Dr. Alesia Tietze, die es mir ermöglicht hat diese Doktorarbeit in ihrem Arbeitskreis anzufertigen. Sie hat mir während meiner Promotion immer zur Seite gestanden und mich dabei unterstützt neuen Ideen nachzugehen und selbstständig zu forschen. Vielen Dank für deine Unterstützung, deine Expertise und die vielen Stunden in denen wir zusammen gesessen, neue Ideen erarbeitet und immer wieder herzlich gelacht haben.

Ebenso herzlich danken möchte ich Herrn Professor Harald Kolmar für die Übernahme des Korreferats und für seine Förderung unseres Arbeitskreises. Vielen Dank für Ihre Unterstützung und die Möglichkeit sich stets mit allen Anliegen an Sie wenden zu dürfen. An dieser Stelle möchte ich dem gesamten Team von Herrn Professor Kolmar danken, das mich während der letzten Jahre begleitet und mir immer wieder mit Rat und Tat zur Seite gestanden hat.

Ein ganz großer Dank geht auch an die Professoren Dr. Gerd Buntkowsky, Dr. Viktor Stein und Dr. Christina Thiele sowie an ihre Arbeitskreise welche mir während meiner Promotion Zugang zu ihren Laboren und Geräten ermöglicht haben. Vielen Dank für eure Freundlichkeit, euren Humor und für die vielen fachlichen Diskussionen die ich in den letzten Jahren mit euch führen durfte.

Ein ebenso großes Dankeschön geht an die MS-Abteilung der TU Darmstadt, insbesondere an Frau Christiane Rudolph, die durch ihre Freundlichkeit und Hilfsbereitschaft eine große Bereicherung war. Vielen Dank für die Zeit und Mühe die ihr euch gegeben habt und für die vielen tollen Resultate. Eurer Fleiß und eure Arbeit haben meine Arbeit erst möglich gemacht.

Mein herzlicher Dank geht auch an Dr. Daniel Tietze sowie an meine Kollegin Lena K. Müller die mich während der letzten Jahre begleitet haben. Vielen Dank für die Zeit und für die vielen Stunden die wir zusammen gearbeitet und auch gelacht haben. Danke für eure Ideen, euren Fleiß und die gute Zusammenarbeit. An dieser Stelle möchte ich mich auch bei Gerke-Fabian Thomas und Alena Kopp bedanken, die ich während ihrer Bachelorarbeiten betreuen durfte. Ich wünsche euch alles Gute für eure Zukunft wo auch immer es euch einmal hinziehen wird.

Besonders möchte ich mich auch bei meiner Familie bedanken, die mich immer unterstützt und mir zur Seite gestanden hat. Danke für eure Geduld und für eure Unterstützung in den letzten Jahren.

Abschließend bedanken möchte ich mich auch bei all denen, die ich nicht im einzeln aufzählen kann und die mich während meiner Promotion unterstützt und begleitet haben. Sie alle haben ihren Teil dazu beigetragen, dass ich mich während meiner Promotion als Mensch und Wissenschaftler weiterentwickeln konnte.

Diese Arbeit entstand während meiner Promotion unter der Leitung von Dr. A. Tietze am Clemens-Schöpf-Institut für Organische Chemie und Biochemie an der Technischen Universität Darmstadt.

Einige Teile dieser Dissertation wurden bereits in folgenden Präsentationen und Publikationen vorgestellt oder veröffentlicht:

Publikationen:

A.C. Baumruck, D. Tietze, A. Stark, A.A. Tietze, Reactions of Sulfur-Containing Organic Compounds and Peptides in 1-Ethyl-3-methyl-imidazolium Acetate, *The Journal of Organic Chemistry*, **2017**, 82, 7538-7545.[1]

A.C. Baumruck, D. Tietze, L.K. Steinacker, A.A. Tietze, Chemical synthesis of membrane proteins: a model study on the influenza virus B proton channel, *Chemical Science*, **2018**, 9, 2365-2375.[2]

Andreas C. Baumruck, Jie Yang, Gerke-Fabian Thomas, Daniel Tietze and Alesia A. Tietze, Ionic liquids as efficient media for native chemical ligation of membrane-associated peptides, (submitted).

Lena K. Müller, Andreas C. Baumruck, Hanna Zhdanova, and Alesia A. Tietze, Challenges and Perspectives in Chemical Synthesis of Highly Hydrophobic Peptides, *Frontiers in Bioengineering and Biotechnology*, **2020**, 8, 162.

Vorträge:

Doktorandentag TU Darmstadt 2017 (05.10.2017):
Carbene-induced reactions of peptides and sulfur containing compounds in imidazolium-based ionic liquids.[1]

Molecular Basis of Life 2017 – Herbsttagung der GBM (24.09.2017 – 27.09.2017):
Synthesis, purification and ligation of membrane proteins using in situ-cleavable solubilizing tail.[2]

Fonds der chemischen Industrie (FCI) Stipendiatentreffen (19.02.2016):
Novel strategies for chemical synthesis of membrane proteins.[2]

Doktorandentag TU Darmstadt 2016 (28.01.2016):
Novel strategies for chemical synthesis of membrane proteins.[2]

Posterpräsentationen:

Molecular Basis of Life 2017 – Herbsttagung der GBM (24.09.2017 – 27.09.2017):
Synthesis, purification and characterisation of membrane proteins using in situ-cleavable solubilizing tail.

Doktorandentag TU Darmstadt 2016 (28.01.2016):
Purification and characterisation of membrane proteins using in situ-cleavable solubilizing tail.

Doktorandentag TU Darmstadt 2019 (15.01.2019):
Reactions of carbenes from the neat ionic liquid with disulfide-containing organic compounds and peptides.[1]

Wallenberg Centre yearly event 2019 in Göteborg (31.01.2019):
Chemical synthesis of influenza virus B protein fragment using removable solubilizing tag.[2]

Table of contents

1. Zusammenfassung 1

2. Summary 5

3. State of the Art 8

3.1. Chemical peptide synthesis – A brief historical overview 8

3.2. Synthesis of peptide thioesters – Precursors for the native chemical ligation ... 11

3.2.1. Direct synthesis of peptide thioesters 11

3.2.2. Thioesterification of the C-terminus on the solid support 11

3.2.3. Thioesterification by thiolysis 12

3.2.4. Post-cleavage thioesterifications 14

3.2.5. Thioesterification by O/N-to-S acyl shift reactions 16

3.3. Synthetic strategies for hydrophobic peptides 22

3.4. Internal modifications as solubilization strategies 23

3.4.1. Synthesis of O-acly isopeptides 23

3.4.2. Side chain and backbone attached solubilizing tags 23

3.4.3. Solubilizing tags at the N-terminus 27

3.4.4. Solubilizing tags at the C-terminus 28

3.5. External conditions as solubilization strategies 30

3.5.1. Detergents and organic solvents as additives for NCL 30

3.5.2. Fluorinated alcohols as co-solvents 30

3.5.3. Ionic liquids as co-solvents 31

3.5.4. Carbene formation in imidazolium based ILs 32

3.6. Post-ligation methods: Desulfurization and Acm deprotection 33

3.6.1. Metal-free desulfurization of peptides 34

3.6.2. Cleavage of the Acm-protection group 35

3.7. The influenza B proton channel sequence BM2(1-51) 36

4. Motivation and Aims of the Thesis 38

5. Results and Discussion 40

5.1. Investigation of internal modifications 40

5.1.1. Synthesis of 2-Hydroxy-3-(triphenylmethyl)thio-propanoic acid 40

5.1.2. Investigation of the stereochemistry of Hmp-peptides 42

5.1.3. Overview of the synthesised peptides 44

5.1.4. Synthesis of N-terminal Cys-peptides 45

5.1.5. Synthesis of model Hmp-peptides 46

5.1.6. Synthesis of complete BM2 Hmp-peptide fragments 53

5.1.7. Summary of resin preparation 58
5.1.8. Summary of resin weights, scales and obtained yields 59
5.1.9. Solubilizing tag-assisted NCL of Hmp-peptides in conventional buffer A 60
5.2. Investigation of external conditions 68
5.2.1. Application of fluorinated alcohols as additives for NCL of Hmp-peptides 68
5.2.2. TFE-assisted NCL of Hmp-peptides in buffer B 69
5.2.3. HFIP-assisted NCL of Hmp-peptides in buffer C 71
5.2.4. Investigation of the ionic liquid [C_2mim][OAc] as reaction media 77
5.2.5. Reaction of thiophenol and diphenyl disulfide in [C_2mim][OAc] 78
5.2.6. Reaction of benzyl mercaptan and dibenzyl disulfide in [C_2mim][OAc] 81
5.2.7. Reaction of [Cys^{22}]BM2(22-35) in [C_2mim][OAc] 84
5.2.8. Effect of water to NHC-induced modifications 87
5.2.9. Evaluation of optimal water content for NCL 88
5.2.10. Ionic liquid-mediated NCL of [Leu^{10}]BM2(1-51) 90
5.3. Development of novel follow-up protocols: desulfurization and Acm-group deprotection 92
5.3.1. HFIP-mediated desulfurization 92
5.3.2. Acm deprotection using conventional procedures 94
5.4. Predominate fold analysis of BM2 peptides by CD spectroscopy 97

6. Conclusion 100

7. Chemicals and Materials 105
7.1. Reagents and solvents for analytic methods 105
7.2. Reagents and solvents for synthetic methods 105
7.3. Laboratory equipment 107

8. Analytical Methods 108
8.1. Analytic methods 108
8.1.1. Analysis of thiols and disulfides in [C_2mim][OAc] 108
8.1.2. Analysis of [Cys^{22}]BM2(22-35) in [C_2mim][OAc] 108
8.1.3. Thin-layer chromatography (TLC) 108
8.1.4. Nuclear magnetic resonance (NMR) spectroscopy 108
8.1.5. Mass spectrometry LC-MS, ESI-MS and MALDI-TOF-MS 109
8.1.6. Reverse-phase high performance liquid chromatography 109
8.1.7. Purification by preparative RP-HPLC 109
8.1.8. UV/Vis spectroscopy 110
8.1.9. Circular dichroism (CD)-spectroscopy 110
8.1.10. Reconstitution of membrane peptides into lipid POPC vehicles 111
8.1.11. SDS-polyacrylamide gel electrophoresis (PAGE) 112

9. Synthetic Methods 112

9.1. Synthesis of Hmp(Trt) 112
9.1.1. 3-Chloro-2-hydroxypropanoic acid 112
9.1.2. 2-Hydroxy-3-(triphenylmethyl)thio-propanoic acid (Hmp(Trt)) 112
9.2. Manual synthesis of model Hmp-peptides 113
9.3. Automated microwave-assisted Fmoc-SPPS 120

10. Development of Ligation Protocols 125
10.1. Summary of ligation experiments 125
10.1.1. Native chemical ligation in buffer A 126
10.1.2. Native chemical ligation in buffer B 127
10.1.3. Native chemical ligation in buffer C 127
10.1.4. Native chemical ligation in buffer D (D1-D6) 128
10.1.5. Native chemical ligation of P27 in buffer D5 128

11. Desulfurization Protocols 129
11.1. Conventional and HFIP-based desulfurization of BM2 peptides 129
11.1.1. Metal-free desulfurization in conventional buffer 129
11.1.2. Metal-free desulfurization in HFIP containing buffer 129

12. Acetaminomethyl (Acm) deprotection 130
12.1. Comparison between silver salts and elemental iodine 130
12.1.1. Acm deprotection using silver trifluoromethanesulfonate 130
12.1.2. Acm deprotection using elemental iodine 130

13. List of Abbreviations 131

14. References 135

15. Appendix 147
15.1. Supporting information for internal modifications 147
15.1.1. Synthesis of model Hmp-peptides (chapter 5.1.5) 147
15.1.2. Test cleavage after ADO, Hmp and Leu coupling 153
15.1.3. Solubility test of the penta-lysine tag 153
15.1.4. Synthesis of complete BM2 peptides (chapter 5.1.6) 154
15.1.5. Analytical RP-HPLC of P22 [Leu^{21}]BM2(17-35) (chapter 5.1.9) 157
15.2. Supporting information for external conditions 158
15.2.1. HFIP-assisted NCL: ESI-MS of ligation product P23 (chapter 5.2.3) 158
15.2.2. TLCs of sulfur compounds in [C_2mim][OAc] (chapter 5.2.5 and 5.2.6) .. 159
15.2.3. Ionic liquid-mediated NCL: ESI-MS P22 (chapter 5.2.9) 160
15.2.4. Ionic liquid-mediated NCL: ESI-MS of P27 (chapter 5.2.10) 161
15.3. Supporting information for follow-up protocols 162
15.3.1. Desulfurization: ESI-MS of product P25 (chapter 5.3.1) 162
15.3.2. Acm deprotection: ESI-MS of product P26 (chapter 5.3.2) 163

15.4. Circular dichroism spectroscopy 164
15.4.1. CD spectroscopy in TFE and phosphate buffer (chapter 5.4)..... 164
15.4.2. CD spectroscopy in POPC liposomes (chapter 5.4)..... 165

1. Zusammenfassung

Die Herstellung gut löslicher Peptide mit Hilfe der Fmoc-basierten Festphasenpeptidsynthese (Fmoc-SPPS) und nativen chemischen Ligation (NCL) ist ein Routineverfahren. Die Ligation größerer Transmembranproteine ist jedoch, aufgrund der geringen Löslichkeit hydrophober Peptidfragmente, schwierig. In konventionellen (wässrigen) Ligationspuffern neigen solch hydrophobe Peptidfragmente zum aggregieren und ausfallen. Es besteht dennoch ein großer Bedarf an effizienten Synthesestrategien für hydrophobe membranassoziierte Peptide und Proteine mit Hilfe chemischer Verfahren. Im Gegensatz zur Proteinexpression ermöglicht die Festphasenpeptidsynthese schnelle und gezielte Modifikationen der Peptidkette, wie den Einbau unnatürlicher Aminosäuren, die Verwendung von Schutzgruppen oder eine präzise Isotopenmarkierung. Daher konzentriert sich diese Arbeit auf die Entwicklung neuer Strategien und Reaktionsbedingungen zur Herstellung hydrophober Transmembranpeptide mittels Fmoc-basierter Festphasenpeptidsynthese und nativer chemischer Ligation. Die Einleitung dieser Dissertation bietet einen Überblick über zahlreiche Synthesestrategien, die in den letzten Jahrzehnten speziell für die Herstellung hydrophober Peptide entwickelt wurden. Im ersten Teil werden Fmoc-kompatible Methoden für die Synthese C-terminaler Thioester präsentiert welche für die native chemische Ligation mit N-terminalen Cysteinpeptiden Verwendung finden (Kapitel **3.2**). In den darauf folgenden Kapiteln sind zahlreiche interne Modifikationen und externe Konditionen beschrieben, die die Löslichkeit hydrophober Peptide erhöhen. Die vorgestellten internen Modifikationen basieren auf dem Einbau temporär gebundener Löslichkeits-Tags, welche nach der Ligation oder Aufreinigung wieder entfernt werden können (Kapitel **3.4**). Die beschriebenen externen Konditionen beruhen auf der Zugabe löslichkeitsverbessernder Additive für Ligationspuffer. Diese Additive umfassen verschiedenste organische Lösemittel, Tenside oder ionische Flüssigkeiten (Kapitel **3.5**). Ein besonders wichtiger Punkt dieses Kapitels ist die Untersuchung der ionischen Flüssigkeit, 1-Ethyl-3-methylimidazoliumacetat [C_2mim][OAc] als alternatives Medium für die native chemische Ligation. Im darauf folgenden Kapitel werden Post-Ligationsstrategien wie die Cystein Desulfurierung und Acetamidomethyl (Acm) Abspaltung vorgestellt (Kapitel **3.6**).

Die während dieser Arbeit entwickelten und untersuchten Methoden zielen darauf ab, die Löslichkeit chemisch hergestellter Peptidfragmente während der Aufreinigung, nativen chemischen Ligation (NCL) und Desulfurierung, zu verbessern. Dafür wurden interne Modifikationsstrategien und unterschiedliche externe Bedingungen getestet (Kapitel **5**). Als Modellpeptid für diese Studien wurde die Influenza B Virus Protonenkanalsequenz BM2(1-51) verwendet (Kapitel **3.7**). Diese Proteinsequenz spielt bei der Vermehrung des Influenza B Virus eine bedeutende Rolle und ist daher für die Entwicklung eines antigrippalen Arzneimittels von hoher Relevanz. Alle vorherigen Versuche BM2(1-51) mit Hilfe der Fmoc-basierten Festphasenpeptidsynthese herzustellen schlugen jedoch fehl.[3] Die im Rahmen dieser Arbeit entwickelten Strategien zur Synthese von BM2(1-51) sind im Folgenden zusammengefasst.

Erhöhung der Löslichkeit durch interne Modifikationen (*Chem. Sci.*, ***2018***)[2]:

Die neu entwickelte interne Modifikationsstrategie beruht auf dem Einbau temporär gebundener Löslichkeits-Tags am C-Terminus von 2-Hydroxy-3-mercaptopropanamid (Hmp) Peptiden. Hmp ist ein trifunktionaler Linker, der über eine O-zu-S Acyl-Umlagerungsreaktion aktive Thioester bilden kann. Dadurch können funktionelle Gruppen oder Löslichkeits-Tags an

den C-Terminus des Peptids gebunden und während der Ligation wieder entfernt werden (temporärer Tag). In Kapitel **5.1** ist die Herstellung kurzer Model Hmp-Peptide und vollständiger BM2 Hmp-Peptide mit unterschiedlichen Löslichkeits-Tags (ADO, ADO_2, $ADO-Lys_5$) beschrieben. In einer ersten Studie wurden die Stereochemie und optimale Synthesebedingungen für Hmp-Peptide getestet. Dabei ist ein Kopplungsprotokoll an Hmp weiterentwickelt worden, welches auf der Mitsunobu-Reaktion basiert. Die Synthese der Modell Hmp-Peptide gelang nach diesem modifizierten Protokoll mittels manueller Fmoc-basierter Festphasenpeptidsynthese (Kapitel **5.1.5**). Für die Herstellung der vollständigen BM2 Hmp-Peptidfragmente wurde eine Kombination aus manueller und automatisierter, Fmoc-basierter Festphasenpeptidsynthese angewendet (Kapitel **5.1.6**). Nach der erfolgreichen Herstellung der kurzen und langen Hmp-Peptide, mit verschiedenen Löslichkeits-Tags, wurden Ligationsstudien in konventionellen (wässrigen) Ligationspuffern durchgeführt (Kapitel **5.1.9**). Dabei konnte gezeigt werden, dass C-terminal gebundene Löslichkeits-Tags wie ADO oder Polylysin keinen negativen Einfluss auf die Ligationseffizienz und Ausbeute haben. Die interne Löslichkeits-Tag Strategie erwies sich als effiziente Methode für die native chemische Ligation von Transmembranpeptiden was durch die Herstellung von [Cys^{22}]BM2(17-35) mit Ausbeuten von über 85% gezeigt werden konnte. Als effizientester Löslichkeits-Tag für lange, hydrophobe BM2 Hmp-Peptidfragmente erwies sich eine Kombination von Pentalysin und einer ADO-Gruppe. Dieser Löslichkeits-Tag wurde für die Ligation der hydrophoben Peptidsequenz [$Cys(Acm)^{11}$][Leu^{21}][Cys^{22}]BM2(1-51), mit einer Ausbeute von 71%, verwendet.[2]

Externe Konditionen *(J. Org. Chem.,* ***2017****)*[1]*, (Chem. Sci.,* ***2018****)*[2]*:*

Die in dieser Arbeit untersuchten externen Bedingungen zur Verbesserung der Löslichkeit beinhalten die Zugabe von Additiven zu konventionellen (wässrigen) Ligationspuffern (Kapitel **5.2**). Als vielversprechende Additive für Ligationsstudien mit langen, hydrophoben Hmp-Peptiden wurden zuerst fluorierte Alkohole wie Trifluorethanol (TFE) oder Hexafluorisopropanol (HFIP) getestet (Kapitel **5.2.1**). Die Ligation mit dem TFE basierten Puffer führte zu einem überraschenden Befund, der auf eine unerwartete TFE vermittelte Carbamylierung von N-terminalen Cysteinresten in Gegenwart von Harnstoff hinwies. Diese durch TFE vermittelte Nebenreaktion wurde in der Literatur nie zuvor beschrieben und führte zu einer deutlichen Reduktion der Ligationsausbeute (Kapitel **5.2.2**). Als effizientestes Ligationsmedium für hydrophobe BM2 Peptide wurde eine Phosphatpuffer/HFIP-basierte Emulsion entwickelt, welche nahezu quantitative Ligationsausbeuten ermöglichte (Kapitel **5.2.3**). Durch Zugabe von HFIP konnten keine Nebenreaktionen des N-terminalen Cysteinrestes beobachtet werden, was ein großer Vorteil im Vergleich zum TFE-basierten Ligationsmedium war. Diese HFIP-basierte Ligationsstrategie wurde erfolgreich für die native chemische Ligation der hydrophoben Peptide [$Cys(Acm)^{11}$][Leu^{21}][Cys^{22}]BM2(1-51) und [Leu^{10}]BM2(1-51) verwendet.[2]

Als weiteres vielversprechendes Ligationsmedium für hydrophobe Hmp-Peptide wurde die ionische Flüssigkeit 1-Ethyl-3-methylimidazoliumacetat ([C_2mim][OAc]) untersucht. In einer ersten Reihe von Experimenten konnte gezeigt werden, dass die reine ionische Flüssigkeit [C_2mim][OAc] mit Thiol- und Disulfid-haltigen Verbindungen wie Thiophenol (PhSH), Benzylmercaptan (BzlSH), Diphenyldisulfid (PhSSPh) und Dibenzyldisulfid (BzlSSBzl) reagieren kann (Kapitel **5.2.5** und **5.2.6**). Die aus NMR-, RP-HPLC- und ESI-MS-Studien gewonnenen Daten stützten einen Reaktionsmechanismus, bei dem Thiole zunächst zu den

entsprechenden Disulfiden oxidiert werden, bevor sie mit *in situ* gebildeten N-heterocyclischen Carbenen (NHCs) reagieren können. Untersuchungen des N-terminalen Cysteinpeptids [Cys^{22}]BM2(1-51) in der ionischen Flüssigkeit [C_2mim][OAc] resultierten in der gleichen Modifizierung der Thiolgruppe wie bei den organischen Modellverbindungen (PhSH, BzlSH, PhSSPh, BzlSSBzl). Darüber hinaus wurden mit Hilfe von ESI-MS weitere Peptidmodifikationen an [Cys^{22}]BM2(22-35) gefunden, die durch die reinen ionischen Flüssigkeit gebildet wurden (Kapitel **5.2.7**). Im weiteren Verlauf dieser Untersuchungen konnte gezeigt werden, dass eine Zugabe von mindestens 30% Wasser ausreichend ist, um NHC-induzierte Peptidmodifikationen vollständig zu unterdrücken (Kapitel **5.2.8**).[1] Basierend auf diesen Erkenntnissen gelang die Entwicklung eines IL-basierten Ligationspuffers, welcher höhere Ausbeuten für hydrophobe Hmp-Peptide erzielte als konventionelle Ligationspuffer. Der optimale Wasseranteil wurde durch eine Serie von Ligationsexperimenten mit kurzen Hmp-Peptiden ermittelt in dem der Wassergehalt für jede Ligation schrittweise um jeweils 10% erhöht wurde (Kapitel **5.2.9**). Als effizientestes Ligationsmedium wurde eine Mischung bestehend aus 60% [C_2mim][OAc], 40% Wasser, 150 mM TCEP HCl und 150 mM Thiophenol ausgemacht. Dieses Mischungsverhältnis zeigte einen pH-Wert von 7.5, welcher sich bereits bei den HFIP-basierten Ligationsexperimenten in Kapitel **5.2.3** als optimal für Hmp-Peptide erwies. Im Vergleich zur nativen chemischen Ligation im HFIP-basierten Puffer war die IL-basierte Ligation jedoch schneller und ermöglichte das Lösen größerer Peptidmengen in kleineren Puffervolumina. Die Vorteile dieses IL-basierten Ligationspuffers konnte durch die Herstellung des finalen Zielpeptids [Leu^{10}]BM2(1-51), mit einer Ausbeute von 76%, demonstriert werden (Kapitel **5.2.10**).

Post-Ligationsmethoden: Desulfurierung und Abspaltung von Acm *(Chem. Sci., **2018**)*[2]:

Obwohl die Desulfurierung löslicher Peptide in der Literatur umfassend beschrieben ist, bleiben schwerlösliche Peptide und Proteine eine Herausforderung. Wie in Kapitel **5.3.1** gezeigt, eignen sich herkömmliche Desulfurierungspuffer im Allgemeinen nicht dafür hydrophobe Transmembranpeptide in Lösung zu bringen und zu desulfurieren. In dieser Arbeit wird ein effizientes Desulfurierungsprotokoll für schwer lösliche Transmembranpeptide vorgestellt, welches für die Desulfurierung des Peptids [Cys(Acm)^{11}][Leu^{21}][Cys^{22}]BM2(1-51) Verwendung fand. Dabei gelang die Desulfurierung mittels einer Phosphatpuffer/HFIP Emulsion in Gegenwart von Glutathion, dem Reduktionsmittel TCEP (Tris(2-carboxyethyl)phosphin) und dem Radikalstarter VA-044 (2,2'-Azobis[2-(2-Imidazolin-2-yl)propan] dihydrochlorid) (Kapitel **11.1.2**). Diese HFIP Emulsion war in der Lage die hydrophoben BM2 Peptide vollständig in Lösung zu bringen und ermöglichte eine nahezu quantitative Umwandlung der Cys22 Ligationstelle zum entsprechenden Ala22.

Eine weitere Post-Ligationsmethode, welche für die Synthese des finalen BM2 Peptids [Leu^{21}]BM2(1-51) Verwendung fand, war die Acm Abspaltung. Dazu wurden zwei unterschiedliche Methoden getestet und miteinander verglichen. Die oxidative Acm Abspaltung mit elementarem Iod sowie die Verwendung von Silbertrifluormethansulfonat (AgOTf) in konzentrierter Trifluoressigsäure. Beide Strategien ermöglichten die Herstellung von [Leu^{21}]BM2(1-51), jedoch mit großen Unterschieden in der Ausbeute. Durch elementares Iod wurde nur eine sehr schlechte Ausbeute von etwa 16% erzielt, während der größte Teil des Peptids oxidiert wurde. Durch die Verwendung von AgOTf gelang jedoch die Synthese des finalen Peptids [Leu^{21}]BM2(1-51) mit einer Ausbeute von 66% (Kapitel **5.3.2**).

Analyse der bevorzugten Faltung mittels CD-Spektroskopie *(Chem. Sci., **2018**)*[2]:

Die bevorzugte Faltung der hergestellten BM2 Peptide wurde mit Hilfe der CD Spektroskopie ermittelt (Kapitel **5.4**). Diese Untersuchungen bestätigten eine bevorzugt alpha-helikale Faltung aller hergestellten BM2 Peptide. Die Analyse der beiden finalen Zielpeptide [Leu^{10}]BM2(1-51) und [Leu^{21}]BM2(1-51) in TFE und POPC Liposomen enthüllte einen alpha-helikalen Anteil von über 60% in der Influenza B Virus Peptidsequenz BM2(1-51). Dieses Ergebnis deutet auf mögliche helikale Strukturen innerhalb der Peptidsequenz 36-44 hin, welche in früheren Studien als unstrukturiert betrachtet wurden.[4]

2. Summary

The chemical production of well soluble peptides by Fmoc-based solid phase peptide synthesis (Fmoc-SPPS) and native chemical ligation (NCL) is a routine procedure. However, native chemical ligation of extended transmembrane proteins is usually hampered by the poor solubility of hydrophobic peptide fragments which tend to aggregate and precipitate in conventional (aqueous) ligation buffers. Nevertheless, there is a great demand for the efficient production of transmembrane peptides/proteins by chemical methods. In contrast to protein expression, chemical peptide synthesis allows a fast incorporation of specific modifications including unnatural amino acids, protecting groups or precise isotopic labelling. Therefore, this thesis is focused on the development of novel strategies and reaction conditions for the synthesis of hydrophobic transmembrane peptides by Fmoc-based solid phase peptide synthesis and native chemical ligation.

This thesis provides an overview of various synthetic strategies for hydrophobic peptides and proteins which were published over the last decades. In the first part, Fmoc-chemistry compatible methods for the synthesis of C-terminal peptide thioesters are presented which can be used for native chemical ligation with N-terminal cysteine peptides (chapter **3.2**). In the following chapters various internal modifications and external conditions are presented which were developed to enhance peptide solubility for purification or native chemical ligation (chapter **3.3**). The internal modification strategies, introduced in this thesis, are based on the incorporation of temporarily bound solubilizing tags (chapter **3.4**). The external conditions, presented in this work, describe the addition of solubility enhancing additives to ligation buffers (chapter **3.5**). These additives comprise different organic solvents, surfactants or ionic liquids. One main focus of this chapter lies in the investigation of ionic liquid 1-ethyl-3-methylimidazolium acetate [C_2mim][OAc] as an alternative ligation media. In the following chapter post-ligation strategies such as cysteine desulfurization and Acm deprotection are presented (chapter **3.6**).

The newly-developed strategies investigated during this work are focused on increasing the solubility of transmembrane peptides during purification, native chemical ligation (NCL) and cysteine desulfurization. Therefore, internal modification strategies and external conditions were tested (chapter **5**). As a model peptide for these studies, the influenza B proton channel sequence BM2(1-51) was chosen (chapter **3.7**). This protein sequence plays an important role in the multiplication of the influenza B virus and is therefore of great relevance for the development of an anti-flu drug. However, all previous attempts to obtain BM2(1-51) by Fmoc-based SPPS failed.[3] The strategies for the synthesis of BM2(1-51) which were developed during this thesis are summarized below.

Solubility enhancement by internal modifications *(Chem. Sci., **2018**)*[2]*:*

The newly-developed internal modification strategy relies on the attachment of temporary bound solubilizing tags at the C-terminus of 2-hydroxy-3-mercaptopropanamide (Hmp) peptides. Hmp is as trifunctional linker which is capable of forming active peptide-thioesters *via* rearrangement over an O-to-S acyl shift reaction. This allows an attachment of functional groups or solubilizing tags at the C-terminus of peptides which are removed during ligation (temporary tag). In chapter **5.1** the synthesis of model Hmp-peptides and complete BM2

Hmp-peptide fragments, with various solubilizing tags (ADO, ADO_2, ADO-Lys_5), is presented. In the first studies the stereochemistry and optimal synthetic conditions for Hmp-peptides were investigated. Thereby, a coupling protocol at the Hmp moiety was further developed which is based on the Mitsunobu reaction. The synthesis of the model Hmp-peptides succeeded with this modified protocol using manual Fmoc-SPPS (chapter **5.1.5**). For the synthesis of complete BM2 Hmp-peptide fragments a combination of manual Fmoc-SPPS (preloading of the resin) and automated, microwave assisted Fmoc-SPPS was applied (chapter **5.1.6**). After successful production of Hmp-peptides with different solubilizing tags, ligation studies in a conventional (aqueous) ligation buffer were performed (chapter **5.1.9**). Thereby, it could be shown that C-terminal bound solubilizing tags such as ADO or polylysine have no negative effect on the ligation efficiency or yield. The internal solubilizing tag strategy in combination with Hmp-peptides turned out to be an efficient method for native chemical ligation (NCL) of transmembrane peptides as demonstrated by the successful NCL of the influenza B proton channel fragment [Cys^{22}]BM2(17-35) with ligation yields of over 85%. The most powerful solubilizing tag for complete, hydrophobic BM2 Hmp-peptides was a combination of pentalysine with an ADO group which was applied for the NCL of the sequence [Cys(Acm)^{11}][Leu^{21}][Cys^{22}]BM2(1-51) with a yield of 71%.[2]

Solubility enhancement by external conditions *(J. Org. Chem.,* ***2017****)*[1] (*Chem. Sci.,* ***2018****)*[2]*:*

The investigation of external conditions includes the addition of solubility improving additives to conventional (aqueous) ligation buffers (chapter **5.2**). At first fluorinated alcohols such as 2,2,2-trifluoroethanol (TFE) or hexafluoro-2-propanol (HFIP) were tested as promising additives for ligation studies with hydrophobic Hmp-peptide fragments (chapter **5.2.1**). The ligation in the presence of TFE led to a surprising finding indicating an unexpected, TFE-promoted, carbamylation of N-terminal cysteine residues by urea. This side reaction in the presence of TFE was never described in literature and led to a dramatic decrease of ligation yield (chapter **5.2.2**). The most efficient medium for the NCL of the hydrophobic BM2 peptide fragments was a phosphate buffer/HFIP-based emulsion which achieved nearly quantitative ligation yields (chapter **5.2.3**). By addition of HFIP no side reactions of N-terminal Cys residues were detectable which was a great advantage compared to the TFE based buffer solution. The HFIP-based strategy was successfully applied for the NCL of the sequence [Cys(Acm)^{11}][Leu^{21}][Cys^{22}]BM2(1-51) and the target peptide [Leu^{10}]BM2(1-51).[2]

The second promising media, the ionic liquid 1-ethyl-3-methylimidazolium acetate ([C_2mim][OAc]), was investigated for the ligation of hydrophobic Hmp-peptides. In a first set of experiments it was demonstrated that the neat ionic liquid [C_2mim][OAc] is capable of reacting with thiol- and disulfide-containing compounds such as thiophenol (PhSH), benzyl mercaptan (BzlSH), diphenyl disulfide (PhSSPh) and dibenzyl disulfide (BzlSSBzl) (chapters **5.2.5** and **5.2.6**). The acquired data from NMR, RP-HPLC and ESI-MS studies supported a reaction mechanism in which thiols are first oxidized to the corresponding disulfides before reacting with *in situ* formed N-heterocyclic carbenes (NHCs). Investigations of the Cys containing model peptide [Cys^{22}]BM2(22-35) into the neat [C_2mim][OAc] resulted in the same modifications of the thiol group as observed for the organic model compounds (PhSH, BzlSH, PhSSPh, BzlSSBzl). Moreover, several different peptide modifications of [Cys^{22}]BM2(22-35) were found by ESI-MS which were formed in neat [C_2mim][OAc] (chapter **5.2.7**). In the further course of these studies it could be demonstrated that the

addition of at least 30% of water was sufficient to supress NHC-induced peptide modifications entirely (chapter **5.2.8**).[1] Based on these results the development of an IL-based ligation buffer succeeded which showed better ligation yields for hydrophobic Hmp-peptides than conventional ligation buffers. The optimal water content of the IL-based ligation buffer was found by a series of ligation studies using short model Hmp-peptides in which the water content was gradually increased by 10% for each ligation (chapter **5.2.9**). The most efficient ligation buffer was a mixture of 60% [C_2mim][OAc], 40% water, 150 mM TCEP HCl and 150 mM thiophenol. This mixture showed a pH of 7.5 which was already found as optimal for the NCL of Hmp-peptides in the HFIP-based ligation buffer of chapter **5.2.3**. However, in comparison with the NCL in the HFIP-based buffer, the IL-based NCL was much faster and allowed the dissolution of more peptide in small buffer volumes. The benefits of the IL-based ligation buffer could be impressively demonstrated by the native chemical ligation of the final target peptide [Leu^{10}]BM2(1-51) with a ligation yield of 76%. This peptide sequence represents a large fragment of the BM2 proton channel (**5.2.10**).

Post-ligation methods: Desulfurization and Acm deprotection (*Chem. Sci.*, ***2018***)[2]:

Although Cys desulfurization of soluble peptides is well described in literature, poorly-soluble peptides/proteins still remain a challenge. Conventional desulfurization buffers are in general unsuitable to dissolve and desulfurate hydrophobic transmembrane domains as demonstrated in chapter **5.3.1**. In this thesis an efficient desulfurization protocol for poorly-soluble transmembrane peptides is presented which was developed for the desulfurization of the BM2 sequence [Cys(Acm)^{11}][Leu^{21}][Cys^{22}]BM2(1-51). The desulfurization could be accomplished using a buffer/HFIP emulsion in the presence of glutathione, the reducing agent TCEP (tris(2-carboxyethyl)phosphine) and the radical initiator VA-044 (2,2'-azobis[2-(2-imidazolin-2-yl)propane] dihydrochloride). This HFIP emulsion was capable of dissolving hydrophobic BM2 peptides entirely and allowed a nearly quantitative conversion of the Cys22 ligation site to the corresponding Ala22 residue.

The second post-ligation method used for the synthesis of the final BM2 peptides was the Acm cleavage from the Cys11 side chain. For the synthesis of the final target peptide [Leu^{21}]BM2(1-51), two different methods were tested and compared including the oxidative cleavage of Acm by elemental iodine or the use of silver trifluoromethanesulfonate (AgOTf). Both strategies showed product formation of the final target peptide [Leu^{21}]BM2(1-51), yet with dramatic differences in the yield. With elemental iodine only very poor yields of approx. 16% were obtained while most of the peptide was oxidized. However, the synthesis of the final peptide [Leu^{21}]BM2(1-51) succeeded by AgOTf with a yield of 66% (chapter **5.3.2**).

Predominate fold analysis of BM2 peptides by CD spectroscopy *(Chem. Sci.*, ***2018***)[2]:

The predominant fold of the synthesised BM2 peptides were investigated by circular dichroism (CD) spectroscopy (chapter **5.4**). These studies confirmed a predominate alpha-helical folding for all investigated BM2 peptides. Analysis of the final target peptides [Leu^{10}]BM2(1-51) and [Leu^{21}]BM2(1-51) in TFE and POPC liposomes revealed an alpha-helical content of about 60% in the influenza B virus proton channel sequence 1-51 indicating possible helical structures between residues 36-44 which were considered structurally disordered in previous studies.[4]

3. State of the Art

3.1. Chemical peptide synthesis – A brief historical overview

Since the first steps of peptide chemistry by T. Curtius and E. Fischer at the beginning of the last century, numerous scientists have constantly searched for new synthetic methods to produce peptides and peptide analogues by total chemical methods.[5] Already in 1904, T. Curtius published the first useful synthetic pathway for benzoylglycines, using the azide-coupling method. This two-step coupling strategy relied on the reaction of an acyl azide with the nucleophile amino group of amino acids.[6] Despite this first practical coupling method, the application was limited to short peptide sequences and unprotected amino acids.

This changed in 1931 with the introduction of the carbobenzoxy (Cbz) group by M. Bergmann.[7] The Cbz-group was stable under basic conditions and could be removed by strong acids or under reductive conditions using hydrogen and palladium catalysts. Bergmanns invention allowed the synthesis of more complex peptides and led to the first total chemical synthesis of the peptide hormones vasopressin and oxytocin. In 1955, Vigneaud was rewarded with the Noble Prize for this work.[8] Shortly after the first successful synthesis of bioactive peptides, the discovery of the tert-butyloxycarbonyl (Boc) group was published by Carpino and colleagues.[9] The Boc group was stable under strong basic conditions but could be easily removed by acidic treatment. One decade later Carpino presented the fluorenylmethyloxycarbonyl (Fmoc) group which was stable under acidic conditions but could be removed by strong bases.[10] Together, both protecting groups enabled an orthogonal protection strategy for chemical peptide synthesis. Nowadays Boc- and Fmoc-protected amino acids are the fundament of the chemical solid-phase peptide synthesis (SPPS).

Simultaneously, new activation agents for carboxyl groups were developed. Usually activation of carboxyl groups can be achieved by introduction of an electron-withdrawing group. This activated intermediate must possess an intrinsic self-stability to prevent premature hydrolysis, enolisation or cyclisation. At the beginning of the last century acyl azides, halides or mixed anhydrides were used as electrophile reactants for aminolysis with unprotected amino acids.[11] Although all these precursors worked well for short sequences, more reliable activation agents were constantly developed. Especially, the development of carbodiimide-based coupling agents by Sheehan and Khorana in the middle of the last century simplified peptide synthesis significantly.[6b, 12] Famous examples for these important activation agents are N,N'-diisopropylcarbodiimide (DIC) and N,N'-dicyclohexylcarbodiimide (DCC).

Although efficient coupling agents and orthogonal protecting groups were already available in the middle of the last century, chemical peptide synthesis in liquid phase was the standard procedure until the end of the 50s. However, chemical synthesis of highly hydrophobic peptides was impractical or even impossible in liquid phase.[13] In 1963, almost 60 years after T. Curtius and E. Fischer, the American chemist Robert Bruce Merrifield solved this problem by the first practical peptide synthesis on a solid resin support. These solid supports are composed of small polymer beads covered with a functional surface.[14] The strategy consists of the stepwise coupling of orthogonal protected amino acids on the resin support followed by deprotection steps.[15] The major advantage of this method is a simple purification after each coupling and deprotection step by filtration. Thereby, peptide chains remain covalently bound to the resin beads. The possibility of automating this process is a further important advantage of this method, allowing a fast chemical peptide synthesis within a few hours.[16]

Depending on the N-terminal protection group and the type of the solid support there are two different strategies which have been developed over time. The first approach that was already introduced by Merrifield relied on the usage of Boc-protected amino acids. In this strategy concentrated TFA is used after every coupling step to remove the N-terminal Boc group from the growing peptide chain. However, the greatest disadvantage of this method is the need for strong and toxic acids such as hydrofluoric acid (HF) in order to cleave the final peptide from the solid support. A more convenient approach is the Fmoc-based SPPS. In this strategy basic conditions are used to remove Fmoc from the N-terminal peptide chain. After synthesis the final peptide sequence can be cleaved and deprotected by a mixture of concentrated TFA, water and scavengers (e.g. anisole, TIPS). In this work all peptides were synthesized with the Fmoc approach.

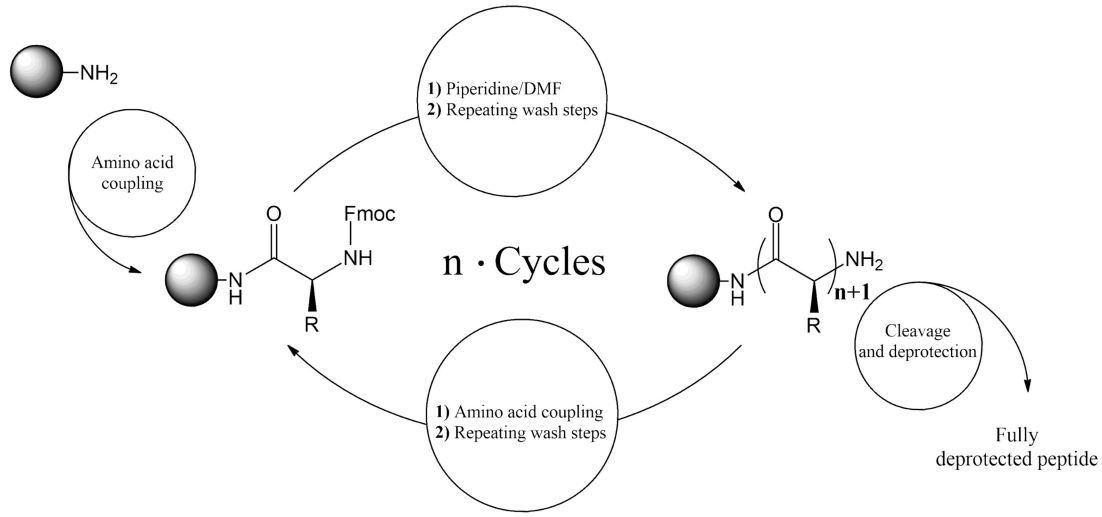

Scheme 3.1: Procedure of the Fmoc-solid phase peptide synthesis (Fmoc-SPPS). The final peptide can be cleaved from the solid support by acidic treatment using a mixture of concentrated TFA and scavengers.

Despite the possibility to automate the procedure, the synthesis of peptides with more than 50 amino acids is usually unprofitable.[17] Fmoc-SPPS of transmembrane related proteins remain an especially complicated challenge. Hydrophobic sequences tend to aggregate on the resin support and minimize access to the N-terminal amino group of the peptide chain. As a result the coupling efficiency decreases with rising chain length.[18]

The limitation of the solid phase peptide synthesis has promoted the development of ligation strategies which can be used to conjugate two or more peptide segments. Today, a large number of ligation/conjugation methods are described in the literature such as the Staudinger ligation, click chemistry or the thiazolidine-forming ligation.[19] However, most of these conjugation strategies lead to non-native peptide bonds between peptide segments. In 1994, Dawson and Kent published a native chemical ligation (NCL) strategy which involved the reaction of an N-terminal cysteine peptide and a C-terminal peptide-α-thioester.[20] The NCL enables a regiospecific conjugation of two or more unprotected peptide fragments under neutral or slightly basic conditions. This reaction is usually performed in aqueous phosphate buffers. The final ligation product is thereby obtained with a native peptide bond. Especially important is the preservation of stereochemistry at the ligation site. During the reaction the nucleophile thiol group of the cysteine peptide attacks the electrophile thioester site. The

generated thioester-peptide intermediate undergoes an N-to-S acyl shift reaction over a five-membered ring transition state.[21] During this rearrangement, the stereochemistry of the C-terminal amino acids is retained. Different studies were able to demonstrate that the final ligation product carries less than 1% D-amino acids after NCL.[22]

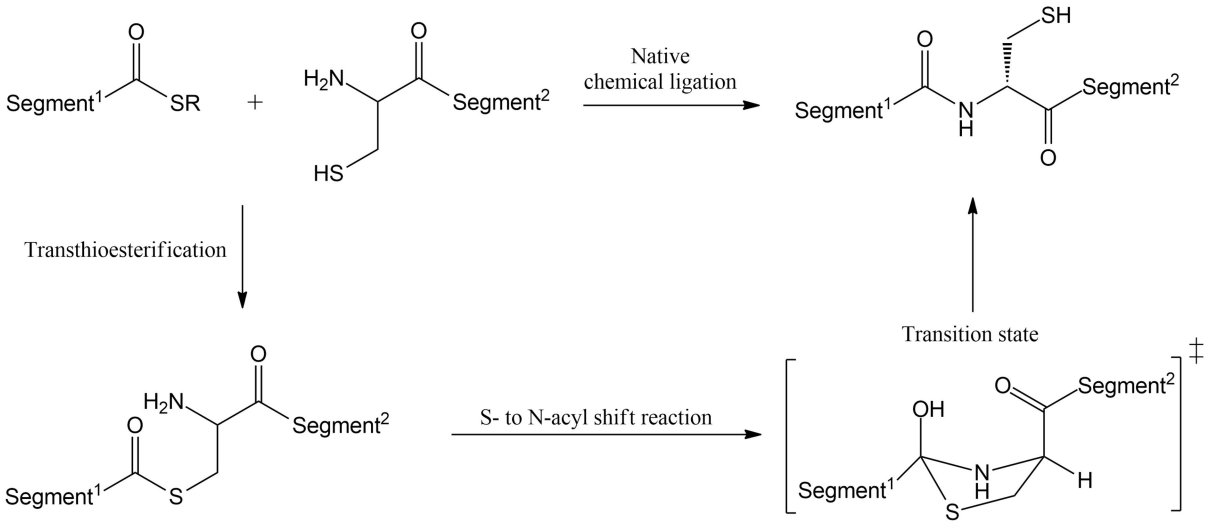

Scheme 3.2: Mechanism of the native chemical ligation (NCL) between the C-terminal peptide-α-thioester and the N-terminal cysteine peptide. The reaction involves an N-to-S acyl shift reaction resulting in a native peptide bond.[21]

After this discovery, NCL became the most popular method for the ligation of peptide fragments and was applied for the synthesis of numerous medium-sized proteins.[23] Several studies were able to demonstrate the value of the ligation strategy with synthesis of peptides with up to 15 kDa.[24] Over time, the strategy was constantly improved by investigation of different ligation buffers, catalysts or reducing agents.[21, 25] Today, dozens of different ligation variations are known such as the thioacid capture, oxo-ester or acyl azide mediated ligation.[26] Through the development of N-terminal cysteine surrogates and efficient desulfurization protocols for different amino acid residues (chapter **3.6**) even ligations in absence of natural cysteine residues are possible.[27]

However, a major drawback of the "classical" ligation method is its restriction to good or at least moderately soluble peptide fragments. Hydrophobic, transmembrane peptides are still especially challenging to ligate in conventional ligation solutions such as guanidinium chloride or urea based phosphate buffers. To counter this issue, a variety of different solubilisation strategies for poorly soluble peptide fragments were developed which will be presented and discussed in chapter **3.3**.

3.2. Synthesis of peptide thioesters – Precursors for the native chemical ligation

Peptide thioesters have become indispensable for chemical synthesis of medium-size proteins by NCL. Nevertheless, their synthetic access can still be difficult in many cases. Especially the production of long and hydrophobic transmembrane domains is often associated with poor yields. Since thioesters are sensitive to aminolysis under basic deprotection conditions, Boc-SPPS was long considered as most efficient method for the synthesis of peptide thioesters. However, the major drawback of the Boc strategy includes the requirement of strong, toxic acids like triflic acid or concentrated hydrofluoric acid (HF). Only in recent years good alternative approaches of HF-free protocols were published.[28] The deprotection of the N-terminal Boc-group by concentrated TFA though, still remains a main disadvantage. Over decades plenty approaches for the Fmoc-based SPPS of peptide thioesters have been investigated. These investigations led to many different methods for the preparation of peptide thioesters which can be classified into five different types, (i) direct, on resin-bound thioester synthesis, (ii) thioesterification of the C-terminus on the solid support, (iii) thioesterification by thiolysis from the solid support, (iv) post-cleavage thioesterification and (v) thioesterification *via* intramolecular O-to-S or N-to-S acyl migration. In following chapters the most promising Fmoc-based strategies for the synthesis of peptide thioesters are summarized.

3.2.1. Direct synthesis of peptide thioesters

The direct synthesis of peptide thioesters by Fmoc-SPPS is usually hampered since labile thioester are not stable under exposure to basic conditions during repetitive deprotection steps using piperidine. However, several groups were able to demonstrate that direct thioester preparation can be achieved if non-nucleophilic bases are used for Fmoc-group deprotection steps. Already in 1998, Aimoto and co-workers synthesised the 15 amino acid (aa) long thioester peptide Verotoxin(11-25)-SR with 24% yield using a conventional Fmoc-SPPS protocol. As a mild deprotection mixture for Fmoc cleavage 25% 1-methylpyrrolidine, 2% hexamethyleneimine, 2% HOBt in NMP/DMSO (1:1, v/v) were applied. This discovery led to the search for mild but more efficient bases for Fmoc deprotection.[29] Two years later, Wade *et al*. described a mixture of 1% 1,8-diazabicyclo[5.4.0]undec-7ene (DBU), 1% 1-hydroxynezotriazole (HOBt) and DMF as useful solution for Fmoc cleavage. The deprotection was performed under continuous flow conditions for 10 min. Although DBU was known as a stronger base compared to piperidine, it showed a lower nucleophilicity.[30] The application of DBU as non-nucleophilic base for thioester peptide synthesis was later further optimised by X. Bu and Z. Guo.[31] During their studies a ratio of 0.88:1 DBU/HOBt showed the best results for Fmoc-group removal while the thioester stayed intact. However, even under these optimized conditions, aminolysis of the thioester bond could not be prevented entirely. Despite this progress, Fmoc-SPPS of thioester peptides longer than 20 amino acids remained problematic.[32]

3.2.2. Thioesterification of the C-terminus on the solid support

An alternative approach to direct thioester synthesis is the thioesterification of the C-terminus while the peptide is linked through the side chain or the backbone on the resin

support. In all these methods the peptide C-terminus is either protected or in an unreactive state during the amino acid coupling and Fmoc deprotection cycles. After Fmoc-SPPS, the C-terminus must be converted to a thioester or thioester precursor (e.g. thioimide) before the final peptide can be cleaved from the resin.[32] In the approach of Crich *et al.* a thioglycinamdie linker was used to connect the peptide chain to the resin support. After Fmoc-SPPS the thioamide group was converted into a thioimide group by a simple S-alkylation with benzyl bromide. After cleavage from the solid support the final peptide was obtained as C-terminal benzyl thioester (scheme **3.3 a**).[33]

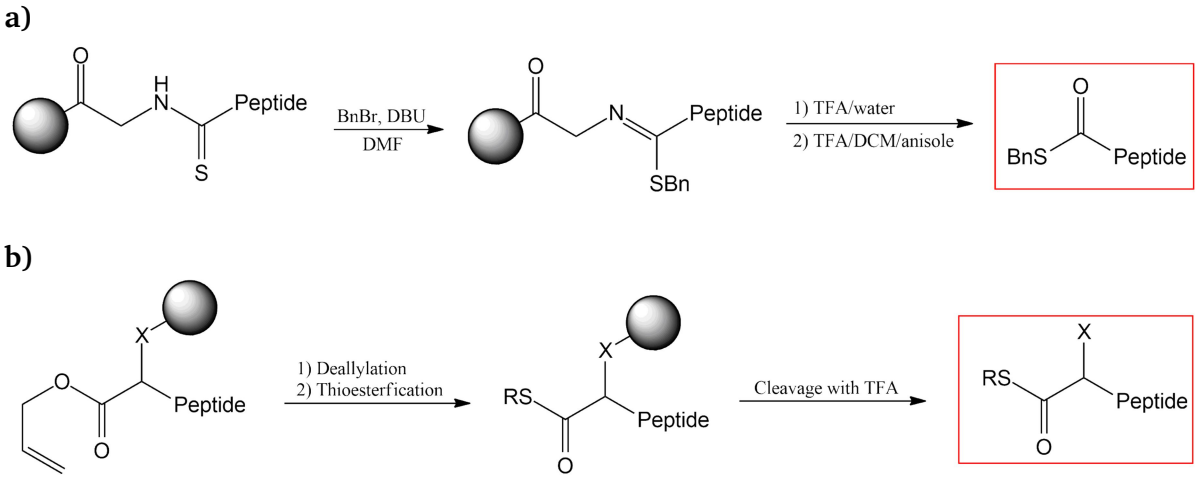

Scheme 3.3: **a)** Thioester production by Crich *et al.*, **b)** Production by Nakahara *et al.* (X=CH_2O, CH_2N, CH_2S).

Another example for the side-chain anchored strategy was published by Nakahara and co-workers. In this approach the C-terminal carboxyl group was protected as allyl ester. After Fmoc-SPPS, the C-terminus was deprotected by deallylation using an Pd(0) catalyst followed by thioesterification with thiophenol, benzyl mercaptan or ethyl-3-mercaptopropionate. The peptides were linked as silyl ether on Wang resin at tyrosine, lysine, cysteine, glutamic or aspartic acid (scheme **3.3 b**).[32, 34] In 2008, Wong *et al.* extended this side chain anchored strategy with the successful synthesis of the glycoprotein erythropoietin (EPO). The thioester peptide EPO(1-28)-SR was obtained with 23% on bromo-(4-methoxyphenyl)methyl resin. After deallylation, the free carboxyl acid was coupled with a glycine thioester using HATU as activator. The final thioester peptide could be released from the resin support by acidic treatment with TFA and scavengers.[32, 35]

3.2.3. Thioesterification by thiolysis

Although numerous approaches are well described in the literature, safety-catch linker strategies remain the most frequently used methods for the synthesis of peptide thioesters. Safety-catch linkers were developed to resist harsh basic or acidic conditions even at higher temperatures or under microwave radiation. This high stability allows the synthesis of thioesters by Fmoc- or Boc-strategies. The peptide cleavage from the resin support requires an activation of the linker. This activation is usually achieved by selective alkylation or cyclisation of the linker site near the peptide C-terminus. After activation, the peptide can be released from the linker by a nucleophile attack of an organic thiol compound

(e.g. thiophenol). The crude peptide is thereby obtained as a fully side chain protected C-terminal thioester. A characteristic feature of all these methods is the side chain deprotection after peptide cleavage from the resin support. However, this additional deprotection step leads to a longer and inconvenient work-up process compared to other methods. One of the most used safety catch linker strategies is the sulfonamdie method developed by Ingenito and co-workers (scheme **3.4 a**).[36] Commercial available resins are preloaded with 4-sulfamylbutyryl linkers. After Fmoc-SPPS the linker is activated by alkylation of the sulfamyl residue with trimethylsilyl diazomethane or iodoacetonitrile. The alkylated linker is then able to release the peptide by thiolysis.[36]

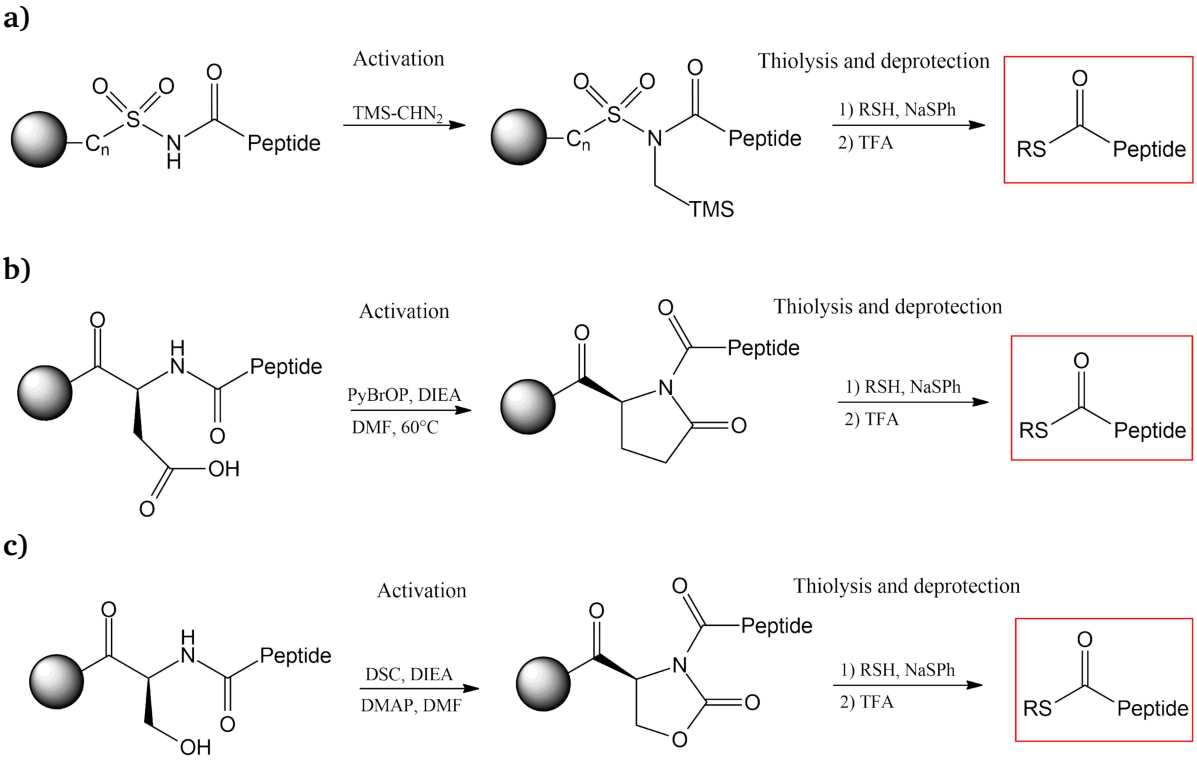

Scheme 3.4: **a)** Safety catch strategy developed by Ingenito for the synthesis of peptide thioesters on sulfamylbutyryl resins,[36] **b)** Thioester synthesis by Jensen and colleges using glutamic acid as linker.[37] **c)** Thioester peptide synthesis by Raj *et al.* using a serine linker[38]

In 2009, the Jensen group developed a Fmoc-based approach for the synthesis of peptide thioesters on a C-terminal glutamic acid linker (scheme **3.4 b**). Although this approach was not directly denoted as "safety catch" strategy the required steps were similar to the safety catch approach of Ingenito and co-workers. The method relies on the thiolysis of a backbone pyroglutamyl imide which is created by cyclisation of C-terminal glutamic acid. After activation the thioester peptide can be released from the resin by thiolysis using a free thiol.[37] A comparable strategy was published in 2017 by Elasha and Raj using a serine linker (scheme **3.4 c**). In this strategy the unprotected amino acid serine acts as a linker surrogate. After Fmoc-SPPS, the C-terminal serine is activated by selective cyclization to a urethane moiety using N,N-disuccinimidyl carbonate. Subsequently, the urethane unit can be displaced by thiolysis releasing the side chain protected peptide as thioester from the solid support. As well as for the safety catch strategy, the peptide can be deprotected by acidic treatment after cleavage from the resin support. Since serine is used as linker, the method can be applied with a great variety of resin types.[38]

3.2.4. Post-cleavage thioesterifications

Thioesterification after cleavage from the solid support is another widely used approach to obtain peptide thioesters. This strategy encompasses many different methods which convert the C-terminus into an active thioester in solution. The oldest and simplest approach relies on the thioesterification of fully side chain protected peptide acids. Usually the Fmoc-SPPS is performed on highly acid-sensitive resins such as HMPB or chlorotrityl resin. After peptide cleavage using mild acidic conditions, the C-terminal carboxyl group is activated in the presence of thiols. As product a fully side chain protected peptide thioester is obtained which must be deprotected in a following procedure.[39] However, solubility problems caused by the high hydrophobic character of fully side chain protected peptides make this method impractical for the synthesis of long membrane peptide domains.

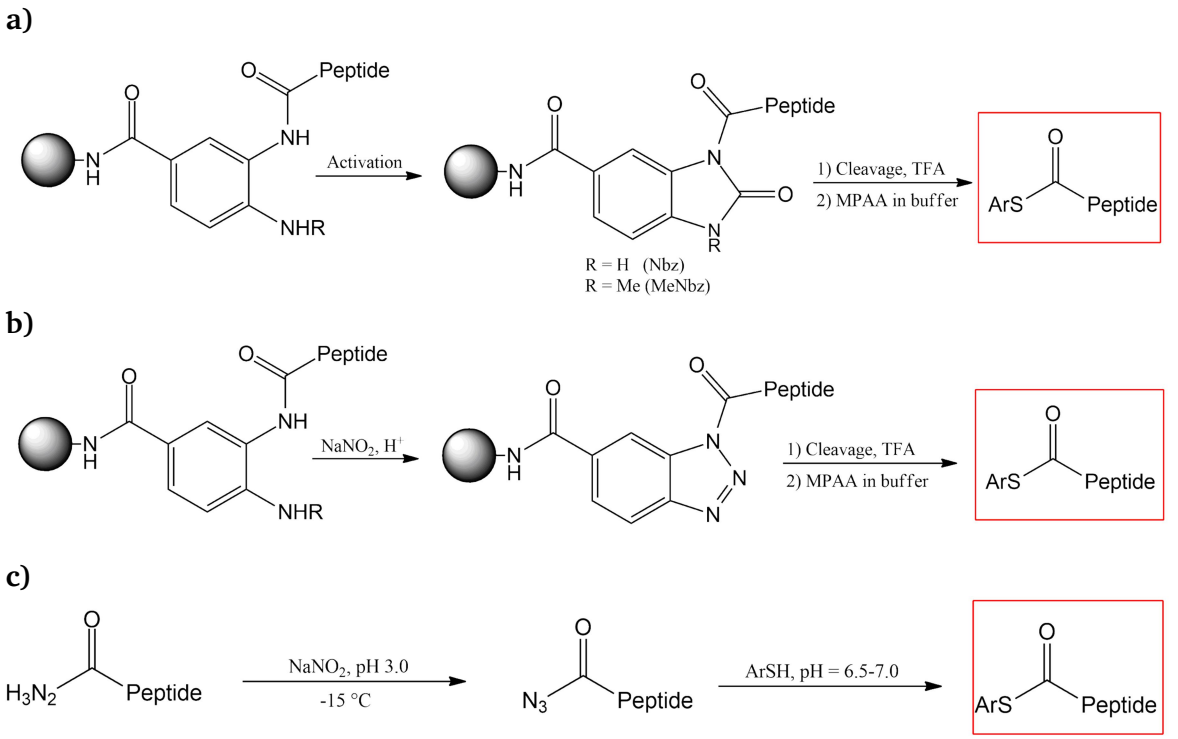

Scheme 3.5: **a)** Dbz (first generation) and MeDbz (second generation) strategy developed by Dawson *et al.*,[40] **b)** activation of the ortho-aminoanilide linker developed by Liu and co-workers using $NaNO_2$.[41], **c)** Ligation of peptide hydrazides by Liu and co-workers. The conversion of the hydrazide group into an azide group can be performed in the ligation buffer using sodium nitrite.[42]

An improved strategy that has received much attention in recent years is the synthesis of N-acyl-benzimidazolinone (Nbz) peptides originally invented by Dawson and co-workers.[40a] In this method peptides were synthesized on ortho-aminoanilide linkers. Activation of this linker is achieved by acetylation with 4-nitrophenylchloroformate which leads to cyclisation of the ortho-amino moiety. The resulting Dbz peptides can be easily cleaved from the resin by acidic treatment using TFA. Since Nbz peptides can be rapidly converted into the corresponding thioester by thiolysis, the direct use of Nbz peptides for the NCL is possible (scheme **3.5 a**). Although the Nbz method is compatible with Fmoc-SPPS, over-acetylation of the ortho-aminoanilide group can inactivate the linker. To diminish those side reactions more carefully Fmoc-SPPS conditions were investigated for the synthesis of Nbz peptides.[43] Additionally, capping steps with acetic anhydride should be avoided to prevent over-acetylation of the unprotected amino group. To counter this problem Blanco-Canosa and

Dawson improved the strategy by introduction of the ortho-(N-methyl)aminoanilide unit as a less sensitive linker. This MeNbz method is more resistant to over-acetylation yet reactive enough for activation *via* 4-nitrophenylchloroformate.[40b] This enhanced MeDbz method was used several times for NCL of cysteine-rich proteins such as cyclotides Kalata B1, MCoTI-II, cyclic peptides, cyclothiodepsipeptides[44] and many more.[45] An impressive example for this method was also made by Sueiras-Diaz *et al*. by the first total chemical synthesis of the Human Growth Hormone consisting of 191 amino acid residues. The synthesis was achieved by sequential native chemical ligation with three peptide fragments.[46] Dbz- and MeDbz-peptides are not only very easily convertible into C-terminal thioesters, these peptides can also be stored safely over a long period of time. Furthermore, the Dbz carboxyl group can be applied for the attachment of C-terminal tags. To date, the Dbz method has been constantly further developed and is therefore one of the most used synthetic pathways for peptide thioesters. Recently, Pala-Pujadas and Blanco-Canosa presented a kinetically controlled NCL on the base of MeDbz-peptides using p-cyano-phenylcarbamate as an activation agent. This strategy was recently used for the chemical synthesis of a 175 amino acid long Sonic Hedgehog protein.[47] Inspired by that work, Tsuda and co-workers further enhanced this protocol using 4-fluorophenyl chloroformate activated MeDbz precursors.[48] This approach was successfully used for the one-pot NCL of three peptide segments which can be controlled over the pH of the ligation solution.[33a]

A further modification of this method is the conversion of the ortho-aminoanilide linker into a benzotriazole leaving group (scheme **3.5 b**). Several works already demonstrated that benzotriazole peptides can be applied for peptide ligation but their synthesis was rather uncomfortable and not suitable for long peptides.[49] In 2015 Liu *et al*. published an improved modification of the Dbz method using sodium nitrite ($NaNO_2$) to convert the ortho-aminoanilide unit into a benzotriazole moiety.[41] These C-terminal benzotriazole peptides reacted similar to Nbz peptides and could be used as thioester precursors directly in the ligation buffer. The method was used for the preparation and NCL of histone H2B from five peptide segments. Additionally, the method was compatible with C-terminal solubilizing tags attached on the aminoanilide moiety which was demonstrated by the preparation of the cyclic protein lactocyclicin Q.[33a, 41]

A further post-cleavage thioesterification method which used sodium nitrite as an activation agent was presented in 2011 by Liu and colleges.[42] The method relies on C-terminal hydrazide peptides which can be easily converted into peptide azides in aqueous ligation buffers (scheme **3.5. c**). At low temperatures and slightly acidic conditions sodium nitrite is capable of reacting chemoselectively with the hydrazide moiety while the rest of the peptide chain remains unmodified. The formed azide group is then immediately replaced by a nucleophile thiol catalyst such as MPAA or thiophenol. This $NaNO_2$-mediated ligation strategy encompasses several advantages, including the simple access of hydrazide peptides trough Fmoc-SPPS and their direct usage in the ligation buffer. Even more important, inactivated peptide hydrazides remain unreactive in NCL and allow orthogonal ligation strategies in combination with peptide thioesters.[33a] Moreover, the stepwise activation of the hydrazide group allows the one-pot ligation of multiple peptide segments from the N- to the C-terminus without the need of cysteine protecting groups.[50] To date, this versatile hydrazide strategy has been applied with the successful ligation of multiple medium-sized proteins such as human α-synuclein[50a], the M2 influenza A proton channel[51], histone H2A[52], Mambalgin-1[50b] and many more.[53]

3.2.5. Thioesterification by O/N-to-S acyl shift reactions

The discovery of Fmoc-compatible thioester generating rearrangement groups was a tremendous progress for the synthesis of peptide thioesters. In this strategy peptides were not directly obtained as thioester after Fmoc-SPPS. Instead, rearrangement units with thiol containing side chains are linked over amide or oxo-ester bonds at the C-terminus. Under slightly basic conditions the free thiol group acts as internal nucleophile which attacks the C-terminal carbonyl unit over a cyclic intramolecular O-to-S or N-to-S acyl shift reaction. The rearrangement relies on an equilibrium that is dependent on temperature, pH and possible substituents next to the carbonyl group. Surprisingly, a similar mechanism was discovered during intein-mediated protein splicing that can be found in eukaryotes, bacteria and archaea.[54] The principle of the O-to-S or N-to-S acyl shift reaction is shown in scheme **3.6**.

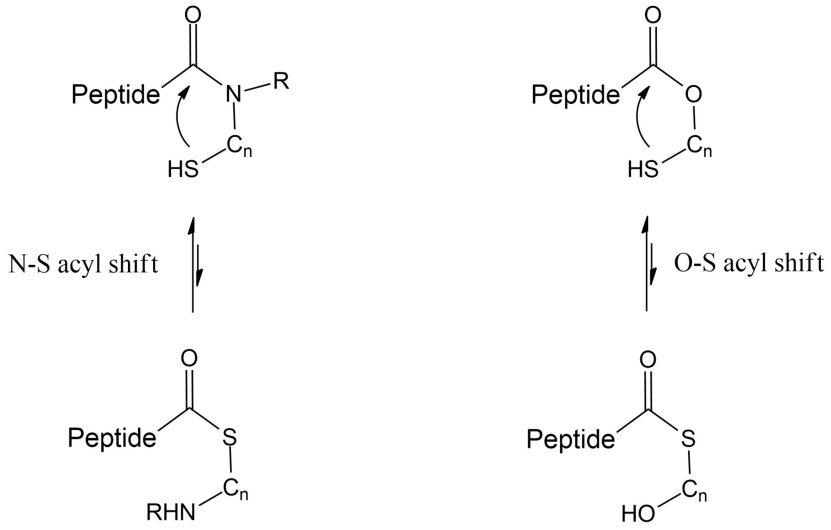

Scheme 3.6: Left: Intramolecular thioesterification by the N-to-S acyl transfer reaction over a cyclic transition state, Right: Intramolecular thioesterification over an O-to-S acyl transfer reaction.

In recent years this revolutionary approach attracted much attention due to constant developments of new rearrangement groups. In 2004, the first discovery of a thioester forming rearrangement group was published by Danishefsky and co-workers. As a rearrangement unit, 2-mercaptophenol was successfully applied reaching ligation yields up to 78%. Encouraged by this success, side chain protected peptide fragments were converted into disulfide-protected 2-mercaptophenyl esters[32] and then used for the NCL of glycopeptides.[55] However, the main drawback of this strategy was the rather complicated synthesis of the peptide thioesters in solution.

In 2006, Bang and Kent published a “kinetically controlled native chemical ligation” which allowed chemical ligation of multiple peptide segments in one reaction vessel. This strategy relied on different ligation rates of peptide-α-thioarylesters and peptide-α-thioalkylesters. In absence of thiophenol were thioalkylesters considered as effectively unreactive while thioarylesters remain reactive.[56] Inspired from that kinetically controlled approach, Zheng *et al.* investigated different thiol-containing oxo-esters which can rearrange to a C-terminal thioester (table **3.1**). For that study, glycine derivatives of oxo esters **1**-**4** were ligated with free cysteine in a phosphate-buffered saline (PBS) solution. The study was primarily focused

on the relationship between the structure of the oxo-ester and the ligation efficiency with cysteine. The conversion, hydrolysis and ligation amounts were determined after 48 h using RP-HPLC analysis (table **3.1**).[57]

Table 3.1: Results of the ligation experiments using oxo-esters **1-4**, after 48 h reaction time, at room temperature. Ligation buffer: 0.2 M PBS, 2% PhSH, 30 mM TCEP, pH=6.5.[57]

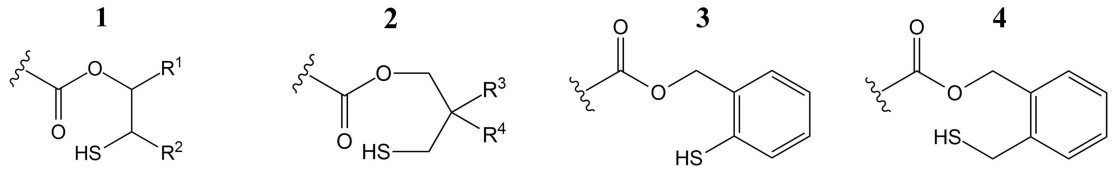

Structure	Substituents	Hydrolysis [%]	Ligation [%]	Conversion [%]
1 1 to 5 acyl shift (fast conversion)	R^1=H, R^2=H	90	10	100
	R^1=Me, R^2=Me	86	11	97
	R^1=COR, R^2=H	6	93	99
	R^1=CONHR, R^2=H	16	84	100
2 1 to 6 acyl shift (slow conversion)	R^3=H, R^4=H	3	8	11
	R^3=OR, R^4=H	2	8	10
	R^3=Me, R^4=Me	2	12	14
3 1 to 6 acyl shift (fast conversion)	aromatic substituent	100	0	100
4 1 to 7 acyl shift (fast conversion)	aromatic substituent	31	38	69

The conversion rate was highly dependent on the number of carbon atoms between the oxygen and sulfur atom. After 48h, rearrangements over 1 to 5 acyl migration (structure **1**) showed nearly 100% conversion, while 1 to 6 acyl shift reactions (structure **2**) reached only about 10%. Furthermore, in the case of a five-membered ring intermediate (structure **1**) substituent R^1= H, Me showed a massive amount of hydrolysis while R^1= COR, CONHR resulted in high ligation yields. These results suggest that the presence of a sterically hindered group near the ligation site seemed to improve the ligation efficiency.

The incorporation of an aryl group (structure **3** and **4**) accelerated the reaction rate significantly. The internal thioesterification over a six-membered ring intermediate was slow for thioalkylesters (structure **2**) but noticeably faster for thioarylesters (structure **3**). After 48 h, oxo-ester **3** showed 100% conversion. However, no ligation product was found. The rearrangement over a seven-membered ring intermediate (structure **4)** showed 69% conversion with a hydrolysis/ligation ratio of approximately 1:1.

Since intramolecular thioesterifications *via* an O-to-S acyl transfer attracted more attention at the beginning of this decade [55, 58] an understanding of the mechanism was required. In theoretical calculations of the O-to-S acyl transfer reaction by the Qing-Xiang group, more detailed information about the hydrolysis and the reactivity-structure relationship were analyzed.[59] It was found that the O-to-S rearrangement, as well as hydrolysis, proceeds over

an anionic stepwise mechanism in which the cleavage of the C-O bond is the rate-limiting step. Surprisingly, the calculated energy barriers of the oxo-ester hydrolysis (+24.3 kcal/mol) and the thioester hydrolysis (+25.5 kcal/mol) for model compound 2-mercaptoethyl acetate led to the assumption that hydrolysis occurs preferably over the oxo-ester.

The O-to-S acyl migration by the anionic stepwise mechanism is initiated by deprotonation of the thiol group followed by a rearrangement over the five-membered ring intermediate (figure **3.1**). The relative free energy of transition state 1 (TS1) is independent from R^1 or R^2 and was calculated for model compound 2-mercaptoethyl acetate (R^1, R^2=H) with 12.5 kcal/mol. Substitution of R^1 and R^2 by bigger groups showed almost no changes for the relative free energy of TS1 (table **3.2**). However, the free energy barrier of transition state 2 (TS2), decreased with rising steric hindrance of R^1 and R^2 (table **3.2,** TS2). Since the energy barrier of the oxo-ester hydrolysis (+24.3 kcal/mol) is also considered as independent from substituents, big space claiming groups for R^1 and R^2 should favour the O-to-S acyl migration.[59]

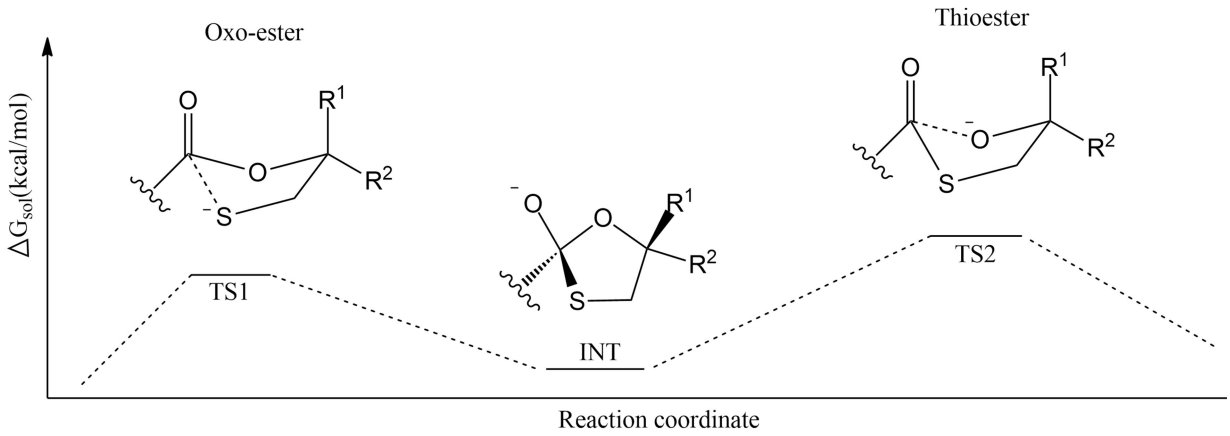

Figure 3.1: The energy barriers of both transition states TS1 and TS2 during the O-to-S acyl migration. The rearrangement occurs over a five-membered ring intermediate (INT).[59]

Especially 2-hydroxy-3-mercaptopropanamide (Hmp) (entry **1.3**, table **3.2)**, with a relative free energy barrier of +16.3 kcal/mol (TS2) and 2-hydroxy-2-methyl-3-sulfanylpropanoic acid (HMSP) (entry **1.4)** with +13.6 kcal/mol (TS2) were calculated as the most efficient rearrangement groups for thioester formation.[59] These theoretical calculations confirm the experimental results of Zheng and co-workers which are depicted in table **3.1**.[57]

Table 3.2: Calculated free energy barriers (in kcal/mol) of TS1 and TS2 with respect to R^1 and R^2.[59]

Entry	Rests	ΔG(TS1)	ΔG(TS2)	Rearrangement group
1.1	R^1=H, R^2=H	12.5	25.1	2-Mercaptoethanol
1.2	R^1=COMe, R^2=H	10.0	23.7	MMPA
1.3	R^1=CONHR, R^2=H	9.5	16.3	Hmp
1.4	R^1=CONHR, R^2=Me	9.9	13.6	HMSP

Although HMSP **1.4** can be easily made from the commercially available precursor methyl 2-methylglycidate using the method of Liu and Maier,[60] no practical applications of this promising rearrangement group have been published so far. However, in contrast to the theoretical model group **1.4**, the Hmp unit **1.3** was used several times to produce peptide

thioesters. Already in 2004, Botti and co-workers published the first method for the preparation of disulfide protected Hmp-peptides. Therefore the resin support was prepared by the coupling of disulfide protected Fmoc-Cys-OH. After deprotection of the Fmoc group, the free amino group was converted into a hydroxyl function using sodium nitrite and slightly acidic conditions (scheme **3.7 a**). The following peptide sequence of NNY-Rantes-(2-33)-Hmp was synthesized using a standard Fmoc-based protocol. According to the authors, the coupling of the first amino acid at Hmp succeeded quantitative by Steglich esterification using HBTU/DIEA with DMAP as a catalyst. However, these quantitative coupling yields through Steglich esterification were not reproducible by other groups. Indeed, later studies demonstrated that Steglich esterification is rather inefficient for the coupling of most amino acids at the Hmp moiety.[2, 60] Nevertheless Botti *et al.* showed that Hmp-peptides can be directly applied for ligations in conventional phosphate buffers. In these ligation experiments, Hmp hydrolysis was observed as a single side reaction with an amount of 12.6%.[61] These results confirmed the findings of Zheng *et al.* who determined Hmp hydrolysis to 16% in 0.2 M PBS buffer (table **3.1**).

The main drawback of Bottis approach was a rather complicated on-resin preparation of Hmp which resulted in low loading capacities. In the following years several groups tried to avoid this disadvantage *via* a complex synthesis of t-butyldimethylsilyl (TBS) protected Hmp.[62] Nevertheless, this rather complicated procedure relied on five synthetic steps which prevented a breakthrough of this method.

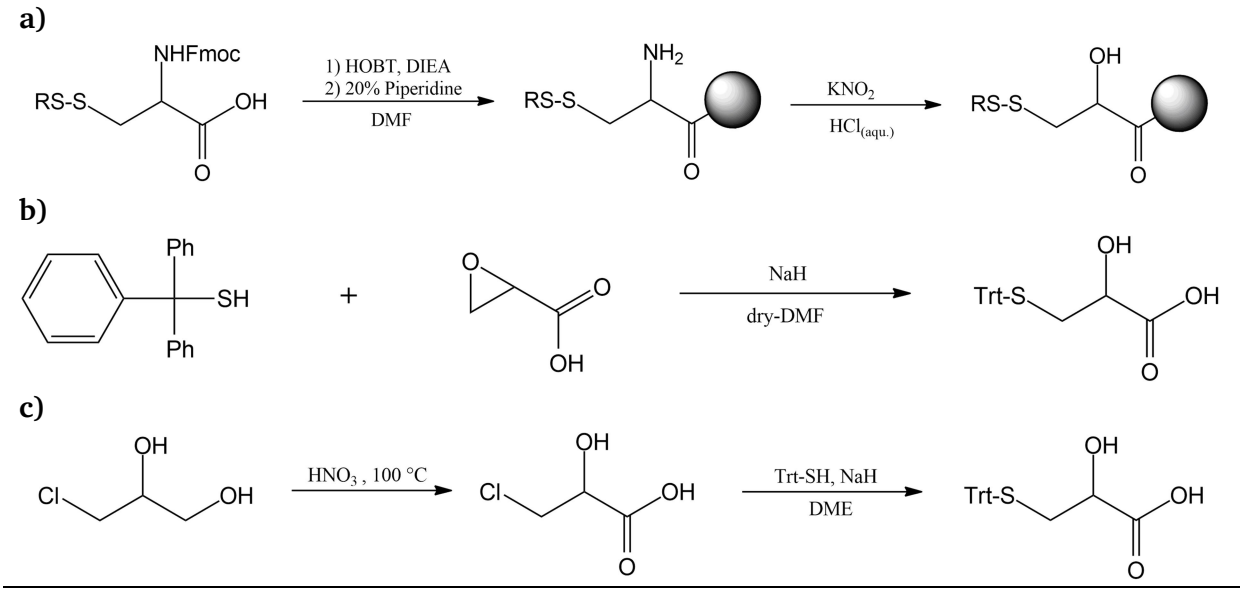

Scheme 3.7: **a)** Synthesis of disulfide protected Hmp on the resin support by Botti *et al.*,[61] **b)** Production of trityl protected Hmp by Liu and Maier,[60] **c)** Synthesis of the trityl protected Hmp by Wisniewski.[63]

In 2013, Liu and Maier introduced an Fmoc compatible, trityl-protected Hmp(Trt) building block which was compatible with Fmoc-SPPS. In contrast to previous approaches, the synthesis of Hmp(Trt) succeeded quickly and simply starting from oxirane-2-carboxylate and triphenylmethyl thiol (scheme **3.7 b**). Additionally, this study presented an efficient method for the coupling of the first amino acid at Hmp(Trt) using the Mitsunobu reaction. Liu *et al.* were also able to increase the yield of the SPPS by using 2-methylpiperidine instead of

piperidine for Fmoc deprotection steps. All these improvements allowed an efficient synthesis of Hmp-peptides with enhanced yields.[60] In their study, Liu and Maier used Hmp-peptides successfully as precursors for the preparation of peptide thioesters. Furthermore they confirmed the results of the ligation experiments from Botti *et al*. using Hmp-peptides directly in NCL.

A very efficient synthetic route for trityl-protected, enantiomerically pure Hmp ((R)-3-chloro-2-hydroxypropanoic acid) was published by K. Wisniewski who applied Hmp(Trt) as a precursor for the synthesis of the oxytocin agonist [L-Hmp^1, Thr^4]OT. In this two-step strategy 3-chloro-1,2-propanediol was first oxidized by 68% nitric acid to 3-chloro-2-hydroxypropanoic acid. Treatment with triphenylmethyl thiol resulted in trityl protected Hmp (scheme **3.7 c**). The main advantage of this method was the simple procedure starting with inexpensive and easily available compounds.[63]

For peptide thioester preparation by O-to-S acyl shift reactions Hmp is a promising rearrangement group. Nevertheless, an alternative and widely investigated approach is the usage of N-to-S acyl shift rearrangement units. In 2002, Vizzavona *et al*. observed an N-to-S acyl transfer at 2-mercapto-4,5-dimethoxybenzyl (Dmmb)-modified peptides during the search for a suitable auxiliary group at the X-Gly ligation site. This unsuspected side reaction occurred under acidic treatment with concentrated TFA.[64] Three years later, this finding was adopted and further expanded by Kawakami and co-workers who developed a Fmoc-based SPPS approach for the preparation of peptide thioesters based on the Dmmb-group. In this method the thioester was generated during peptide cleavage with concentrated TFA resulting from an acid-induced N-to-S acyl transfer.[65] Soon after this discovery it was realized that the intramolecular thioesterification via N-to-S acyl shift reactions was a powerful method for thioester peptide preparation. In the following years, the numbers of new developed N-to-S acyl rearrangement units exploded. Nowadays, thioesterification by the N-to-S acyl transfer reaction is a widely used “gold standard” technique for the preparation of peptide thioesters.[66] Most of these rearrangement groups are compatible with Fmoc-SPPS and can be directly used in NCL. The main advantage of N-to-S acyl rearrangement groups is the stable amide bond which is less prone to hydrolysis than the oxo-ester bond. However, this higher stability causes lower reaction rates for the N-to-S acyl shift reaction.[66c, 67]

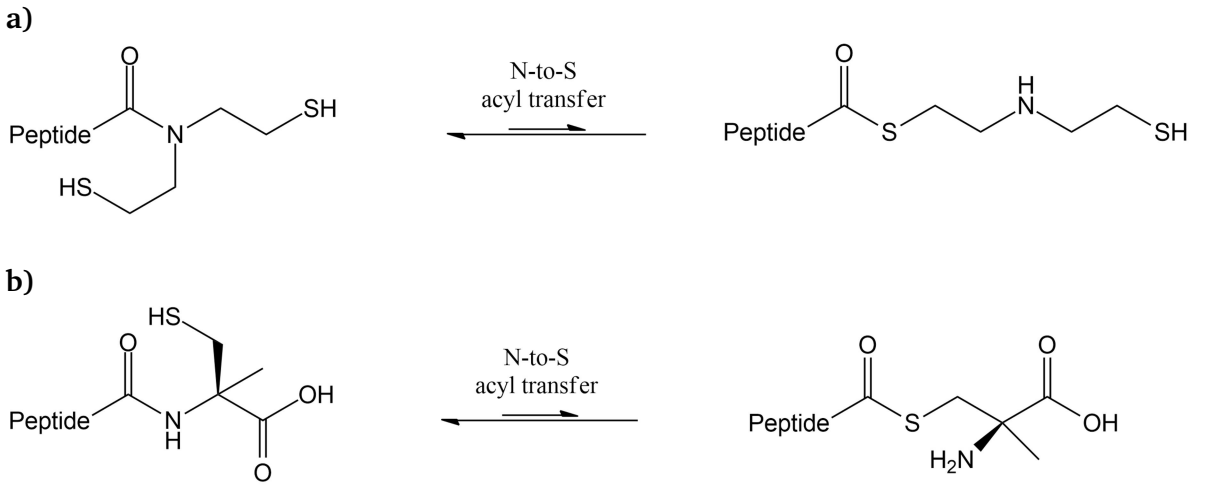

Scheme 3.8: **a)** N-to-S-acyl transfer reaction of SEA modified peptides to the activated thioester[68], **b)** Rearrangement of α-methylcysteine to a C-terminal peptide thioester.[69]

A widely applied strategy using N-to-S shift reactions is the SEA ligation with bis(2-sulfanylethy-l)amino (SEA) modified peptides (scheme **3.8 a**).[70] This method was introduced and published by the O. Melnyk and C. Liu group.[68] The enhanced reactivity of the SEA motif relies on the presence of two β-mercaptoethyl groups which are bound to the N-atom. In this motif one thiol group is always aligned for an intramolecular attack at the peptide C-terminus. This SEA mediated thioesterification occurs *via* a five-membered ring intermediate.[71] Since its discovery, the SEA strategy was successfully applied for the total chemical synthesis of multiple medium-sized proteins such as cyclic O-acyl isopeptides, small ubiquitin-like modifier (SUMO) proteins and 15 kDa polypeptides.[24b, 72]

In 2014, another promising N-to-S acyl shift reaction was introduced by the Offer group (scheme **3.8 b**). The strategy was successfully used for the synthesis of the bovine pancreatic trypsin inhibitor (BPTI) and murine KC (mKC), the mouse functional homologue of interleukin 8.[69] In this study two C^{α}-substituted cysteine analogues AMP (2-amino-2-methylpropane-1-thiol) and α-methylcysteine were investigated as potential thioester-producing rearrangement groups (figure **3.2**). The activation of the amide bond was achieved by the additional methyl group at the C^{α}-carbon atom which caused a dramatic acceleration of the acyl shift reaction. The additional methyl group at the C^{α}-atom reduced the free energy barrier of the cyclic transition state and facilitated the cleavage of the amide bond. This so called gem-dimetyl effect, which can be observed at α-methylcysteine, was thoroughly investigated and summarized by M. Jung and G. Piizzi and is also kwon for a number of different organic reactions and cyclizations.[73]

The main advantage of this promising method was the high stability of the thioester peptide in conventional ligation buffers. In contrast to the O-to-S acyl shift reaction α-methylcysteine showed no signs of hydrolysis during NCL. A second advantage of α-methylcysteine was its compatibility with the widely used Fmoc-SPPS. However, the main disadvantage of this method was the minor reaction rate. Although the usage of α-methylcysteine peptides turned out to be an efficient method for the ligation of membrane peptides, α-methylcysteine is not commercially available and its precursors are prohibitively expensive.

a) HMSP **b)** AMP **c)** α-methylcysteine

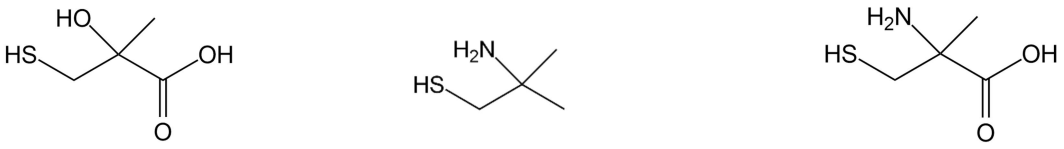

Figure 3.2: **a)** structure of 2-hydroxy-2-methyl-3-sulfanylpropanoic acid, **b)** 2-amino-2-methylpropane-1-thiol, **c)** structure of α-methylcysteine.[59, 69]

Interestingly, α-methylcysteine resembles the theoretically designed rearrangement group HMSP (2-hydroxy-2-methyl-3-sulfanylpropanoic acid) which was proposed by the Qing-Xiang group and discussed above in table **3.2**.[59] Similar to AMP and α-methylcysteine, HMSP carries an additional methyl group at the C^{α}-atom (figure **3.2**). However, HMSP is not deeply investigated so far as rearrangement group for ligation studies. In further studies, HMSP could be a promising rearrangement unit for the synthesis of peptide thioesters.

3.3. Synthetic strategies for hydrophobic peptides

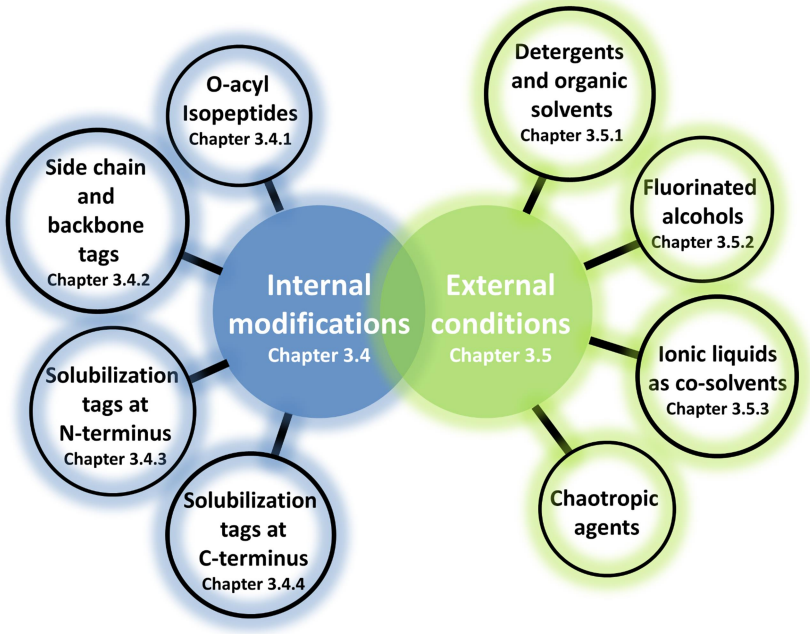

Figure 3.3: Internal modifications and external conditions used as strategies to improve the solubility of hydrophobic peptides during NCL or peptide purification.[74]

The synthesis of hydrophobic proteins by NCL is a recurring challenge in modern peptide science. Especially transmembrane peptide/protein domains, which are naturally located in cell membranes, often precipitate/aggregate in all known aqueous ligation buffers. Strong intra- and intermolecular interactions of hydrophobic sequences tend to form secondary structures like β-sheets which further decrease the solubility of peptides/proteins. Over decades, different methods have been developed to counter solubility problems of transmembrane proteins. These methods can be divided into two different groups.[74]

The first group of solubility-improving strategies include external conditions which use detergents, organic solvents or fluorinated alcohols as additives in aqueous buffer solutions. A less studied method is the usage of ionic liquids as media for oxidative folding or NCL.

The second group of solubility-improving strategies include internal modifications of the peptide chain. These modifications encompass the incorporation of depsi-motifs (O-acyl isopeptides) or the attachment of permanent and temporarily bound solubilizing tags, respectively. Of special interest are temporarily bound solubilizing tags, since they can be removed from the final target peptide. This requires a cleavable linker, which must be tracelessly cleaved from the peptide chain under defined conditions. In contrast to temporarily bound tags, permanently bound tags are mostly applied for recombinant protein expression since cleavable linkers are usually difficult to incorporate by recombinant methods. Famous examples for recombinant solubilizing tags are solubility enhancing ubiquitous (SNUT), aggregation-resistant proteins, glutathione-S-transferase (GST) and polyionic amino acid sequences with chargeable side chains (Asp-, Lys-, Arg-, Glu-, His-tags).[75] The following chapters give a precise insight into temporarily bound tags which can be incorporated by chemical methods.

3.4. Internal modifications as solubilization strategies

3.4.1. Synthesis of O-acly isopeptides

A well-studied method to increase peptide solubility by internal modifications of hydrophobic peptides is the synthesis of O-acly isopeptides (depsipeptides) which contain oxo-ester bonds within the primary sequence.[76] These oxo-esters are located at threonine or serine residues and can be incorporated by Fmoc-SPPS. The depsi-motif prevents the formation of unfavourable secondary structures (e.g. β-sheets) which tend to aggregate and participate in aqueous ligation buffers. After ligation, the natural peptide sequence can be obtained under slightly basic conditions, since the depsipeptides tend to rearrange over an O-to-N acyl shift reaction to from the native peptide bond. An important example of the power of this strategy is the successful ligation of the highly hydrophobic β-amyloid peptide Aβ42 which is related to Alzheimer's disease (scheme **3.9**).[77]

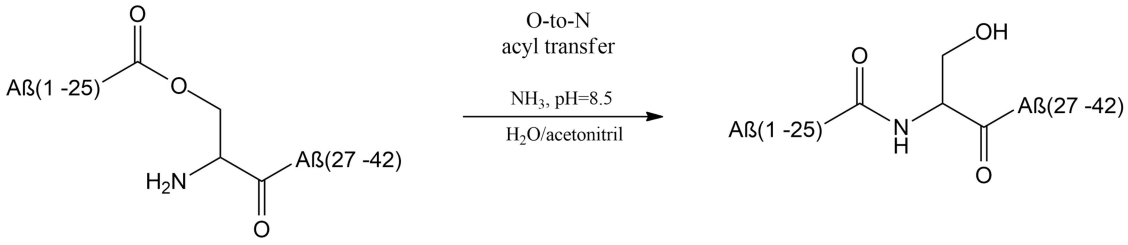

Scheme 3.9: Rearrangement of O-acyl isopeptides to the natural peptide sequence under slightly basic conditions. The irreversible O-to-N acyl transfer reaction occurs over a five-membered ring intermediate.[77b]

3.4.2. Side chain and backbone attached solubilizing tags

Despite the great variety of possible recombinant solubilizing tags, non-native solubilizing tags can hardly be incorporated by protein expression. The chemical peptide synthesis, however, can be performed using native or non-native building blocks. Frequently used examples for non-native solubilizing tags are hydrophilic polymers such as poly(ethyleneglycol)polyamide (PPO) or poly-8-amino-3,6-dioxaoctanoic acid (ADO).[2, 78] Nevertheless, natural amino acids represent the most used building blocks for solubilizing tags. Especially basic amino acids such as histidine, lysine or arginine are frequently incorporated in solubility enhancing sequences.

Kato *et al*. compared the differences between polylysine and polyarginine tags with the help of the model peptide bovine pancreatic trypsin inhibitor (BPTI-22). They found that the solubility-improving effect was not only dependent on the number of basic amino acids but also the location of the tag was an important factor. Attachment on the C-terminus seemed to increase peptide solubility more than N-terminal-bound tags. Furthermore, polyarginine tags showed a slightly higher solubility potential as their polylysine counterparts. However, the differences between polyarginine and polylysine tags were negligible for sequences shorter than 5 amino acids.[79] Surprisingly, Albericio and co-workers came to opposite results. In their HPLC studies, peptides with linear polylysine tags showed a greater increase in polarity than their polyarginine counterparts.[80] Due to this controversial finding, polylysine and polyarginine tags were considered similarly efficient.

The attachment of solubility enhancing tags at the side chain or backbone is one of the most favored methods to increase peptide solubility.[35] Side chain or backbone linked tags provide several advantages over C-terminal or N-terminal tags. The attachment of large groups or tags, far away from the C-terminus, reduces steric hindrance at the ligation site. Additionally, the high number of functional groups alongside the side chain offers various anchor points for solubility tags. Despite these benefits, the synthesis of thioester peptides with side chain or backbone modifications is challenging. Due to lower safety risks, Fmoc-SPPS is the most applied method for production of those peptide thioesters (chapter **3.2**). Last decade, a remarkable number of new linker types and backbone modifications were developed which enabled the attachment of permanent or temporarily bound polyionic tags at the peptide chain. Especially important are temporarily bound tags, since they can be removed from the final target peptide after native chemical ligation or purification.

Temporarily bound solubilizing tags:

Table **3.3** shows a comprehensive selection of temporary linker types and solubilizing tags which were successfully applied for the synthesis or purification of hydrophobic peptides.

Table 3.3: Backbone and side chain modification strategy to attach solubilization tags on hydrophobic peptides.

Peptide	SPPS	Modifi. site	Solubility tag	Reference
AYVLWYA	Fmoc	Tyr	Nmec tag[a]	Wahlström *et al.*, **2008** [81]
ACP(65-74)	Fmoc	Tyr, Asp	TEGBz tag	L. Kocsis *et al.*, **2008** [82]
KWLPFLA	Fmoc	Trp	Nmbu tag[a]	Wahlström *et al.*, **2009** [83]
hEPO(43-77)	Fmoc	Glu, Lys	polyarginine	Z. Tan *et al.*, **2011** [84]
LC31(1-114)	Fmoc	Gln	polyarginine[c]	Y. Huang *et al.*, **2013** [85]
AM2(1-97)	Fmoc	Gly backbone	polyarginine[b]	J. Zheng *et al.*, **2014** [51]
H4(1-102)	Fmoc	Cys	tri-arginine[b]	S. Maity *et al.*, **2016** [86]
Aβ(1-48)	Fmoc	backbone	polyarginine[b]	C. Zuo *et al.*, **2016** [87]
HCV p7	Fmoc	backbone	polyarginine[b]	J. Zheng *et al.*, **2016** [43]
GroES(1-97) L31(1-70)	Fmoc	Lys	polylysine[b] PEG_2[b]	M. Kay *et al.*, **2016** [88]
Aβ(1-42)	Fmoc	Lys	oNb-OEG3[b,c]	J. Karas *et al.*, **2017** [89]
AM2(1-97)	Fmoc	backbone	polyarginine[b]	S. Tang *et al.*, **2017** [90]
Model peptide	Fmoc	Lys	KKK, RRR[b]	S. Tsuda *et al.*, **2018** [48]
hepatitis B Cp (1-149)	Fmoc	Cys	deka-lysine	S. Tsuda et al., **2018** [91]
PYY(3-36)	Fmoc	Lys	PEG_{22}	Castelletto *et al.*, **2018** [78b]
BM2(1-51)	Fmoc	Cys	polylysine[b]	S. Tsuda *et al.*, **2019** [92]

a: used for purification via HPLC.
b: used for purification and native chemical ligation.
c: photocleavable tag.

Solubilizing tags attached to a side chain of peptides:

One of the first attempts to incorporate temporarily bound solubilizing tags at the side chain of peptides was made by K. Wahlström and co-workers.[81] Wahlström introduced two side chain protecting groups (Nmec and Nmbu) with solubility improving properties, for tyrosine (Tyr) and tryptophan (Trp) residues. Both protected building blocks Fmoc-Tyr(Boc-Nmec) and Fmoc-Trp(Boc-Nmbu) were compatible with Fmoc-based SPPS and could be easily incorporated by standard coupling conditions (figure **3.4**).

The strategy was developed and tested by the synthesis of short model peptides (table **3.3**). During peptide cleavage using a TFA cleavage cocktail, the Boc group was removed releasing Nmec or Nmbu carrying peptides. The resulting deprotected peptide chain was positively charged at Nmec or Nmbu residues and showed a greatly improved solubility. Although this strategy was only used to improve the solubility of peptides during purification *via* RP-HPLC, this approach is also applicable for ligation studies with hydrophobic transmembrane peptides containing Tyr and Trp residues. After purification, the Nmec and Nmbu tags can be traceless removed from the peptide chain under basic conditions (pH ~9.5).[81, 83]

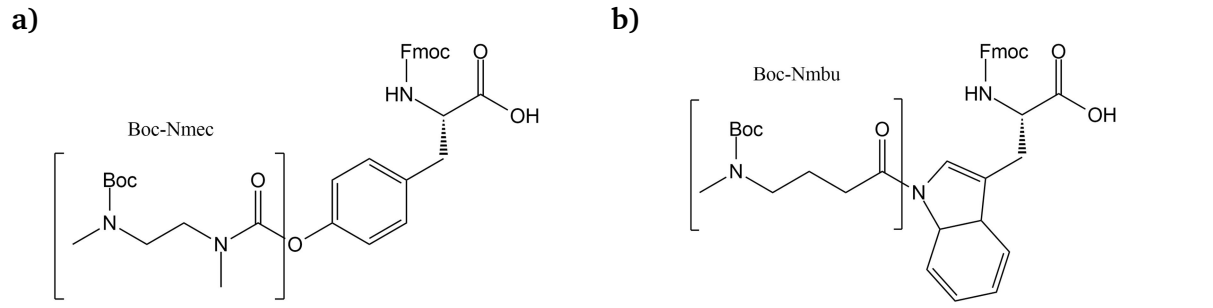

Figure 3.4: Solubility improving amino acid building blocks **a)** Fmoc-Tyr(Boc-Nmec) and **b)** Fmoc-Trp(Boc-Nmbu) suitable for Fmoc-SPPS. Boc protecting groups are removed during peptide cleavage from the solid support.[81, 83]

Despite this interesting approach, the method of Wahlström *et al*. is limited to tyrosine and tryptophan residues. However, numerous solubility improving tags were published over the last decades (table **3.3**). Most of these developed linker types and solubilizing units are compatible with Fmoc-based SPPS. For instance, Tan *et al*. used the side chains of Glu and Lys for the synthesis of glycosylated human erythropoietin (hEPO). Here, arginine subunits were attached over 6-hydroxyhexanoic acid linkers at Glu and Lys residues.[84] Huang *et al*. coupled polyarginine tags at Gln using a photo cleavable nitrobenzyl linkers for the synthesis of the autophagosomal marker protein LC3-II.[85] Maity and co-workers used the side chain of Cys to attach tri-arginine tags at Phacm (phenylactamidomethyl) linker. The strategy was applied for the NCL of the histone protein H4.[86] The Kay group coupled a combination of PEG_2 and polylysine tags at a Ddae (4,4-dimethyl-2,6-dioxocyclohexylidene-3-[2-(2-aminoethoxy) ethoxyl]-propan-1-ol) linker to modify the side chain of lysine. This method was also successfully applied for the NCL of an Ebola virus C20 peptide and the 70-residue ribosomal protein L31.[88]

In 2018, Tsuda and Yoshiya presented a polyionic tag that was composed of several lysine residues, attached on a trityl anchor.[93] This trityl-polylysine tag was able to react selectively with thiol groups and was therefore considered a promising tool to attach solubilizing tags on

cysteine residues of fully deprotected peptides. Ingeniously, this reaction could be performed in HFIP which has long been known as a superb solvent for hydrophobic membrane peptides.[94] Already in 2014, Mochizuki et al. described that tritylation of unprotected Cys-containing peptides can be efficiently achieved in neat HFIP.[95] Shortly after this invention, the advantage of this method was impressively demonstrated by the successful synthesis of a 149-amino acid capsid protein from hepatitis B.[91] However, a major drawback of this method was a very low yield after attachment of the trityl tag at cysteine. Furthermore, this trityl tag strategy was not compatible with thioester-forming rearrangement groups which produce thioester *via* O-to-S- or N-to-S-acyl shift (chapter **3.2.5**).

Solubilizing tags attached to the backbone of peptides:

A completely different approach that does not require a suitable peptide side chain is the attachment of solubility enhancing groups at a backbone of a peptide. Temporarily attached linkers along the backbone are not only anchor points for tags, but also prevent the formation of unfavorable secondary structures like β-sheets which are considered as possible reason for peptide aggregation.

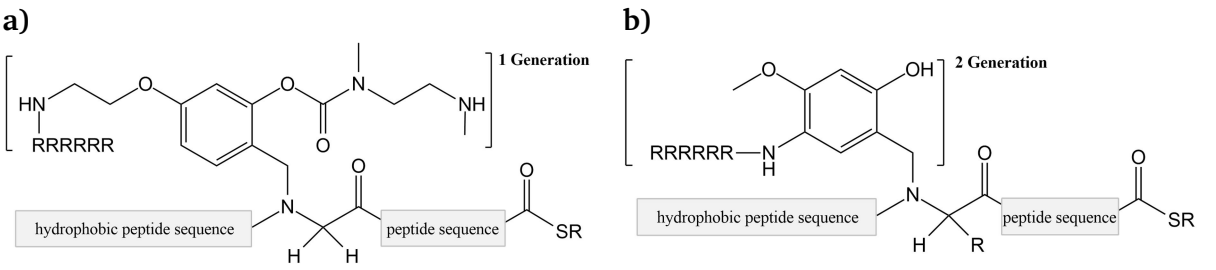

Figure 3.5: **a)** First generation of linkers for the removable backbone modification (RBM) strategy. **b)** second generation of linkers.

One of the strategies using backbone-attached solubilizing tags is the removable backbone modification (RBM) strategy developed by the Liu group. Initially, the method was invented to increase the solubility of medium-sized transmembrane proteins during NCL. The feasibility of this strategy was impressively demonstrated by the total chemical synthesis of the membrane-embedded domain of the potassium channel Kir5.1.[51]

The first generation of RBM linkers used modified glycine derivatives to attach a polyarginine tag to the backbone of hydrophobic peptides (figure **3.5a**). However, the synthesis of this glycine derivative was rather tedious. Additionally, the strategy could only be used for peptides with glycine residues in the natural sequence. These disadvantages encouraged the Liu group to develop a second generation of RBM linkers which were compatible with all natural amino acids (figure **3.5b**). This second generation of linkers was much easier to synthesize and is one of the most promising approaches for the synthesis of highly hydrophobic peptide thioesters.[74] The strategy was adopted for the total chemical synthesis of various difficult peptides using Fmoc-based SPPS and NCL.[43] One of the examples was published by Tang and co-workers who achieved the synthesis of the influenza A virus proton channel sequence AM2(1-97) using the RBM strategy.[90] Another example was reported by Zuo and Zheng who applied the second generation RBM strategy for the NCL of β-amyloid peptides which are linked to Alzheimer's disease.[87]

3.4.3. Solubilizing tags at the N-terminus

The temporary attachment of hydrophilic tags to a peptide N-terminus is another possible strategy to enhance peptide solubility. The nucleophilic character of the amino group and the low steric hindrance are two main reasons why the N-terminus is an ideal anchor point for solubility-improving tags. Since decades, this idea is used supporting the native chemical ligation or purification of poorly soluble, recombinant proteins.[75, 96] However, examples for total chemical synthesis of peptides with N-terminal attached solubilizing tags are sparely represented in the literature. One main reason for the restricted application of the N-terminal tag strategy is their limitation to the thioester fragment. Highly hydrophobic N-terminal cysteine peptides are not suitable for this method since a free N-terminus in form of cysteine is required for the ligation. Therefore, most N-terminal solubilizing tags published were used for purification purposes by preparative HPLC or affinity chromatography. Table **3.4** shows examples of N-terminal attached solubilizing tags and linkers which were developed over the last two decades.

Table 3.4: Summary of N-terminal solubilization tag strategies for poorly soluble peptides.

Peptide	SPPS	Linker	Solubility tags	Reference
PQFVQNINIENLFR	Boc	Ntl	Poly-(RGG)[a]	Robillard *et al.*, **1999** [97]
ALFCYRANGCSPKGYS	Fmoc	Canaline	KKK, RRR[b]	S. Tsuda *et al.*, **2018** [48]
Insulin A chain	Fmoc	Ddae	KKK[c]	Disotuar *et al.*, **2019** [98]

a: used for purification via HPLC.
b: used for purification and native chemical ligation.
c: disulfide ligation with B chain.

Englebretse and Robillard first described an approach by attachment of a polyarginine-di-glycine tag through a base-labile urethane linker at the peptide N-terminus. After purification, the linker was removed by treatment with a mild aqueous base. However, the method was only compatible with the Boc-based SPPS, because the prepared Ntl-linker 2-[(2-Aminoethyl)sulfonyl]ethanol was highly base-labile.[97]

Recently, Disotuar *et al.* presented a cleavable N-terminal tri-lysine tag to improve the solubility of the insulin A chain. This tag was coupled over a PEG spacer at a Ddae (4,4-dimethyl-2,6-dioxocyclohexylidene-3-[2-(2-aminoethoxy) ethoxyl]-propan-1-ol) linker. The Ddae linker could be removed using a hydrazine-based buffer at a pH of 7.5. Although this strategy was not thought to improve the solubility during NCL, this approach can be applied for hydrophobic peptide thioesters.[98]

A promising strategy for NCL-mediated synthesis of hydrophobic peptides was presented by Tsuda and colleagues who applied the non-proteinogenic amino acid canaline as an N-terminal linker between a polyarginine tag and the poorly soluble part of the sequence. In contrast to previous methods, canaline-containing peptides can be synthesised by standard Fmoc-SPPS. Interestingly, canaline can be attached at both the N-terminus and the side chain of lysine, which makes the method especially versatile. In combination with the kinetically controlled ligation (KCL), the canaline strategy can also be applied for N-to-C assembling of peptides. After ligation, the linker could be removed with a slightly acidic treatment in an ammonium acetate buffer.[48]

3.4.4. Solubilizing tags at the C-terminus

So far the most published solubilizing tag strategy for hydrophobic peptides is the attachment to the C-terminus. This approach is usually accompanied by less steric hindrance compared to backbone modification methods, thus facilitating the incorporation of solubilizing tags into the peptide sequence during the SPPS. Table **3.5** present a comprehensive selection of C-terminal solubilizing tags investigated over recent years.

Table 3.5: Summary of C-terminal solubilizing tag strategies for chemical synthesis of hydrophobic peptides.

Peptide	SPPS	Linker	Sol. tags	Reference
CP10(42-55)	Boc	glycolamide ester	tetra-arginine[a]	Alewood *et al.*, **1996** [99]
TMPs	Fmoc	4-Hmb-oxo-ester	$(GK)_n$[b]	Choma *et al.*, **1998** [100]
Vpu(2-31)	Boc	thioester	PPO_2[h]	Becker *et al.*, **2004** [78a]
ORL1(288–370)	Boc	MPA-thioester	penta-arginine[e]	Sato *et al.*, **2005** [101]
DGK, KcsA	Boc	MPA-thioester	hexa-arginine[e]	Kent *et al.*, **2007** [102]
[D83A]RNase	Boc	MPA-thioester	hexa-arginine[e]	Boerema *et al.*, **2007** [103]
HIV 1 protease	Boc	MPA-thioester	deka-arginine[e]	Johnson *et al.*, **2007** [104]
IGF1(1-70)	Boc	MPA-thioester	tetra-arginine[e]	Sohma *et al.*, **2008** [105]
Insulin glargine	Fmoc	4-Hmb-oxo-ester	penta-lysine[a]	Hossain *et al.*, **2009** [106]
NY-ESO-1	Fmoc	HMBA-oxo-ester	hexa-arginine[a]	Harr. *et al.*, **2009** [107]
mouse INSL5, B	Fmoc	4-Hmb-oxo-ester	penta-lysine[a]	Belgi *et al.*, **2011**[108]
DAGK (46-121)	Boc	MPA-thioester	hexa-arginine[e]	Lahiri *et al.*, **2011**[109]
C1q (68-134)	Boc	MPA-thioester	penta-lysine [e]	Yang *et al.*, **2013** [110]
DEN2C (21-100)	Boc	MPA-thioester	hexa-arginine[e]	Zhan *et al.*, **2013** [111]
α-Conotoxins	Fmoc	PAM-oxo-ester	tetra-lysine[a]	Peigneur *et al.*, **2014** [112]
Q11	Fmoc	Mmsb-oxo-ester	polylysine[c]	Albericio *et al.*, **2014** [113]
Aβ40	Fmoc	Amide ester	polylysine[a,d]	Wetzel *et al.*, **2014** [114]
Lactocyclicin Q	Fmoc	Dbz-amide	hexa-arginine[f]	Wang *et al.*, **2015** [41]
IFITM3	Fmoc	No linker	hepta-arginine[g]	Bode *et al.*, **2017** [115]
SUMO-2, Ub	Fmoc	Dbz-amide	hexa-arginine[f]	Brik *et al.*, **2017** [116]
BM2(1-51)	Fmoc	Hmp-thioester	penta-lysine[e]	Baumruck *et al.*, **2018** [2]
Model peptides	Fmoc	Dbz-amide	tri-arginine[e]	Tsuda *et al.*, **2018** [48]

a: used for purification via HPLC.
b: used for purification and thioether coupling.
c: used for fragment condensation.
d: removed by Carboxypeptidase B (CPB).
e: used to improve the solubility of the C-terminal thioester peptide for NCL.
f: used to improve the solubility of the N-terminal Cys peptide during NCL.
g: used to improve the solubility of the N-terminal peptide for KAHA ligation.
h: used to improve the solubility of the N-terminal peptide for oxime ligation.

The C-terminal tag strategy was first described in 1996 by Englebretsen and Alewood who coupled a poly-glycine-arginine tag to a base labile glycolamide ester.[99] However, this approach was only compatible with Boc-based SPPS and was used to dissolve peptides for purification by preparative RP-HPLC. Two years later, Choma and Englebretsen published a Fmoc-SPPS compatible strategy using 4-Hmb (4-hydroxymethyl benzoic acid) oxo-ester as a linker. This approach was additionally applied for the coupling of two transmembrane protein segments by thioether ligation.[100] Over the course of time oxo-ester linkers were applied in combination with polyarginine or polylysine tags to improve handling and purification of poorly soluble peptides such as Q11,[113] insulin glargine[106] or NY-ESO-1.[107b]

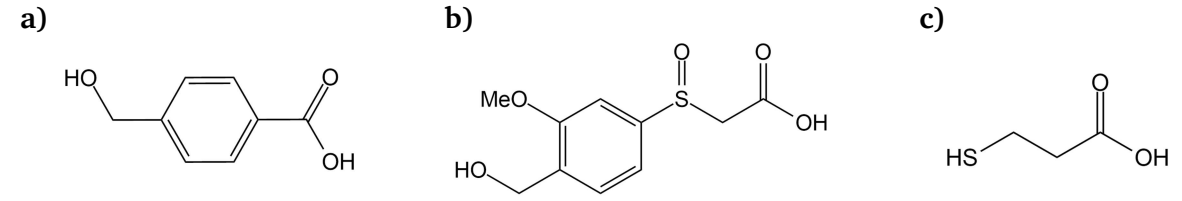

Figure 3.6: **a)** 4-(Hydroxymethyl)benzoic acid (4-Hmb) linker by Englebretsen, **b)** 2-Methoxy-4-methylsulfinylbenzyl alcohol (Mmsb) linker by Albericio,[80] **c)** 3-Mercaptopropionic acid (3-MPA) linker by Sato and Aimoto.[101]

In 2004, Becker *et al*. suggested the use of a PPO (polyethylene glycol-polyamide) auxiliary in the thioester moiety to improve the solubility of the HIV (human immunodeficiency virus) protein sequence Vpu(2-31). The strategy was used to couple the Vpu (viral protein u) domain to a small peptide template *via* oxime ligation.[78a] In the same year, Sato and co-workers proposed a similar approach for the NCL of the hydrophobic transmembrane peptide ORL1 (opioid receptor like 1). The strategy relied on a good soluble penta-arginine tag with 3-MPA (3-mercaptopropionic acid) as a linker.[101] In the following years this idea was adopted by several groups for the synthesis of different poorly soluble peptides such as KcsA,[102] IGF1(1-70),[105] DAGK(46-121)[109] and DEN2C(21-100).[111] However, the main drawback of this method was the need of Boc chemistry for the synthesis of the thioester segment.

Fmoc-based synthetic routes for the synthesis of peptide thioesters with C-terminal solubility tags are barely reported in the literature. One main reason is that thioesters are base-labile during the Fmoc-deprotection step. Less basic deprotection agents as described by Wade *et al*.[30] or Guo and co-workers[31], allow only the synthesis of short thioester peptides. The most promising approach so far is the Dbz or MeDbz strategy by Blanco-Canosa and Dawson (chapter **3.2.4**).[40] Indeed, this approach was used to improve the solubility of hydrophobic peptides during the ligation of lactocyclicin Q,[41] SUMO-2 or ubiquitin(1-93).[116] Nevertheless, the Dbz linker is prone to inactivation and uncontrollable side reactions through over-acetylation. Capping steps using acetic anhydride should also be avoided which makes it difficult to obtain clean products for longer sequences. Furthermore, an additional activation step must be introduced for the synthesis of Dbz peptides using toxic chemicals such as 4-nitrophenylchloroformate.[40b] Another but more convenient Fmoc-SPPS compatible strategy for the synthesis of thioester peptides with C-terminal solubility tags is the usage of thioester-forming rearrangement groups such as Hmp or α-methylcysteine (chapter **3.2.5**). In contrast to Dbz- or MeDbz-peptides are Hmp-peptides compatible with capping steps and independent from activation steps with toxic chemicals. Surprisingly, this strategy has never been widely used in the peptide chemistry community so far.

3.5. External conditions as solubilization strategies

3.5.1. Detergents and organic solvents as additives for NCL

Conventional ligation buffers like urea or guanidinium chloride based solutions with good water soluble compounds such as disodium phosphate, TCEP and MPAA are unfortunately only applicable for the ligation of soluble peptide fragments. Hydrophobic or poorly water soluble peptides precipitate under these conditions. For this reason, solubility-improving additives were searched or developed for decades.

The solubility of hydrophobic peptides during ligation can be enhanced by the addition of detergents or organic solvents.[74] Multiple short to medium-size peptides have been successfully ligated in the presence of detergents or bilayer forming surfactants.[117] Fujii and co-workers introduced the lipid bilayer-assisted NCL of membrane-embedded chemokine receptors (CXCR4) in the presence of 1-palmitoyl-2-oleoylphosphatidylcholine (POPC) or sodium dodecyl sulfate (SDS).[118] Kochendoerfer and colleges used 1-monooleoyl-rac-glycerol (MO) bilayers to ligate transmembrane domains of bacteriorhodopsin (*Halobacterium salinarium*) [119] and Becker *et al.* applied dodecylphosphocholine (DPC) or octylglycoside (OG) as solubilizing detergents for the ligation of *Escherichia coli* diacylglycerol kinase (DAGK).[109] Despite this success, detergents and surfactants often led to problems during purification *via* RP-HPLC which is a disadvantage of these methods.

A further method is the addition of organic solvents such as dimethylformamide (DMF), dimethyl sulfoxide (DMSO) or N-methyl-2-pyrrolidone (NMP) to the ligation buffer. This approach was deeply investigated by Dittmann and co-workers.[120] Especially the usage of DMF as an organic ligation media was used for NCL of transmembrane peptides such as small chromopeptides or even the entire sensory rhodopsin II/transducer complex containing two transmembrane helices.[120-121] Of particular importance is the use of fluorine-containing organic solvents or ionic liquids as potential additive in phosphate buffers. Both strategies will be presented and discussed in the following sections.

3.5.2. Fluorinated alcohols as co-solvents

The use of fluorinated alcohols as powerful solvents for the synthesis of organic compounds (e.g. imidazoles, quinolones, Hantzsch esters etc.) has been discussed for a long time.[122] Soon after their first descriptions as superior solvents, they also found applications in peptide synthesis. Especially trifluoroethanol (TFE) and hexafluoroisopropanol (HFIP) attracted much attention as effective media for both solution phase[123] and solid phase peptide synthesis of difficult or poorly soluble peptides.[124] Both solvents also gained wide use in the field of peptide analysis.[125] Several NMR- and CD-studies were able to demonstrate that TFE promote the formation of secondary structures (α-helices, β-sheets) in proteins.[126] Urry *et al.* concluded that fluorine-containing solvents mimic the natural environment of membrane proteins.[126b] Molecular dynamic simulations, by Roccatano *et al.* suggest that these structure-stabilizing effects are induced by the accumulation of TFE molecules around the peptide chain. This TFE layer represents a dielectric environment in which intramolecular peptide hydrogen bonds are favored.[127] Competing hydrophobic interactions in contrast were considered as rather low, so that stabilizing effects of secondary structures were preferred.[128]

In 1988, Narita and Obana conducted profound solubility experiments with poorly soluble model peptides in a variety of different organic solvents. They found that HFIP has the highest solubilizing potential for hydrophobic peptides followed by HMPA and DMSO.[129] Today, multiple studies describe TFE or HFIP as highly effective co-solvents for the ligation of transmembrane peptides. DeGrado *et al.*[130] as well as Mei Hong *et al.*[131] used TFE containing phosphate buffers for the ligation of the M2 proton channel of influenza A. Liu *et al.* investigated HFIP as an potent additive for the chemical ligation of membrane proteins and hydrophobic antibiotics such as trifolitoxin.[94] In contrast to other solvent improving additives such as SDS, DMF or DMSO, fluorinated alcohols possess a low boiling point and minor viscosity which allows simple peptide purification by preparative RP-HPLC.

Although fluorinated alcohols like HFIP and TFE are known to promote or accelerate some organic reactions, possible peptide modifications have not been reported so far.[132] Nevertheless, in combination with TCEP, MPAA or urea are TFE or HFIP-induced peptide modifications possible.[2] Until now, ligation experiments with Hmp-peptides in TFE or HFIP containing phosphate buffers were never investigated. Especially interesting is therefore the effect of fluorinated alcohols on the ligation yield of Hmp-peptides.

An alternative approach to the addition of fluorinated alcohols to conventional ligation buffers is the use of ionic liquids (ILs) as ligation media. Ionic liquids gathered much attention in recent years due to their unique solvent properties for peptides. The following section will discuss the advantages and disadvantages of ILs as additives or ligation media for hydrophobic peptides.

3.5.3. Ionic liquids as co-solvents

During recent decades, interest in more environmentally friendly solvents has increased tremendously. Promising alternative solvents are ionic liquids (ILs), which can be considered as organic salts with melting points near room temperature.[133] Although ILs were known for over a century, very little research on their unique properties were performed for a long period of time.[134] Nevertheless, ILs provide countless advantages over more traditional organic solvents such as negligible vapour pressure, high thermal stability and low flammability.[135] Additionally, ILs offer the possibility to tailor their physical and chemical properties for the purpose of interest primarily by structural modifications of the cation or by exchange of the anion. Since several years, ILs attract more attention in the scientific community as solvents for classical organic reactions such as the Knoevenagel condensation[136], Robinson annulation[137] or Diels-Alder reactions.[138] The great number of possible applications and different ILs led to an explosion of publications in this area.[134, 139]

Especially interesting is the application of ILs as media for biomolecules such as DNA,[140] RNA,[141] enzymes[142] and proteins.[143] Some ILs simultaneously show excellent solvation properties for hydrophilic and hydrophobic biomolecules which is primarily useful for hydrophobic peptides and proteins. In particular imidazolium-based ionic liquids such as 1-ethyl-3-methylimidazolium acetate ([C_2mim][OAc]) seem to be a favourable reaction media for hydrophobic proteins like conotoxins or transmembrane peptides.[144] Different studies underline the structure stabilizing effects of imidazolium cations to the native protein structure.[145] Although the underlying molecular interactions are not fully understood so far, it is thought that imidazolium cations minimize the formation of non-native protein isoforms

and stabilize the energetic ground state of secondary and tertiary structures.[146] Additionally, imidazolium based ionic liquids supply optimal conditions for the oxidation of cysteine residues in the presence of air.[144b, 147] In several studies Tietze, Imhof and co-workers demonstrated that [C_2mim][OAc] is a highly efficient, biocompatible media for the oxidative folding of cysteine-rich conopeptides. The newly developed method showed multiple advantages over conventional buffer solutions such as a reduced reaction time, no need for redox-active reagents and an increase in peptide concentration by three orders of magnitude.[144, 148]

Another possible application for ILs is their usage as ligation media for poorly soluble peptides such as transmembrane domains of ion or proton channels. Thioester hydrolysis in aqueous ligation buffers is the most important side reaction of the NCL. A reduction of the water content by addition of ILs is one possible approach to increase the final ligation yield. Due to their special solvent properties, ionic liquids are particularly promising as media for membrane associated peptides. Already in 2010, Braga *et al*. showed that organic thioesters are stable in the imidazolium based ionic liquid 1-butyl-3-methylimidazolium hexafluorophosphate (BMIM-PF_6). However, they never examined the liquid as a media for ligation experiments.[149] In the following years, the usage of ionic liquids as solvents for NCL has been reported several times.[135, 150] In 2012, Imhof and colleagues tested a variety of different imidazolium based ionic liquids for the NCL of tridegin, a 66-mer peptide inhibitor of the coagulation factor XIIIa. This study demonstrated that acetate is the most effective anion for NCLs in imidazolium based ionic liquids.[151] Two years later, Kühl *et al*. investigated the influence of different C-terminal amino acids by NCL of multiple model peptides in [C_2mim][OAc].[152] For these studies C-terminal 3-mercaptopropionate thioester were applied which could be obtained on 4-sulfamylbutyryl resins using the safety catch linker strategy by Ingenito and co-workers (chapter **3.2.3**).[36] However, these ligation studies were accompanied by severe side reactions involving alkylation, cyclisation and disulfide formation of the cysteine residue.[152] Some publications reported the existence of N-heterocyclic carbenes in [C_2mim][OAc].[153] Nevertheless, carbene involved peptide modifications caused by ILs were never investigated thoroughly. Of particular interest are these investigations for ligation studies with thioester forming rearrangement groups such as SEA or Hmp peptides, since the thiol group must be unprotected during the ligation.

3.5.4. Carbene formation in imidazolium based ILs

Already in 1964, NMR studies by Olofson and co-workers gave the first pieces of evidence that positively charged, heterocyclic compounds such as 1,3-dimethylimidazolium iodide react like carbenes.[154] Three decades later Arduengo and Kline confirmed these observations by the isolation and characterisation of the first kinetic and thermodynamic stable imidazolium-based carbene.[155] In the following years, multiple studies proved that imidazolium-based ionic liquids such as [C_2mim][OAc] contain traces of highly reactive N-heterocyclic carbenes (NHCs).[155-156] In 2010, Nyulaszi and colleagues found that the amount of NHCs formation in ILs is dependent on the strength of the basic anion.[157]

Different chemical reactions were applied as indirect indicators for the existence of NHCs in [C_2mim][OAc]. Aggarwal and Mereu observed unexpected side reactions of imidazolium-based ionic liquids with aldehydes.[158] Cooks and co-workers achieved the first experimental

measurements of the proton affinity of N-heterocyclic carbenes in the gas phase[159] and Gurau *et al*. were able to identify the [C_2mim][$H(OAc)_2$][C_2mim^+-COO^-] complex after chemisorption of carbon dioxide in concentrated [C_2mim][OAc]. Moreover, the authors reported on the fast release of carbon dioxide after the addition of water, leading to the formation of [C_2mim][HCO_3].[160]

Sulfur and sulfur-containing amino acids like cysteine seem to be especially sensitive towards NHC-related modifications in [C_2mim][OAc]. Previous studies by Rodriguez *et al*. were able to detect 1-ethyl-3-methylimidazole-2-thione as a reaction product of neat [C_2mim][OAc] with elemental sulfur.[161] Although [C_2mim][OAc] was frequently described as a superior solvent for hydrophobic, cysteine-rich peptides, possible carbene related modifications of the peptide chain have never been investigated thoroughly. Such unpredictable side reactions can severely limit the application of ionic liquids as possible ligation media.

3.6. Post-ligation methods: Desulfurization and Acm deprotection

The selective desulfurization of cysteine provides the possibility to ligate peptides and proteins next to an alanine residue. Since alanine is a common amino acid in proteins, this strategy allows access to sequences without naturally occurring cysteine residues. The first description of protein desulfurization was made in 1951 by Cooley and Wood who applied Raney nickel catalysts for the desulfurization of casein and albumin.[162] However, this method was not restricted to cysteine alone, it also showed heavy amounts of methionine desulfurization. Twenty years later, Cheng *et al*. tested various temperatures and pH conditions to determine the mildest conditions for a specific cysteine desulfurization. These efforts led to the first selective desulfurization of the proteins hemoglobin, lysozyme and α-lactalbumin.[163] Since then the usage of Raney nickel was for a long time the only reliable method for a selective desulfurization of cysteine in proteins. In 2001, Yan and Dawson achieved a breakthrough by the combination of NCL and cysteine desulfurization. This study expanded the NCL-desulfurization strategy by the introduction of Pd/Al_2O_3 catalysts.[164]

However, the selective desulfurization of the ligation site in the presence of multiple free thiol groups was a major problem at that time. This was solved by Pentelute and Kent who introduced the acetaminomethyl (Acm) group for the protection of multiple cysteine residues within the peptide chain. In this study, Raney nickel induced conversion of cysteine to alanine could be successfully applied for the total chemical synthesis of the peptide hormone amylin and the small trypsin inhibitor protein EETI-II.[165] These pioneering works encouraged several groups to extend the NCL-desulfurization strategy to other desulfurization agents and amino acid surrogates.[166] Meanwhile the “alanine ligation” strategy has been expanded to the usage of unnatural β- or γ-mercapto amino acids derivatives, which enable the NCL at almost each amino acid.[167] A significant step was also made by the development of the metal-free, radical-based desulfurization which is described in the following section and was a basis of the strategy development within this thesis.

3.6.1. Metal-free desulfurization of peptides

The metal-related desulfurization using Ni or Pd catalysts is often associated with low yields of peptide recovery. The large surface of the sponged metal catalyst frequently leads to adsorption and aggregation of denatured peptides. In addition unexpected modifications such as hydrogenation of tryptophan or demethylthiolization of methionine have been observed.[164] A major disadvantage is also the instability of the thiazolidine (Thz) protecting group during the metal-related desulfurization, which is frequently applied for N-terminal protection during multiple segment ligations.[168]

In 1956, F. Hoffmann *et al.* reported on desulfurization of organic mercaptans using trialkylphophites under thermal or photochemical conditions.[169] Later, this work was continued by C. Walling and co-workers who initiated the reaction by catalytic amounts of azobisisobutyronitrile (AIBN).[170] Four decades later A. González and G. Valencia were the first who proposed the specific desulfurization of cysteine and cysteine derivatives in peptides and proteins by means of photochemical initiated desulfurization with triethylphosphite. However, this study was only conducted with simple amino acids and allowed no deeper conclusions about possible side reactions or peptide modifications.[171] This was changed in 2007 by Q. Wan and S. Danishefsky who introduced the first selective free-radical desulfurization of glycopolypeptides in the presence of TCEP, the radical initiator 2,2'-azobis[2-(2-imidazolin-2-yl)propane] dihydrochloride (VA-044) and a free thiol as a proton donator (scheme **3.10**).[172]

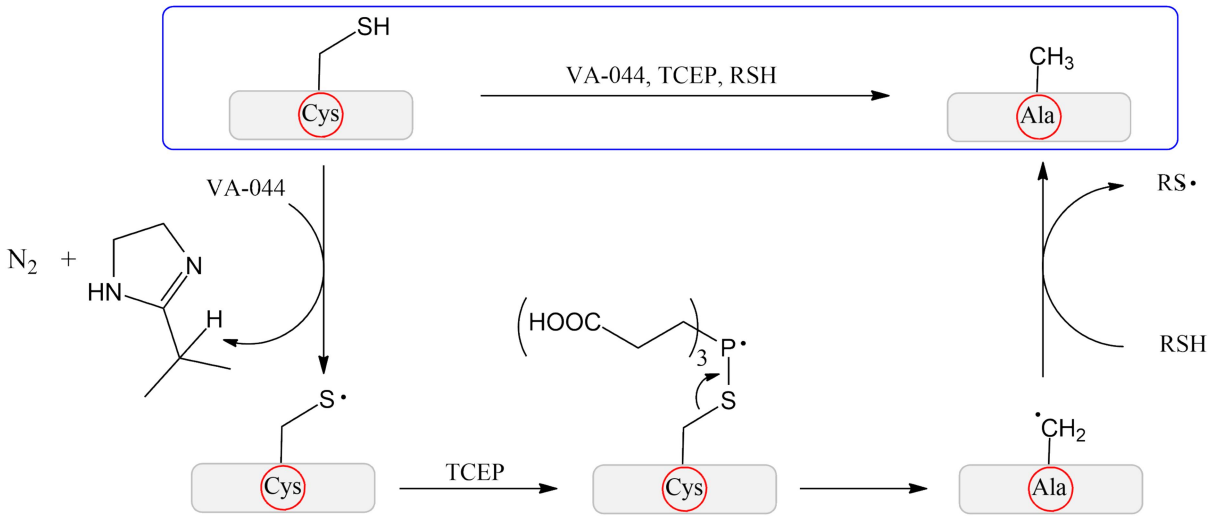

Scheme 3.10: Proposed reaction mechanism of the radical-based desulfurization of cysteine using TCEP and the radical initiator VA-044.

The reaction is compatible with conditions used for the native chemical ligation and can be performed as a one-pot ligation and desulfurization procedure.[173] Today, the free radical-based desulfurization by Danishefsky is one of the easiest and most efficient strategies to convert cysteine or other unnatural mercapto amino acids into their desulfurated counterparts. This radical-based desulfurization relies on the reaction of the thiol group with trisubstituted organic phosphines. In the presence of a radical initiator, the thiol function of cysteine is deprotonated under formation of the thiyl radical. This radical intermediate reacts

with TCEP to create a phosphoranyl radical which is decomposed in the further course of the reaction, creating an alkyl radical. The final alanine residue is created after abstraction of a hydrogen atom from a proton donating thiol compound such as glutathione. This hydrogen exchange creates a new thiyl radical which can restart the radical cycle or react with another thiyl radical.[168, 174] In combination with the native chemical ligation this desulfurization strategy was chosen for the synthesis of multiple proteins.[175]

Very recently, the P-B desulfurization method was reported from the X. Li group who described TCEP activation by boron compounds (e.g. $NaBH_4$, $LiEt_3BH$) as a particularly mild alternative to the metal-based or radical-initiated desulfurization. In contrast to the radical initiation, the P-B desulfurization proceeds *via* a ylide like phosphine–borane complex. Possible radical based side reactions like the cleavage of sensible photochemical amino acid derivatives could be prevented by this approach. In addition, the authors describe this strategy as a reliable and robust method with high yields. So far this method has been successfully applied for the synthesis of ubiquitin, γ-synuclein, and histone H2A.[176] Due to solubility problems, desulfurization of hydrophobic transmembrane peptides using the mentioned above methods is frequently incomplete or even impossible, which clearly represents an urgent need for the development of desulfurization strategies for highly hydrophobic peptides.

3.6.2. Cleavage of the Acm-protection group

The sulfhydryl function of cysteine is by far the most reactive group within the sequence of native proteins. In nature, thiol groups play a crucial role for maintaining the active conformation of proteins over disulfide bonds or as a splicing site for inteins.[177] From the chemical point of view, cysteine represents a possible ligation site for the native chemical ligation.[20a] The high reactivity of cysteine makes the search for reliable and efficient protecting groups necessary. A protecting group that has gained particular importance alongside the trityl and MeBzl[178] group is the acetaminomethyl (Acm) group. Since its first description Acm-protected cysteine has been used multiple times for the total chemical synthesis of medium-sized proteins by NCL and desulfurisation.[179]

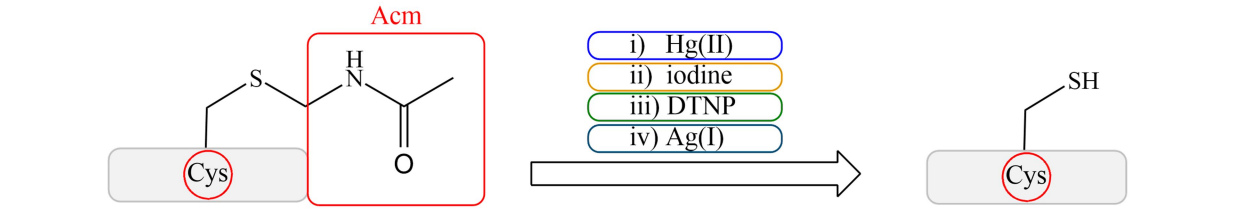

Figure 3.7: Acm deprotection of peptides by different deprotection agents described in literature.

In general Acm is stable under basic, acidic or reductive conditions which allow its use for Fmoc- and Boc-chemistry as well as a protecting group for reductive desulfurizations. Challenging is the mild removal of Acm in the presence of an unprotected peptide chain with a variety of functional groups. Over the course of time several deprotection strategies for Acm have been published. The first removal strategy was proposed by Veber and co-workers using mercury (Hg) ions under release of H_2S.[180] Nevertheless, due to the high toxicity of mercury, this method is rather unpopular. Another strategy relies on the oxidative removal of Acm by

elemental iodine. This method is particularly useful for Acm removal of two adjacent Acm protected cysteine residues resulting in disulfide formation.[181] However, some sources describe Acm deprotection with iodine also for peptides with only one Acm protected thiol group within the peptide sequence.[182] Other strategies, that were investigated thoroughly, involve the usage of sulfur containing organic compounds such as 2-pyridine sulfenyl chloride[183] or 2,2′-dithiobis(5-nitropyridine) (DTNP).[184] However, most of these methods suffer from unexpected side reactions and peptide modifications.

The most practical method is the usage of silver salts such as silver tetrafluoroborate ($AgBF_4$)[185] or silver acetate (AgOAc).[186] Fujii and colleges discovered that especially silver trifluoromethanesulfonate (AgOTf) in the presence of 2% anisole, dissolved in concentrated TFA, is one of the most efficient mixtures for Acm cleavage.[187] Since then, AgOTf mediated Acm cleavage has been used in multiple publications after NCL and cysteine desulfurization.[188]

3.7. The influenza B proton channel sequence BM2(1-51)

Every year more than 3-5 million people worldwide suffer from an infection with influenza A, B or C with 250.000-500.000 deaths.[189] The consistently high number of new infections and yearly death toll surpasses even the cases of breast cancer-related deaths in the united states and places influenza in the top ten causes of premature death.[190] Despite the existence of vaccines, patients who suffer from immunodeficiency or show allergies against vaccine components are unsuitable for immunization. The investigation and development of antiviral drugs for a complementary therapy is therefore an essential aim of medical research. As potential target for antiviral drug treatment M2 proton channels were identified which belong to the smallest known *bona fide* ion channels with exceptionally high ion selectivity.[191] M2 proton channels are embedded in the virus particle membrane and function as pH gated proton channels. At the beginning of the infection the virus particle enters the cell by receptor-mediated endocytosis. The low pH in the endosome causes a selective transport of protons through the M2 channel pore that increases the pH in the virus capsule.[192] This acidification leads to dissociation of the matrix protein 1 (M1) from the ribonucleoprotein (RNP) allowing the release of viral ribonucleoproteins (vRNPs) into the cytoplasm of the host cell. This process is essential to the replication of all influenza virus subtypes.[193]

It is thought that over 20% of all influenza infections in recent years are related to the influenza B variant.[194] While some antiviral drugs like M2 proton channel inhibitors (e.g. amantadine, rimantadine) are available for the influenza A treatment, no effective M2 inhibitors for influenza B exist.[195] Several groups investigated structural properties of BM2 to understand the function of the proton channel.[189a, 190, 196] BM2 is a 109 amino acid long, left-handed, integral type III protein which is embedded as a homotetramer in the membrane of the virus capsid. The coiled-coil arrangement of the four TM domains form a stable channel pore by itself, which conducts protons highly selectively and unidirectionally from the N- to the C-terminus.[197] The BM2 proton channel of influenza B is functional similar to its influenza A counterpart but shares only 24% sequence homology with AM2.[195] Despite the minor sequence homology between BM2 and AM2, both channel variants possess the important HXXXW sequence motif. In BM2 this motif is located inside the channel pore including the residues His19 and Trp23 (figure **3.8**).[4]

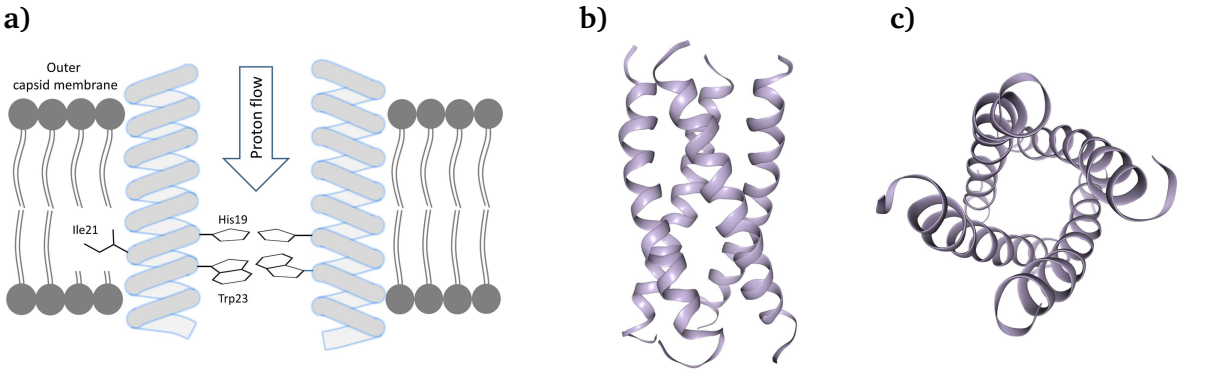

Figure 3.8: **a)** HXXXW motif (His19, Trp23) within the open BM2 channel pore. Amino acid Ile21 in the WT is directed to the hydrophobic membrane. **b)** BM2 homotetramer side view.[B] **c)** BM2 channel pore formed by the stable arrangement of the four TM domains.[B]

Mutation studies in which one of these amino acids are replaced proved that both amino acids are essential for the function of the channel.[198] In recent years, further important core-lining residues were identified by NMR studies in lipid bilayers. Mei Hong and co-workers were able to investigate the proton conduction and hydration of the BM2 channel pore. They also provided further evidence for the contribution of His27 to the proton-dissociation rate of His19, which regulates the channel activity.[196a] As a result the pKa value of His19 in BM2 is significant lower than that of His37 in AM2. Based on multiscale computer simulations, Zheng *et al*. even proposed the existence of a second, reversed WxxxH motif within the BM2 channel pore due to the interaction of His29 and Trp23.[189a] In addition, the channel interior of BM2 is also lined with a number of polar residues which accelerate the proton flux rate across the channel pore. It is thought that several Ser, Gln and Asn residues create a hydrophilic pathway that relays protons to the WxxxH gating element. In fact, mutation studies of one of these polar residues showed significantly decreases in channel activity.[4, 197]

WT BM2(1-109)

Rndm. α-helical TMD Rndm. unknown helical

10 20 30 40 50

MLEPFQILSI CSFILSALHF LAWTIGHLNQ IKRGINMKIR IKGPNKETIN

60 70 80 90 100

REVSILRHSY QKEIQAKETM KEVLSNNMEI LSDHIIIEGL SAEEIIKMGE

109

TVLEIEELH

Figure 3.9: Peptide sequence of the 109 amino acid long influenza B M2 proton channel (PDB database: 2KIX). The dark letters show the peptide sequence BM2(1-51) which was synthesized during this thesis.[4, 195]

Previous studies obtained BM2 by expression in *Escherichia coli* or *Xenopus oocytes* fused with a polyhistidine or glutathione S-transferase tag (GST).[199] Very recently, Mei Hong *et al*. expressed uniformly ^{13}C- and ^{15}N-labelled His_6-TEV-BM2(1-51) for NMR studies in POPC/POPG bilayers. This domain was chosen since BM2(1-51) includes the proton conduction channel pore as well as the cytoplasmic section for membrane targeting.[195] They found that residues 6-28 form a well-ordered α-helix, which represent the trans membrane domain (TMD) of the BM2 channel, while residues 1-5 and 29-35 showed chemical shifts of a random coil.[195] However, residues 36-44 remained structurally unknown.

4. Motivation and Aims of the Thesis

The total chemical synthesis of membrane-associated peptides and medium-sized proteins offers many advantages over alternative strategies, such as protein expression. Synthetic peptides can be synthesised faster, customized depending on the purpose of research or isotopically labelled (e.g. ^{13}C, ^{15}N).[2] Moreover, the combination of SPPS and NCL is by far the shortest and fastest route to obtain the peptide of interest in a multi-milligram scale. Although preparation of good water soluble proteins by NCL is a routine procedure, chemical synthesis of medium-sized, hydrophobic peptides is often accompanied by poor solubility, aggregation and inefficient ligation yields.[200] Synthetic access by "classical" ligation strategies is usually limited due to solubility problems of hydrophobic peptide fragments in the ligation buffer.

An especially important class of hydrophobic peptides and proteins include membrane proteins which make up more than 23% of the human proteome.[201] Today, membrane proteins are targets for more than 60% of all available pharmaceutical drugs as they are involved in essential biochemical processes inside and outside of the cell membrane.[201a, 202] In the past, structure-based drug design with the help of membrane proteins led to the development of new and improved pharmaceutical ingredient as for G protein-coupled receptors (GPCRs)[203], proton channels[204], voltage gated-ion channels[205] and many more.[206] Reliable synthetic routes for transmembrane peptides, which allow the production of hydrophobic peptides in multi-milligram amounts, are therefore essential for the molecular characterisation and function studies of transmembrane peptides. Over the last decades, the development of new synthetic approaches for hydrophobic peptides and transmembrane proteins turned into a "booming" field in modern peptide chemistry (chapter **3.3**).

This thesis is focused on the development of an oxo-ester based ligation strategy, employing internal modifications and external conditions, in order to facilitate chemical production of highly hydrophobic peptides and protein domains at a multi-milligram scale. For that purpose, temporary solubilizing tags (internal modifications) and the addition of fluorinated alcohols or ionic liquids (external conditions) were studied and discussed. The results of these experiments represented within this thesis contribute and enable the structural and functional characterizations of transmembrane proteins (TMP), interaction studies of TMPs potential drug leads or development of membrane-based bio-inspired materials.

Overall, the following five aims can be formulated and represent the content of this thesis (Figure **4.1**):

(i) Development of a novel strategy for the synthesis of transmembrane peptides by combination of oxo-ester Hmp-peptides and C-terminal solubilizing tags;

(ii) Exploration of the NCL based on the strategy developed in part (i) and comparison of a set of removable solubilizing tags;

(iii) Exploration of NCL based on the strategy developed in part (i) in terms of variation of ligation media: application of fluorinated alcohols as additives;

(iv) Exploration of NCL based on the strategy developed in part (i) in terms of variation of ligation media: application of ionic liquid [C_2mim][OAc] as ligation media;

(v) Development of novel follow-up protocols: desulfurization and Acm-group cleavage.

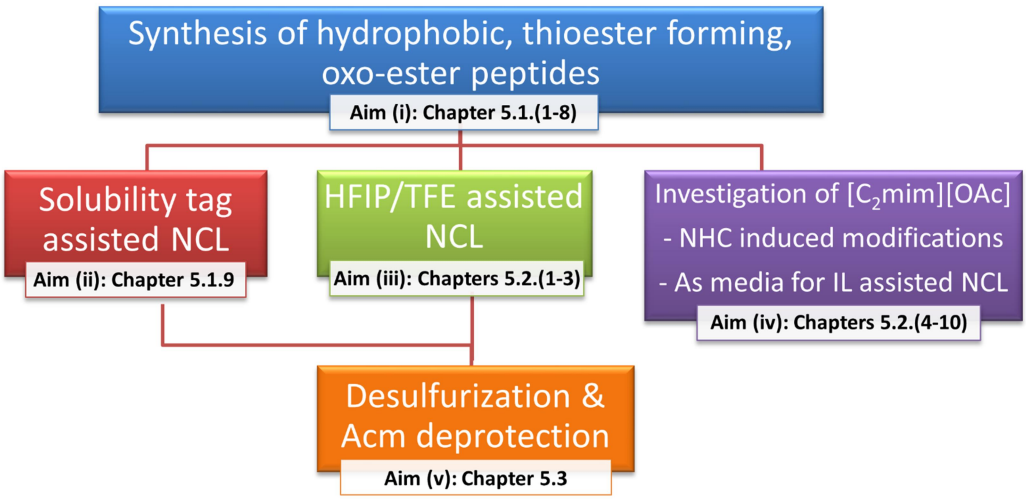

Figure 4.1: Schematic representation of thesis aims.

A peptide of interest which represents a promising drug target and gathered much attention in recent years is the influenza virus B protein BM2, especially its fragment BM2(1-51), since it includes part of the sequence which is not yet structurally characterized. Various attempts have been undertaken to chemically synthesize the BM2(1-51) sequence at once,[3] however, all attempts failed. These circumstances make BM2(1-51) an ideal model system for the development of a new production strategy for highly hydrophobic peptides. The ligation strategy developed during this thesis was used for the synthesis of the final target peptides [Leu^{10}]BM2(1-51) and [Leu^{21}]BM2(1-51) which are presented in table **4.1**.

Synthesized variants of BM2(1-51)

[Leu^{21}]BM2(1-51)	MLEPFQILSI CSFILSALHF **L**AWTIGHLNQ IKRGINMKIR IKGPNKETIN R
[Leu^{10}]BM2(1-51)	MLEPFQILS**L** CSFILSALHF IAWTIGHLNQ IKRGINMKIR IKGPNKETIN R

Table 4.1: Sequences of [Leu^{21}]BM2(1-51) and [Leu^{10}]BM2(1-51) which represent the final target peptides of this thesis.

The synthesized peptide variants [Leu^{10}]BM2(1-51) and [Leu^{21}]BM2(1-51) can be applied for structural investigations of the BM2 proton channel sequence of influenza B. Analysis by circular dichroism (CD) spectroscopy can be used to determine the alpha-helical content within the BM2(1-51) sequence. Since some sections of BM2(1-51) are still structural uncharacterised, these studies contribute to the structural elucidation of this promising drug target.

5. Results and Discussion

5.1. Investigation of internal modifications

5.1.1. Synthesis of 2-Hydroxy-3-(triphenylmethyl)thio-propanoic acid

In recent decades the thioester-forming rearrangement group Hmp was proposed several times for the synthesis of C-terminal, thioester-forming, oxo-ester peptides.[62] Already P. Botti *et al.*[61] and F. Liu[60] *et al.* were able to demonstrate that Hmp-peptides can serve as precursors for the production of peptide thioesters. However, no commercial access and comparatively high hydrolysis rates limited the interest in Hmp-peptides within the scientific community. In order to facilitate the access to Hmp, an economically useful route for synthesis was investigated during this thesis. As most valuable economically route, the strategy by K. Wisniewski was adopted and modified in the course of this work (chapter **3.2.5**). In the two-step strategy by K. Wisniewski trityl-protected Hmp(Trt) was produced by oxidation of (R)-3-chloro-1,2-propanediole to (R)-3-chloro-2-hydroxypropanoic acid using 68% nitric acid followed by substitution of the chlorine leaving group with triphenylmethyl thiol (scheme **3.7c**). In the literature enantiopure (L)-Hmp(Trt) was obtained with an overall yield of 58%.[63] However, the use of the enantiopure precursor (R)-3-chloro-1, 2-propanediole is expensive compared to the use of inexpensive, racemic 3-chloro-1, 2-propanediole as a precursor.

During this thesis a protocol for the production of racemic, trityl-protected Hmp was developed based on the previous work of K. Wisniewski *et al.* (chapter **9.1**). As a result an improved protocol was created which allowed the production of racemic Hmp(Trt) with an overall yield of 66%. The cheaper precursor 3-chloro-1, 2-propanediole and the higher yield are the main advantages of the newly developed protocol which represent an economically more valuable synthetic route for the production of trityl-protected Hmp.

After synthesis following protocols **9.1.1** and **9.1.2**, the final Hmp(Trt) building block was obtained as a white powdered solid which could be applied using a standard coupling procedure by Fmoc-based SPPS. The structure and purity of racemic Hmp(Trt) was confirmed by NMR spectroscopy and LC-MS. In Figure **5.1** the LC-MS of the synthesized Hmp(Trt) building block is depicted. The chromatogram shows one main product peak at 12.9 min. Mass spectra of the retention time between 12.72 – 13.17 min shows the negative charged molecular ion peak of $[Hmp(Trt)\text{-}O^-]^-$ at 362.9 m/z and the negatively charged fragmentation product $[Trt\text{-}S^-]^-$ at 275.2 m/z.

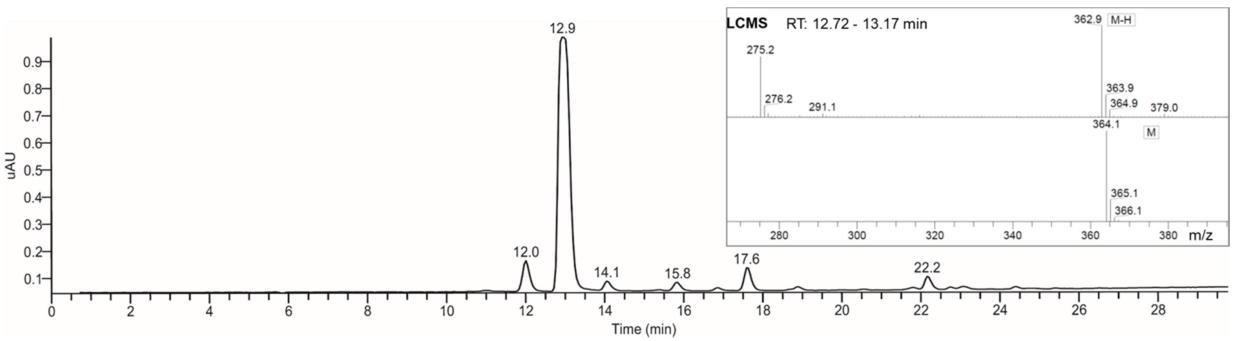

Figure 5.1: LC-MS measurement of the racemic Hmp building block. Liquid chromatography was performed at 220 nm wavelength. The main peak at 12.9 min belongs to Hmp(Trt).

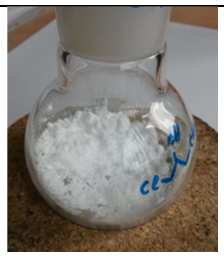

Intermediate 3-Chloro-2-hydroxypropanoic acid

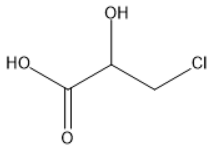

Structure of intermediate
3-Chloro-2-hydroxypropanoic acid

2-Hydroxy-3-(triphenylmethyl)thio-propanoic acid

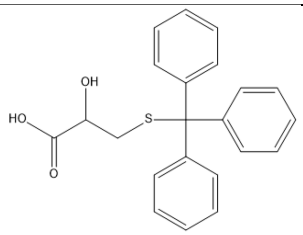

Structure of the final product 2-Hydroxy-3-(triphenylmethyl)thio-propanoic acid (Hmp(Trt))

Figure 5.2: Pictures and chemical structures of the synthesized intermediate 3-chloro-2-hydroxypropanoic acid (upper picture) and the final product 2-Hydroxy-3-(triphenylmethyl)thio-propanoic acid (lower picture).

a) ^{1}H-NMR in DMSO-D6

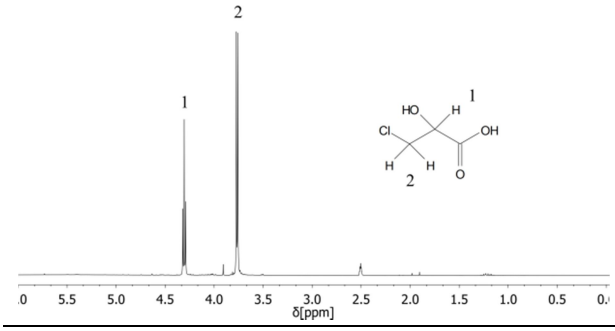

b) ^{13}C-NMR in DMSO-D6

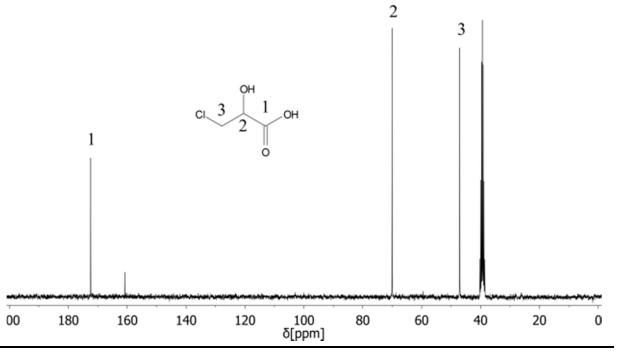

Figure 5.3: 3-Chloro-2-hydroxypropanoic acid in DMSO-D6 at 300 MHz, **a)** ^{1}H-NMR (DMSO, 300 MHz, 300 K): δ (ppm) = 4.32 – 4.29 (t, 2H), 3.77 – 3.76 (d, 1H) 2.52 and **b)** ^{13}C-NMR (DMSO, 300 MHz, 300 K): δ = 172.40, 70.05, 47.08, 39.95 – 38.84.

a) ^{1}H-NMR in $CDCl_3$

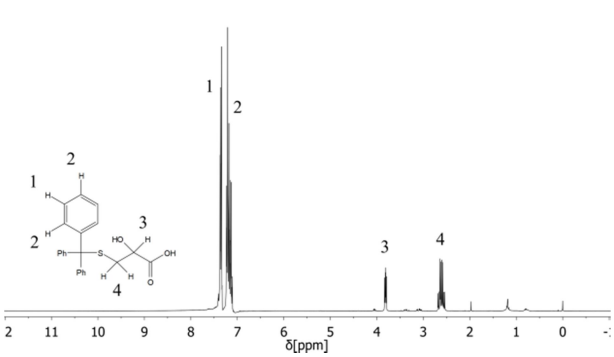

b) ^{13}C-NMR in $CDCl_3$

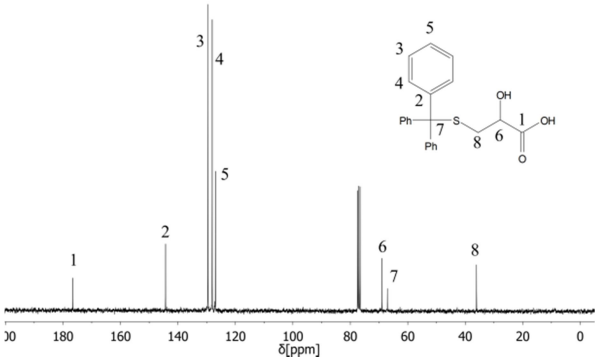

Figure 5.4: 2-Hydroxy-3-(triphenylmethyl)thio-propanoic acid in $CDCl_3$ at 500 MHz, **a)** ^{1}H-NMR ($CDCl_3$, 500 MHz, 300 K): δ (ppm) = 2.63 (2H, CH_2^{β}), 3.81 (1H, CH^{α}), 7.12-7.38 (15H, Trt) and **b)** ^{13}C-NMR ($CDCl_3$, 500 MHz, 300 K): δ (ppm) = 36.10 (CH_2^{β}), 67.05 (Ph_3, CH^{α}), 68.96, 126.92, 127.16, 128.06, 129.54, 144.32 (phenyl).

5.1.2. Investigation of the stereochemistry of Hmp-peptides

The production of stereochemically pure peptides is one of the most important issues in chemical peptide synthesis. While peptide expression in bacteria or yeasts usually lead to stereochemically pure L-amino acid composed peptides, chemical peptide synthesis can cause racemisation of amino acid residues. To reduce those unwanted side reactions, additives like HOAt (1-hydroxy-7-azabenzotriazol) are commonly utilized for Fmoc-SPPS.

However, peptides synthesised under novel coupling conditions or with different coupling reactants such as DEAD and PPh_3 need to be investigated for their stereochemistry. For this reason, two peptide variants Phe-(L-Leu)-Hmp and Phe-(D-Leu)-Hmp were synthesized according to instruction **9.2**. Since Hmp(Trt) was obtained and used as a racemic mixture, two peaks for each of both peptide variants were expected in the chromatogram (figure **5.6**). The first amino acids L-Leu or D-Leu, respectively, were coupled by the Mitsunobu reaction using the method of Liu *et al.*[60] In order to evaluate the amount of racemization, both peptides were analysed by RP-HPLC and ESI mass spectrometry. The figures below show the structures and stereochemistry of the expected model peptides.

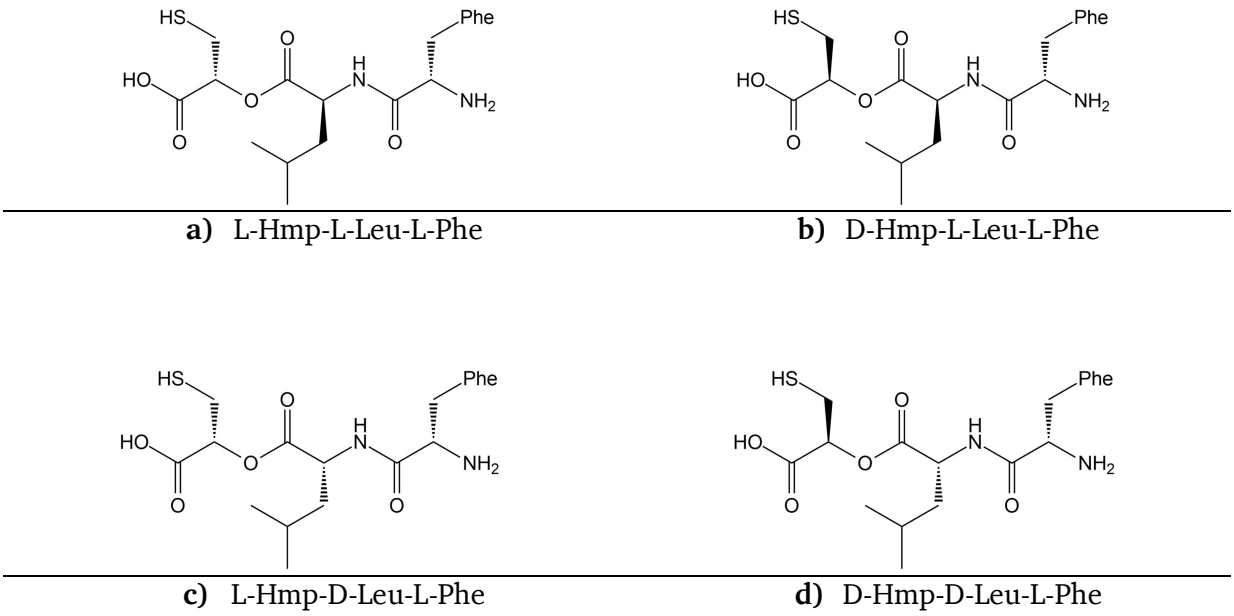

a) L-Hmp-L-Leu-L-Phe **b)** D-Hmp-L-Leu-L-Phe

c) L-Hmp-D-Leu-L-Phe **d)** D-Hmp-D-Leu-L-Phe

Figure 5.5: Structures of obtained peptide diastereomers with three stereogenic centers.

All four peptide variants **a)**, **b)**, **c)** and **d)** are diastereomers with three different stereocenters. These diastereomers have the same molecular weight but different retention times in the chromatogram. In Figure **5.6** the chromatograms of Hmp-L-Leu-Phe and Hmp-D-Leu-Phe are compared. Both upper chromatograms show two peaks with different retention times. Although all diastereomers differ only in stereochemistry, retention times with differences of more than 1 min can be observed. This experiment impressively shows the effect of stereochemistry on the RP-HPLC results. Even more important is that no racemisation products can be observed in the chromatogram which makes the used coupling conditions practical for the synthesis of Hmp-peptides.

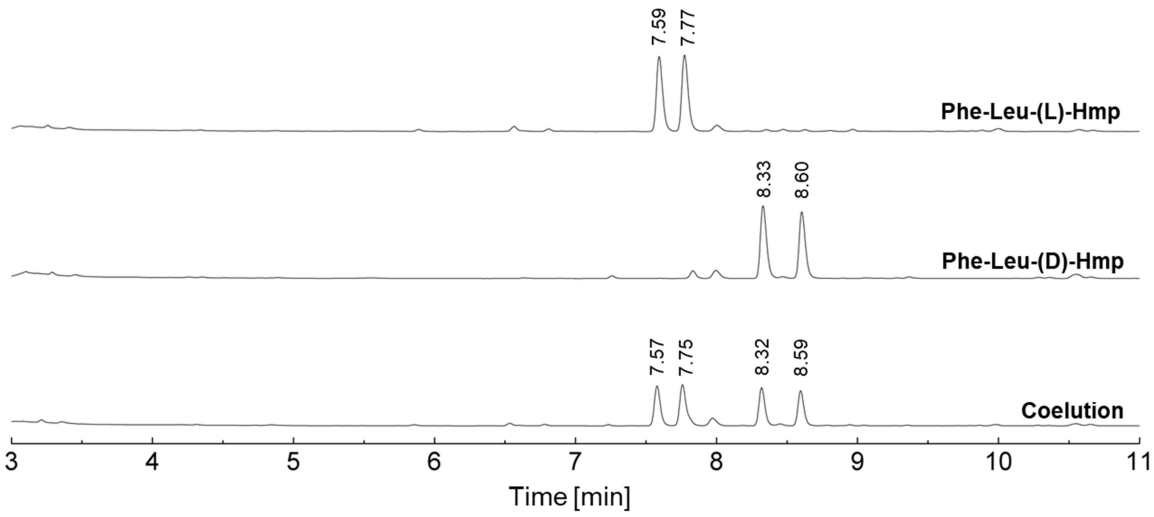

Figure 5.6: Stacked RP-HPLC chromatograms of dipeptides L-Phe-L-Leu-Hmp (upper chromatogram) and L-Phe-D-Leu-Hmp (middle chromatogram). The lower chromatogram displays the coelution of both peptides. RP-HPLC conditions: C18 column (150 x 4 mm, 100 Å pore diameter, 3 µm particle size), gradient 0 – 80% acetonitrile in 15 min, flow rate 1 ml/min.

ESI-MS results of both peptide variants Phe-(L)-Leu-Hmp and Phe-(D)-Leu-Hmp have the same isotopic pattern and molecular weight of 382.18 m/z. The experimental isotopic pattern of both diastereomers is in perfect line with the simulated isotopic pattern (figure **5.7**).

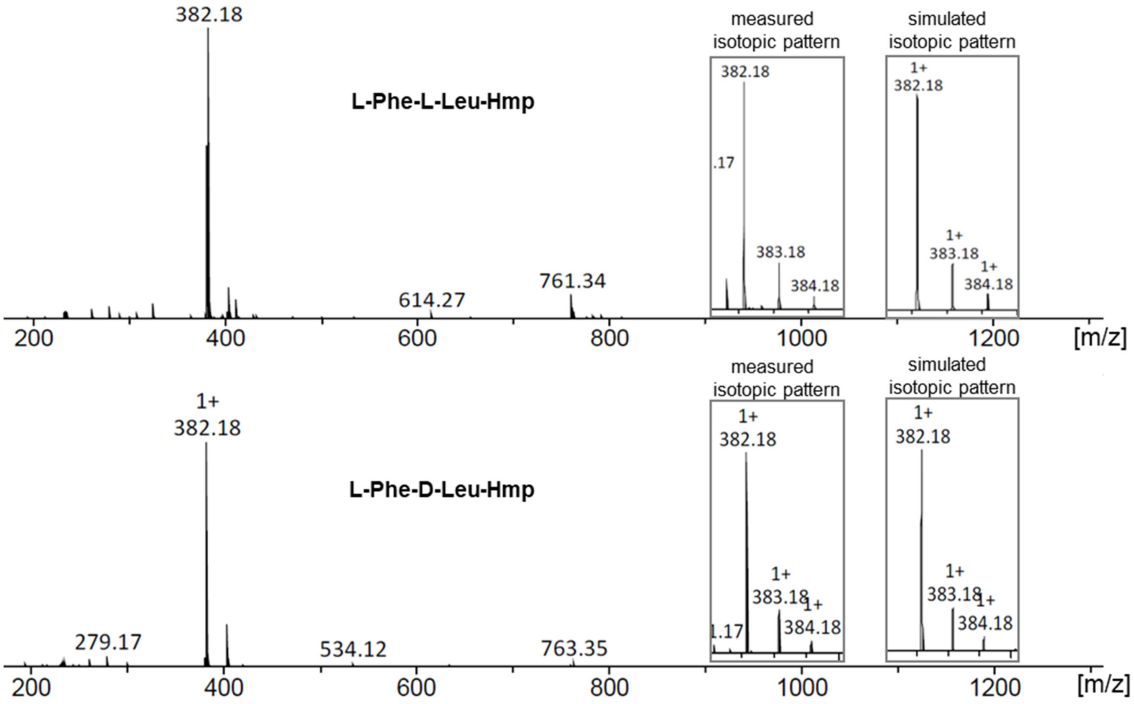

Figure 5.7: ESI-MS of model peptides L-Phe-L-Leu-Hmp (upper spectrum) and L-Phe-D-Leu-Hmp (lower spectrum).

5.1.3. Overview of the synthesised peptides

As mentioned in chapter **4**, the influenza virus B protein was chosen as a model system for this thesis mainly because of its important role in the multiplication cycle of influenza B. The hydrophobic character makes BM2(1-51) to an ideal model peptide for the development of new synthetic strategies for transmembrane peptides. This chapter is focused on the development of efficient synthetic routes for transmembrane peptides by combination of oxo-ester Hmp-peptides, as thioester-forming precursors, in combination with C-terminal solubilizing tags. In order to test this strategy, short model Hmp-peptides were synthesised by Fmoc-based SPPS. As a model sequence the first five amino acids of the BM2 ligation site were chosen.

The following tables provide an overview of the N-terminal cysteine peptides (table **5.1**), the model Hmp-peptides (table **5.2**) and the complete Hmp-peptide fragments (table **5.3**) which were synthesised during this thesis.

Table 5.1: Synthesized N-terminal Cys peptides, *(a)* monoisotopic molecular mass and *(b)* average molecular mass.

No.	N-terminal Cys Peptides	Formula	M_W[Da][a]	M_W[Da][b]
P1	[Cys^{22}]BM2(22-35)	$C_{73}H_{120}N_{24}O_{17}S$	1636.96	1637.95
P2	[Cys^{22}]BM2(22-51)	$C_{154}H_{264}N_{52}O_{39}S_2$	3529.97	3532.20
P3	[Cys^{11}]BM2(11-51)	$C_{214}H_{353}N_{65}O_{52}S_2$	4729.64	4732.64

Table 5.2: Synthesized model Hmp-peptides, *(a)* monoisotopic molecular mass and *(b)* average molecular mass.

No.	BM2 Model Hmp-Peptides	Formula	M_W[Da][a]	M_W[Da][b]
P4	[Ile^{21}]BM2(17-21)-Hmp	$C_{33}H_{50}N_8O_7S$	702.36	702.86
P5	[Ile^{21}]BM2(17-21)-Hmp-ADO	$C_{39}H_{61}N_9O_{10}S$	847.43	848.02
P6	[Ile^{21}]BM2(17-21)-Hmp-ADO_2	$C_{45}H_{72}N_{10}O_{13}S$	992.5	993.18
P7	[Leu^{21}]BM2(17-21)-Hmp	$C_{33}H_{50}N_8O_7S$	702.36	702.86
P8	[Leu^{21}]BM2(17-21)-Hmp-ADO	$C_{39}H_{61}N_9O_{10}S$	847.43	848.02
P9	[Leu^{21}]BM2(17-21)-Hmp-ADO_2	$C_{45}H_{72}N_{10}O_{13}S$	992.5	993.18
P10	[Leu^{21}]BM2(17-21)-Hmp-Lys_5	$C_{63}H_{109}N_{17}O_{13}S$	1343.81	1344.71
P11	[Leu^{21}]BM2(17-21)-Hmp-ADO-Lys_5	$C_{69}H_{122}N_{19}O_{15}S$	1488.91	1489.89
P12	[Leu^{21}]BM2(17-21)-Hmp-ADO_2-Lys_5	$C_{75}H_{131}N_{19}O_{19}S$	1633.959	1635.02
P13	[Leu^{21}]BM2(17-21)-Hmp-Arg_5	$C_{63}H_{109}N_{27}O_{13}S$	1483.842	1484.78
P14	[Leu^{21}]BM2(17-21)-Hmp-ADO-Arg_5	$C_{69}H_{120}N_{28}O_{16}S$	1628.916	1629.93
P15	[Leu^{21}]BM2(17-21)-Hmp-ADO_2-Arg_5	$C_{75}H_{131}N_{29}O_{19}S$	1773.99	1775.09

Table 5.3: Complete Hmp-peptide fragments of BM2, *(a)* monoisotopic mass and *(b)* average mass.

No.	Complete BM2 Hmp-Peptide Fragments	Formula	M_W[Da][a]	M_W[Da][b]
P16	[Leu^{10}]BM2(1-10)-Hmp	$C_{59}H_{96}N_{12}O_{16}S_2$	1292.65	1293.59
P17	[Ile^{21}]BM2(1-21)	$C_{116}H_{181}N_{25}O_{27}S_2$	2420.30	2421.96
P18	[$Cys(Acm)^{11}$]BM2(1-21)-Hmp	$C_{122}H_{190}N_{26}O_{30}S_3$	2595.33	2597.17
P19	[$Cys(Acm)^{11}$]BM2(1-21)-Hmp-ADO_2	$C_{134}H_{212}N_{28}O_{36}S_3$	2885.47	2887.48
P20	[$Cys(Acm)^{11}$]BM2(1-21)-Hmp -ADO-Lys_5	$C_{158}H_{261}N_{37}O_{38}S_3$	3380.88	3383.19

5.1.4. Synthesis of N-terminal Cys-peptides

The N-terminal cysteine peptides **P1** [Cys^{22}]BM2(22-35), **P2** [Cys^{22}]BM2(22-51) and **P3** [Cys^{11}]BM2(11-51) were synthesized by automated, microwave-assisted Fmoc-based SPPS according to instruction **9.3**. The synthesis of **P1** and **P2** succeeded by a standard Fmoc-SPPS coupling cycle while additional washing steps were necessary to obtain the 41-mer peptide **P3** (appendix **15.1.4**).[207] The purification of the crude peptides was performed *via* preparative RP-HPLC following instruction **8.1.7**. All N-terminal cysteine peptides were analysed by analytical RP-HPLC and mass spectrometry. For peptides **P1** and **P2**, MALDI-TOF-MS was used while peptide **P3** was identified by ESI-MS. All products showed the correct molecular weight and isotopic pattern which were in line with the simulated patterns. Analytical RP-HPLCs displayed clean products with one main peak at 7.89 min (**P1**), 8.18 min (**P2**) and 14.60 min (**P3**), respectively. The yields of the peptides are summarized in table **5.4**.

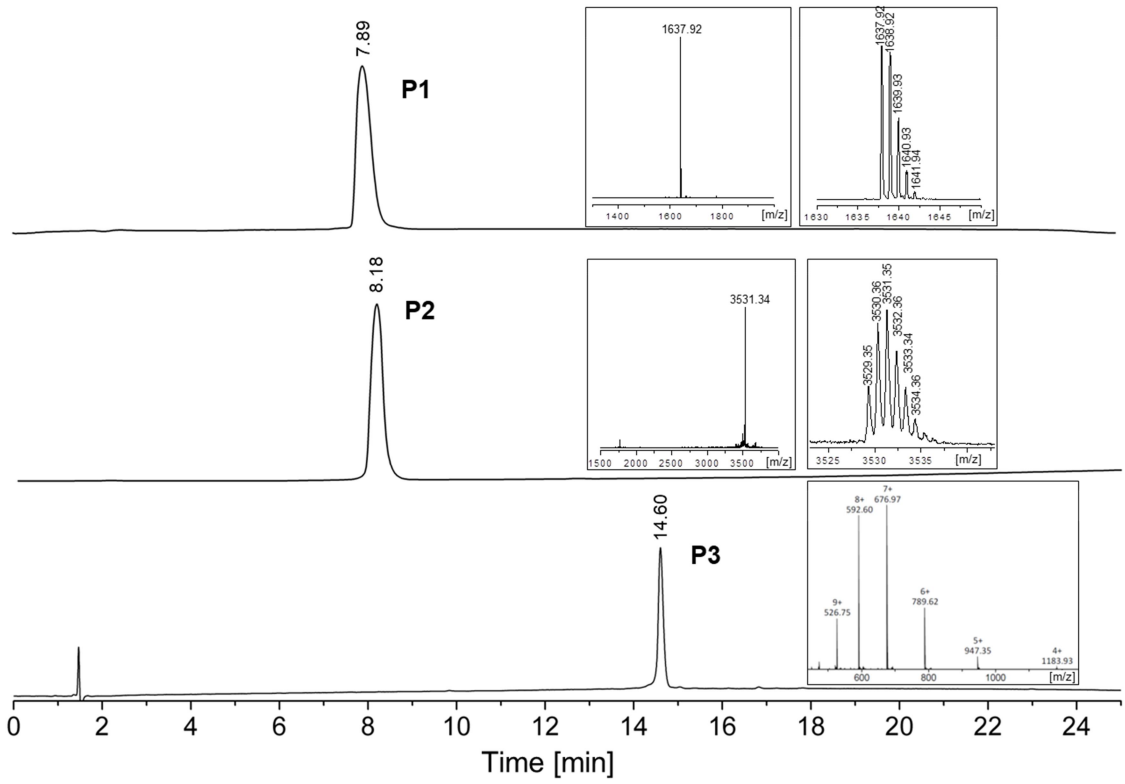

Figure 5.8: Analytical RP-HPLC of N-terminal cysteine peptides. **P1** [Cys^{22}]BM2(22-35), C18 column (150 x 4 mm, 100 Å pore diameter, 3 µm particle size), gradient 20 - 80% acetonitrile in 20 min, flow rate 1 ml/min. **P2** [Cys^{22}]BM2(22-51), C18 column (150 x 4 mm, 100 Å pore diameter, 3 µm particle size), gradient 20 - 40%, flow rate 1 ml/min. **P3** [Cys^{11}]BM2(11-51), C4 column (125 x 4 mm, 300 Å pore diameter, 5 µm particle size), gradient 20 - 95% acetonitrile in 30, flow rate 1 ml/min.

Table 5.4: Results of N-terminal cysteine peptides **P1**, **P2** and **P3**.

Entry	Peptide	Found [m/z]	Crude	Purified	Yield
P1	[Cys^{22}]BM2(22-35)	1637.92^{1+}	192 mg	85.2 mg	26.0%
P2	[Cys^{22}]BM2(22-51)	3529.35^{1+}	528 mg	40.7 mg	6.2%
P3	[Cys^{11}]BM2(11-51)	676.67^{7+}	478.6 mg	63.4 mg	5.3%

5.1.5. Synthesis of model Hmp-peptides

The first three isoleucine carrying model Hmp-peptides **P4** [Ile^{21}]BM2(17-21)-Hmp, **P5** [Ile^{21}]BM2(17-21)-Hmp-ADO and **P6** [Ile^{21}]BM2(17-21)-Hmp-ADO$_2$ were synthesized by manual Fmoc-SPPS according to procedure **9.2**. In this first study, the most efficient coupling and Fmoc-deprotection conditions were tested based on previous experiments by F. Liu and co-workers.[60] While Hmp(Trt) could be easily coupled using a standard Fmoc-based protocol, the coupling of the next amino acid at Hmp(Trt) turned out to be decisive step for the production of Hmp-peptides. The first tested coupling method described by F. Liu *et al.* relied on the Steglich esterification of the amino acid at the Hmp(Trt) moiety.[60] However, the coupling of Fmoc-Ile-OH was not possible and completely failed. A second more efficient coupling protocol by the F. Liu group relied on the Mitsunobu reaction between Fmoc-Ile-OH and the Hmp(Trt) moiety.[60, 208] However, this single coupling protocol resulted in only 34% loading capacity of isoleucine on the resin support.[60] The most efficient procedure, a double coupling protocol developed during this thesis, resulted in much higher loading capacities of over 60% for all tested amino acids (protocol **9.2**). All following amino acids in the peptide sequence were coupled by standard Fmoc-based SPPS conditions. The final peptides were cleaved from the resin support by a standard TFA cleavage protocol. Figure **5.9** shows the RP-HPLC chromatograms of crude peptides **P4**, **P5** and **P6** where both diastereomers can be observed as a result of the use of racemic Hmp as discussed in chapter **5.1.2**.

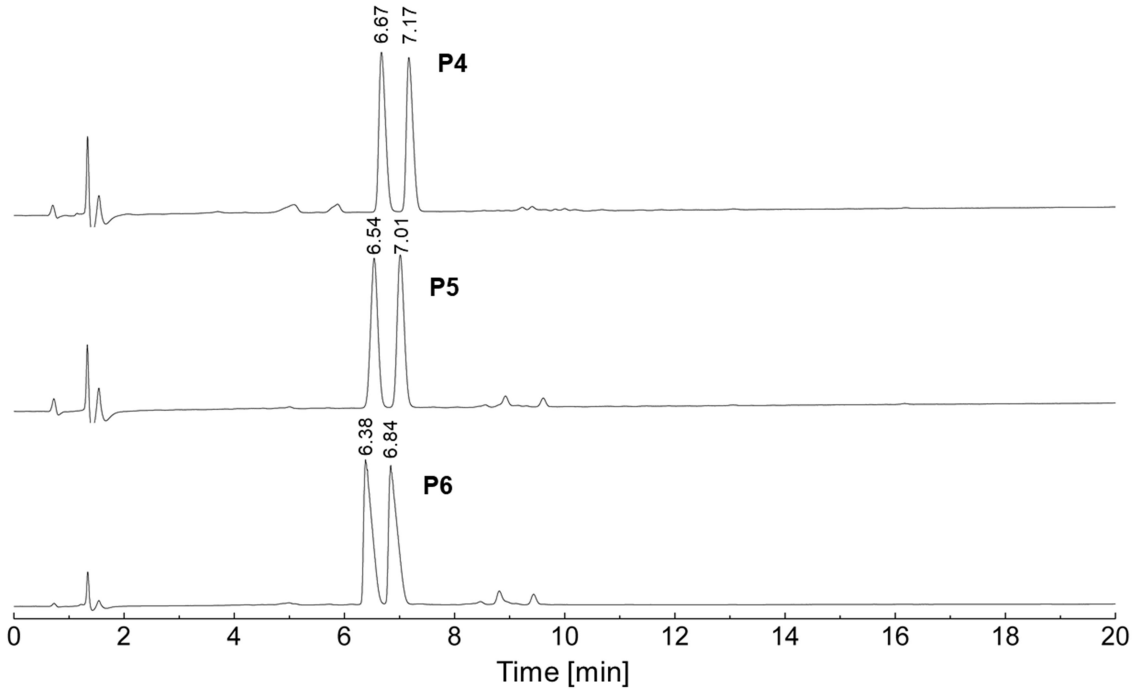

Figure 5.9: Analytical RP-HPLC of crude peptides **P4**, **P5** and **P6**. HPLC conditions: C18 column (150 x 3.9 mm, 100 Å pore diameter, 5 µm particle size), gradient 20 – 50% acetonitrile in 20 min, flow rate 1 ml/min.

Table 5.5: Results of model Hmp-peptides **P4**, **P5** and **P6**.

Entry	Peptide	Theo. [m/z]	Found [m/z]	Crude	Yield
P4	[Ile^{21}]BM2(17-21)-Hmp	352.18^{2+}	352.19^{2+}	11.0 mg	19.3%
P5	[Ile^{21}]BM2(17-21)-Hmp-ADO	424.72^{2+}	424.72^{2+}	14.0 mg	73.6%
P6	[Ile^{21}]BM2(17-21)-Hmp-ADO$_2$	497.26^{2+}	497.26^{2+}	11.2 mg	50.2%

To confirm the presence of diastereomers, the model peptide **P4** was investigated by LC-MS. Both peaks in the chromatogram showed the same molecular weight and isotopic pattern in the mass spectra (figure **5.10**).

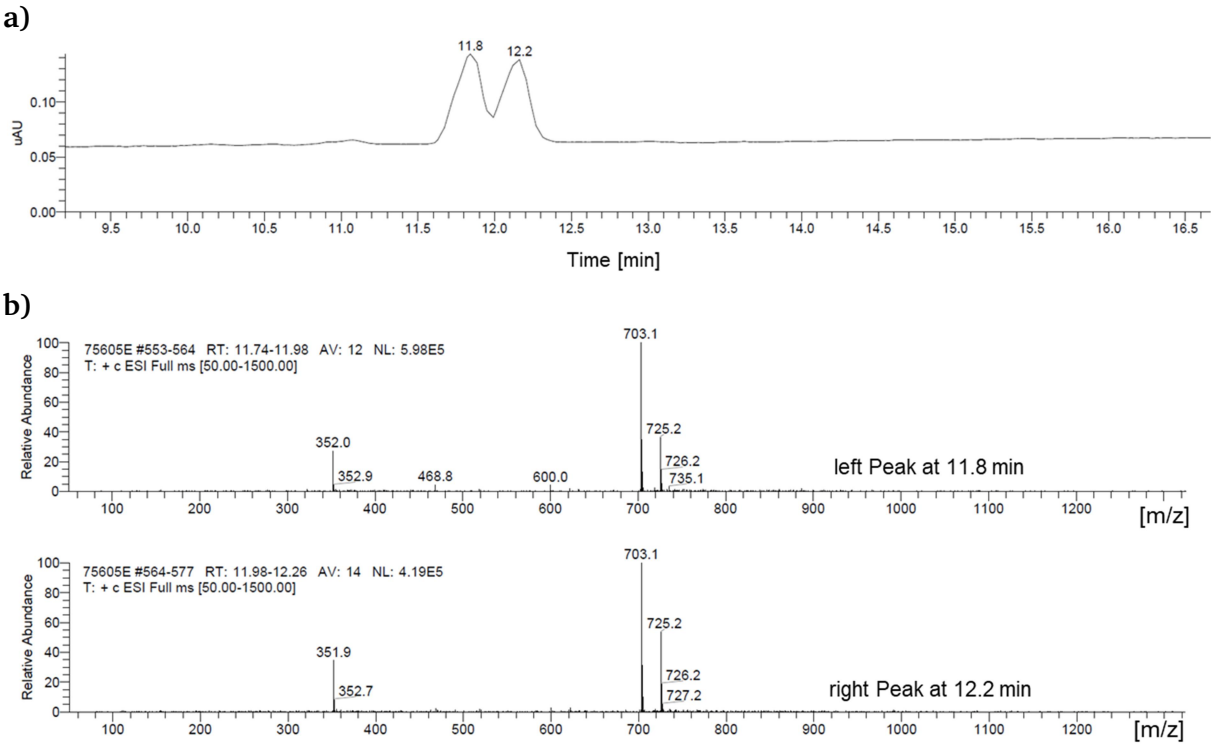

Figure 5.10: **a)** LC-MS of crude peptide **P4**. RP-HPLC conditions: C8 column (150 x 4.6 mm, 5 µm particle size), gradient 20 - 80% acetonitrile in 25 min, flow rate of 0.5 ml/min, **b)** MS of the separated diastereomers. The upper spectrum shows the retention time at 11.8 min. The lower mass spectrum shows the retention time of 12.2 min. Both peaks have the same isotopic pattern.

Since Hmp is a trifunctional linker, peptides with temporarily attached solubilizing tags can be produced. This approach was investigated with the attachment of 8-(9-Fluorenylmethyloxycarbonyl-amino)-3,6-dioxaoctanoic acid (ADO) and ADO_2 tags at the Hmp moiety. The ADO chain is composed of alternating carbon and oxygen units which can interact with polar protic solvents. This interaction is thought to increase the solubility of hydrophobic peptides. Due to minor interactions with the stationary phase of the column, retention times to a faster elution can be observed in RP-HPLC if ADO units are attached at the C-terminus (figure **5.9**). The shorter retention times of model peptides **P5** and **P6** indicate a minor change of the hydrophobicity compared to the non-ADO carrying peptide **P4**. This result showed that the ADO tag can not only be used to increase the distance between the ligation site and the solubilizing tag, ADO units can also be applied directly as solubility-enhancing tags for short hydrophobic peptide sequences. In combination with polyionic tags such as polylysine or polyarginine, ADO represents an efficient solubility-improving spacer.

While the synthesis of the Ile-carrying peptides **P4**, **P5** and **P6** succeeded with the newly developed double coupling protocol by the Mitsunobu reaction, the C-terminal isoleucine moiety represented a potential obstacle for subsequent ligation experiments. It is long known that some amino acids such as Ile at the C-terminal ligation site significantly influence the ligation efficiency. Already Liu *et al.* were able to demonstrate that ligation yields at

C-terminal Ile moieties dramatically drop.[60] For this reason, amino acid Ile21 was mutated to Leu21 for the production of the three leucine carrying model peptides **P7** [Leu^{21}]BM2(17-21)-Hmp, **P8** [Leu^{21}]BM2(17-21)-Hmp-ADO and **P9** [Leu^{21}]BM2(17-21)-Hmp-ADO$_2$. Similar to previous experiments two diastereomers could be detected in each chromatogram of all three peptide variants. Again, ADO carrying peptides **P8** and **P9** displayed shorter retention times in HPLC. However, the peak area of the first peak decreased with raising length of the ADO spacer. Analysis *via* ESI-MS revealed the same isotopic pattern for each diastereomer. All three crude peptides showed only small amounts of impurities in the chromatogram. Due to their high purity, model peptides **P7**, **P8** and **P9** were directly used for the following ligation experiments without further purification.

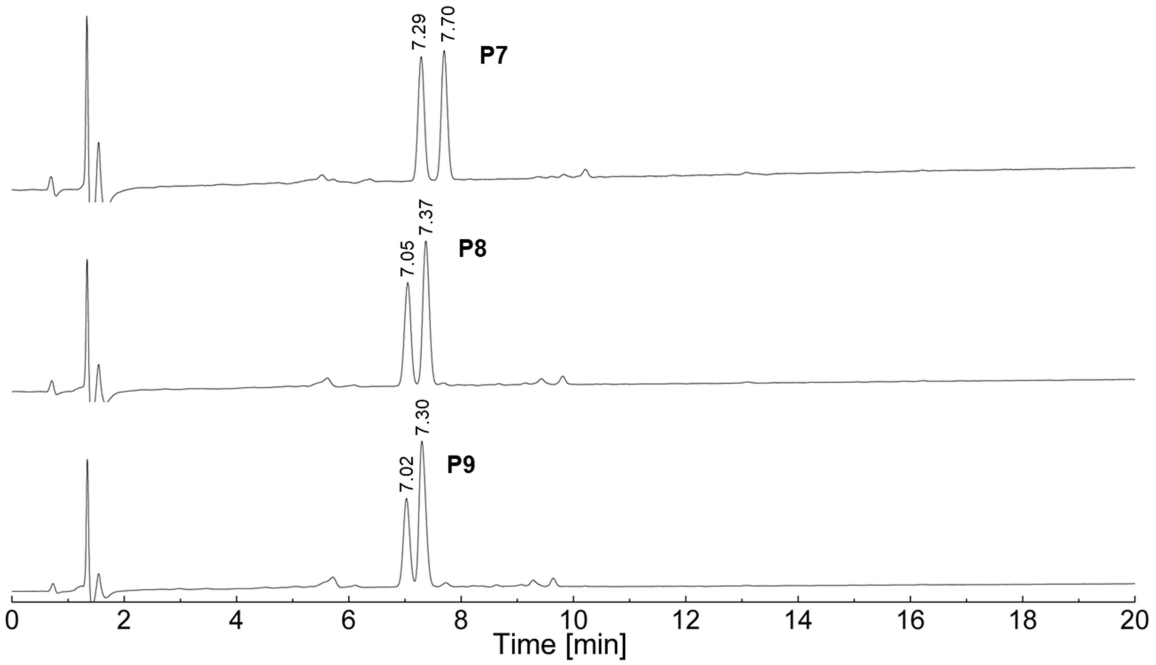

Figure 5.11: Analytical RP-HPLC of crude peptides **P7**, **P8** and **P9**. HPLC conditions: C18 column (150 x 3.9 mm, 100 Å pore diameter, 5 µm particle size), gradient 20 - 50% acetonitrile in 20 min, flow rate 1 ml/min.

The synthesis on ADO preloaded resin caused a drop of resin loading from 0.25 mmol/g for peptide **P7** to 0.19 mmol/g for peptide **P8** and 0.18 mmol/g for peptide **P9**. Surprisingly, the loading capacity of ADO preloaded resins dropped with an increasing spacer length. One explanation for this finding is the exceeding of the optimal spacer length, which is more likely to form undefined "knot-like" structures, which limiting access to the N-terminus of the spacer.

Table 5.6: Results of model Hmp-peptides **P7**, **P8** and **P9**.

Entry	Peptide	Theo. [m/z]	Found [m/z]	Crude	Yield
P7	[Leu^{21}]BM2(17-21)-Hmp	352.18^{2+}	352.18^{2+}	71.8 mg	61.9%
P8	[Leu^{21}]BM2(17-21)-Hmp-ADO	424.72^{2+}	424.72^{2+}	38.3 mg	54.8%
P9	[Leu^{21}]BM2(17-21)-Hmp-ADO$_2$	497.26^{2+}	497.26^{2+}	28.1 mg	34.3%

Peptides with penta-lysine tags

In order to develop temporarily-bound solubilizing tags, which are expected to dissolve highly hydrophobic peptides, penta-lysine tags were attached at the Hmp moiety. The amino acid lysine carries a primary amino group which is chargeable under acidic conditions. The protonated form of lysine dramatically raises the solubility of hydrophobic peptides. Previous studies indicate that lysine is the most efficient amino acid for the dissolution of poorly water soluble peptides.[80] However, the steric hindrance of the bulky 2-methylpropan-2-yl)oxycarbonyl (Boc) side chain of Fmoc-L-Lys(Boc)-OH can lead to a low resin loading after coupling of multiple lysine residues. In order to find optimal synthetic conditions three different model peptides **P10** [Leu^{21}]BM2(17-21)-Hmp-Lys$_5$, **P11** [Leu^{21}]BM2(17-21)-Hmp-ADO-Lys$_5$ and **P12** [Leu^{21}]BM2(17-21)-Hmp-ADO$_2$-Lys$_5$ were synthesized. All peptides were synthesized manually on penta-lysine preloaded resin supports according to instruction **9.2**. HPLC analysis of the crude peptides revealed several side products. In Figure **5.12** the chromatograms of the crude products **P10**, **P11** and **P12** are highlighted.

Peptide **P10** was synthesized without any spacer unit between Hmp and the penta-lysine tag. However, the synthesis of **P10** failed (figure **5.12** upper chromatogram). The HPLC chromatogram of crude product **P10** showed no main peak that could be assigned to the searched peptide. Moreover, MALDI-TOF-MS were not able to identify the calculated mass in crude product **P10**. The big steric hindrance of the penta-lysine tag was considered a reason for the unsuccessful synthesis. The second model peptide **P11** and the third model peptide **P12** were variants with one and two ADO spacer units between Hmp and the penta-lysine tag.

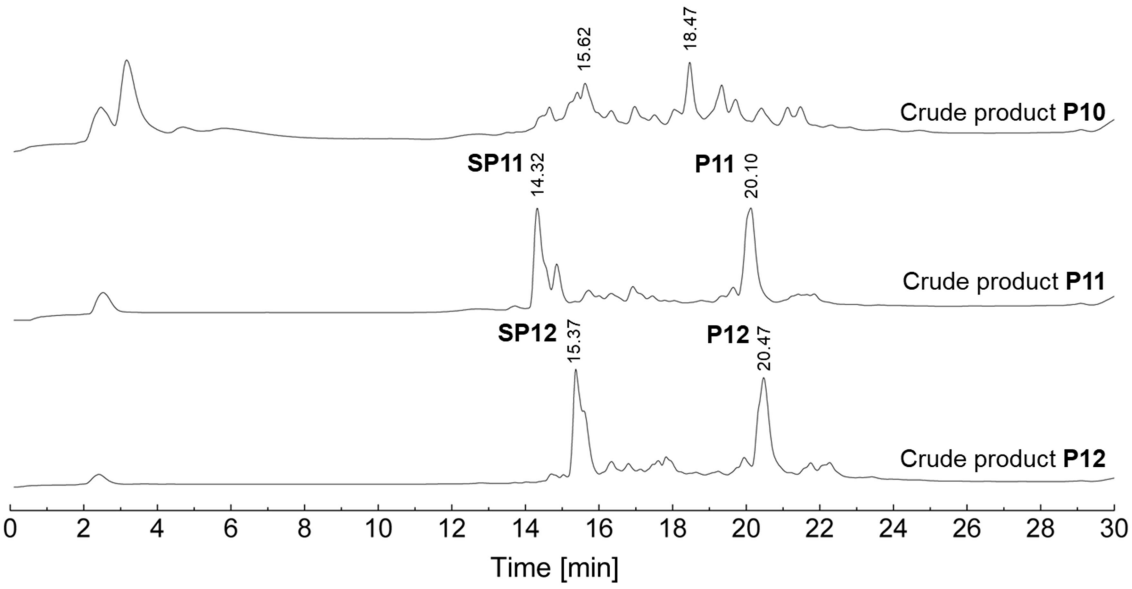

Figure 5.12: Analytical RP-HPLC of peptide **P10** (upper chromatogram), **P11** (middle chromatogram) and **P12** (lower chromatogram). RP-HPLC was performed with a C18 column (150 x 4 mm, 100 Å pore diameter, 3 µm particle size). Gradient: 0 –50% acetonitrile in 20 min, flow rate 1 ml/min.

The chromatograms of crude peptides **P11** and **P12** showed two main products, at 14.32 min and 20.12 min for crude peptide **P11**, and 15.37 min and 20.47 min for crude peptide **P12**, respectively. MALDI-TOF MS measurements of these main peaks confirmed the right peptides at retention times of 20.12 min and 20.47 min corresponding to **P11** and **P12**. The main side

products **SP11** and **SP12** were identified as $(Leu)_2$-Hmp-ADO-Lys_5 and $(Leu)_2$-Hmp-ADO_2-Lys_5. To investigate the production of side product **SP11**, test cleavages after the coupling of ADO (**1**), Hmp (**2**) and Leu (**3**) were performed. These results proved that side product **SP11** was formed during the Mitsunobu reaction. The mass spectra of these test cleavages are shown in the appendix (chapter **15.1.2**).

Table 5.7: Found molecular weights and possible products after the test cleavages (1), (2) and (3).

Entry	Test cleavage	Found [m/z]	Found product
1	ADO-Lys_5	803.66^{1+}	ADO-Lys_5
2	Hmp-ADO-Lys_5	907.67^{1+}	Hmp-ADO-Lys_5
3	Leu-Hmp-ADO-Lys_5	1132.81^{1+}	$(Leu)_2$-Hmp-ADO-Lys_5

After cleavage from resin and lyophilisation, crude peptides **P11** and **P12** were purified according to instruction **8.1.7** and analysed *via* analytical RP-HPLC and MAILDI-TOF-MS. Both peptides showed the typical double peak for Hmp-peptides, however, the difference in the retention time of both diastereomers was too small for baseline separation.

The chromatograms showed no signs of impurities or oxidised side products. The mass spectra and measured isotopic pattern were in accordance with the simulated isotopic pattern of the expected chemical formulas for **P11** and **P12** (figure **5.13**).

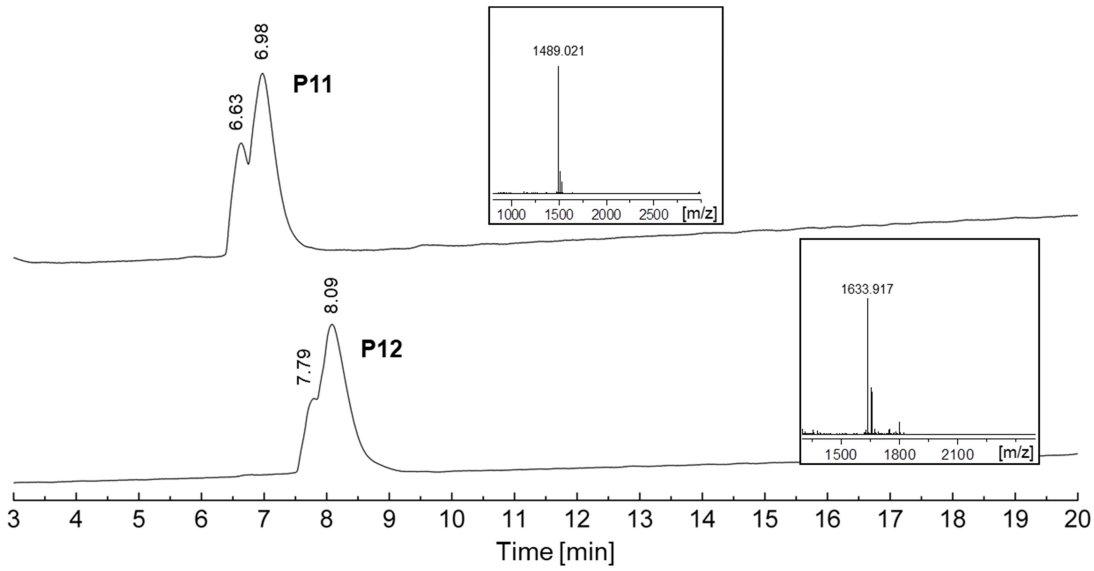

Figure 5.13: Analytical RP-HPLC of model peptides **P11** and **P12**. HPLC was performed with a C18 column (150 x 4 mm, 100 Å pore diameter, 3 µm particle size), gradient 15 - 45% acetonitrile in 30 min, flow rate 1 ml/min.

Table 5.8: Results of Hmp-model peptides **P11** and **P12**.

Entry	Peptide	Found [m/z]	Crude	Purified	Yield
P11	[Leu^{21}]BM2(17-21)-Hmp-ADO-Lys_5	1489.02^{1+}	35.7 mg	1.36 mg	1.10%
P12	[Leu^{21}]BM2(17-21)-Hmp-ADO_2-Lys_5	1633.92^{1+}	42.2 mg	2.35 mg	1.74%

Peptides with penta-arginine tags

In multiple studies arginine tags were used to enhance peptide solubility for purification or NCL.[103-104, 115-116] Similar to polylysine, polyarginine tags can be protonated under acidic conditions thus increasing the charge of the peptide. In this study the synthesis of three penta-arginine carrying model Hmp-peptides was tested. For the synthesis of the model peptides **P13** [Leu^{21}]BM2(17-21)-Hmp-Arg$_5$, **P14** [Leu^{21}]BM2(17-21)-Hmp-ADO-Arg$_5$ and **P15** [Leu^{21}]BM2(17-21)-Hmp-ADO$_2$-Arg$_5$ the resin was preloaded with penta-arginine using a standard Fmoc-SPPS protocol according to instruction **9.2**.

Model peptide **P13** was composed of five BM2-derived amino acids (BM2(17-21)), the Hmp group and penta-arginine as a tag. The model peptides **P14** and **P15** were synthesized with a distant increasing ADO or ADO$_2$ spacer between Hmp and the C-terminal solubilizing tag. Table **5.9** shows the sequences and chemical formulas of model peptides **P13**, **P14** and **P15**.

Table 5.9: Sequences of the penta-arginine carrying model peptides **P13**, **P14** and **P15**.

Entry	Chemical formula	Peptide sequence
P13	$C_{63}H_{109}N_{27}O_{13}S$	ALHFL-Hmp-RRRRR
P14	$C_{69}H_{120}N_{28}O_{16}S$	ALHFL-Hmp-ADO-RRRRR
P15	$C_{75}H_{131}N_{29}O_{19}S$	ALHFL-Hmp-ADO$_2$-RRRRR

Figure **5.14** displays the RP-HPLC chromatograms of the obtained crude products **P13**, **P14** and **P15**. All chromatograms have one main peak at 14.97 min (**P13**), 15.87 min (**P14**) and 16.48 min (**P15**). To identify these main products MALDI-TOF mass spectroscopy was used (figure **5.15**).

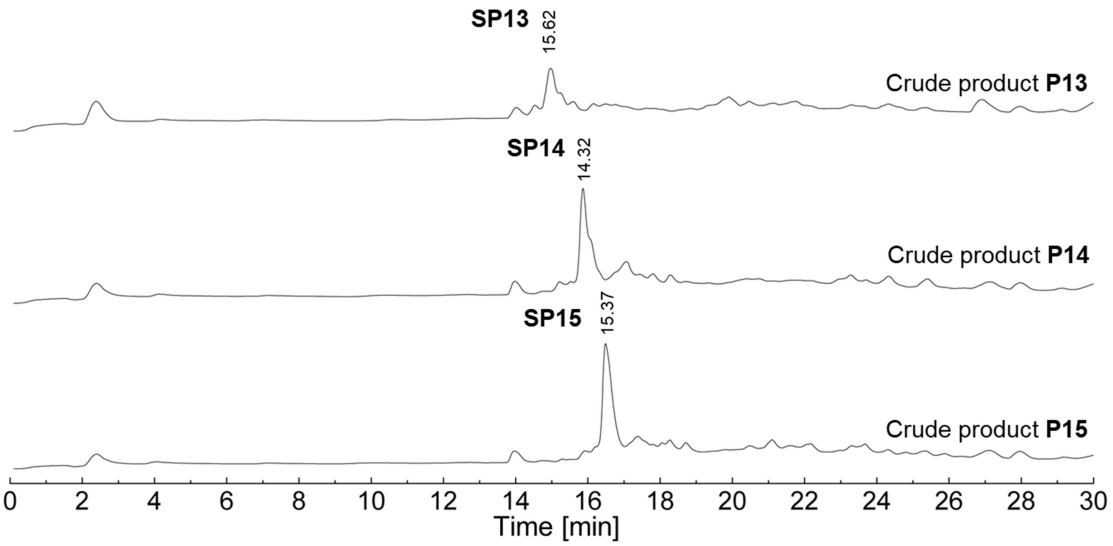

Figure 5.14: Analytical RP-HPLC chromatograms of crude product **P13** (upper chromatogram), crude product **P14** (middle chromatogram) and crude product **P15** (lower chromatogram). HPLC measurements were performed with a C18 column (150 x 4 mm, 100 Å pore diameter, 3 µm particle size), gradient 0 - 50% acetonitrile in 20 min, flow rate 1 ml/min.

After peak separation by RP-HPLC, the samples were prepared for mass spectrometry following instruction **8.1.5**. In the samples of the crude products **P13**, **P14** and **P15** the signal and the isotopic pattern of the uncoupled sequences Hmp-Arg_5, Hmp-ADO-Arg_5 and Hmp-ADO_2-Arg_5 were identified.

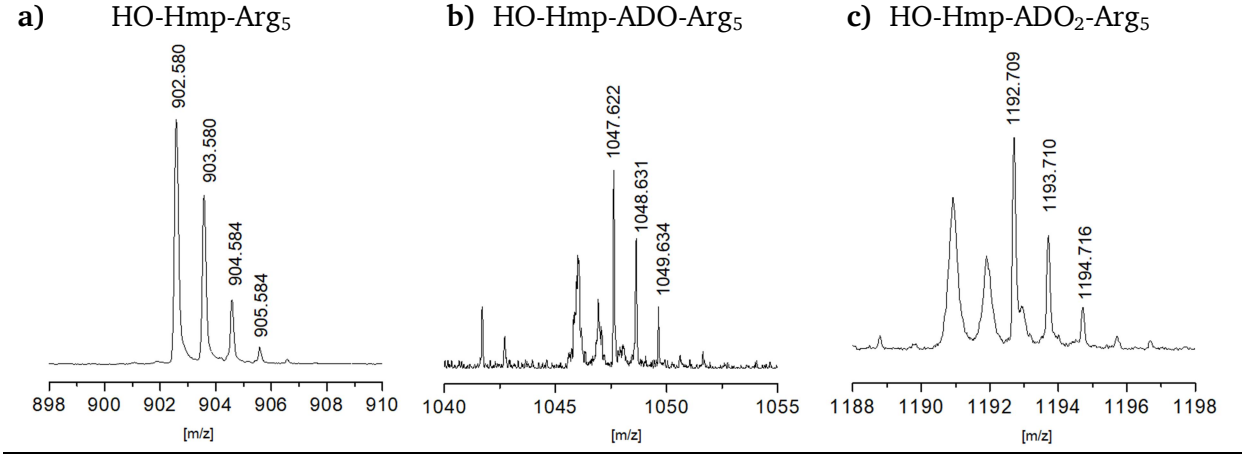

Theoretical monoisotopic mass
SP 13: $C_{33}H_{67}N_{21}O_7S$
$[M+H]^+$ = 902.53 m/z

Theoretical monoisotopic mass
SP 14: $C_{39}H_{78}N_{22}O_{10}S$
$[M+H]^+$ = 1047.60 m/z

Theoretical monoisotopic mass
SP 15: $C_{45}H_{89}N_{23}O_{13}S$
$[M+H]^+$ = 1192.58 m/z

Figure 5.15: Mass spectrometry of crude products **P13**, **P14** and **P15**. HCCA was used as matrix for MALDI-TOF-MS.

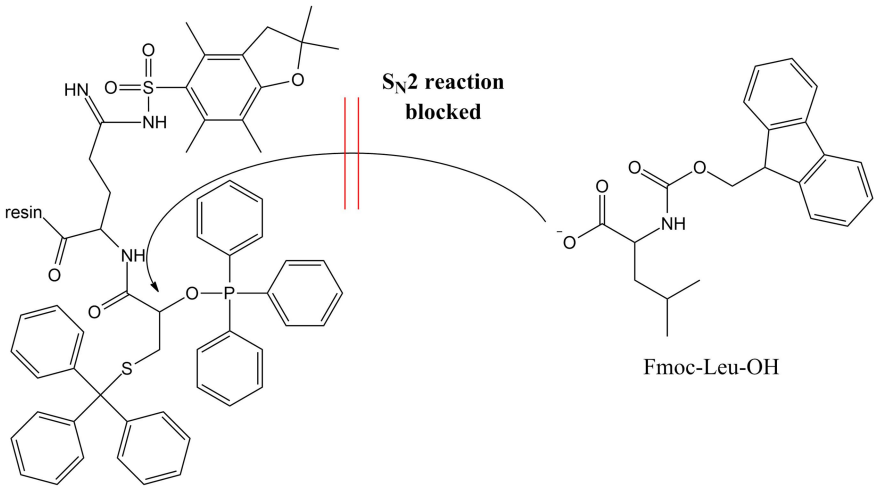

Figure 5.16: Mechanism of the Mitsunobu reaction with leucine as nucleophile at a penta-arginine preloaded resin. The steric hindrance and bulky Pbf protecting group of arginine prevent an efficient nucleophile attack.

These results can be explained by the high steric hindrance of the Arg(Pbf) side chain which prevents the amino acid coupling in the Mitsunobu reaction. The S_N2 mechanism of the Mitsunobu reaction, in which the deprotonated carboxyl group of leucine acts as nucleophile, relies on accessibility of the C^{α}-carbon atom of the Hmp group. However, bulky groups in the vicinity of Hmp(Trt), reduce or even prevent a successful attack of Fmoc protected amino acids. Even with ADO_2 as spacer, no product formation could be observed by RP-HPLC and MALDI-TOF-MS.

5.1.6. Synthesis of complete BM2 Hmp-peptide fragments

Synthesis of P16 [Leu^{10}]BM2(1-10)-Hmp

The synthesis of **P16** BM2(1-10)-Hmp was performed by automated, microwave-assisted Fmoc-SPPS according to instruction **9.3**. The Hmp group and the first two amino acids leucine and serine were coupled manually following procedure **9.2**. In order to protect the basic labile oxo-ester bond of Hmp, 2-metylpiperidin (2-MP) was applied for the deprotection of the N-terminal Fmoc group. For peptide cleavage and deprotection a standard cleavage protocol was applied. The RP-HPLC of crude peptide **P16** showed the characteristic double peak that belongs to the peptide diastereomers **P16a** and **P16b**. For ligation experiments both peaks were purified by preparative RP-HPLC. After peak separation diastereomers **P16a** and **P16b** were reinjected and analysed by analytical RP-HPLC and ESI-MS (figure **5.17**). The isotopic patterns of both diastereomers were in accordance with the simulated isotopic patterns.

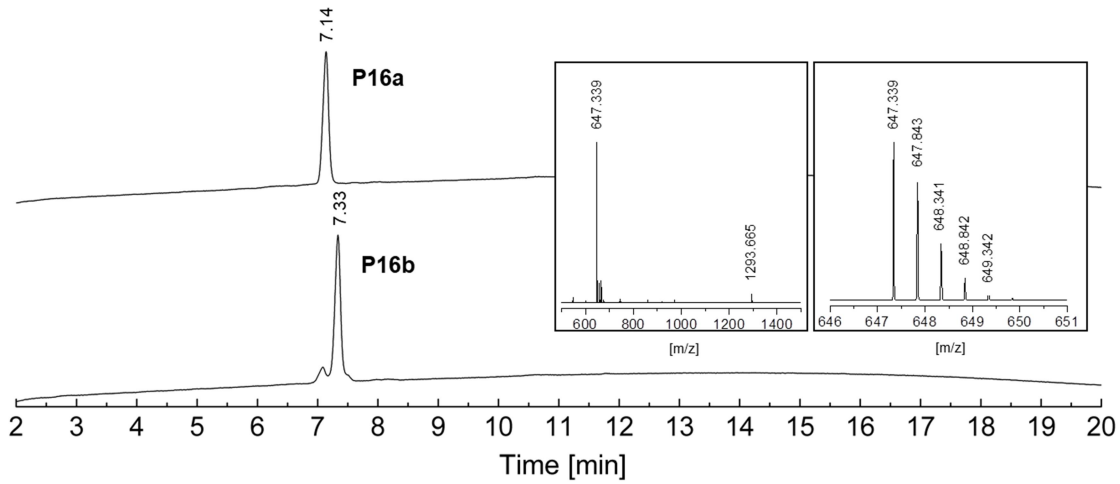

Figure 5.17: Analytical RP-HPLC and ESI-MS of purified peptides **P16a** and **P16b**. HPLC conditions: C4 column (MultoHigh U C4, 100 x 4 mm), gradient 25 -99% acetonitrile in 20 min, flow rate 1 ml/min.

Since the Hmp(Trt) building block was used as a racemic mixture, the probability for the formation of both diastereomers was equal. Diastereomer **P16a** was acquired with a yield of 16.5 mg (5.1%) and diastereomer **P16b** was obtained with 20.4 mg (6.3%). In table **5.10** the theoretical and the real obtained yields of **P16a** and **P16b** are listed.

Table 5.10: Results of Hmp-peptide diastereomers **P16a** and **P16b**.

Entry	Dia.	Peptide	Found [m/z]	Crude	Purified	Yield
P16a	1	[Leu^{10}]BM2(1-10)-Hmp	647.339^{2+}	99.5 mg	16.5 mg	5.1%
P16b	2	[Leu^{10}]BM2(1-10)-Hmp	647.339^{2+}	99.5 mg	20.4 mg	6.3%

Because the amino acid sequence of peptide **P16** was derived from the N-terminal hydrophobic part of BM2(1-51) low solubility was expected. The purified peptide diastereomers **P16a** and **P16b** could not be dissolved in acetonitrile/water based solvent mixtures. However, mixtures of TFE or HFIP with water (1 : 2, v/v) were capable of dissolving the purified peptides. The low solubility during the purification and analysis of these BM2 fragments showed the advantage associated with the C-terminal solubilizing tag strategy.

Synthesis of P17 BM2(1-21)-NH_2

The 21-mer peptide **P17** BM2(1-21)-NH_2 was synthesized without a C-terminal Hmp unit and was used as a reference peptide for solubility tests and CD spectroscopy. Fmoc-SPPS succeeded in using a standard protocol according to instruction **9.3**. After peptide cleavage and lyophilisation, crude peptide **P17** was obtained as white solid which was highly hydrophobic and insoluble in several different tested mixtures of acetonitrile and water.

For preparative RP-HPLC only small amounts (approx. 10 mg) of the crude peptide **P17** could be dissolved in a mixture containing 2.5 ml TFE and 2.5 ml 0.1% TFA. Therefore, **P17** was pre-dissolved in the organic liquid and slowly diluted with the same amount of 0.1% TFA. After purification, peptide **P17** was reinjected in analytical RP-HPLC and analysed *via* MALDI-TOF-MS. HPLC analysis displayed a single peak at 12.55 min that could be assigned to the desired product. The mass spectrum showed the expected monoisotopic signal at 2421.19 m/z. Below the analytical RP-HPLC chromatogram, the MALDI-TOF mass spectrum and isotopic pattern of the purified peptide **P17** is highlighted (figure **5.18**).

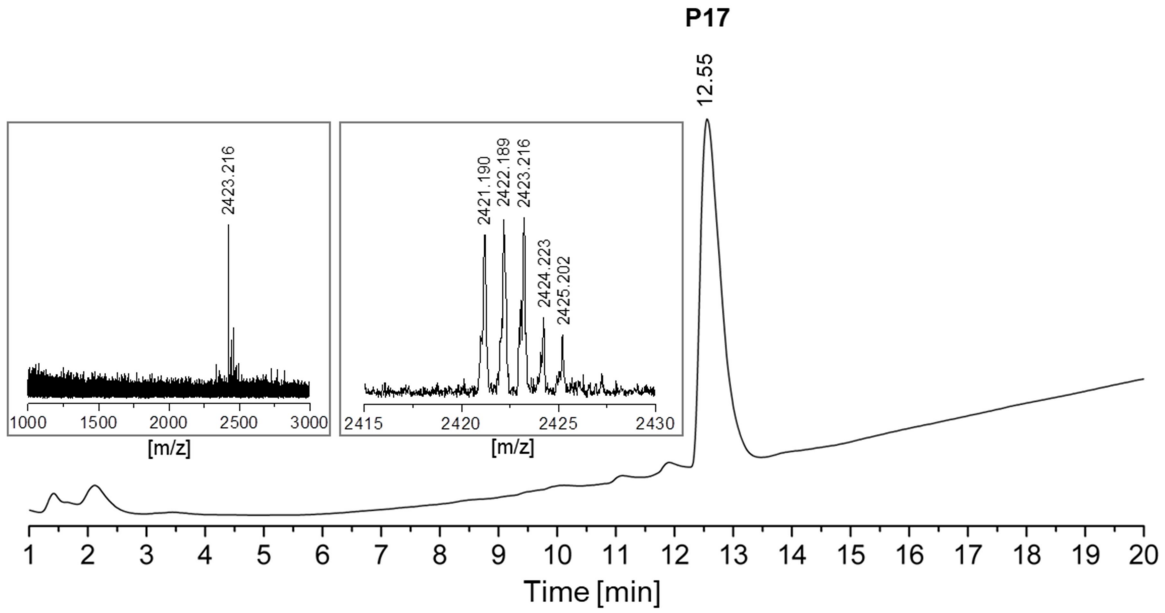

Figure 5.18: Analytical RP-HPLC and MALDI-TOF-MS of purified peptide **P17**. HPLC was performed using a C18 column (150 x 4 mm, 100 Å pore diameter, 3 µm particle size), gradient 50 - 99% acetonitrile in 15 min, flow rate 1 ml/min.

After purification 9.5 mg (4.4%) of peptide **P17** was obtained. The purified peptide was used as a reference substance for CD spectroscopy and analytical RP-HPLC. Table **5.11** shows the obtained amounts and the yield of the purified peptide.

Table 5.11: Results of peptide **P17**.

Entry	Peptide	Found [m/z]	Crude	Purified	Yield
P17	BM2(1-21)-NH_2	2421.19^{1+}	89.5 mg	9.5 mg	4.4%

Synthesis of P18 [Leu^{21}]BM2(1-21)-Hmp

Hmp-peptide **P18** was synthesized according to instruction **9.3**. Since the C-terminal oxo-ester bond of Hmp turned out to be sensitive against piperidine, the less basic 2-metylpiperidine was used for Fmoc deprotection. Crude peptide **P18** was cleaved from the solid phase and released from side chain protecting groups like described in procedure **9.2**. The chromatogram of the crude product showed two main peaks which could be assigned to peptide diastereomers **P18a** and **P18b**. Crude peptide **P18** was as poorly soluble as the hydrophobic peptide **P17**. Due to the poor solubility only small amounts of **P18** could be purified. For preparative RP-HPLC 20 mg were dissolved in 2.5 ml TFE and 2.5 ml water (0.1% TFA). After peak separation the purified fraction was reinjected in analytical RP-HPLC and further analyzed by MALDI-TOF-MS. The MALDI-TOF-MS measurements of the purified peptide **P18** were performed according to instruction **8.1.5**. The measured mass spectra and isotopic pattern of both diastereomers **P18a** and **P18b** were in accordance with the theoretical isotopic pattern. The results of MALDI-TOF-MS and analytical RP-HPLC are highlighted below (figure **5.19**).

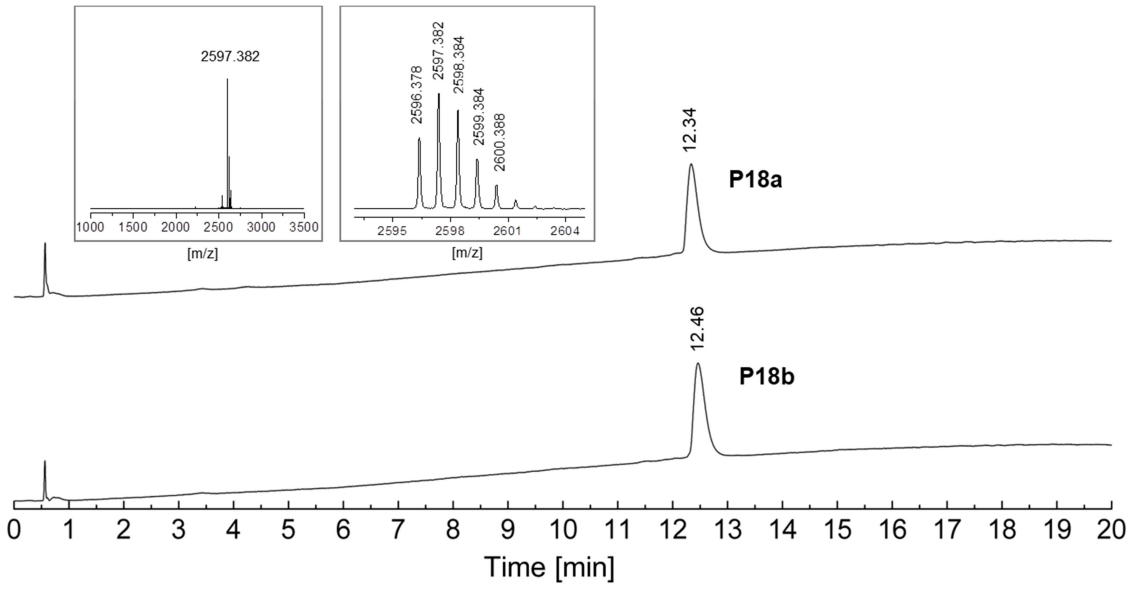

Figure 5.19: Analytical RP-HPLC and MALDI-TOF-MS of purified peptides **P18a** and **P18b**. HPLC conditions: C4 column (MultoHigh U C4, 100 x 4 mm), gradient 10 -20% acetonitrile in 5 min followed by a gradient of 20 -70% acetonitrile in 20 min, flow rate 2 ml/min.

Both chromatograms showed purified products with a single peak at 12.34 min and 12.46 min. After peak separation of both diastereomers, the purified fractions were frozen and lyophilised. The final diastereomers **P18a** and **P18b** were obtained as a white solid which were absolutely insoluble in acetonitrile/water mixtures.

Table 5.12: Results of Hmp-peptide diastereomers **P18a** and **P18b**.

Entry	Dia.	Peptide	Found [m/z]	Crude	Purified	Yield
P18a	1	[Leu^{21}]BM2(1-21)-Hmp	2596.31^{1+}	160.30 mg	4.9 mg	0.85%
P18b	2	[Leu^{21}]BM2(1-21)-Hmp	2596.37^{1+}	160.30 mg	5.2 mg	0.89%

Synthesis of P19 [Leu^{21}]BM2(1-21)-Hmp-ADO$_2$

The Hmp-peptide **P19** was synthesized with a C-terminal ADO$_2$ tag according to instructions **9.2** and **9.3**. Therefore the ADO$_2$ tag, the Hmp unit and the first two amino acids leucine and phenylalanine were coupled manually. Loading determination by UV/Vis spectroscopy revealed a loading capacity of 0.23 mmol/g after coupling of leucine by the Mitsunobu reaction. After cleavage from the solid support 140.20 mg of crude peptide **P19** were obtained. This crude product was poorly soluble in water/acetonitrile based mixtures despite the C-terminal ADO$_2$ tag. For analytical purposes **P19** was dissolved in a mixture of 70% TFE and 30% water (0.1% TFA). RP-HPLC of the crude peptide showed the typical diastereomer double peak of **P19a** and **P19b**. After preparative RP-HPLC, the purified diastereomers were lyophilized and reinjected in analytical RP-HPLC. The chromatograms of the reinjections are depicted below (figure **5.20**).

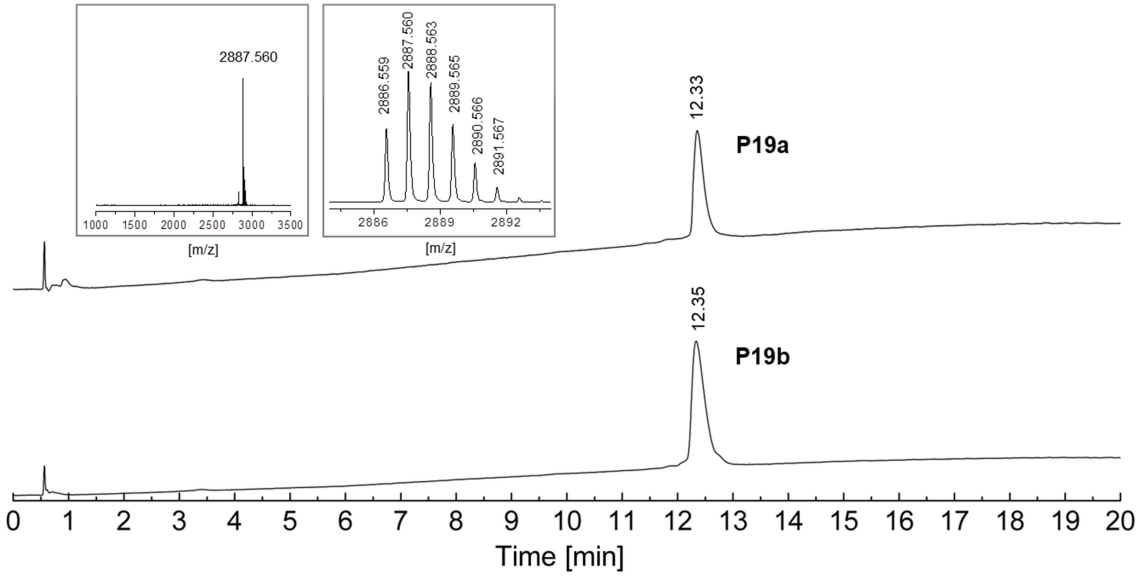

Figure 5.20: Analytical RP-HPLC and MALDI-TOF-MS of purified peptides **P19a** and **P19b**. HPLC conditions: C4 column (MultoHigh U C4, 100 x 4 mm), gradient 10 - 20% acetonitrile in 5 min followed by a gradient of 20 - 70% acetonitrile in 20 min, flow rate 2 ml/min.

Both chromatograms of **P19a** and **P19b** showed pure product peaks without further impurities. For identification of the peaks the reinjected diastereomers **P19a** and **P19b** were analysed by MALDI-TOF-MS. The measured isotopic pattern displayed the exact theoretical mass of the expected peptides.

Table 5.13: Results of Hmp-peptide diastereomers **P19a** and **P19b**.

Entry	Dia.	Peptide	Found [m/z]	Crude	Purified	Yield
P19a	1	[Leu^{21}]BM2(1-21)-Hmp-ADO$_2$	2886.56^{1+}	140.20 mg	4.0 mg	1.5%
P19b	2	[Leu^{21}]BM2(1-21)-Hmp-ADO$_2$	2886.56^{1+}	140.20 mg	5.3 mg	2.0%

Synthesis of P20 [Leu^{21}]BM2(1-21)-Hmp-ADO-Lys$_5$

Because BM2(1-21) turned out to be extremely hydrophobic and poorly soluble in previous experiments, the attachment of a C-terminal penta-lysine tag was tested. The resin support was prepared following instruction **9.2**. After manual coupling of the penta-lysine tag, resin loading dropped from 0.33 mmol/g to a final loading capacity of 0.1 mmol/g. The following peptide sequence was synthesised by automated, microwave-assisted Fmoc-SPPS according to instruction **9.3**.

After cleavage and lyophilisation crude peptide **P20** was obtained as good water soluble solid which was purified *via* preparative HPLC. The purified product was reinjected in analytical RP-HPLC and analysed by MALDI-TOF-MS. Mass analysis showed the exact calculated monoisotopic weight and isotopic pattern of the searched peptide sequence. The HPLC chromatogram of the purified peptide **P20** displayed a single peak at a retention time of 10.36 min. Although all previous synthesized Hmp-peptides were obtained as mixtures of two diastereomers, the purified product **P20** showed no double peak even when a smaller acetonitrile gradient was applied (figure **5.21**).

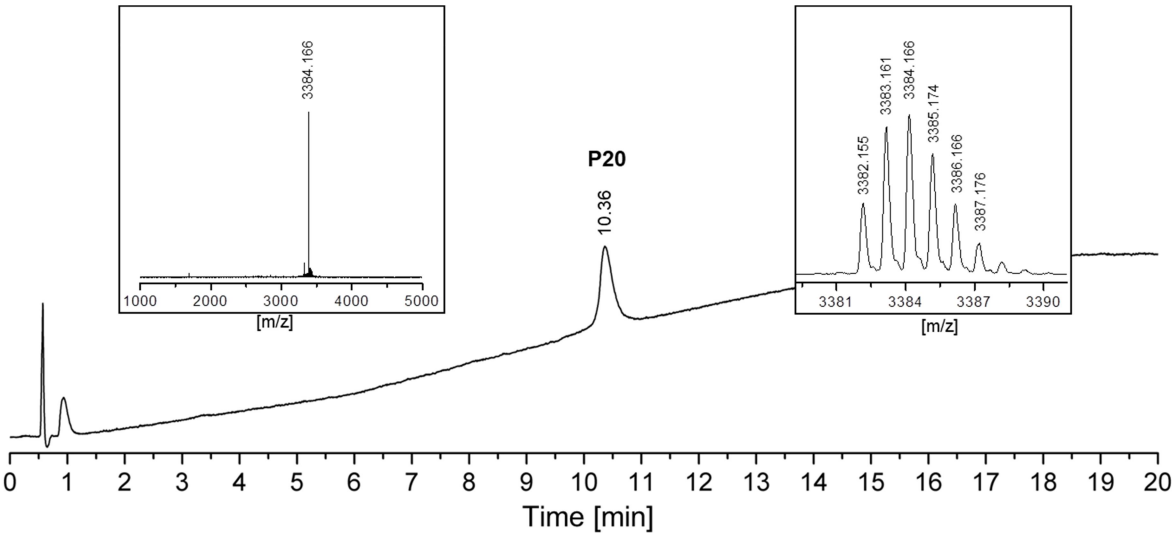

Figure 5.21: Analytical RP-HPLC and MALDI-TOF-MS of peptide **P20**. RP-HPLC was performed with a C4 column (MultoHigh U C4, 100 x 4 mm), gradient 10 - 20% acetonitrile in 5 min followed by 20 - 70% acetonitrile in 20 min, flow rate 2 ml/min.

The solubility of peptide **P20** was significantly increased in comparison to previous synthesised peptides **P18** and **P19**. In the appendix (chapter **15.1.3)** the suspension of peptide **P18** without a solubilizing tag and the solution of peptide **P20** with a C-terminal penta-lysine tag are compared. After purification and lyophilisation 4.3 mg (0.56%) of **P20** were obtained.

Table 5.14: Results of Hmp-peptide **P20**.

Entry	Peptide	Found [m/z]	Crude	Purified	Yield
P20	[Leu^{21}]BM2(1-21)-Hmp-ADO-Lys$_5$	3382.15^{1+}	266.4 mg	4.3 mg	0.56%

5.1.7. Summary of resin preparation

The decisive step in the synthesis of Hmp-peptides is the coupling of the first amino acid at the unprotected hydroxyl function of Hmp. The efficiency of the Mitsunobu reaction is not only dependent on the type and the properties of the solid support, but also on the length of the spacer and the type of amino acid used as a building block for the solubilizing tag. Table **5.15** shows the resin loadings after the Mitsunobu reaction of peptides **P4** - **P20**. The size of the solubilizing tag and the distance to Hmp seem to be the most limiting factors for an efficient Mitsunobu reaction.

Solubilizing tags composed of the amino acid arginine as in the case of model peptides **P13**, **P14** and **P15** result in tremendously low loading capacities under 0.05 mmol/g. This minor resin loading can be explained by steric hindrance caused by the bulky Pbf protecting group of arginine. However, pentalysine was found to be a good alternative for the synthesis of solubilizing tags. Considering the loading growth starting from peptide **P10** (0.09 mmol/g) to peptide **P12** (0.13 mmol/g), the length of the ADO spacer unit is a second decisive factor for an efficient Mitsunobu reaction.

Table 5.15: Influence of the amino acids and spacers to the resin loading after Mitsunobu reaction.

No.	Peptide Name	Tag	Spacer	Loading[a]
P4	[Ile^{21}]BM2(17-35)-Hmp	*n.s.t.*	*n.s.*	0.19[c]
P5	[Ile^{21}]BM2(17-35)-Hmp-ADO	ADO	*n.s.*	0.15[d]
P6	[Ile^{21}]BM2(17-35)-Hmp-ADO_2	ADO_2	*n.s.*	0.14[d]
P7	[Leu^{21}]BM2(17-35)-Hmp	*n.s.t.*	*n.s.*	0.25[b]
P8	[Leu^{21}]BM2(17-35)-Hmp-ADO	ADO	*n.s.*	0.19[b]
P9	[Leu^{21}]BM2(17-35)-Hmp-ADO_2	ADO_2	*n.s.*	0.18[b]
P10	[Leu^{21}]BM2(17-35)-Hmp-Lys_5	Lys_5	*n.s.*	0.07[b]
P11	[Leu^{21}]BM2(17-35)-Hmp-ADO-Lys_5	Lys_5	ADO	0.09[b]
P12	[Leu^{21}]BM2(17-35)-Hmp-ADO_2-Lys_5	Lys_5	ADO2	0.13[b]
P13	[Leu^{21}]BM2(17-35)-Hmp-Arg_5	Arg_5	*n.s.*	0.048[b]
P14	[Leu^{21}]BM2(17-35)-Hmp-ADO-Arg_5	Arg_5	ADO	0.050[b]
P15	[Leu^{21}]BM2(17-35)-Hmp-ADO_2-Arg_5	Arg_5	ADO2	0.053[b]
P16	[Leu^{10}]BM2(1-10)-Hmp	*n.s.t.*	*n.s.*	0.23[b]
P18	[Cys(Acm)^{11}][Leu^{21}]BM2(1-21)-Hmp	*n.s.t.*	*n.s.*	0.25[b]
P19	[Cys(Acm)^{11}][Leu^{21}]BM2(1-21)-Hmp-ADO_2	ADO_2	*n.s.*	0.23[b]
P20	[Cys(Acm)^{11}][Leu^{21}]BM2(1-21)-Hmp-ADO-Lys_5	Lys_5	ADO	0.09[b]

a *Loading after solid phase Mitsunobu reaction in [mmol/g].*
b *AmphiSpheres RAM 40 resin with a start loading of 0.33 mmo/g.*
c *AmphiSpheres RAM 40 resin with a start loading of 0.27 mmo/g.*
d *Tentagel resin with a start loading of 0.18 mmol/g.*
n.s.t. *No solubility tag.*
n.s. *No spacer.*

5.1.8. Summary of resin weights, scales and obtained yields

The used scale, resin weights and obtained yields of the synthesized peptides are summarized in table **5.16**. Short model Hmp-peptides **P4 - P9** were used as crude peptides in all the following analytic steps and ligation experiments. All other peptides were purified before usage by preparative RP-HPLC following instruction **8.1.7**.

The obtained yields of the long Hmp-peptides **P16** - **P20** were under 5% after purification and are only half as high as for the synthesis of the N-terminal cysteine peptides **P1**, **P2** and **P3**. These low yields can be explained by the dropping of resin loading through the Mitsunobu reaction.

Table 5.16: Summary of the start resin weights, scales, received peptide amounts and obtained yields after Fmoc-SPPS of N-terminal cysteine peptides and C-terminal Hmp-peptides.

No.	Resin [g]	Scale [mmol]	Theo. obtained Amount [mg]	Real obtained Amount [mg]	Yield [%]
P1	0.5[f]	0.20	327.4	192[b]/85.2[a]	58.64[b]/26.2[a]
P2	0.68[d]	0.184	648.10	528[b]/40.7[a]	81.46[b]/6.2[a]
P3	0.75[c]	0.250	1183.07	479.0[b]/63.46[a]	40.48[b]/5.36[a]
P4	0.30[c]	0.081	56.89	11.0	19.3[b]
P5	0.125[e]	0.023	19.0	14.0	73.6[b]
P6	0.125[e]	0.023	22.3	11.2	50.2[b]
P7	0.5[c]	0.165	115.9	71.8	61.9[b]
P8	0.25[c]	0.083	69.9	38.3	54.8[b]
P9	0.25[c]	0.083	81.9	28.1	34.3[b]
P10	0.25[c]	0.083	110.9	31.0	27.9[b]
P11	0.25[c]	0.083	122.8	35.7[b]/1.36[a]	29.07[b]/1.1[a]
P12	0.25[c]	0.083	134.8	42.2[b]/2.35[a]	31.30[b]/1.74[a]
P13	0.25[c]	0.083	122.4	*n.p.*	*n.y.*
P14	0.25[c]	0.083	134.4	*n.p.*	*n.y.*
P15	0.25[c]	0.083	146.35	*n.p.*	*n.y.*
P16	0.758[c]	0.250	1292.65	100.5[b]/36.9[a]	7.77[b]/2.9[a]
P17	0.27[c]	0.089	215.40	89.5[b]/9.5[a]	41.5[b]/4.4[a]
P18	0.68[c]	0.225	582.39	160.3[b]/10.1[a]	27.5[b]/1.7[a]
P19	0.27[c]	0.089	257.09	140.2[b]/9.3[a]	54.5[b]/3.6[a]
P20	0.68[c]	0.225	758.89	266.4[b]/4.3[a]	35.1[b]/0.56[a]

a *Purified product.*
b *Crude product.*
c *AmphiSpheres RAM 40 resin with a start loading of 0.33 mmo/g.*
d *AmphiSpheres RAM 40 resin with a start loading of 0.27 mmo/g.*
e *Tentagel resin with a start loading of 0.18 mmol/g.*
f *Rink Amide MBHA resin with a start loading of 0.40 mmol/g.*
n.p. *No product.*
n.y. *No yield.*

5.1.9. Solubilizing tag-assisted NCL of Hmp-peptides in conventional buffer A

The usage of Hmp-peptides for NCL of transmembrane peptides offers several advantages over alternative ligation strategies which do not enable the attachment of solubilizing tags. The solubilizing tag-assisted Hmp strategy allows an efficient ligation of hydrophobic and poorly soluble peptide fragments in conventional (aqueous) ligation buffers as well as a simple purification using standard methods such as preparative RP-HPLC.

In the ligation buffer Hmp rearrange over an O-to-S acyl shift reaction forming an active thioester at the peptide C-terminus. In the presence of MPAA a peptide-thioaryl ester is formed which is capable of undergoing a ligation with a N-terminal Cys-peptide. Since the solubilizing tag is removed together with Hmp during the ligation, final target peptides are acquired without any modifications. The scheme below shows the ligation strategy (i) which was investigated during this work (figure **5.22**).[2]

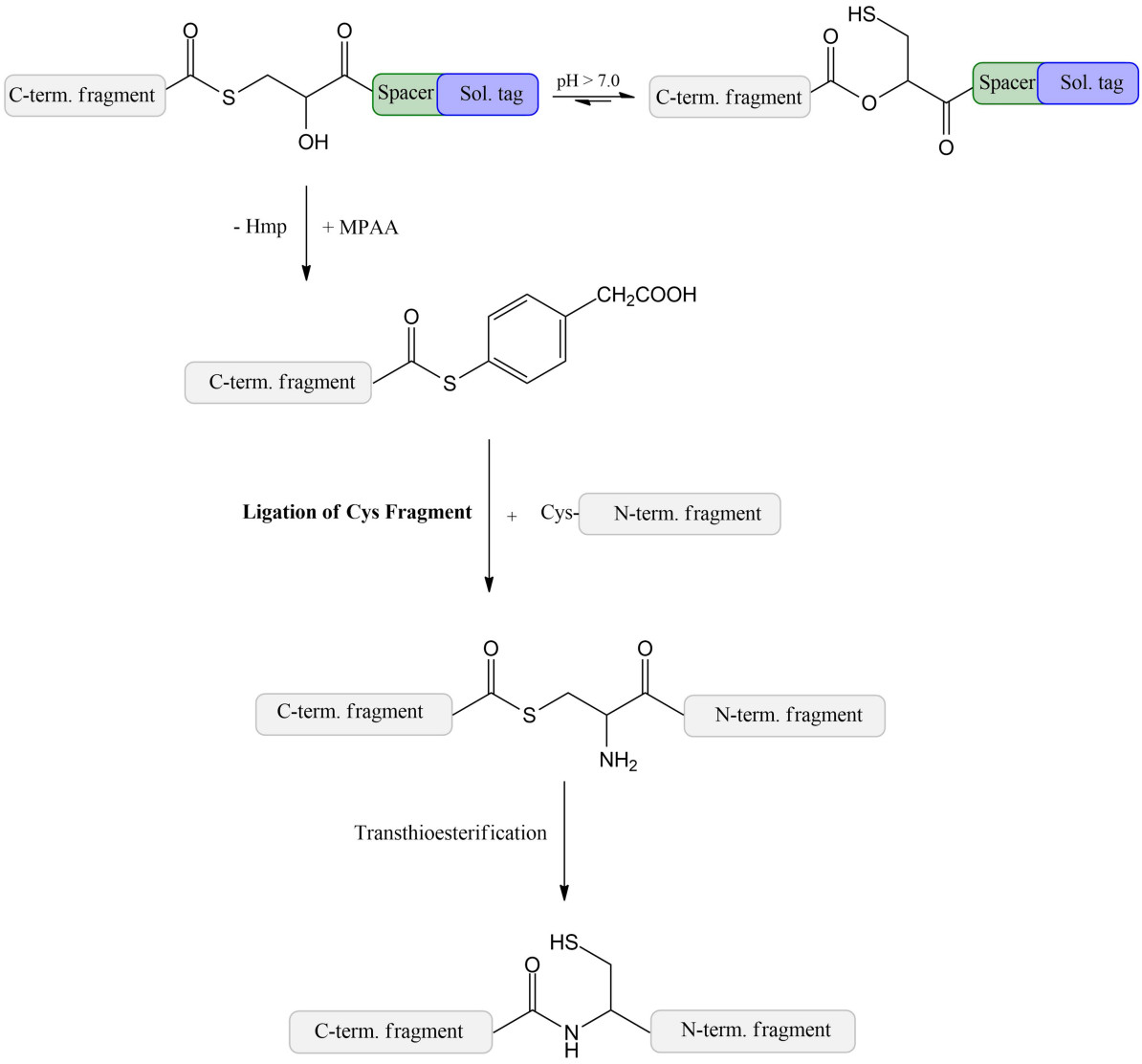

Figure 5.22: Native chemical ligation of BM2 peptides using Hmp as thioester-forming rearrangement group and anchor for a C-terminal solubilizing tag.[2]

For the investigation of ligation strategy (i), in conventional ligation buffer **A**, 8 M urea, 0.2 M disodium phosphate, 150 mM TCEP HCl and 150 mM MPAA was used. In order to find optimal conditions for the NCL in buffer **A**, a set of six different model Hmp-peptides (**P4**, **P7**-**P9**, **P11**-**P12**) was employed and ligated with the N-terminal Cys peptide **P1** (figure **5.32**). The sequence of these model Hmp-peptides was derived from the BM2 ligation site, comprising the residues BM2(17-21). The N-terminal Cys peptide **P1** was composed of the influenza virus BM2 sequence 22-35. [Cys^{22}]BM2(17-35) was acquired as a ligation product (appendix chapter **15.1.5**).

In the first ligation experiment, using the model peptides **P4** [Ile^{21}]BM2(17-21)-Hmp and **P7** [Leu^{21}]BM2(17-21)-Hmp, the difference between C-terminal isoleucine and leucine was tested. Hmp-peptides **P8** – **P12** were used to investigate the influence of different types of solubilizing tags to the ligation efficiency. After detailed investigation of yields and hydrolysis rates in buffer **A**, the long proton channel sequence **P23** [$Cys(Acm)^{11}$][Leu^{21}][Cys^{22}]BM2 (1-51) could be synthesised by the NCL of peptide **P20** [$Cys(Acm)^{11}$][Leu^{21}]BM2(1-21)-Hmp-ADO-Lys_5 with the N-terminal cysteine peptide **P2** [Cys^{22}]BM2(22-51). All ligation experiments in ligation buffer **A** were performed at room temperature under a nitrogen atmosphere. Ligation yields of the short model peptides were calculated using the relative peak areas acquired from RP-HPLC. The yield of the final ligation product **P23** was calculated using the weight of the purified product.

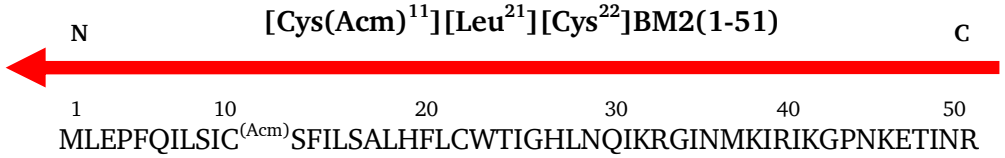

Sequences of model peptides:

P1: CWTIGHLNQIKRGI
P4: ALHFI-Hmp
P7: ALHFL-Hmp
P8, P9: ALHFL-Hmp-ADO_{1-2}
P11, P12: ALHFL-Hmp-ADO_{1-2}-Lys_5

Sequences of complete BM2 fragments:

P2: CWTIGHLNQIKRGINMKIRIKGPNKETINR
P20: MLEPFQILSIC(Acm)SFILSALHFL-Hmp-ADO-Lys_5

Figure 5.23: Amino acid sequences of the final target peptide **P23** [$Cys(Acm)^{11}$][Leu^{21}][Cys^{22}]BM2(1-51) and the precursors **P1**, **P2**, **P4**, **P7**, **P8**, **P9**, **P11**, **P12** and **P20**.

Table 5.17: Ligation experiments of the solubilizing tag-assisted NCL in buffer **A**.

Entry	Ligation product	Cys-peptide	Hmp-peptide	Sol. tag
P21	[Ile^{21}]BM2(17-35)	P1	P4	*n.s.t.*
P22	[Leu^{21}]BM2(17-35)	P1	P7	*n.s.t.*
	[Leu^{21}]BM2(17-35)	P1	P8	ADO
	[Leu^{21}]BM2(17-35)	P1	P9	ADO_2
	[Leu^{21}]BM2(17-35)	P1	P11	ADO-Lys_5
	[Leu^{21}]BM2(17-35)	P1	P12	ADO_2-Lys_5
P23	[$Cys(Acm)^{11}$][Leu^{21}][Cys^{22}]BM2(1-51)	P2	P20	ADO-Lys_5

n.s.t. *No solubilizing tag.*

NCL of model Hmp-peptides P4 and P7 in conventional ligation buffer A

In the first ligation experiments the two model Hmp-peptides **P4** [Ile^{21}]BM2(17-21)-Hmp and **P7** [Leu^{21}]BM2(17-21)-Hmp were ligated to product **P21** [Ile^{21}]BM2(17-35) and **P22** [Leu^{21}]BM2(17-35), respectively. As N-terminal cysteine peptide **P1** [Cys^{22}]BM2(22-35) was used. In this experiment, the influence of the C-terminal ligation site on the ligation efficiency was tested. Already Liu and Mayer were able to demonstrate that the formation of the MPAA-thioester intermediate is highly dependent on the C-terminus.[60] Especially the amino acids Thr, Val and Ile seem to decrease reaction rates and ligation yields. However, reaction rates and ligation yields of C-terminal bound Leu were comparable with less sterically hindered amino acids such as Gly or Ala. In order to investigate this finding on Hmp-peptides, **P4** and **P7** were ligated and compared under the same conditions. As ligation media conventional urea-based buffer **A** was applied following ligation protocol **10.1.1**.

Table 5.18: Results for ligation experiments of **P4** and **P7** in buffer **A**.

Ligation	No.	Product	Buffer	Time	Hydrolysis	Yield
a)	P21	[Ile^{21}]BM2(17-35)	A	6 h	97%	3%
b)	P22	[Leu^{21}]BM2(17-35)	A	2 h	13%	87%

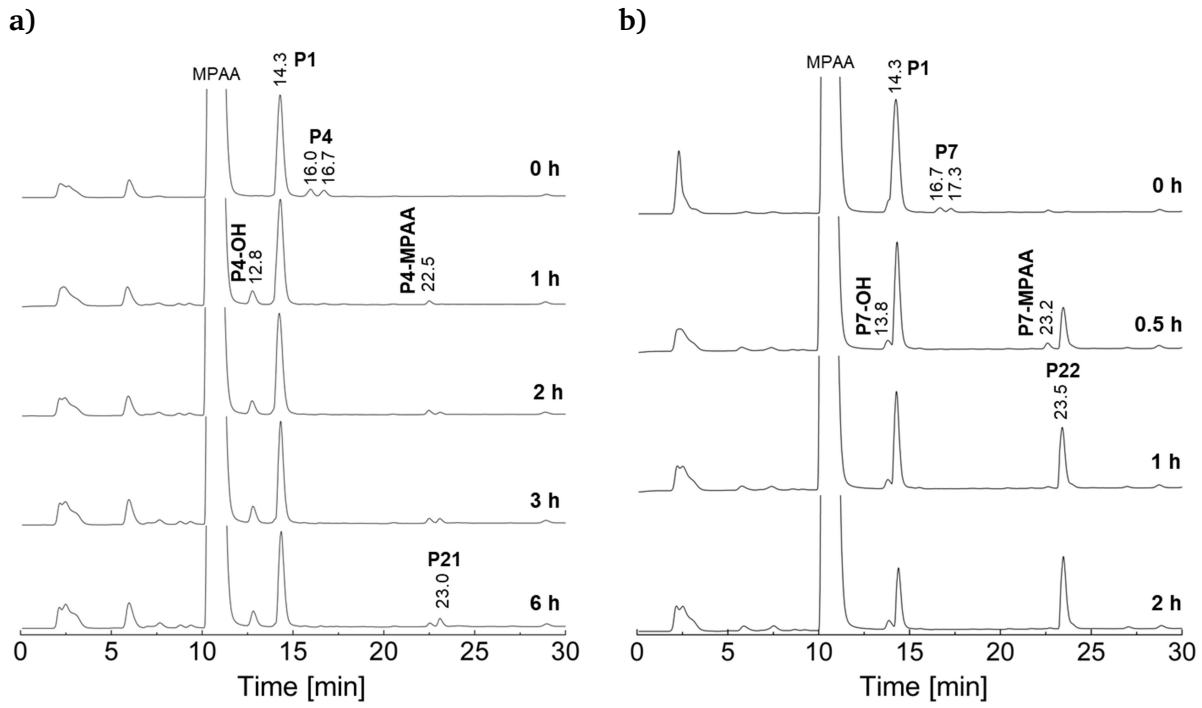

Figure 5.24: Stacked chromatograms of ligation experiments **a)** and **b)**. HPLC conditions: C18 column (150 x 4 mm, 100 Å pore diameter, 3 µm particle size). Gradient: 15 – 45% acetonitrile in 30 min using a flow rate of 1 ml/min. **P4-OH/P7-OH**: hydrolysis side product, **P4-MPAA/P7-MPAA**: thioester intermediate, **P21/P22**: ligation products.

The ligation of **P4** was accompanied by high hydrolysis rates (97%) and low ligation yields (3%). After 1 h, peptide **P4** was completely converted into hydrolysis product **P4-OH** (12.8 min) and into a small amount of the MPAA thioester intermediate **P4-MPAA** (22.5 min). After 6 h, a small peak at a retention time of 23.0 min appeared which could be assigned to ligation product **P21** [Ile^{21}]BM2(17-35).

In contrast to the isoleucine carrying peptide **P4** was the ligation of the leucine counterpart **P7** successful. Already after 30 min a high peak at 23.50 min was detectable which could be identified as ligation product **P23** [Leu^{21}]BM2(17-35). In ligation buffer **A** the reaction was completed after 2 h showing only a small amount of peptide hydrolysis (**P7-OH**) at a retention time of 13.8 min. The yield of the ligation reached 87%. Similar to previous studies by Liu *et al*. ligation at C-terminal isoleucine resulted in very low ligation yields of 3% which were unprofitable for long BM2 segments.[60] In order to identify all reaction products, all appearing peaks were separated by RP-HPLC and analysed *via* MALDI-TOF-MS.

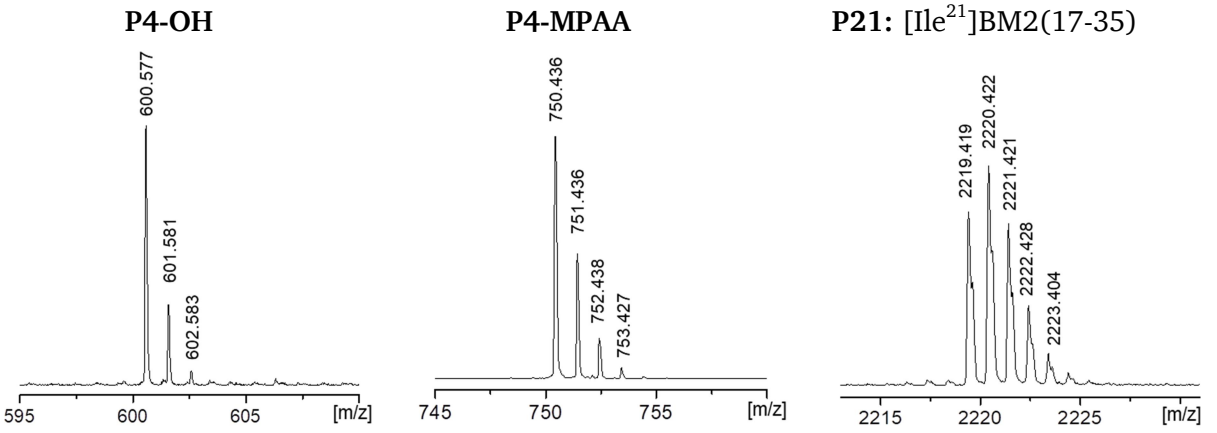

Theoretical monoisotopic mass
$C_{30}H_{45}O_6N_7$
$[M+H]^+$ = 600.350 m/z

Theoretical monoisotopic mass
$C_{38}H_{51}O_7N_7S$
$[M+H]^+$ = 750.364 m/z

Theoretical monoisotopic mass
$C_{103}H_{163}N_{31}O_{22}S$
$[M+H]^+$ = 2219.238 m/z

Figure 5.25: MALDI-TOF-MS and isotopic pattern of the ligation experiment **a)**: **P4-OH**: Hmp hydrolysis side product, **P4-MPAA**: thioester intermediate, **P21**: ligation product [Ile^{21}]BM2(17-35).

a) **P22**: Experimental MALDI-TOF-MS

b) Isotopic pattern $[M+1H]^{1+}$

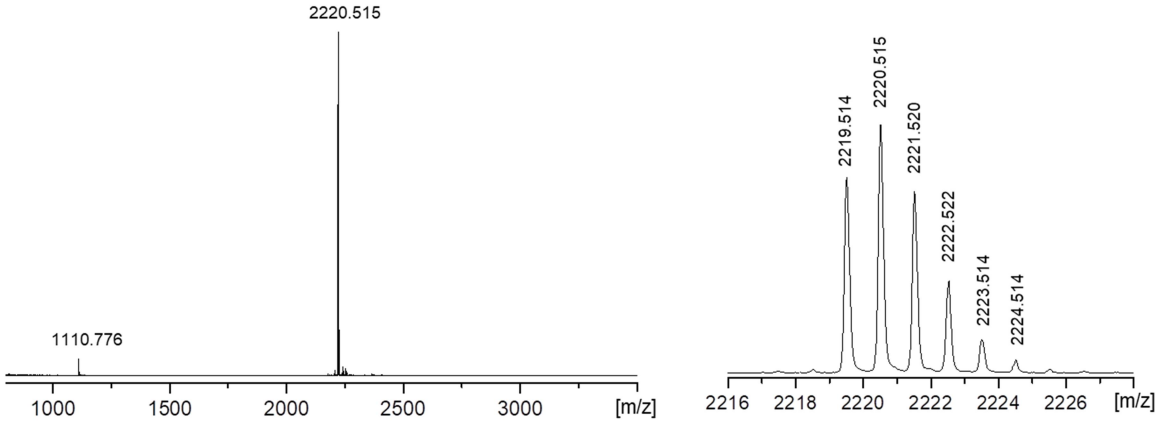

Theoretical average masses
$C_{103}H_{163}N_{31}O_{22}S$
$[M+1H]^{1+}$ = 2220.670 m/z $[M+2H]^{2+}$ = 110.838 m/z

Theoretical monoisotopic mass
$C_{103}H_{163}N_{31}O_{22}S$
$[M+1H]^{1+}$ = 2219.238 m/z

Figure 5.26: MALDI-TOF-MS and isotopic pattern of the ligation experiment **b)**: Mass spectrum of final ligation product **P22** (left) and the isotopic pattern (right).

NCL of model Hmp-peptides P8 and P9 in conventional ligation buffer A

The NCL of the ADO and ADO_2 containing peptides **P8** [Leu^{21}]BM2(17-21)-Hmp-ADO and **P9** [Leu^{21}]BM2(17-21)-Hmp-ADO_2 with model peptide **P1** [Cys^{22}]BM2(22-35) were performed in ligation buffer **A** using the conditions described in protocol **10.1.1**. **P22** [Leu^{21}]BM2(17-35) was obtained as a product of this reaction.

These ligation experiments aimed to evaluate the effect of C-terminal ADO groups at the ligation yield and the amount of hydrolysis. After 30 min, the ligation product **P22** was detected at 23.5 min. Both ligations were completed after 2 h reaching a yield between 85-86%. The amount of Hmp hydrolysis was in line with Hmp-peptides without C-terminal ADO tags and was calculated to be 14-15%. The comparison of both ligations confirmed that there is no difference in the ligation rate or yield, independent from the length of the C-terminal ADO group. The ligation product **P22** was identified *via* MALDI-TOF-MS. In figure **5.27** the results of both ligation experiments are shown.

Table 5.19: Results for ligation experiment of **P8** and **P9** in buffer **A**.

Ligation	No.	Product	Buffer	Time	Hydrolysis	Yield
a)	P22	[Leu^{21}]BM2(17-35)	A	2 h	14%	86%
b)	P22	[Leu^{21}]BM2(17-35)	A	2 h	15%	85%

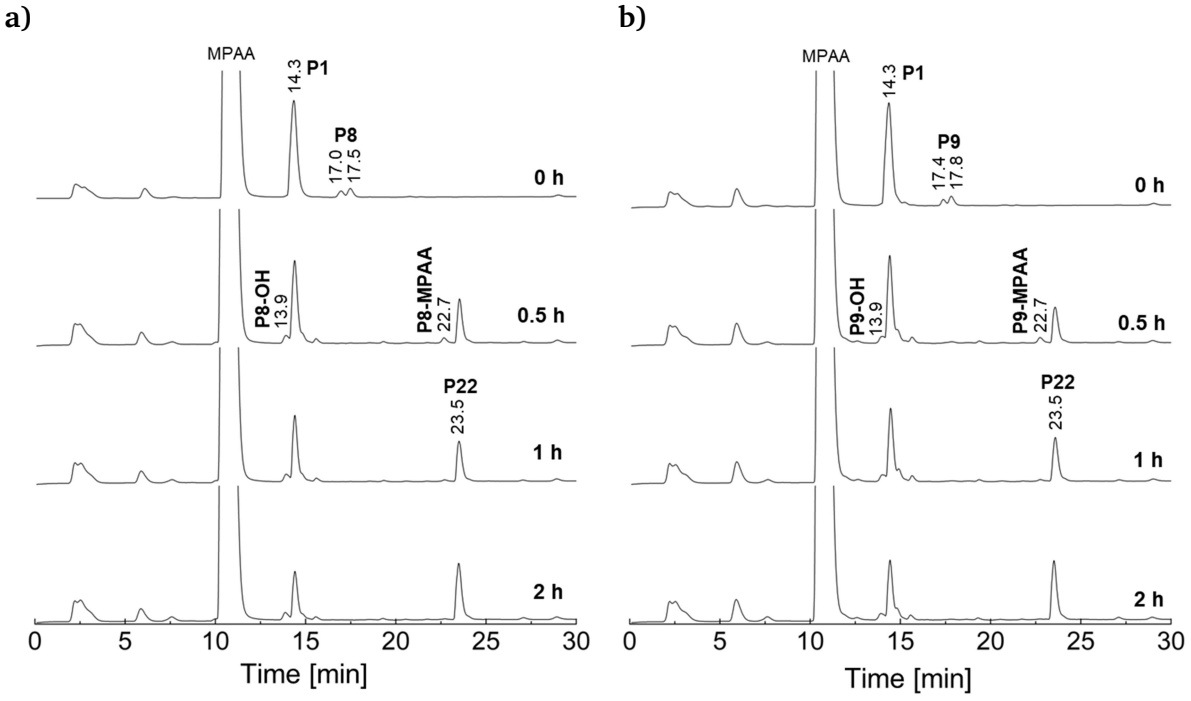

Figure 5.27: Stacked chromatograms of ligation experiments **a)** and **b)**. HPLC conditions: C18 column (150 x 4 mm, 100 Å pore diameter, 3 µm particle size). Gradient: 15 – 45% acetonitrile in 30 min using a flow rate of 1 ml/min. **P8-OH/P9-OH**: hydrolysis side product, **P8-MPAA/P9-MPAA**: thioester intermediate, **P22**: ligation product.

NCL of model Hmp-peptides P11 and P12 in conventional ligation buffer A

One key experiment on the solubilizing tag-assisted ligation strategy was the NCL of the penta-lysine carrying model peptides **P11** [Leu^{21}]BM2(17-21)-Hmp-ADO-Lys$_5$ and **P12** [Leu^{21}]BM2(17-21)-Hmp-ADO$_2$-Lys$_5$ following instruction **10.1.1**. In this ligation experiment the influence of the sterically demanding penta-lysine tag on the ligation yield, retention time and hydrolysis was tested.

Figure **5.28** shows the chromatograms of these experiments. Both penta-lysine carrying starting peptides gave very broad and small peaks in the HPLC and were detected at 6 min (**P11**) and 7.6 min (**P12**). After 30 min, product **P22** [Leu^{21}]BM2(17-35) was obtained at a retention time of 25.1 min. Both ligation experiments reached yields of over 80% and proved that the steric demanding penta-lysine tag had only a small negative effect on the ligation yield. In comparison with previous ligation experiments, slightly higher hydrolysis amounts between 17-19% were observed.

Table 5.20: Results for ligation experiment of **P11** and **P12** in buffer **A**.

Ligation	No.	Product	Buffer	Time	Hydrolysis	Yield
a)	P22	[Leu^{21}]BM2(17-35)	A	2 h	19%	81%
b)	P22	[Leu^{21}]BM2(17-35)	A	2 h	17%	83%

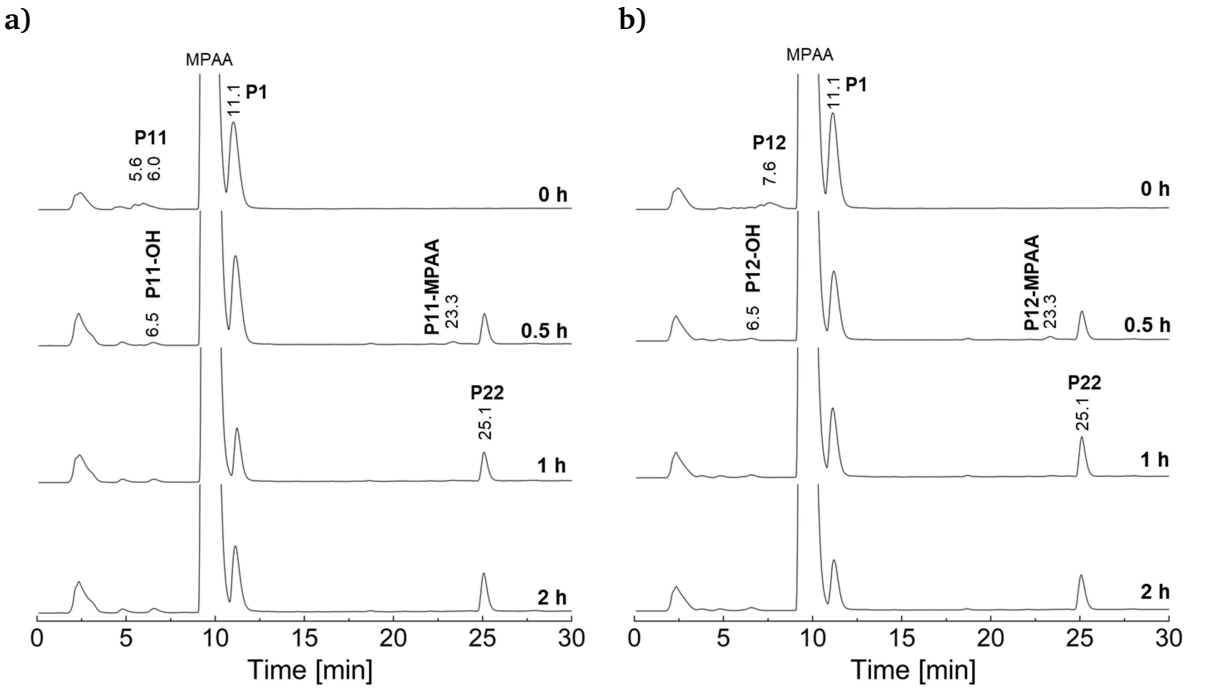

Figure 5.28: Stacked chromatograms of ligation experiments **a)** and **b)**. HPLC conditions: C18 column (150 x 4 mm, 100 Å pore diameter, 3 µm particle size). Gradient: 20 – 40% acetonitrile in 30 min using a flow rate of 1 ml/min. **P11-OH/P12-OH**: hydrolysis side product, **P11-MPAA/P12-MPAA**: thioester intermediate, **P22**: ligation product.

NCL of the complete BM2 Hmp-peptide P20 in conventional ligation buffer A

The main goal of the solubilizing tag-assisted ligation strategy was the production of **P23** [Cys(Acm)^{11}][Leu^{21}][Cys^{22}]BM2(1-51) in the conventional ligation buffer **A**. The good soluble Hmp peptide **P20** [Cys(Acm)^{11}][Leu^{21}]BM2(1-21)-Hmp-ADO-Lys$_5$ was composed of the hydrophobic sequence [Cys(Acm)^{11}]BM2(1-21), the thioester forming Hmp group and the C-terminal ADO-Lys$_5$ solubilizing tag. As a counterpart for the ligation, the N-terminal Cys peptide **P2** [Cys^{22}]BM2(22-51) was applied. Both peptide segments were entirely soluble in the aqueous ligation buffer **A**. In contrast to ligation experiments with short model Hmp-peptides, ligation of long peptide **P20** took 24 h. Reaction progress was thereby followed by analytical RP-HPLC. Figure **5.29** shows the stacked RP-HPLC chromatograms of the ligation experiment. Initial peptides **P2** and **P20** were found at 4.7 min and 11.5 min, respectively. After 2 h, ligation product **P23** [Cys(Acm)^{11}][Leu^{21}][Cys^{22}]BM2(1-51) was detected at 14.5 min. The final ligation product **P23** was obtained with a yield of 71%. Due to the insolubility of thioester intermediate **P20-MPAA**, no complete conversion could be achieved. After 24 h, 11% of thioester intermediate **P20-MPAA** was left. The amount of hydrolysis side product **P20-OH** was calculated to be 18%.

Table 5.21: Results for ligation experiment of **P20** in buffer **A**.

No.	Product	Buffer	Time	Hydrolysis	Yield
P23	[Cys(Acm)^{11}][Leu^{21}][Cys^{22}]BM2(1-51)	A	24 h	18%	71%

Amino acid sequence P23:MLEPFQILSIC(Acm)SFILSALHFLCWTIGHLNQIKRGINMKIRIKGPNKETINR

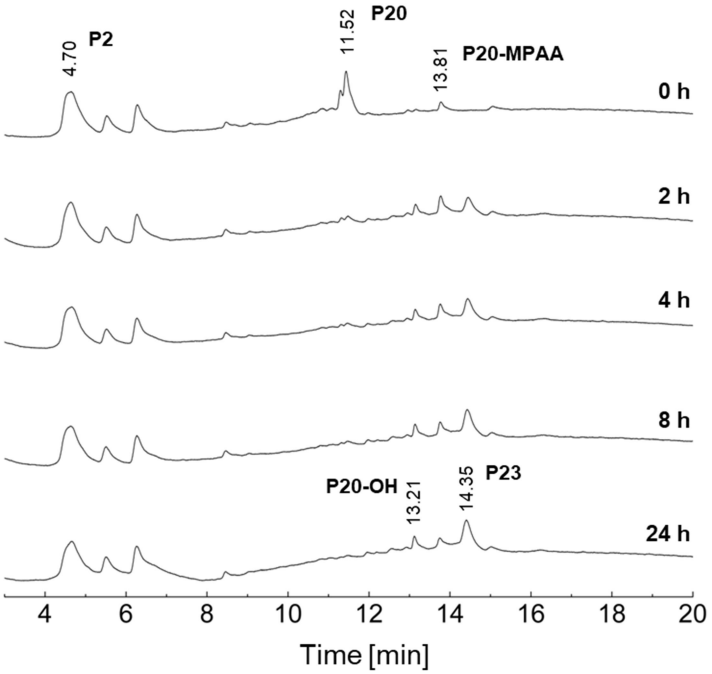

Figure 5.29: Stacked chromatograms for the ligation of Hmp-peptide **P20**. HPLC conditions: C4 column (100 x 4 mm, 100 Å pore diameter, 5 µm particle size). Gradient: 10 – 20% acetonitrile in 5 min followed by 70% acetonitrile in 20 min, rate of 2 ml/min. **P20-OH**: hydrolysis side product, **P20-MPAA**: thioester intermediate, **P23**: ligation product.

In order to identify all new appearing peaks in the chromatogram, ESI-MS analysis was performed. MS showed the expected isotopic pattern of hydrolysis product **P20-OH** and MPAA thioester intermediate **P20-MPAA** at 13.2 min and 13.8 min.

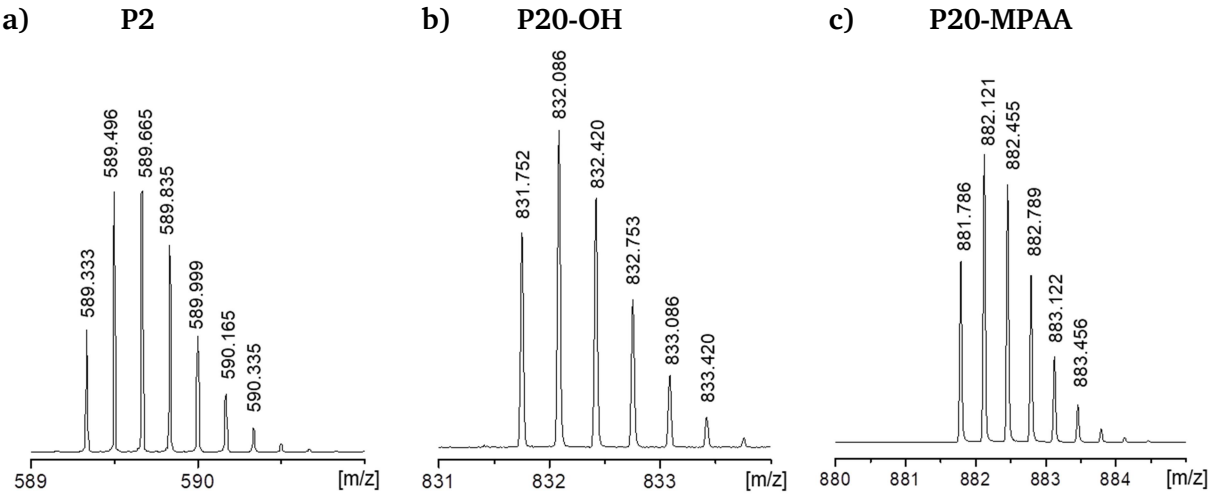

Theoretical monoisotopic mass
$C_{154}H_{264}O_{39}N_{52}S_2$
$[M+6H]^{6+}$ = 589.336 m/z

Theoretical monoisotopic mass
$C_{119}H_{184}N_{25}O_{29}S_2$
$[M+3H]^{3+}$ = 831.445 m/z

Theoretical monoisotopic mass
$C_{127}H_{191}N_{25}O_{30}S_3$
$[M+3H]^{3+}$ = 881.786 m/z

Figure 5.30: ESI-MS and isotopic pattern of the separated peaks from the ligation experiment. **a) P2:** Cys peptide, **b)**: **P20-OH**: hydrolysis side product, **c): P20-MPAA**: thioester intermediate.

Figure **5.31** shows the ESI mass spectrum of ligation product **P23** and the experimental isotopic pattern of the $[M+5H]^{5+}$ ion. The experimental isotopic pattern of ligation product **P23** is in perfect accordance with the simulated pattern of formula $C_{273}H_{447}N_{77}O_{67}S_4$.

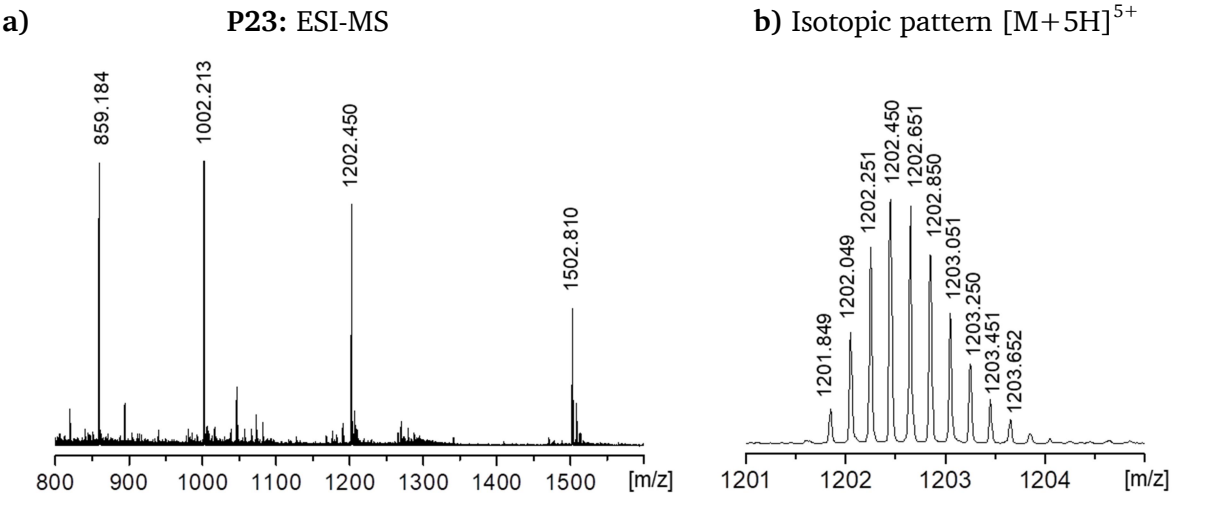

Theoretical average masses
$[M+4H]^{4+}$ = 1503.063 m/z
$[M+5H]^{5+}$ = 1202.652 m/z
$[M+6H]^{6+}$ = 1002.378 m/z
$[M+7H]^{7+}$ = 859.325 m/z

Theoretical monoisotopic mass
$C_{273}H_{447}N_{77}O_{67}S_4$
$[M+5H]^{5+}$ = 1201.864 m/z

Figure 5.31: ESI-MS and isotopic pattern of ligation product **P23**. The experimental isotopic pattern shows the expected monoisotopic molecular weight and isotopic pattern of chemical formula $C_{273}H_{447}N_{77}O_{67}S_4$.

5.2. Investigation of external conditions

5.2.1. Application of fluorinated alcohols as additives for NCL of Hmp-peptides

As alternative strategy to the solubilizing tag-assisted NCL of poorly soluble Hmp-peptides the usage of fluorinated co-solvents was tested. The addition of organic solvents was not only tested to enhance peptide solubility but also to reduce the water content of the ligation buffer. This reduced water content could reduce Hmp hydrolysis and increase the ligation yield.

The TFE-based ligation (buffer **B**) and the HFIP-based ligation (buffer **C**) were investigated by the native chemical ligation of product **P23** [Cys(Acm)^{11}][Leu^{21}][Cys^{22}]BM2(1-51). All ligation experiments were carried out at room temperature and under a nitrogen atmosphere according to instructions **10.1.2** (buffer **B**) and **10.1.3** (buffer **C**).

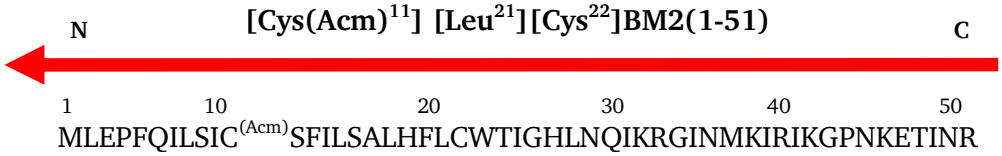

P2: CWTIGHLNQIKRGINMKIRIKGPNKETINR
P16: MLEPFQILSL-Hmp
P18: MLEPFQILSIC$^{(Acm)}$SFILSALHFL-Hmp
P19: MLEPFQILSIC$^{(Acm)}$SFILSALHFL-Hmp-ADO$_2$

Figure 5.32: Amino acid sequences of the final target peptide **P23** [Cys(Acm)^{11}][Leu^{21}][Cys^{22}]BM2(1-51) and the precursors **P2**, **P16**, **P18** and **P19**.

Table 5.22: Performed ligation experiments with long Hmp-peptides in ligation buffer **B** and **C**.

Entry	Ligation product	Cys-peptide	Hmp-peptide	Ligation buffer
P23	[Cys(Acm)^{11}][Leu^{21}][Cys^{22}]BM2(1-51)	P2	P18a	B
	[Cys(Acm)^{11}][Leu^{21}][Cys^{22}]BM2(1-51)	P2	P18a	C
	[Cys(Acm)^{11}][Leu^{21}][Cys^{22}]BM2(1-51)	P2	P18b	C
	[Cys(Acm)^{11}][Leu^{21}][Cys^{22}]BM2(1-51)	P2	P19a	C
	[Cys(Acm)^{11}][Leu^{21}][Cys^{22}]BM2(1-51)	P2	P19b	C
P27	[Leu^{10}]BM2(1-51)	P3	P16a	C
	[Leu^{10}]BM2(1-51)	P3	P16b	C

a *Hmp-peptide diastereomer 1.*
b *Hmp-peptide diastereomer 2.*

5.2.2. TFE-assisted NCL of Hmp-peptides in buffer B

TFE is long known as excellent solvent for poorly soluble peptides and was investigated multiple times for its folding improving properties (chapter **3.5.2**).[126a, 209] Kwon and Tietze have already described the ligation of the influenza A proton channel sequence M2(22-71) using TFE as co-solvent.[131] However, TFE containing phosphate buffers have never been tested as ligation media for Hmp-peptides. In this study, the effect of TFE to the ligation yield and Hmp hydrolysis was investigated.

For the ligation of the poorly soluble Hmp-peptide **P19a** [Cys(Acm)^{11}][Leu^{21}]BM2(17-21)-Hmp-ADO$_2$ a mixture of 33% TFE and 67% of ligation buffer **A** was prepared. As N-terminal cysteine fragment peptide **P2** [Cys^{22}]BM2(22-51) was chosen. Peptide **P23** [Cys(Acm)^{11}][Leu^{21}][Cys^{22}]BM2(1-51) was expected as ligation product. In contrast to the conventional phosphate buffer **A**, peptide **P19a** was completely soluble in the presence of TFE (buffer **B)**. RP-HPLC and ESI-MS indicated the formation of the MPAA-thioester intermediate **P19-MPAA** (14.9 min) and hydrolysis product **P19-OH** (14.0 min) immediately after the start of the ligation. The expected ligation product **P23** was detected after 1 h at a retention time of 15.3 min. After 8 h, 35% of thioester intermediate **P19-MPAA** was still left while the hydrolysis product reached 24%. The hydrophobic ligation product **P23** [Cys(Acm)^{11}][Leu^{21}][Cys^{22}]BM2(1-51) was obtained with a yield of 32%.

Table 5.23: Results for ligation experiment of **P19a** in buffer **B**.

No.	Product	Buffer	Time	Hydrolysis	Yield
P23	[Cys(Acm)^{11}][Leu^{21}][Cys^{22}]BM2(1-51)	B	8 h	24%	32%

Amino acid sequence P23:MLEPFQILSIC(Acm)SFILSALHFLCWTIGHLNQIKRGINMKIRIKGPNKETINR

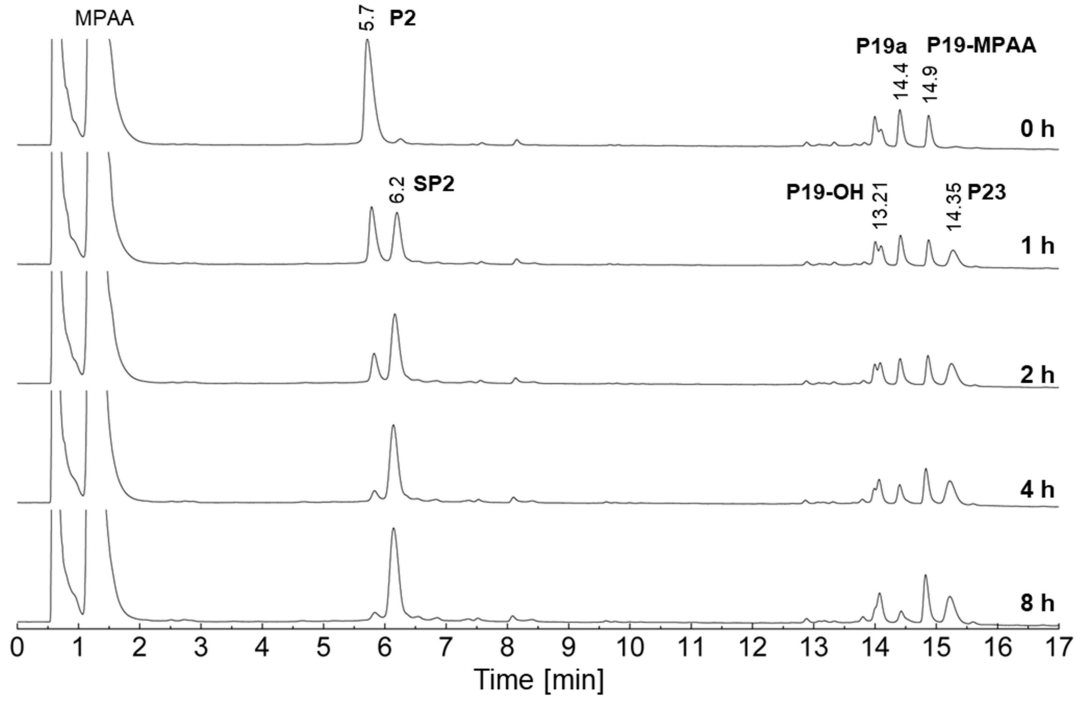

Figure 5.33: Ligation experiment in buffer **B**. HPLC conditions: C4 column (MultoHigh U C4, 100 x 4 mm). Gradient: 10 – 20% acetonitrile in 5 min followed by 20 – 70% acetonitrile in 20 min, flow rate 2 ml/min.

Figure **5.34b** displays the ESI-MS and isotopic pattern of ligation product **P23** with the formula $C_{273}H_{447}N_{77}O_{67}S_4$. Interestingly, the formation of an unknown side product **SP2** could be observed at a retention time of 6.2 min that continuously increased over a period of 8 h. Side product **SP2** turned out as unreactive during the ligation and led to an interruption after 4 h. The mass spectrum and isotopic pattern of side product **SP2** is in line with formula $C_{155}H_{262}O_{40}N_{52}S_2$ and shows an exact mass increase of 26 Da.

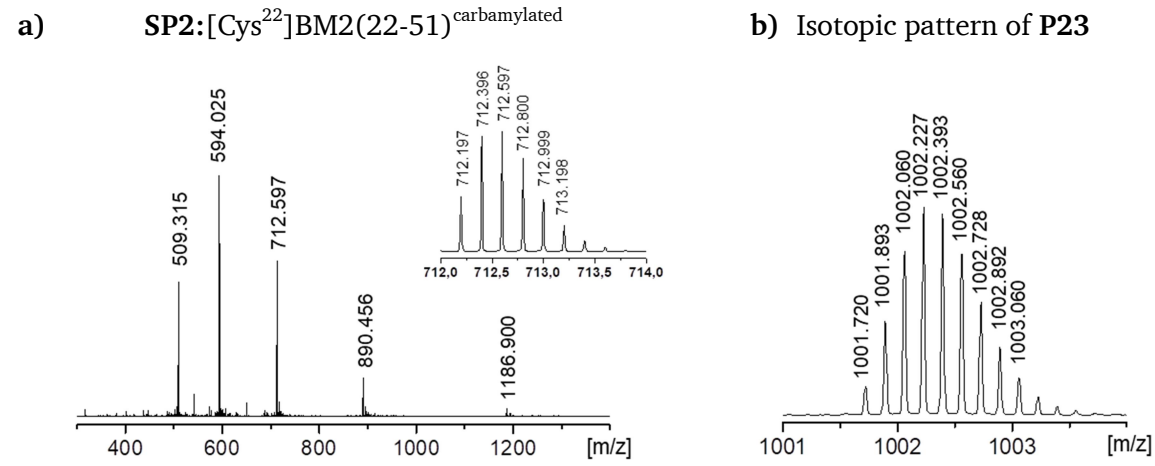

Theoretical average masses

$[M+4H]^{4+}$ = 890.558 m/z $[M+6H]^{6+}$ = 594.041 m/z

$[M+5H]^{5+}$ = 712.648 m/z $[M+7H]^{7+}$ = 509.322 m/z

Theoretical monoisotopic mass

$C_{273}H_{447}N_{77}O_{67}S_4$

$[M+6H]^{6+}$ = 1001.721 m/z

Figure 5.34: **a)** ESI-MS of side product **SP2** with the isotopic pattern, b) Isotopic pattern of ligation product **P23**. For exact ESI-MS to the third decimal place the mass spectrometer was recalibrated using a peptide standard.

The fact that **SP2** was unreactive during the native chemical ligation led to the assumption that the N-terminal cysteine residue of peptide **P2** was modified in ligation buffer **B**. A possible structure that can be assigned to the found mass spectrum and chemical formula $C_{155}H_{262}O_{40}N_{52}S_2$ is shown in figure **5.35**. The formation of a 2-oxo-4-thiazolidine modification at the N-terminus nicely explains the loss of reactivity during the ligation and explains the found mass increase of exact 26 Da.

Figure 5.35: Possible side product **SP2** that was formed during the NCL in buffer **B**. The isotopic pattern of this theoretical structure is in perfect line with formula $C_{155}H_{262}O_{40}N_{52}S_2$.

The formation of **SP2** can be explained by carbamylation of the cysteine residue. Carbamylation of proteins has been reported in the literature for lysine[210] and cysteine[211] residues as result of cyanate formation derived from urea.[212] In solution, ammonium cyanate and urea are in equilibrium.[213] Stark *et al*. were able to demonstrate that carbamylation can be followed by cyclisation to a five membered ring intermediate.[214] Especially, thiol groups were carbamylated more rapidly than any other functional groups within the peptide chain.[215] This finding suggest that TFE could promote carbamylation of N-terminal cysteine peptides in the presence of urea. As result buffer **B** turned out as ineligible for the NCL of **P23**.

5.2.3. HFIP-assisted NCL of Hmp-peptides in buffer C

Ligation of Hmp-peptide P18 with N-terminal Cys peptide P2

Since the TFE-assisted ligation in buffer **B** led to an unexpected modification of peptide **P2**[Cys^{22}]BM2(22-51), a different buffer system was tested. As an alternative co-solvent for TFE, the secondary alcohol HFIP was tested as an additive for the preparation of ligation buffer **C**. Similar to TFE, HFIP has also long been known as an excellent solvent for hydrophobic peptides with folding promoting properties. Previous ligation experiments confirmed that a pH over 7 is necessary for a successful ligation in the presence of HFIP.[94] For Hmp-peptides, the optimal pH was found to be 7.5. Buffer **C** was composed of 33% HFIP and 67% of ligation buffer **A** following procedure **10.1.3**. HPLC analysis of the cysteine-containing peptide **P2** in buffer **C** showed no signs of N-terminal modifications. Additionally, both peptide diastereomers **P18a** or **P18b** were completely soluble in buffer **C**. The ligation was started by pre-dissolving the peptides **P2** and **P18** in HFIP followed by the addition of buffer **A**.

Table 5.24: Results for ligation experiments of **P18a** and **P18b** in buffer **C**.

Ligation	Dia.	Product	Buffer	Time	Hydrolysis	Yield
a)	1	[Cys(Acm)^{11}][Leu^{21}][Cys^{22}]BM2(1-51)	C	24 h	6%	94%
b)	2	[Cys(Acm)^{11}][Leu^{21}][Cys^{22}]BM2(1-51)	C	24 h	5%	95%

Amino acid sequence P23:MLEPFQILSIC(Acm)SFILSALHFLCWTIGHLNQIKRGINMKIRIKGPNKETINR

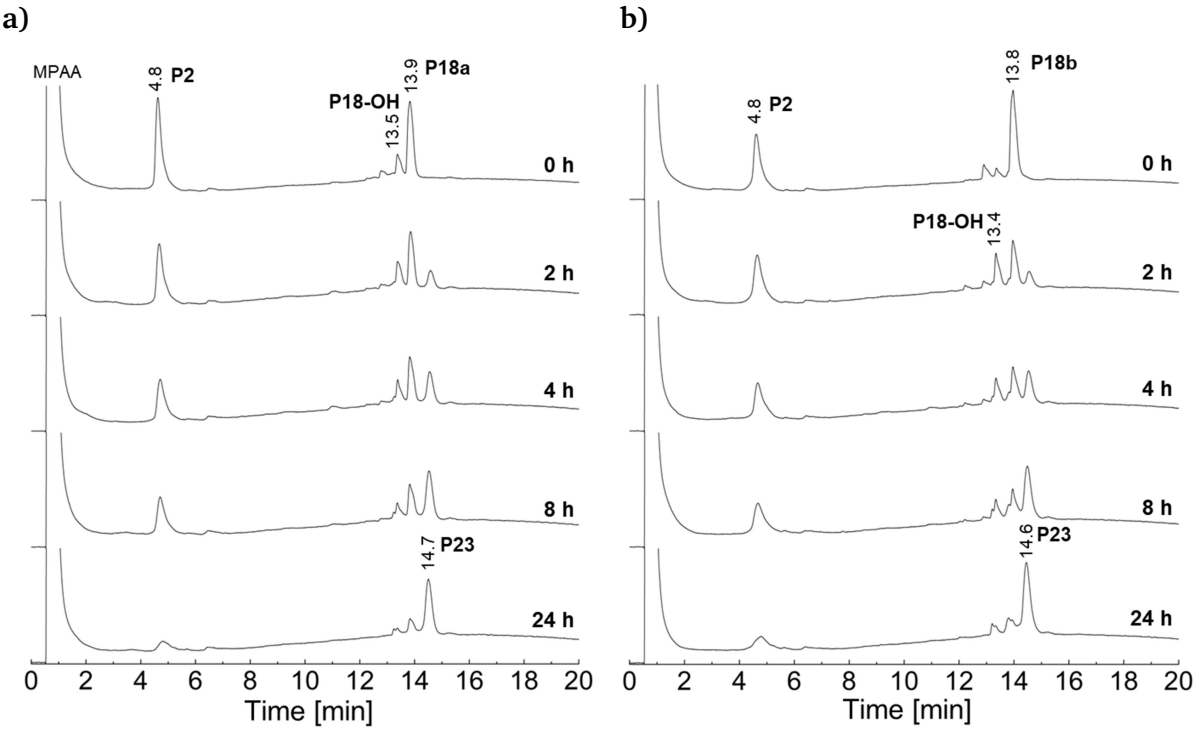

Figure 5.36: Stacked chromatograms of the ligation experiments **a)** and **b)**. HPLC conditions: C18 column (150 x 4 mm, 100 Å pore diameter, 3 µm particle size). Gradient: 15 – 45% acetonitrile in 30 min, flow rate of 1 ml/min. **P18-OH**: hydrolysis side product, **P23**: ligation product.

At the beginning of the ligation, peptide **P2** (4.8 min), hydrolysis product **P18-OH** (13.5 min) and Hmp-peptide diastereomers **P18a**/**P18b** (13.9/13.8 min) were visible in the chromatogram. After 2 h, product **P23** [Cys(Acm)^{11}][Leu^{21}][Cys^{22}]BM2(1-51) was detectable at 14.7 min (figure **5.36**). After 24 h, both ligations were completed showing no differences between the peptide diastereomers **P18a** and **P18b**. Except Hmp hydrolysis no further side reaction could be observed in buffer **C**. An interesting finding during NCL in buffer **C** was the unexpectedly high stability of the Hmp moiety at pH of 7.5. In previous experiments Hmp turned out to be extremely prone to hydrolysis at pH values higher than 7.0. Surprisingly, HFIP addition was not only able to increase the peptide dissolution it was also able to reduce the amount of Hmp hydrolysis considerably. In contrast to ligation experiments in buffer **A** or **B**, NCL in buffer **C** reached nearly quantitative ligation yields. At the end of the ligation, 94% yield for **P18a** and 95% yield for **P18b** were obtained.

To identify and compare both ligation products ESI-MS spectra were recorded from all captured peaks in the chromatogram. In figure **5.37** the entire mass spectrum and isotopic pattern of both ligation products **P23** are illustrated. Both experimental isotopic patterns displayed the expected monoisotopic mass of **P23** and were in perfect agreement with the simulated isotopic pattern of chemical formula $C_{273}H_{447}N_{77}O_{67}S_4$.

a) **P23:** ESI-MS

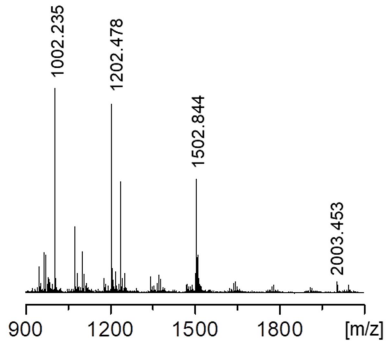

Theoretical average masses
$[M+4H]^{4+}$ = 1503.063 m/z
$[M+5H]^{5+}$ = 1202.652 m/z

b) **P23** of ligation a)

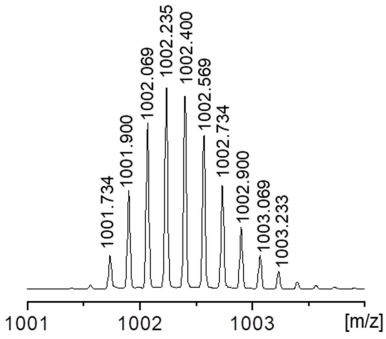

Theoretical monoisotopic mass
$C_{273}H_{447}N_{77}O_{67}S_4$
$[M+6H]^{6+}$ = 1001.721 m/z

c) **P23** of ligation b)

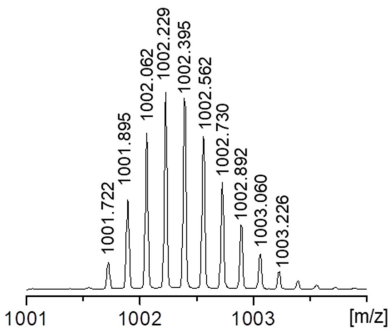

Theoretical monoisotopic mass
$C_{273}H_{447}N_{77}O_{67}S_4$
$[M+6H]^{6+}$ = 1001.721 m/z

Figure 5.37: Comparison of ESI mass spectrum and isotopic pattern of ligation products **P23** [Cys(Acm)^{11}][Leu^{21}][Cys^{22}]BM2(1-51).

The successful synthesis of product **P23** in buffer **C** was a breakthrough. The reduction of water content by HFIP addition especially suppressed Hmp hydrolysis. The experiment demonstrated that HFIP is an excellent co-solvent to produce hydrophobic transmembrane peptides out of Hmp-peptide fragments. In subsequent experiments, buffer **C** was also used for the ligation of different peptide segments. Moreover, the high dissolution potential makes ligation buffer **C** an excellent media for other peptide modifications such as Cys desulfurization, since it did not cause any unwanted modifications at both fragments. In the further course of this work buffer **C** was investigated as a solvent system for Cys desulfurization of poorly soluble, hydrophobic transmembrane peptides (chapter **5.3**).

Ligation of Hmp-peptide P19 with N-terminal Cys peptide P2

Further evidence for the efficiency of ligation buffer **C** was the successful ligation of **P23** [Cys(Acm)^{11}][Leu^{21}][Cys^{22}]BM2(1-51) using the peptide diastereomers **P19a** or **P19b** [Leu^{21}]BM2(17-21)-Hmp-ADO$_2$. Both peptides were modified with a C-terminal ADO$_2$ tag. As N-terminal Cys peptide **P2** [Cys^{22}]BM2(22-51) was applied. Both peptide fragments were completely soluble in buffer **C**. In figure **5.38** the stacked chromatograms of both ligation experiments are compared. The N-terminal cysteine peptide **P2** was detected at a retention time of 4.6 min. After 2 h, the MPAA intermediate **P19-MPAA** (14.5 min) and ligation product **P23** (14.5 min) were visible. The ligation was completed after 24 h and showed no unexpected side reactions. Peptide **P18a** reached a yield of 81% which was explained by a slightly higher pH adjustment (pH 7.7) during the preparation of the ligation buffer. However, **P18b** resulted in 95% ligation yield at a pH of 7.5 which was in line with previous experiments in buffer **C** at the same pH value.Similar to previous ligation experiments with short model Hmp-peptides, **P8** and **P9** (chapter **5.1.9**) the ADO$_2$ tag had no negative effect on the ligation yield.

Table 5.25: Results for ligation experiments of **P19a** and **P19b** in buffer **C**.

Ligation	Dia.	Product	Buffer	Time	Hydrolysis	Yield
a)	1	[Cys(Acm)^{11}][Leu^{21}][Cys^{22}]BM2(1-51)	C	24 h	18%	82%
b)	2	[Cys(Acm)^{11}][Leu^{21}][Cys^{22}]BM2(1-51)	C	24 h	5%	95%

Amino acid sequence P23:MLEPFQILSIC(Acm)SFILSALHFLCWTIGHLNQIKRGINMKIRIKGPNKETINR

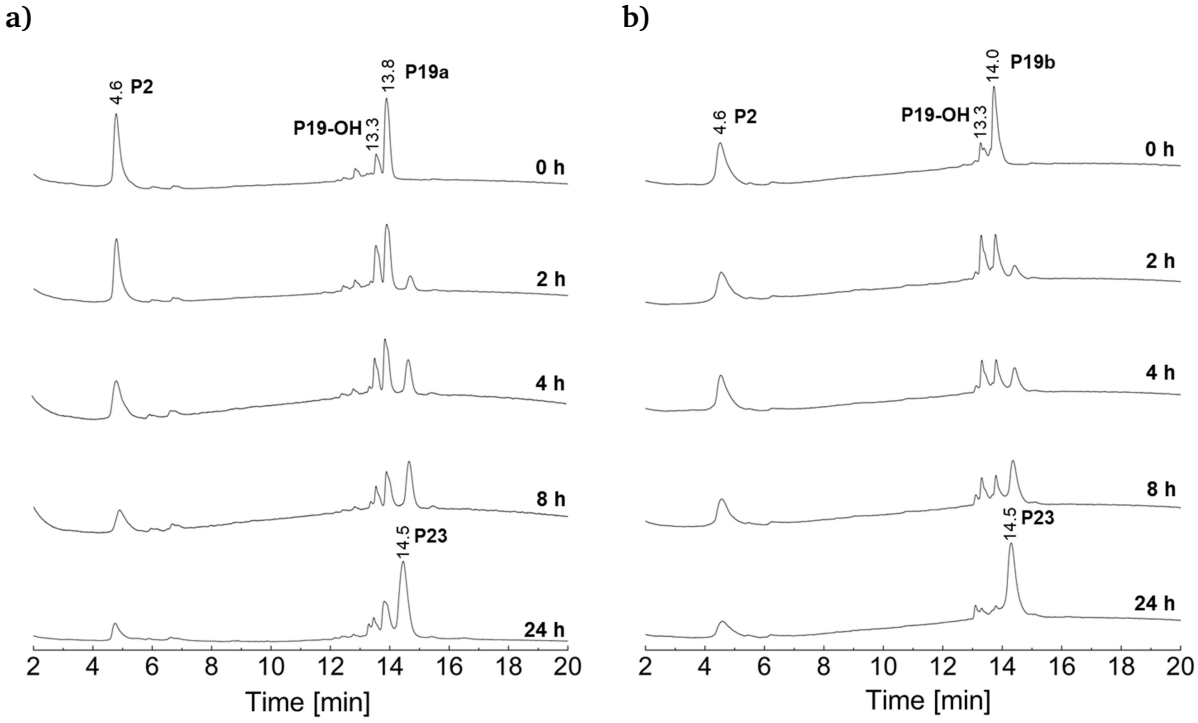

Figure 5.38: Stacked chromatograms of the ligation experiments **a)** and **b)**. HPLC conditions: C18 column (150 x 4 mm, 100 Å pore diameter, 3 µm particle size). Gradient: 15 – 45% acetonitrile in 30 min, flow rate of 1 ml/min. **P19-OH**: hydrolysis product, **P23**: ligation product.

The final ligation product **P23** [Cys(Acm)^{11}][Leu^{21}][Cys^{22}]BM2(1-51) that was produced by NCL in buffers **A**, **B** and **C** was purified *via* preparative RP-HPLC according to procedure **8.1.7**. In figure **5.39** the analytical reinjection of product **P23** is depicted. The chromatogram displays one single peak at 14.47 min and no further impurities. After purification **P23** was analysed by ESI-MS and SDS-PAGE.

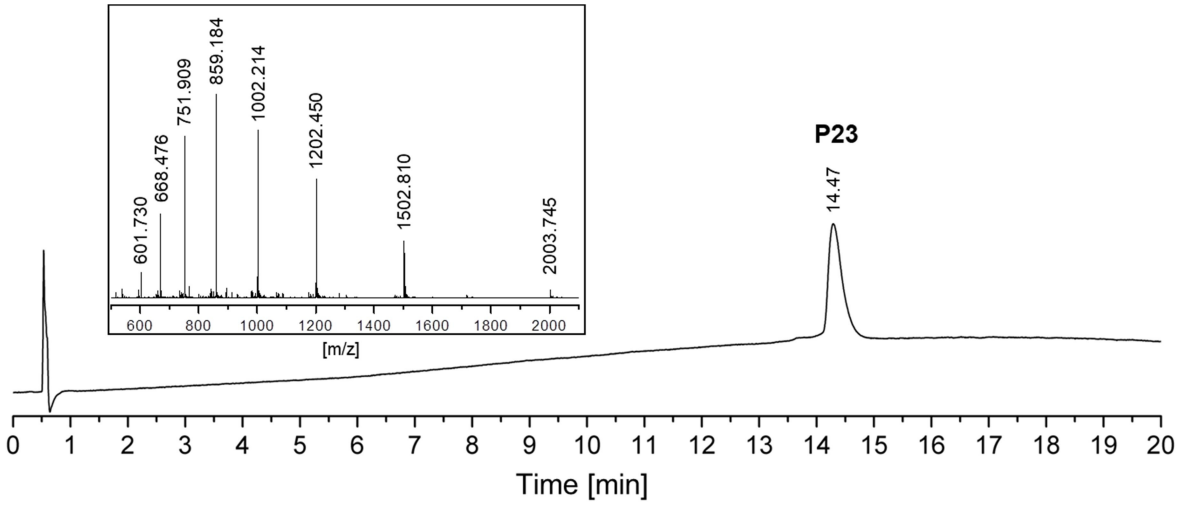

Figure 5.39: Analytical RP-HPLC chromatogram and ESI-MS of ligation product **P23**. HPLC conditions: C4 column (MultoHigh U C4, 100 x 4 mm). Gradient: 10 - 20% acetonitrile in 5 min followed by 20 - 70% acetonitrile in 20 min, flow rate 2 ml/min.

Figure **5.40** shows the result of the SDS-polyacrylamide gel electrophoresis (SDS-PAGE) in ligation buffer **A** (**LB**), the diluted ligation buffer **A** (**DLB**) and the purified peptide **P23**. The peptides were denaturated in the presence of dithiothreitol (DTT), for 10 min, at 95°C according to instruction **8.1.11**. Compared to the coloured marker (**M**), all fractions show a protein mass between 5-10 kDa that belongs to ligation product **P23** with an average molecular weight of 6008.2 Da.

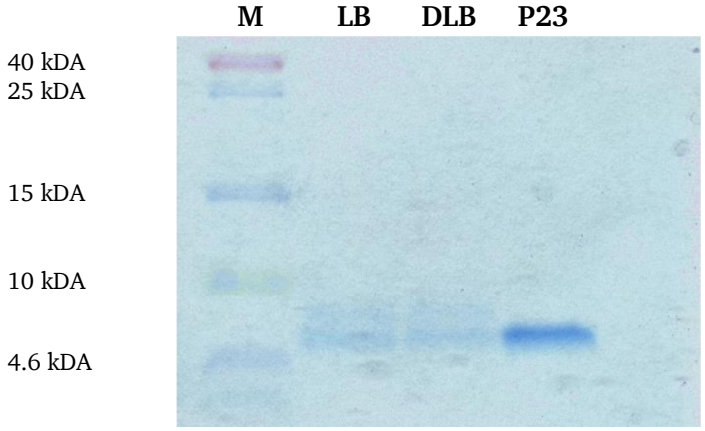

Figure 5.40: SDS-PAGE of ligation product **P23** in the presence of reducing agent DTT, (**LB**) ligation buffer, (**DLB**) diluted ligation buffer (buffer A/water (1:1, v/v)) and the purified ligation product peptide (**P23**). SDS page was performed using 20% acrylamide gel that was prepared from acrylamide / bisacrylamide solution (29:1). Coomassie G-250 was used for staining.

Ligation of Hmp-peptide P16 with N-terminal Cys peptide P3

Buffer **C** was also investigated for the native chemical ligation of **P27** [Leu^{10}]BM2(1-51) using the Hmp-peptide diastereomer **P16a** or **P16b** [Leu^{10}]BM2(1-10)-Hmp and the N-terminal cysteine peptide **P3** [Cys^{11}]BM2(11-51). Again, all peptide segments were soluble in buffer **C**. Already at the beginning of the reaction, ligation product **P27** was detected at 21.49 min. Nevertheless, the reaction took 24 h until Hmp-peptides **P16a** or **P16b** disappeared entirely. At the end of the reaction, hydrolysis product **P16-OH** was detected at 14.80 min. After 24 h, ligation yields of 87% for **P16a** and 88% for **P16b** were achieved.

Table 5.26: Results for ligation experiments of **P16a** and **P16b** in buffer **C**.

Ligation	Dia.	Product	Buffer	Time	Hydrolysis	Yield
a)	1	[Leu^{10}]BM2(1-51)	C	24 h	13%	87%
b)	2	[Leu^{10}]BM2(1-51)	C	24 h	12%	88%

Amino acid sequence P23:MLEPFQILSLCSFILSALHFLCWTIGHLNQIKRGINMKIRIKGPNKETINR

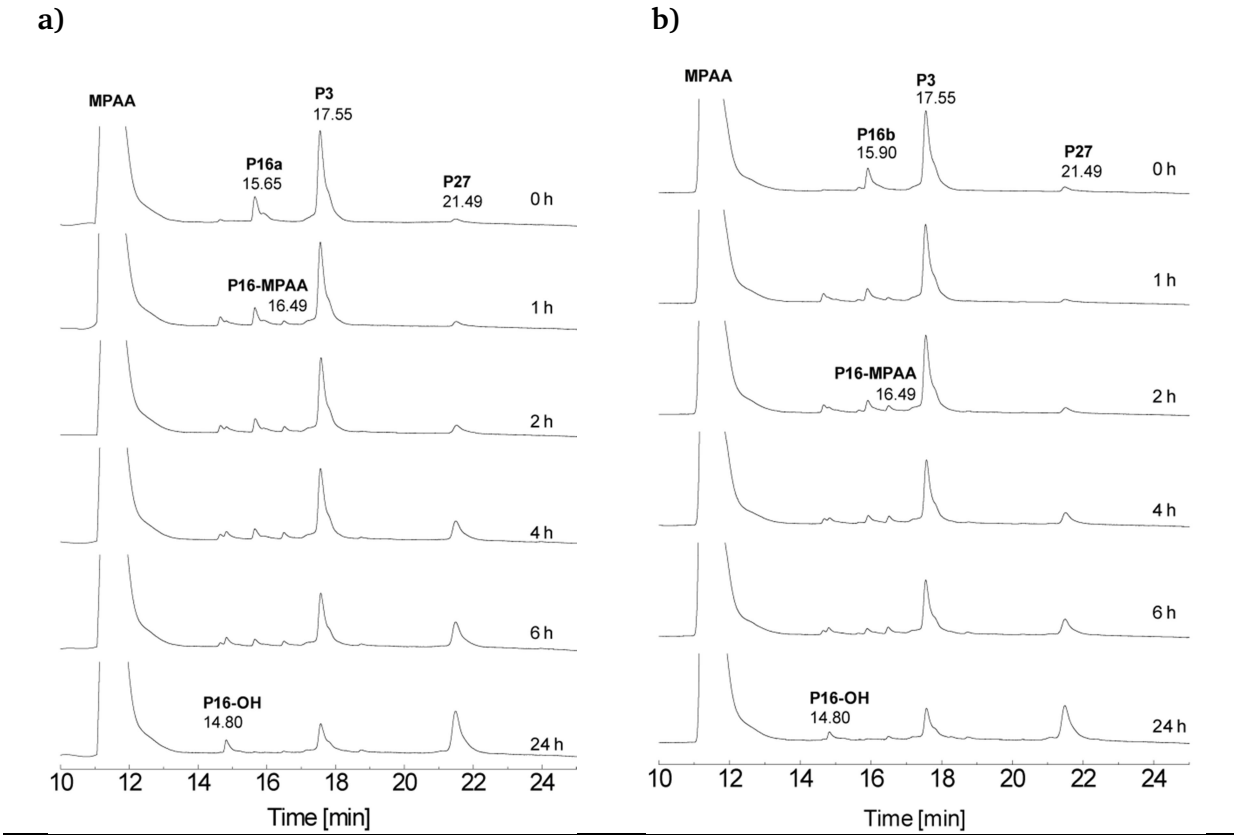

Figure 5.41: Stacked chromatograms of the ligation experiments **a)** and **b)**. HPLC conditions: C18 column (150 x 4 mm, 100 Å pore diameter, 3 µm particle size). Gradient: 10% acetonitrile for 3 min followed by 99% acetonitrile in 30 min, flow rate: 1 ml/min. **P16-OH**: hydrolysis product, **P16-MPAA**: thioester intermediate, **P23**: ligation product.

The use of peptide fragments **P16** and **P3** provided a great advantage compared to the ligation of Hmp-peptides **P18** [Leu^{21}]BM2(17-21)-Hmp or **P19** [Leu^{21}]BM2(17-21)-Hmp-ADO$_2$ with **P2** [Cys^{22}]BM2(22-51). The additional incorporation of Acm protected Cys11 followed by Cys22 desulfurization and Acm deprotection was unnecessary, since Cys11 occurs in the native peptide sequence of BM2(1-51). As final ligation product peptide **P27** [Leu^{10}]BM2(1-51) was acquired. After purification following procedure **8.1.7**, final ligation

product **P27** [Leu^{10}]BM2(1-51) was analyzed *via* RP-HPLC and ESI-MS (figure **5.42**). Analysis *via* RP-HPLC analysis showed the product peak at a retention time of 19.95 min. The experimental monoisotopic mass and isotopic pattern of product **P27** were in line with the simulated isotopic pattern of formula $C_{270}H_{442}N_{76}O_{66}S_3$.

a) Analytical RP-HPLC of [Leu^{10}]BM2(1-51)

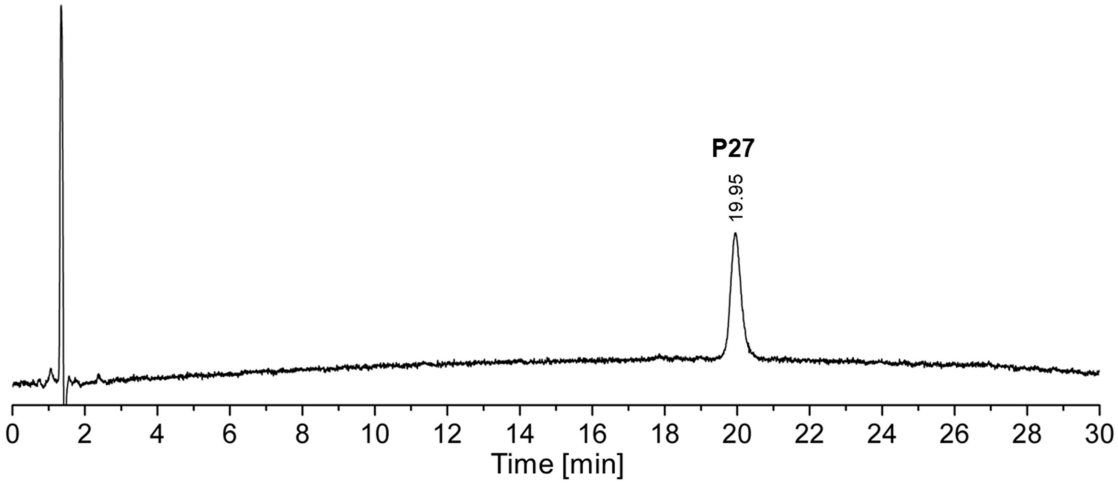

b) ESI-MS of **P27** [Leu^{10}]BM2(1-51)

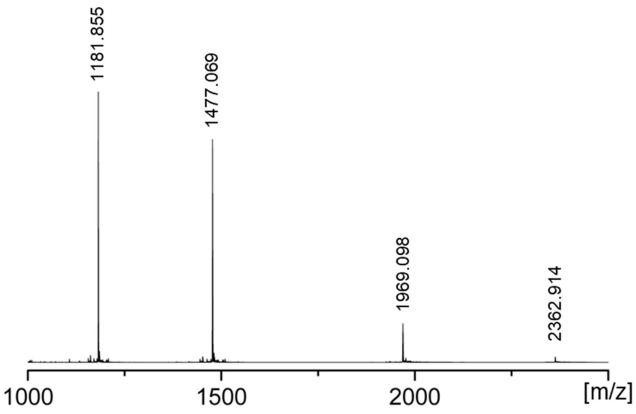

c) Isotopic pattern of **P27**

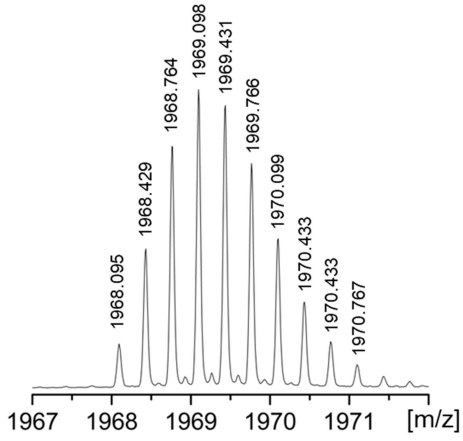

Theoretical average masses

$[M+5H]^{5+}$ = 1182.023 m/z $[M+3H]^{3+}$ = 1969.367 m/z

$[M+4H]^{4+}$ = 1477.277 m/z $[M+2H]^{2+}$ = 2951.644 m/z

Theoretical monoisotopic mass

$C_{270}H_{442}N_{76}O_{66}S_3$

$[M+3H]^{3+}$ = 1968.098 m/z

Figure 5.42: **a)** Analytical RP-HPLC chromatogram of ligation product **P27**. HPLC was performed with a C4 column (MultoHigh U C4, 100 x 4 mm), gradient: 40–70% acetonitrile in 30 min, flow rate 1 ml/min, **b)** experimental ESI-MS and **c)** isotopic pattern of peptide **P27**.

5.2.4. Investigation of the ionic liquid [C_2mim][OAc] as reaction media

Study of 1-Ethyl-3-methyl-imidazolium acetate reactivity towards biomolecules

The low toxicity, the capability of dissolving highly hydrophobic peptides and the folding-inducing properties make 1-ethyl-3-methyl-imidazolium acetate ([C_2mim][OAc]) to an ideal media for poorly water soluble membrane peptides. However, some publications report about the generation of N-heterocyclic carbenes (NHCs) in the neat ionic liquid [C_2mim][OAc] (chapter **3.5.4**).[155-156] Since the amino acid cysteine is the most chemically reactive group within the peptide chain, unexpected modifications of cysteine are possible in the presence of [C_2mim][OAc]. In order to identify those side products and to suppress unwanted side reactions, experiments with small sulfur-containing model compounds were performed. In a first study the organic compounds thiophenol (PhSH), diphenyl disulfide (PhSSPh), benzyl sulfide (BzlSH) and dibenzyl disulfide (BzlSSBzl) were dissolved in the neat ionic liquid [C_2mim][OAc] and analysed *via* RP-HPLC, TLC, ESI-MS and NMR spectroscopy.

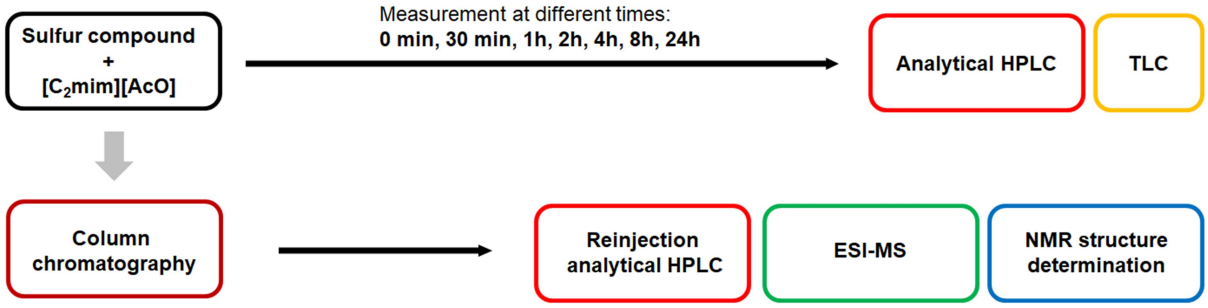

Figure 5.43: Analytical and preparative methods for the investigation of NHC-induced modifications of sulfur-containing model compounds and N-terminal cysteine peptides.

The simple structure of organic sulfur-containing compounds allowed a fast structure determination by NMR. In a follow-up study, using model peptide **P1** [Cys^{22}]BM2(22-35), possible peptide modifications by the neat ionic liquid [C_2mim][OAc] were investigated by ESI-MS. Finally, conditions in which NHC formation can be entirely supressed were searched. These findings allowed the development of ionic liquid based ligation buffers on the basis [C_2mim][OAc].

Table 5.27: Sulfur containing compounds which were dissolved and analysed in [C_2mim][OAc].

Entry	Model compound	Abbreviation
C1	Thiophenol	PhSH
C2	Benzyl sulfide	BzlSH
C5	Diphenyl disulfide	PhSSPh
C6	Dibenzyl disulfide	BzlSSBzl
P1	CWTIGHLNQIKRGI	[Cys^{22}]BM2(22-35)

5.2.5. Reaction of thiophenol and diphenyl disulfide in [C_2mim][OAc]

To understand NHC-induced chemical modifications of sulfur-containing substances thiophenol **C1** and diphenyl disulfide **C2** were dissolved and analyzed in the neat [C_2mim][OAc] according to procedure **8.1.1**. Both substances showed good solubility in the ionic liquid. The reaction is characterised by two equilibriums which are represented in figure **5.44**. A first equilibrium between the reduced form **C1** and the oxidized form **C2** and a second equilibrium between the positive charged imidazolium cation and the neutral deprotonated imidazolium carbene.

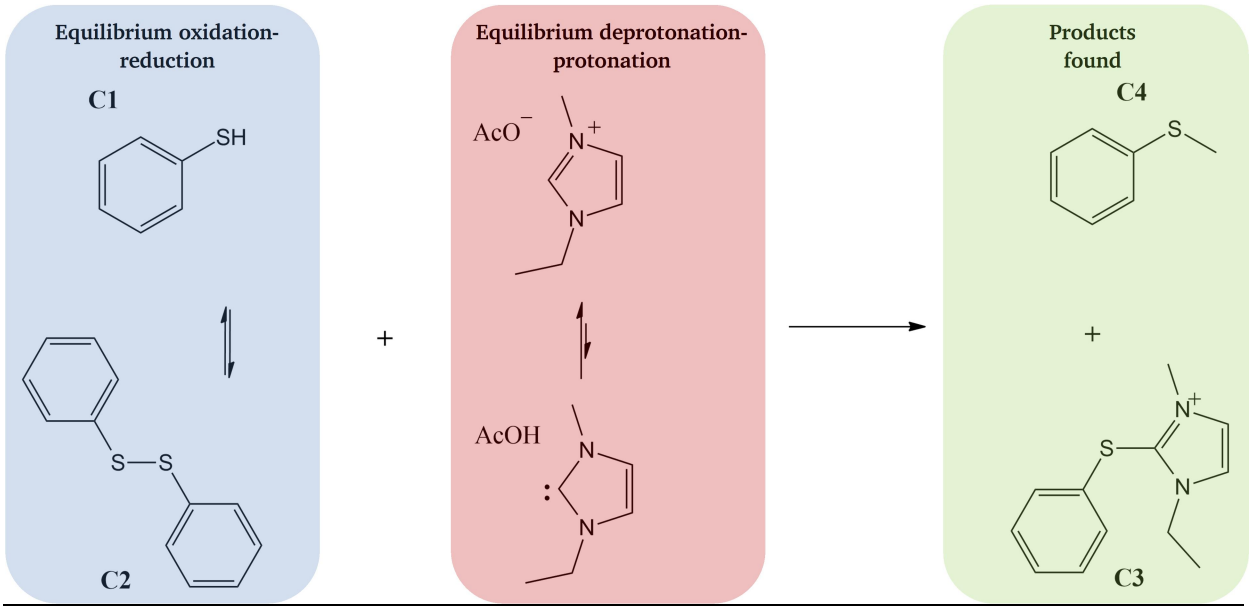

Figure 5.44: NHC formation and modification of thiophenol **C1** and diphenyl disulfide **C2** in neat [C_2mim][OAc].

After dissolution and HPLC analysis of **C1** in neat [C_2mim][OAc], three different peaks appeared at 4.49 min, 10.79 min and 19.39 min (figure **5.45**). The peak at 10.79 min was assigned to educt **C1**. After 5 min reaction time, significant amounts of oxidation product **C2** was detected at 19.39 min. Additionally, a peak at 4.49 min appeared directly at the start of the reaction. According to NMR spectroscopy and ESI-MS, this peak was identified as reaction product **C3** (figure **5.4.6**). After 8 h, starting compound **C1** was almost completely transformed into product **C3**. After 12 h reaction time, product **C3** was isolated as orange liquid by column chromatography applying a mixture of acetonitrile and water (9:1, v/v) as mobile phase.

Approximately 4 h after dissolution of compound **C1** in the neat [C_2mim][OAc], product **C4** was detected at a retention time of 12.39 min. After 72 h reaction time, product **C4** was left as the main product. However, product **C4** was difficult to isolate *via* column chromatography and vacuum evaporation. Therefore, product **C4** was directly extracted with cyclohexane-d12 from the reaction mixture and analyzed by NMR (figure **5.4.7**). Surprisingly, reaction product **C4** could be identified as thioanisole indicating a second possible side-reaction of aromatic thiols in the neat ionic liquid. Obviously, [C_2mim][OAc] was also capable of methylating the thiol group of aromatic thiols such as thiophenol. Interestingly, only the methylated but not the ethylated form was obtained in this reaction.

The dissolution and analysis of diphenyl disulfide (**C2**) in the neat ionic liquid [C_2mim][OAc] led to the same products as the reaction of thiophenol (**C1**). However, formation of **C3** and **C4** was distinctly faster when **C2** was used as starting compound, indicating that diphenyl disulfide is the actual reactant in this reaction. In the case of diphenyl disulfide (**C2**) as starting compound, product **C3** was obtained as the main product after 5 min reaction time. The methylated product **C4** was already detected after 2 h reaction time. Both experiments are compared in the RP-HPLC chromatograms in figure **5.45**.

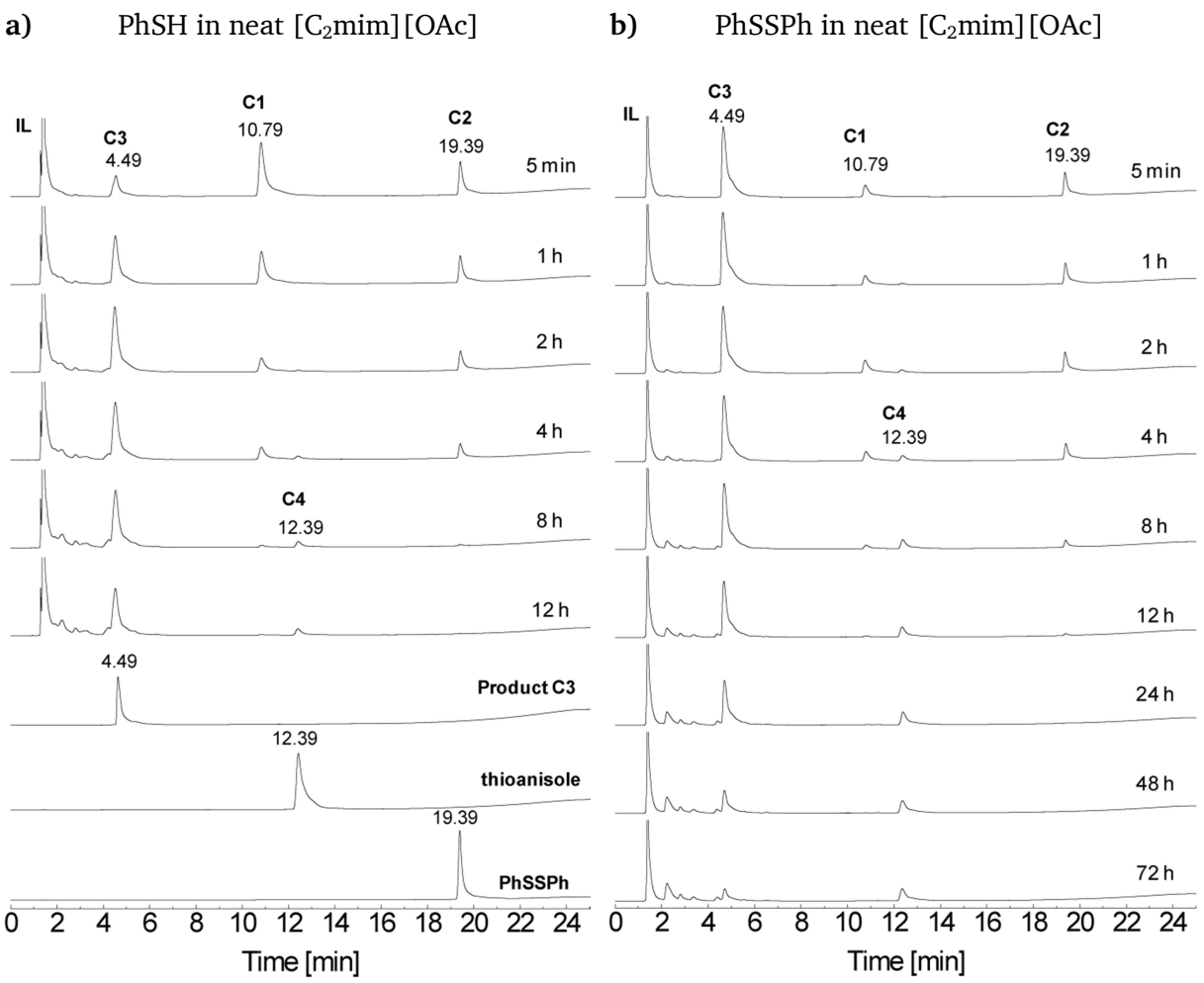

Figure 5.45: Analytical HPLCs of **C1** thiophenol and **C2** diphenyl disulfide in neat [C_2mim][OAc] at 240 nm. HPLC conditions: C8 column (125 x 4 mm, 120 Å pore diameters, 5 µm particle size), 20–55% acetonitrile (0.1% TFA) in 15 min followed by a gradient of 55–95% acetonitrile (0.1% TFA) for 7 min, flow rate of 1 ml/min.

The obtained data proved that aromatic sulfur groups are highly prone to chemical modifications in [C_2mim][OAc]. The finding that **C2** (diphenyl disulfide) reacts faster than **C1** (thiophenol) supports the idea that thiol groups are first oxidized to the disulfide before they react with *in situ* formed NHCs.

a) ^{1}H-NMR in D_2O **b)** ^{13}C-NMR in D_2O

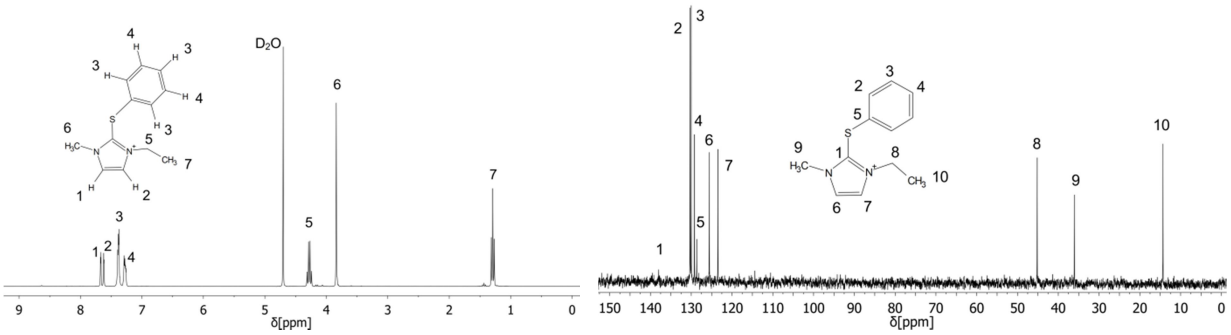

c) ESI-MS of compound C3

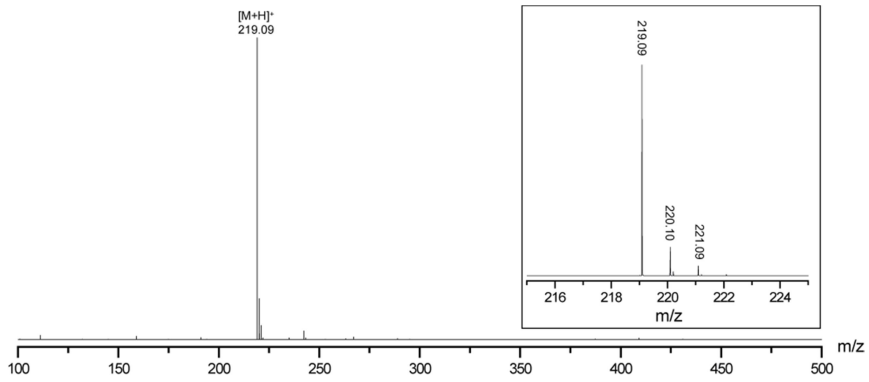

Figure 5.46: **a)** ^{1}H-NMR and **b)** ^{13}C-NMR spectra of product **C3** in D_2O, c) ESI mass spectrum and isotopic pattern of compound **C3**.

Product C3: ^{1}H-NMR (300 MHz, D_2O) δ = 7.7 (d, J = 2.2 Hz, 1-H), 7.6 (d, J = 2.2 Hz, 1-H), 7.4 (m, 3-H, Ar), 7.3 (m, 2-H, Ar), 4.3 (q, J = 7.3 Hz, 2-H), 3.8 (s, 3-H), 1.3 (t, J = 7.3 Hz, 3-H) ppm. ^{13}C NMR (D_2O) δ = 130.3, 130.0, 129.2, 128.6, 123.6, 123.5, 45.17, 36.1, 14.3 ppm.

a) ^{1}H-NMR in D_2O **b)** ^{13}C-NMR in D_2O

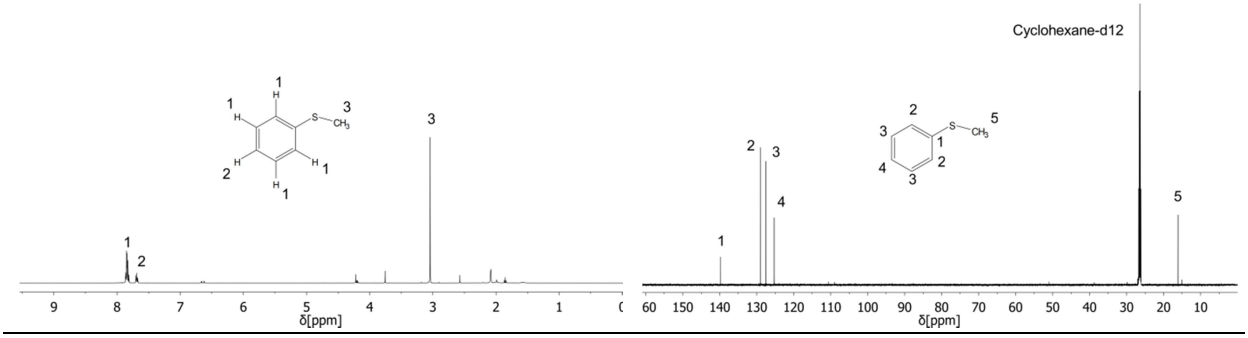

Figure 5.47: **a)** ^{1}H-NMR and **b)** ^{13}C-NMR spectra of product **C4** in cyclohexane-d12.

Product C4: ^{1}H-NMR (500 MHz, cyclohexane-d_{12}) δ = 7.88-7.80 (m, 4-H, Ar), 7.70-7.67 (m, 1-H, Ar), 3.04 (s, 3-H) ppm. ^{13}C-NMR (cyclohexane-d_{12}) δ =139.8, 129.0, 127.5, 125.3, 16.1 ppm.

5.2.6. Reaction of benzyl mercaptan and dibenzyl disulfide in [C_2mim][OAc]

To investigate chemical reactions of thiols which are not directly bound on aromatic systems, benzyl mercaptan (BzlSH) **C5** and dibenzyl disulfide (BzlSSBzl) **C6** were analyzed in neat [C_2mim][OAc] by RP-HPLC, thin-layer chromatography (TLC), ESI-MS and NMR spectroscopy. Again, both substances were completely soluble in the ionic liquid. Shortly after dissolution, benzyl mercaptan **C5** was immediately oxidized to dibenzyl disulfide **C6** which was much faster than the oxidation of thiophenol **C1** to diphenyl disulfide **C2** in previous experiments. After oxidation of **C5** to **C6**, new reaction products **C7**, **C8** and **C9** occurred in the chromatograms (figure **5.49**). This observation was further evidence that thiols were first oxidized to disulfides before they are modified by *in situ* generated imidazole-carbenes in [C_2mim][OAc].

At the beginning of the reaction, product **C8** (5.31 min) was generated by the reaction of dibenzyl disulfide **C6** and the imidazole-carbene. In contrast to previous experiments, reaction product **C8** was not stable in [C_2mim][OAc] and further converted to reaction products **C7** (2.82 min) and **C9** (18.44 min). According to the results of the RP-HPLC, dibenzyl disulfide (**C6**) was completely converted after 2 h at room temperature. Collection and analysis of products **C7**, **C8** and **C9** revealed the structures highlighted in figure **5.48**.

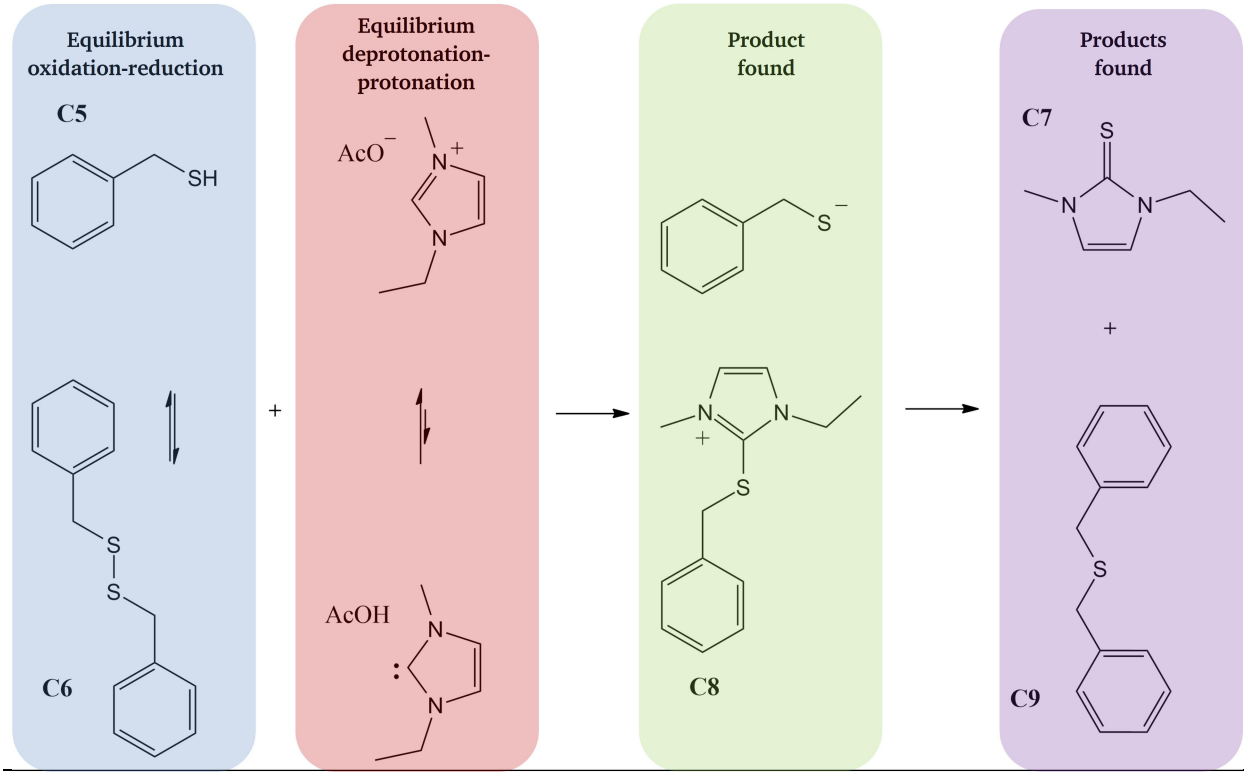

Figure 5.48: NHC formation and modification of benzyl mercaptan **C5** and dibenzyl disulfide **C6** in neat [C_2mim][OAc].

The instability of **C8** in the ionic liquid can be explained by the additional methylene group between the sulfur atom and the aromatic aryl system. Considering the existence of reaction products **C7** and **C9** it is supposed that the methylene group in product **C8** can be attacked by

the nucleophile benzyl mercaptan anion which leads directly to the formation of **C7** and **C9**. For an unambiguous identification, reaction products **C7**, **C8** and **C9** were collected by column chromatography following the procedure in **8.1.1** and analysed *via* NMR spectroscopy and ESI-MS. The isolated and purified product **C7** was a dark orange liquid which was easily soluble in water. Product **C8** was obtained as a highly viscous liquid which could be concentrated under reduced pressure.

In order to verify these results, dibenzyl disulfide (**C6**) was directly dissolved in the neat [C_2mim][OAc] and analysed in the same manner as benzyl mercaptan. The dissolution and analysis of dibenzyl disulfide **C6** in the ionic liquid led to the same products as the dissolution of benzyl mercaptan (**C5**). However, formation of **C7**, **C8** and **C9** was faster starting with dibenzyl disulfide (**C6**)**.** Similar to the observation made by the dissolution of thiophenol (**C1**) and diphenyl disulfide (**C2**)**,** the direct use of the disulfide **C6** resulted in a faster product formation for its reduced form **C5**. In the case of **C6** as a starting compound, the main product **C7** was already detectable after 5 min reaction time (figure **5.49**).

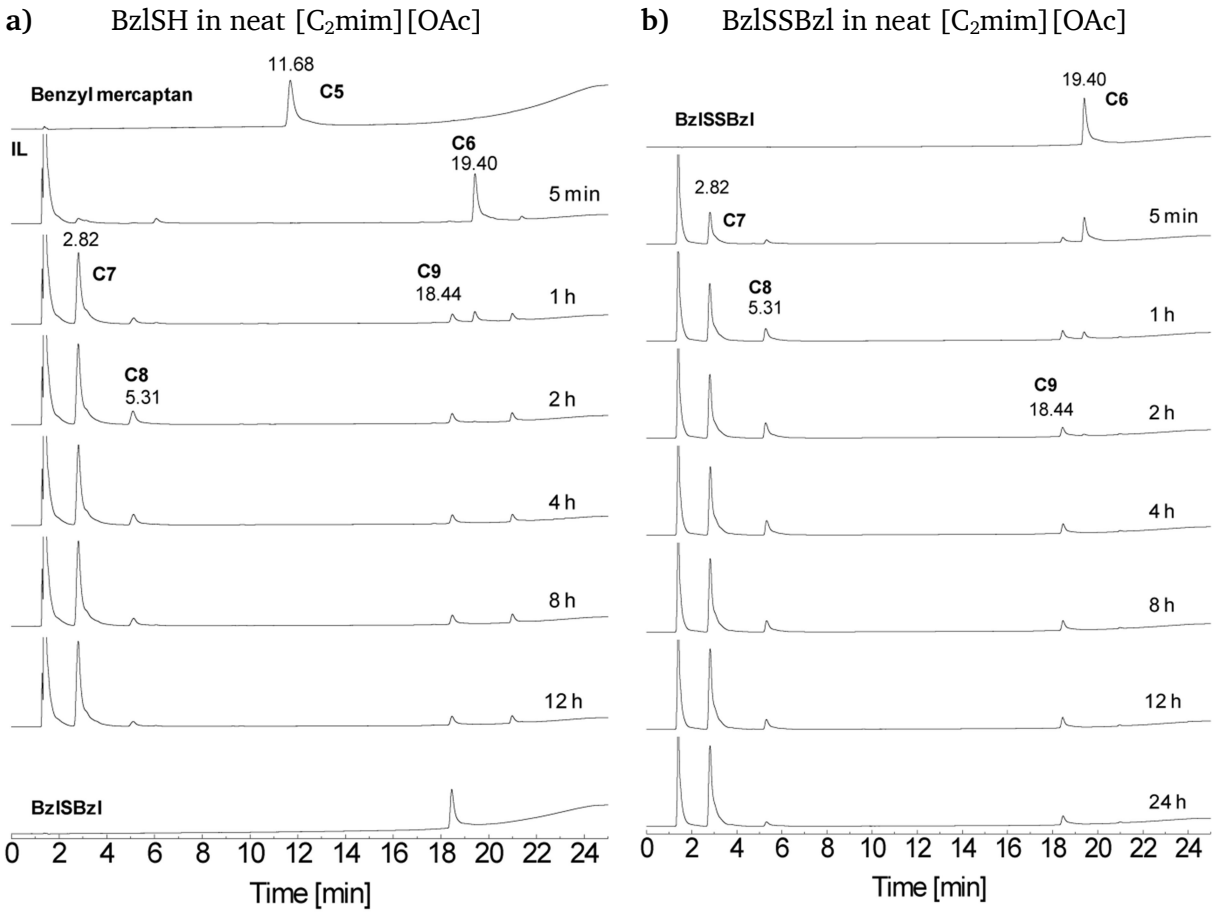

Figure 5.49: Analytical RP-HPLC of **C5** benzyl mercaptan and **C6** dibenzyl disulfide in neat [C_2mim][OAc] at 240 nm using a C8 column (125 x 4 mm, 120 Å pore diameters, 5 µm particle size). HPLC conditions: 20–55% acetonitrile (0.1% TFA) in 15 min followed by a gradient of 55–95% acetonitrile (0.1% TFA) for 7 min using a flow rate of 1 ml/min.

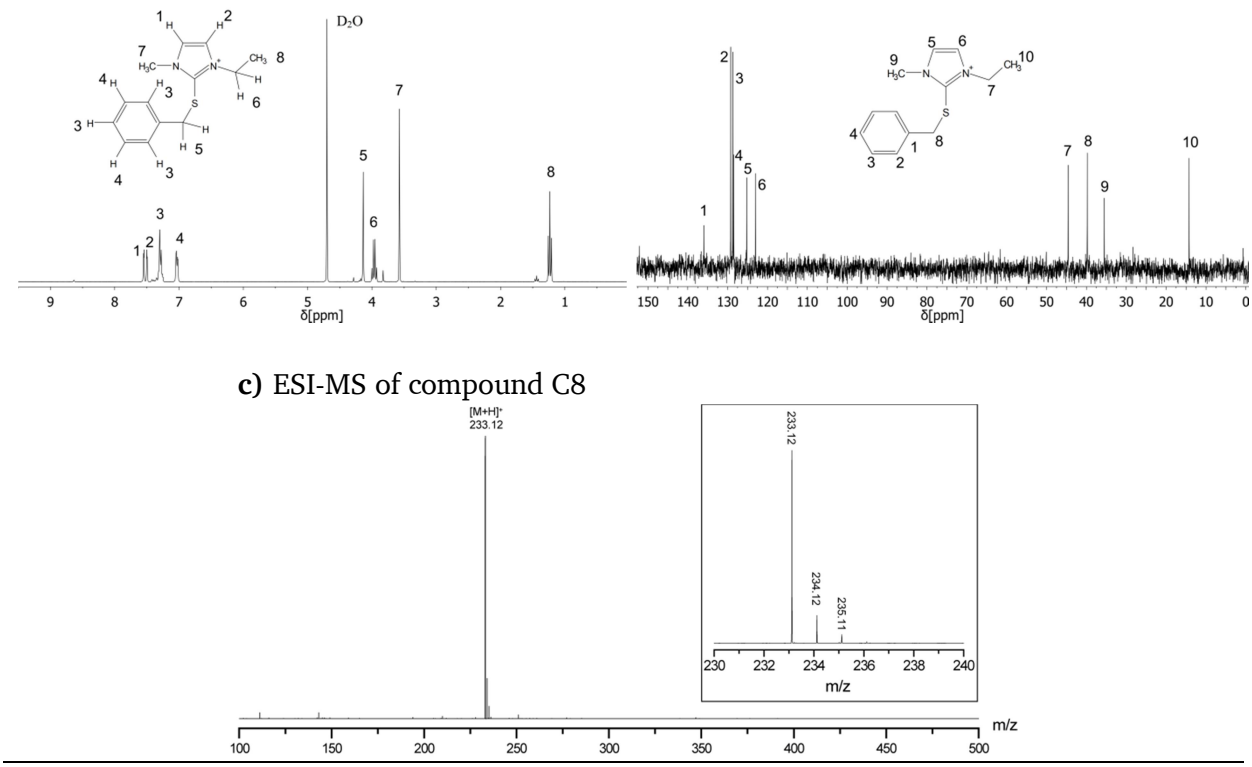

Figure 5.50: **a)** ^{1}H-NMR and **b)** ^{13}C-NMR spectra of product **C8** in D_2O, **c)** ESI mass spectrum and isotopic pattern of compound **C8**.

Product C8: ^{1}H-NMR (300 MHz, D_2O) δ = 7.5 (d, J = 2.1 Hz, 1-H), 7.5 (d, J = 2.2 Hz, 1-H), 7.3-7.2 (m, 3-H), 7.1-7.0 (m, 2-H), 4.1 (s, 2-H), 4.0 (q, J = 7.3 Hz, 2-H), 3.6 (s, 3-H), 1.2 (t, J = 7.4 Hz, 3-H) ppm. ^{13}C-NMR (D_2O) δ = 136.0, 129.2, 128.7, 128.5, 125.2, 123.0, 44.6, 39.8, 35.5, 14.2 ppm.

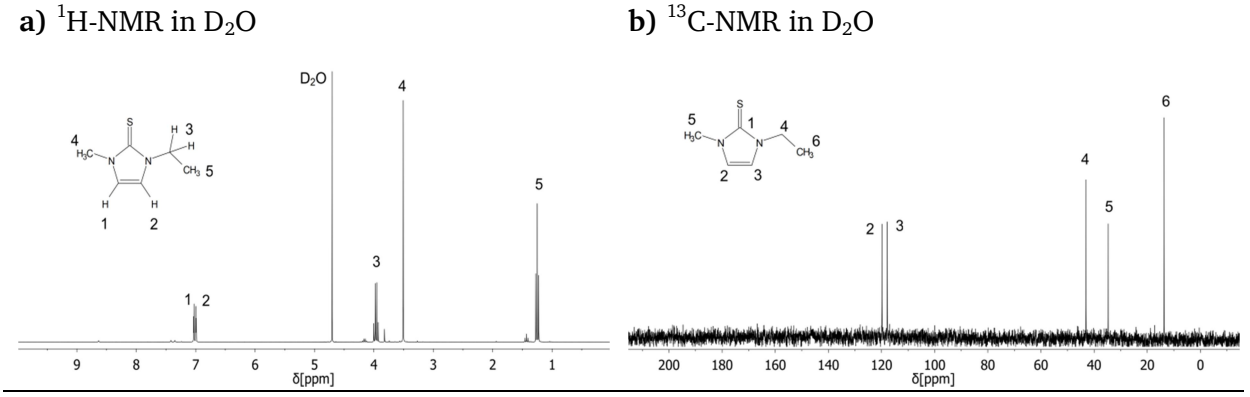

Figure 5.51: **a)** ^{1}H NMR and **b)** ^{13}C NMR spectra of product **C7** in D_2O.

Product C7: ^{1}H-NMR (300 MHz, D_2O) δ = 7.0 (d, J = 2.3 Hz, 1-H), 4.0 (q, J = 7.3 Hz, 2_H), 3.5 (s, 3-H), 1.2 (t, J = 7.3 Hz, 3-H) ppm.^{13}C-NMR (D_2O) δ = 119.8, 117.8, 43.0, 34.7, 13.6 ppm.

5.2.7. Reaction of [Cys^{22}]BM2(22-35) in [C$_2$mim][OAc]

In the further course of this work possible modifications of cysteine-containing peptides by neat [C$_2$mim][OAc] were examined with respect to the identified chemical modifications of the model organic compounds **C1**/**C2** and **C5**/**C6**. As a model peptide for this experiment, the N-terminal cysteine peptide **P1** [Cys^{22}]BM2(22-35) was applied. After dissolution of **P1** in neat [C$_2$mim][OAc] reaction progress was monitored by analytical RP-HPLC according to instruction **8.1.2**. All new occurring peaks in the chromatograms were collected and analysed by ESI-MS. The experimental isotopic pattern and the calculated mass spectrum of **P1** [Cys^{22}]BM2(22-35) in [C$_2$mim][OAc] resulted in the expected reaction products and allowed the identification of several unexpected side products.

After dissolution of **P1** in neat [C$_2$mim][OAc] two peaks at 9.67 min and 16.53 min were detected in the chromatogram. The peak at 9.67 min could be assigned to starting peptide **P1** by a reference chromatogram of **P1** in water (0.1% TFA). ESI-MS analysis of the newly formed product **P1e** at 16.53 min showed the monoisotopic mass of the disulfide of peptide **P1** (Figure **5.54c**). Similar to the rapid oxidation of the organic thiols **C1** and **C5** in [C$_2$mim][OAc] model peptide **P1** was immediately oxidized to disulfide **P1e** shortly after dissolution in the ionic liquid. After 30 min, two new products **P1a** at 7.99 min and **P1b** at 9.24 min appeared in the chromatogram. The isotopic pattern of product **P1a** was in perfect agreement with the proposed structure (figure **5.52)**.

[Cys^{22}]BM2(22-35) in [C$_2$mim][OAc]

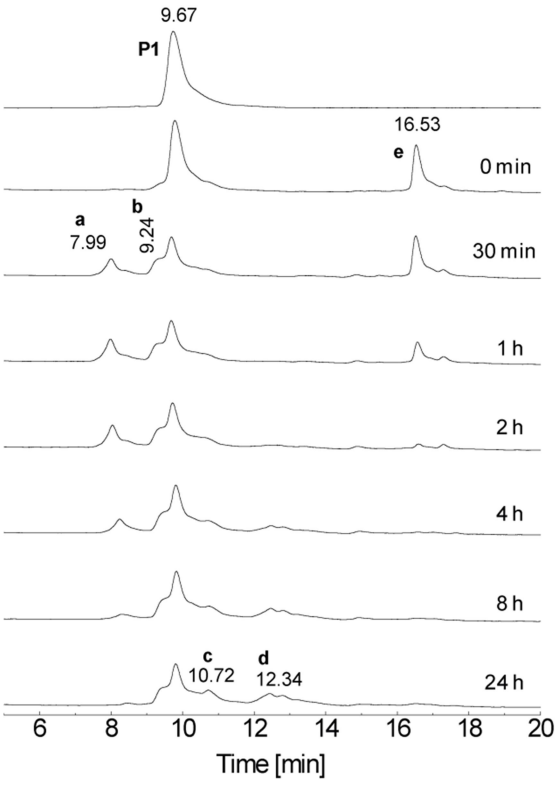

No.	Proposed structures
P1	IGRKIQNLHGITWC
P1a, a	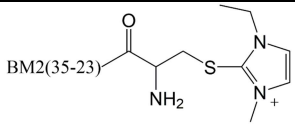
P1b, b	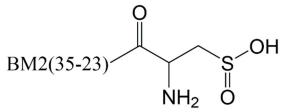
P1c, c	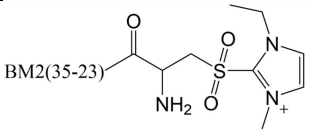
P1d, d	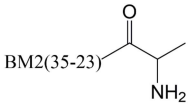
P1e, e	IGRKIQNLHGITW**CC**WTIGHLNQ IKRGI

Figure 5.52: Left: RP-HPLC experiment of **P1** [Cys^{22}]BM2(22-35) in neat [C$_2$mim][OAc] over 24 h. Right: Numbers and presumed structures of the products identified by LC-MS.

After 1 h, the peak area of the peptide disulfide **P1e** clearly decreased indicating that the disulfide bond was not stable in the reaction mixture. At a retention time of 10.72 min a new product **P1c** occurred which continually increased over 24 h. The mass spectrum of **P1c** was in line with the chemical structure highlighted in figure **5.52**. After 4 h, a new peak **P1d** was detected at a retention time of 12.34 min. Surprisingly, this product showed the mass of the desulfurated peptide **P1** as a result of the conversion of Cys22 to Ala22.

a) Experimental spectra of **P1a**

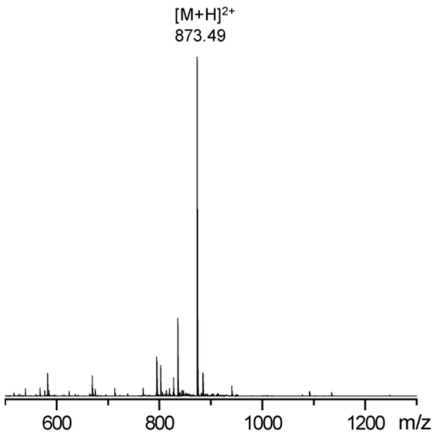

Theoretical monoisotopic mass
$C_{79}H_{129}N_{26}O_{17}S$
$[M+H]^{2+}$ = 873.49 m/z

b) Experimental spectra of **P1b**

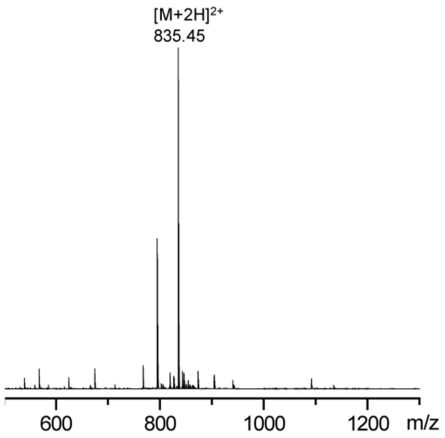

Theoretical monoisotopic mass
$C_{73}H_{120}N_{24}O_{19}S$
$[M+2H]^{2+}$ = 835.45 m/z

Figure 5.53: **a)** MS of reaction product **P1a** which is formed between the imidazolium-carbene and peptide **P1**. **b)** MS of the oxidized product **P1b** at a retention time of 10.72 min.

a) Experimental spectra **P1c**

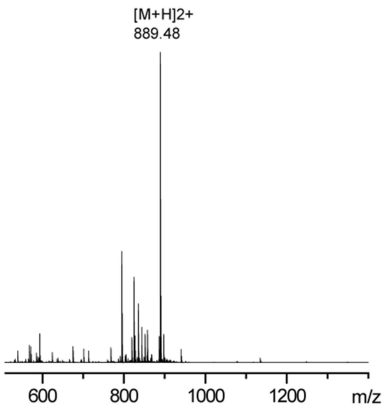

Theoretical monoisotopic mass
$C_{79}H_{129}N_{26}O_{19}S$
$[M+H]^{2+}$ = 889.48 m/z

b) Experimental spectra **P1d**

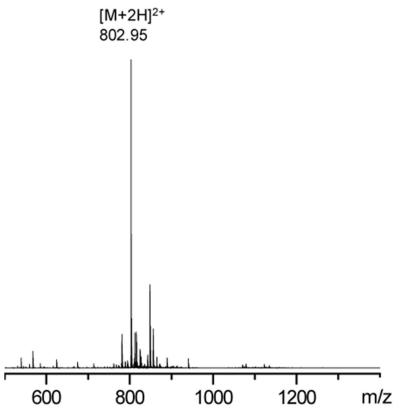

Theoretical average masses
$C_{73}H_{120}N_{24}O_{17}$
$[M+2H]^{2+}$ = 803.47 m/z

c) Experimental spectra **P1e**

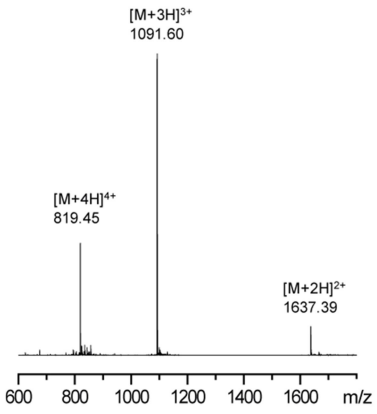

Theoretical monoisotopic mass
$C_{146}H_{238}N_{48}O_{34}S_2$
$[M+3H]^{3+}$ = 1091.60 m/z

Figure 5.54: **a)** MS of reaction product **P1c** at a retention time of 10.72 min. **b)** MS of the desulfurization product **P1d** collected at 12.34 min. **c)** MS of the oxidized product **P1e** at 16.53 min.

The collected data from RP-HPLC, LC-MS and NMR analysis confirmed the suspected formation of N-heterocyclic carbenes (NHCs) in the neat ionic liquid [C_2mim][OAc] which is proposed by numerous sources in the literature.[154-155, 216] All identified reaction products and modifications of organic model compounds **C1**, **C2**, **C5**, **C6** and peptide **P1** [Cys^{22}]BM2(22-35) can be explained by the existence of NHCs in the neat ionic liquid. The proposed reaction scheme for the NHC formation is highlighted below (figure **5.55**).[1]

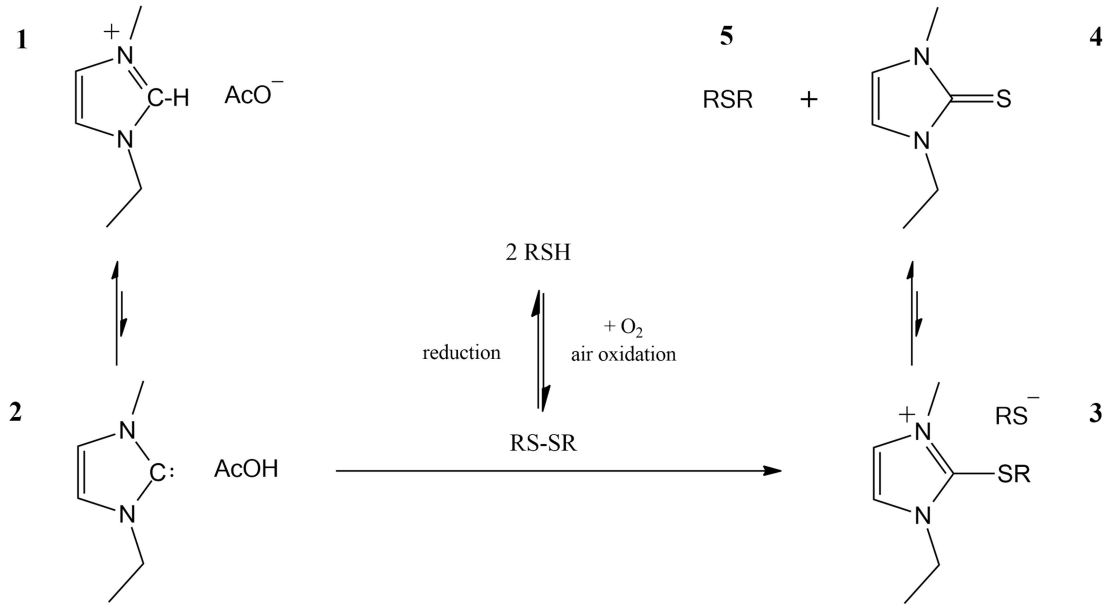

Figure 5.55: Possible formation of N-heterocyclic carbenes (NHC) in the neat ionic liquid [C_2mim][OAc]. These *in situ* formed carbenes can react with sulfur-containing compounds and cysteine side chains in proteins.[1]

In the proposed mechanism, carbene formation is the result of an equilibrium between the protonated **(1)** and deprotonated **(2)** imidazolium cation. The reaction is initiated through the deprotonation of the C(2) atom at the imidazolium cation.[1] Amyes *et al*. as well as Cheng *et al.* were able to calculate the pKa value of the 1-ethyl-3-methylimidazolium cation to 22.1 which is similar to that of fluorene derivatives which are widely used in organic chemistry and well known for their ability to give off protons under basic conditions.[217]

These results support the presumption of a possible C(2) deprotonation by the acetate anion confirming the results of previous studies by L. Nyulaszi and colleagues.[157] In the further course of the reaction, the formed imidazolium carbene **(2)** reacts with disulfides to form an imidazolium-thio intermediate **(3)** which further decays to 1-ethyl-3-methylimidazole-2-thione **(4)** and the corresponding thioether **(5)**.

In the further course of this work 1-ethyl-3-methyl-imidazolium acetate ([C_2mim][OAc]) was investigated as potential ligation media for hydrophobic peptides. Therefore, the addition of polar protic solvents such as water was tested to supress NHC formation. The following chapter summarizes and discusses these studies (**5.2.8**).

5.2.8. Effect of water to NHC-induced modifications

Considering the mechanism of NHC formation in figure **5.55**, proton donating co-solvents such as water should reduce the carbene formation in [C_2mim][OAc] and decrease unexpected peptide modifications. To test this theory model peptide **P1** [Cys^{22}]BM2(22-35) was dissolved and analyzed in different mixtures of [C_2mim][OAc] and water from 10 to 30% (v/v). Indeed, RP-HPLC analysis, according to instruction **8.1.2**, showed that the reaction rate of the peptide modification slowed down with rising concentrations of water.

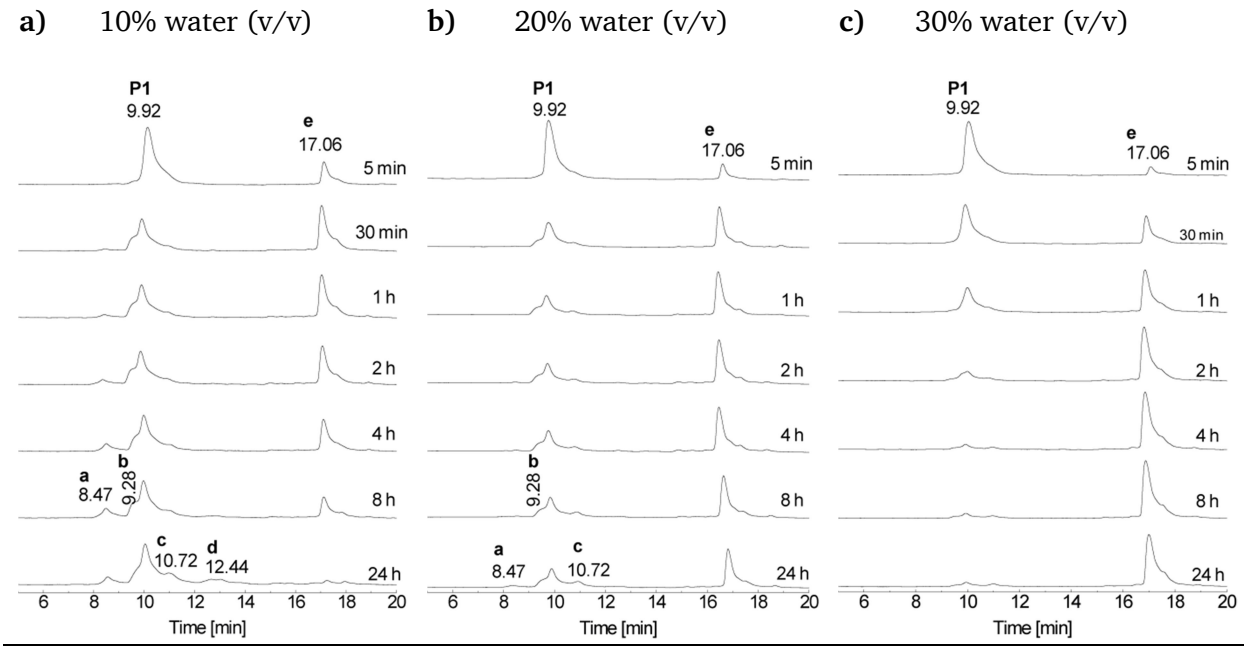

Figure 5.56: Reaction progress of model peptide **P1** [Cys^{22}]BM2(22-35) in mixture of [C_2mim][OAc] with **a)** 10% water, **b)** 20% water and **c)** 30% water. HPLC conditions: 20 - 30% acetonitrile in 20 min, flow rate 1 ml/min.

The presence of 10% water in the reaction solution showed a minor influence on the formation of the side products **P1a-P1d.** However, the generation of these side products was distinctively slower compared to the formation in the neat ionic liquid. After 30 min, only a small amount of product **P1a** was detectable in the chromatogram. Although the formation of side products was not fully suppressed by the addition of 10% water, the influence of the increased water content was clearly visible compared to the neat ionic liquid (chapter **5.2.7**). Similar to the reaction in neat [C_2mim][OAc], the peak of the dimerized peptide **P1e** disappeared over a time period of 24 h indicating that the oxidized form of peptide **P1** was the most reactive. The addition of 20% water further decreased the reaction rate of the side product formation. After 24 h, only a very small amount of product **P1a** appeared in the chromatogram. However, the oxidized reaction products **P1b** and **P1c** were still detectable after 1 h. In contrast to the experiment with 10% of water, the peptide disulfide **P1e** was still detectable after 24 h at 20% water content. At a water percentage of 30%, no NHC-induced side reactions were detectable in the chromatogram. Only the disulfide **P1e** was detectable at 17.06 min which was left as a single peak after 4 h. The results proved that a water content of at least 30% is necessary to supress the NHC-induced modifications. In the further course of this work [C_2mim][OAc]/water mixtures were investigated as possible ligation media for hydrophobic Hmp-peptides.

5.2.9. Evaluation of optimal water content for NCL

The first study investigated the optimal water content for the IL-mediated native chemical ligation. Therefore, ligation buffers **D1**-**D6** were prepared with rising amounts of water according to instruction **10.1.4**. In each ligation experiment the water content was increased by 10% as highlighted in table **5.28**. As model reaction for these experiments cysteine peptide **P1** [Cys^{22}]BM2(22-35) (3.62 min) and Hmp-peptide **P7** [Leu^{21}]BM2(17-21)-Hmp (7.57/8.33 min) were ligated to product **P22** [Leu^{21}]BM2(17-35) (21.57 min). The only observable side reaction was Hmp hydrolysis at 5.13 min (figure **5.57**).

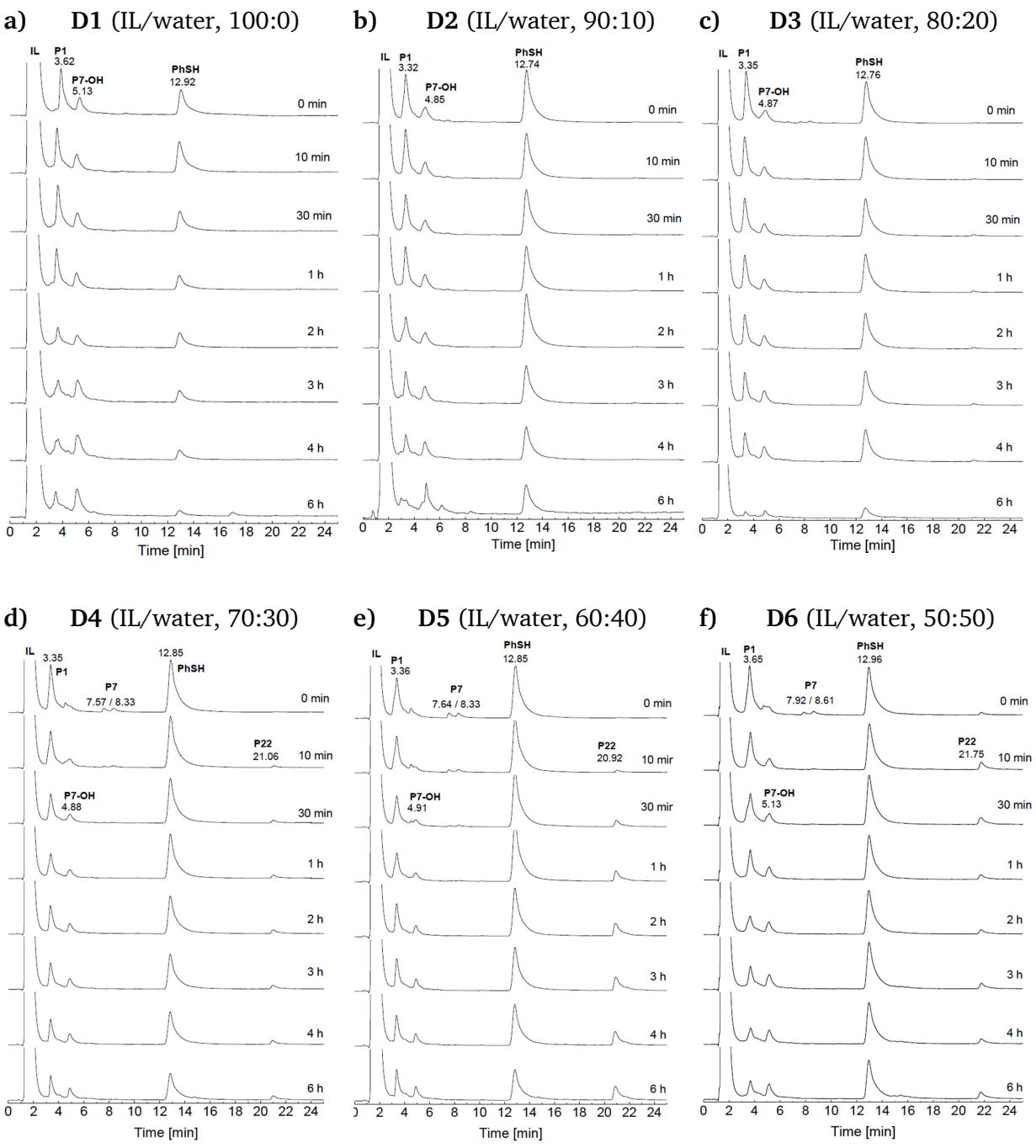

Figure 5.57: Ligation experiments in buffer **D1**-**D6** with **P1** [Cys^{22}]BM2(22-35) and **P7** ALHFL-Hmp. HPLC was performed with a C8 column (125 x 4 mm, 120 Å pore diameters, 5 µm particle size). Gradient: 25 - 35% acetonitrile in 30 min, flow rate 1 ml/min. **PhSH** (thiophenol), **P7-OH** (hydrolysis product of **P7**).

The high solubility potential of the IL-based buffers allowed much higher peptide concentrations for peptides **P1** [Cys^{22}]BM2(22-35) and **P7** [Leu^{21}]BM2(17-21)-Hmp compared to aqueous ligation buffers usually applied for NCL. In contrast to conventional ligation buffers denaturing agents such as urea or guanidinium chloride were not necessary for the preparation of buffers **D**. Also, the addition of buffer salts like disodium phosphate was unnecessary. Except for [C_2mim][OAc] and water only TCEP HCl and thiophenol were added to the ligation solution. The pH of the solution was highly dependent on water content and was ideal for buffers **D5** and **D6**. However, the highest solubility potential for hydrophobic peptides was found in buffers **D1**-**D3**.

Table 5.28: Composition, pH values and ligation yields in buffers **D1**–**D6**.

Buffer	[C_2mim][OAc] [%]	Water [%]	Measured pH	Ligation yield [%]
D1	100	0	11.4	0
D2	90	10	10.5	0
D3	80	20	9.5	10.1
D4	70	30	8.7	40.8
D5	60	40	7.6	71.7
D6	50	50	6.8	55.6

In buffers **D1** and **D2** no ligation product was observable. Already at the start of the reaction Hmp-peptide **P7** [Leu^{21}]BM2(17-21)-Hmp was entirely hydrolysed to side product **P7-OH**. The high pH value seemed to destroy peptide **P1** whose peak area decreased constantly over a time period of 6 h. In buffer **D3** ligation yields of 10% were achieved (figure **5.58**). A significant improvement could be observed in buffer **D4** with a ligation yield of 41%. After 6 h, the best ligation yields for product **P22** [Leu^{21}]BM2(17-35) were achieved in buffer **D5** with a water content of 40 % and a pH of 7.6 while ligation in buffer **D6** resulted in peptide precipitation. In the following course of this work, buffer **D5** was further used as a ligation media for the long and hydrophobic BM2 fragments.

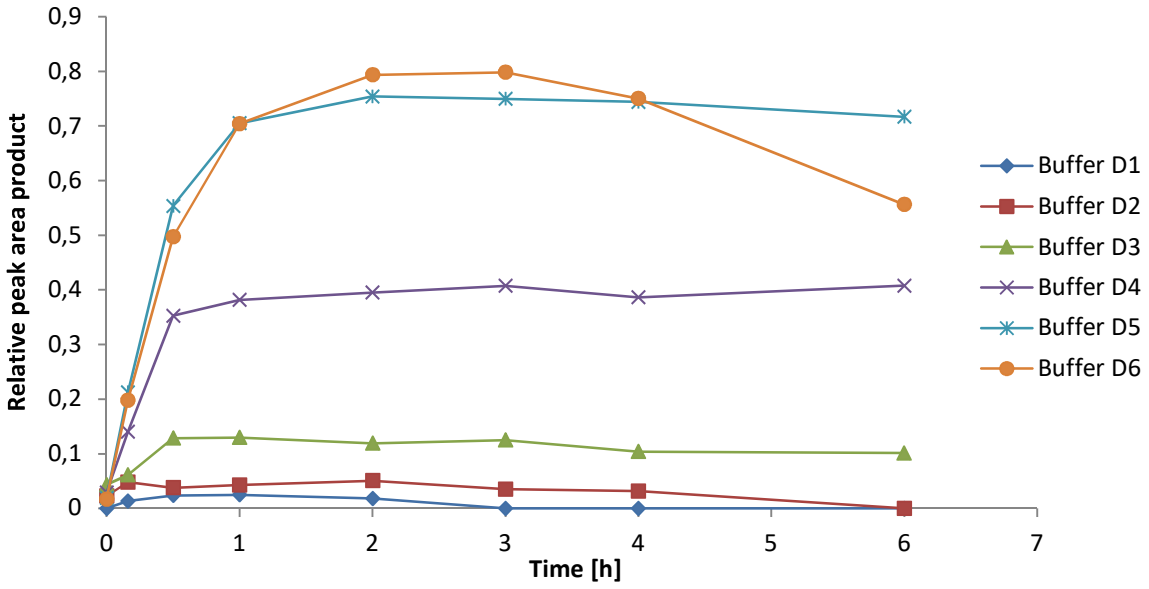

Figure 5.58: Relative peak area of ligation product **P22** [Leu^{21}]BM2(17-35) against the reaction time.[218]

5.2.10. Ionic liquid-mediated NCL of [Leu^{10}]BM2(1-51)

In order to test ligation buffer **D5** for the synthesis of transmembrane peptides, product **P27** [Leu^{10}]BM2(1-51) was produced by ligation of the N-terminal cysteine peptide **P3** [Cys^{11}]BM2(11-51) and the hydrophobic Hmp-peptide diastereomer **P16a** or **P16b** [Leu^{10}]BM2(1-10)-Hmp. The ligation was performed according to instruction **10.1.5** and monitored *via* analytical RP-HPLC over 24 h (figure **5.59**). The high water content (40 %) and the presence of TCEP prevented modifications of the peptide chain. As single side reaction, hydrolysis product **P16-OH** appeared at 14.80 min. However, the amount of Hmp hydrolysis was slightly higher than for ligations in the HFIP-based buffer **C** (figure **5.41**). Already at the start of the reaction ligation product **P27** was detectable at 21.49 min. After 24 h, ligation yields of 76% for **P16a** and 73% for **P16b** were obtained. The final ligation product could be separated from ligation buffer **D5** by preparative RP-HPLC following protocol **8.1.7**. Analysis *via* ESI-MS revealed the expected molecular mass and isotopic pattern of formula $C_{270}H_{442}N_{76}O_{66}S_3$ which was identical to the ligation product **P27** obtained in the HFIP-based ligation buffer **C** (figure **5.60**).

Table 5.29: Results for ligation experiments of **P16a** and **P16b** in buffer **D5**.

Ligation	Dia.	Product	Buffer	Time	Hydrolysis	Yield
a)	1	[Leu^{10}]BM2(1-51)	D5	24 h	24%	76%
b)	2	[Leu^{10}]BM2(1-51)	D5	24 h	27%	73%

Amino acid sequence of P27: MLEPFQILSLCSFILSALHFLCWTIGHLNQIKRGINMKIRIKGPNKETINR

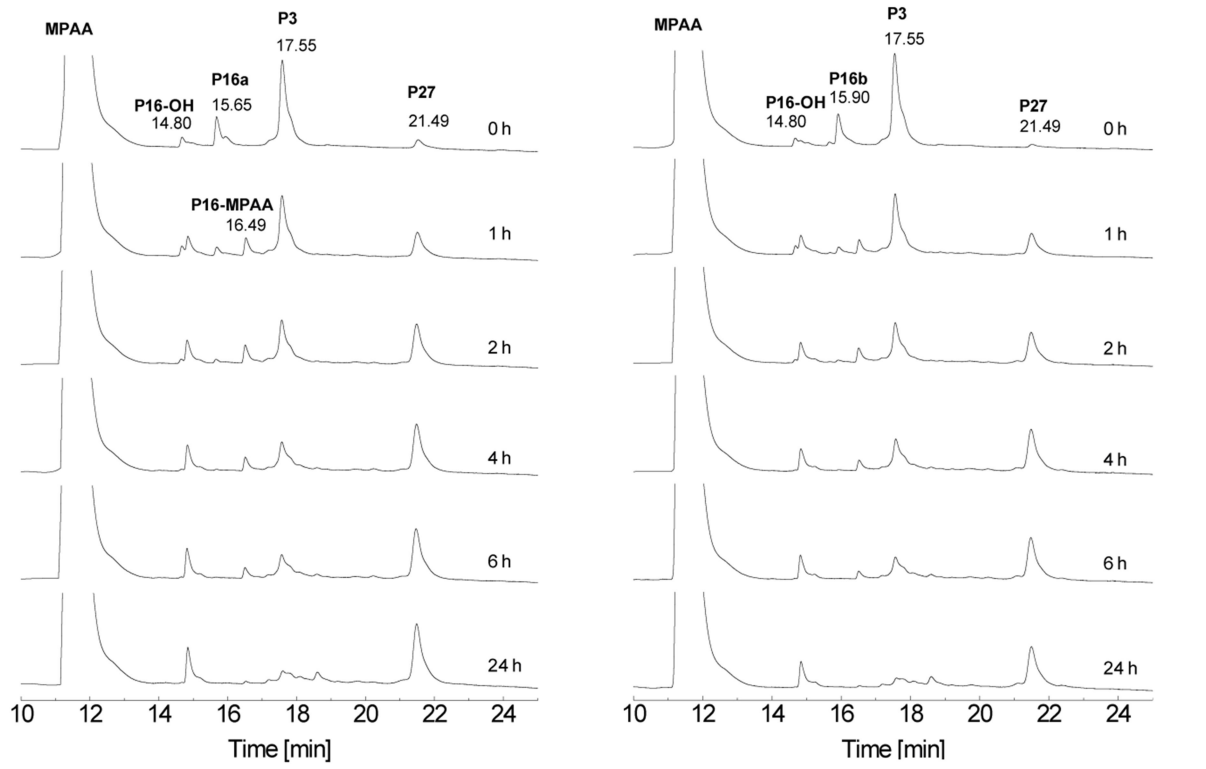

Figure 5.59: Stacked chromatograms of NCL of **P3** + **P16a** and **P3** + **P16b**. HPLC was performed with a C18 column (150 x 4 mm, 100 Å pore diameter, 3 µm particle size). Gradient: 10% acetonitrile for 3 min followed by 99% acetonitrile in 30 min, flow rate 1 ml/min. **P16-MPAA**- BM2(1-10)-MPAA, **P16-OH**- BM2(1-21)-COOH.

In conclusion, the ionic liquid based ligation buffer **D5** is an excellent ligation media for hydrophobic transmembrane peptides. The NCL of [Leu^{10}]BM2(1-51) in the ionic liquid-based buffer **D5** was successful.

RP-HPLC analysis of the purified ligation product **P27** [Leu^{10}]BM2(1-51) showed one single peak at a retention time of 19.91 min and no further impurities. The experimental monoisotopic mass and isotopic pattern of ligation product **P27** was in excellent agreement with the simulated isotopic pattern.

a) Analytical RP-HPLC of [Leu^{10}]BM2(1-51)

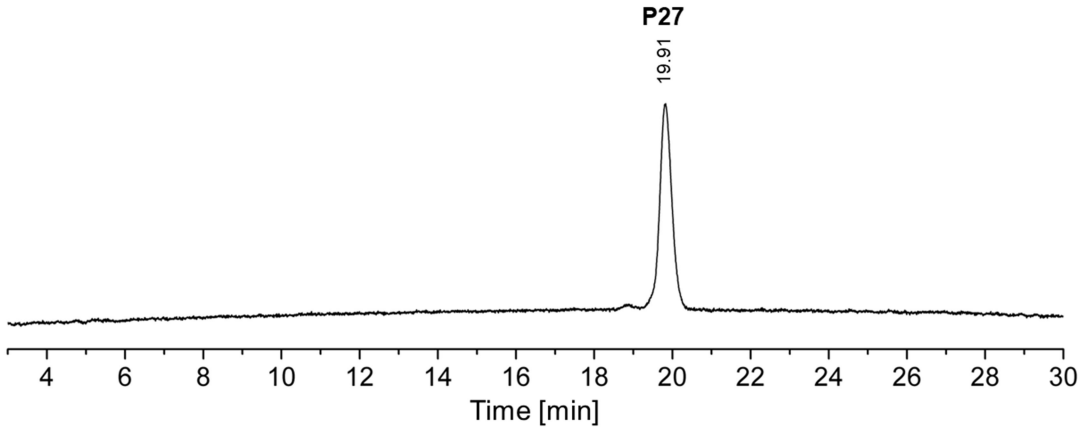

b) ESI-MS of **P27** [Leu^{10}]BM2(1-51)

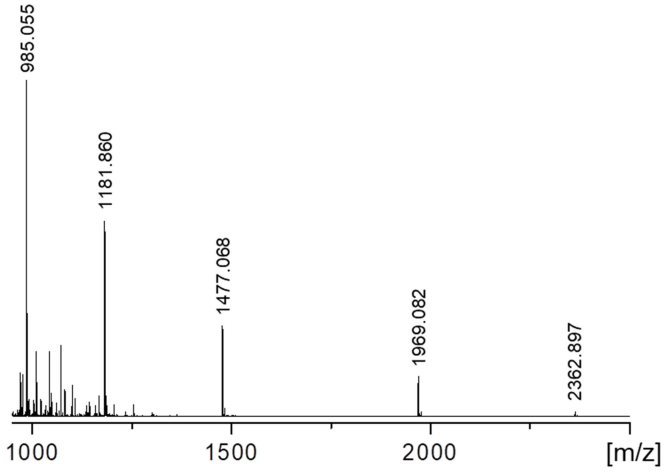

c) Isotopic pattern of **P27**

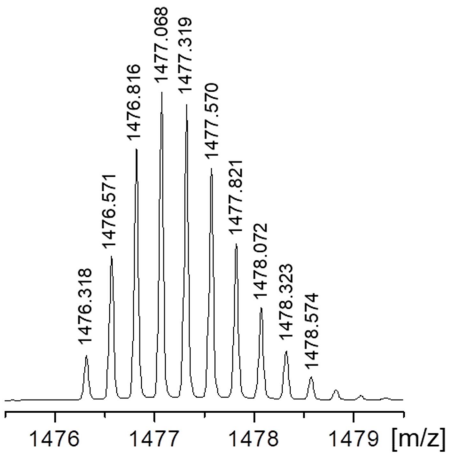

Theoretical average masses

$[M+6H]^{6+}$ = 985.187 m/z
$[M+5H]^{5+}$ = 1182.023 m/z
$[M+4H]^{4+}$ = 1477.277 m/z
$[M+3H]^{3+}$ = 1969.367 m/z

Theoretical monoisotopic mass

$C_{270}H_{442}N_{76}O_{66}S_3$
$[M+4H]^{4+}$ = 1476.325 m/z

Figure 5.60: **a)** Analytical RP-HPLC chromatogram of ligation product **P27**. HPLC was performed with a C4 column (MultoHigh U C4, 100 x 4 mm). Gradient: 40 – 70% acetonitrile in 30 min, flow rate 1 ml/min, **b)** experimental ESI-MS and **c)** isotopic pattern of peptide **P27**.

5.3. Development of novel follow-up protocols: desulfurization and Acm-group deprotection

5.3.1. HFIP-mediated desulfurization

Since cysteine is a rather rare amino acid in most native peptide sequences, other amino acid residues were investigated for decades as possible ligation sites. The combination of the native chemical ligation followed by conversion of cysteine to alanine is the most utilized ligation strategy for peptides without native cysteine residues at the ligation site. One of the fastest and most efficient methods is the free-radical-based desulfurization in the presence of VA-044 and TCEP (chapter **3.6.1**). Ingeniously, TCEP can also be used in the NCL as a reducing agent that prevents unintended oxidation of thiol groups. The similar compositions of ligation and desulfurization buffers provide the opportunity to combine both methods. This one-pot ligation and desulfurization strategy was first published by Yan and Dawson and was used numerous times as a successful pathway for the synthesis of various peptides.[164] However, most publications describe the desulfurization of well water soluble peptides. The desulfurization of highly hydrophobic and poorly water soluble peptides and proteins is rarely presented in the literature. Especially, hydrophobic transmembrane peptides such as BM2(1-51) are usually not soluble in standard desulfurization buffers.

A further aim of this thesis is the development of an appropriate desulfurization buffer for poorly-soluble peptides. Therefore, peptide **P23** [Cys(Acm)^{11}][Leu^{21}][Cys^{22}]BM2(1-51) was converted to desulfurization product **P25** [Cys(Acm)^{11}][Leu^{21}]BM2(1-51). In a first study, peptide **P23** was tried to desulfurize using a conventional, water-based desulfurization buffer (instruction **11.1.1**). However, as expected, the hydrophobic peptide **P23** was not soluble in aqueous buffer solutions resulting in peptide precipitation. Encouraged by the good solubility in ligation buffer **C**, an HFIP-based desulfurization buffer was tested for the synthesis of **P25** [Cys(Acm)^{11}][Leu^{21}]BM2(1-51) (instruction **11.1.2**). Both experiments are compared below.

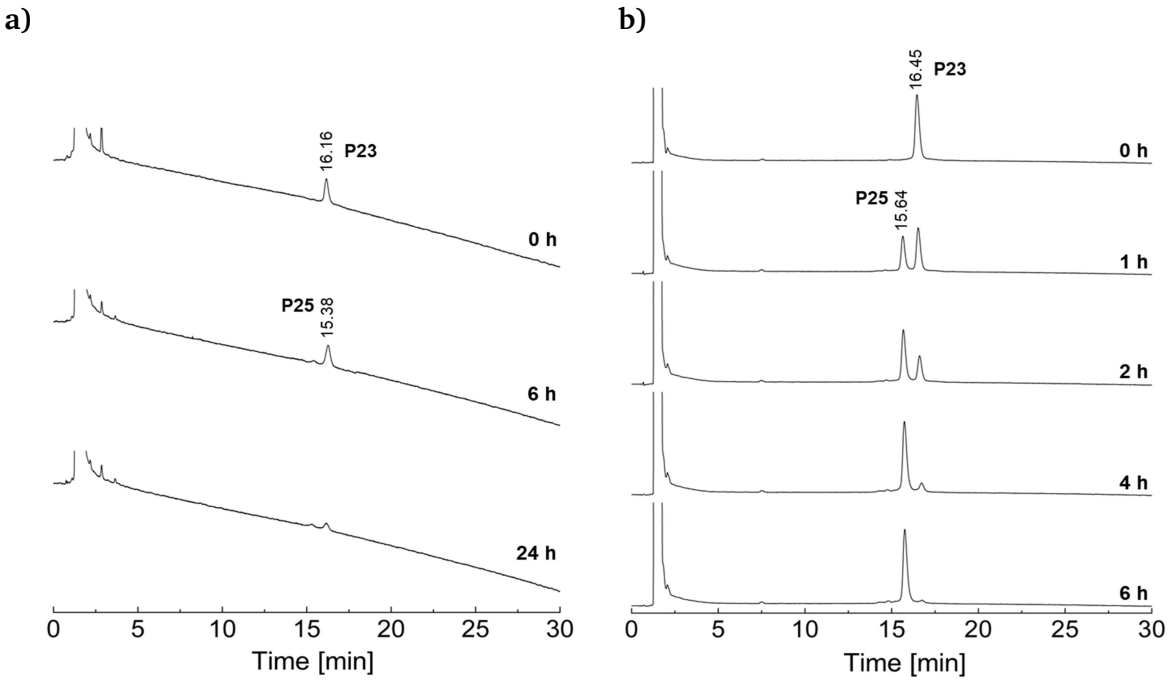

Figure 5.61: **a)** Desulfurization of peptide **P23** in commonly used aqueous desulfurization buffer. **b)** Desulfurization of peptide **P23** in HFIP-based buffer. HPLC conditions: C4 column, gradient: 45–70% ACN in 30 min, 1 ml/min.

Due to the poor solubility of **P23** [Cys(Acm)^{11}][Leu^{21}][Cys^{22}]BM2(1-51) in the aqueous buffer solution, almost no conversion to product **P25** [Cys(Acm)^{11}][Leu^{21}]BM2(1-51) was detectable in the chromatogram (figure **5.61a**). The addition of HFIP led to the formation of two separated phases: an upper phase, which contained well water soluble compounds like sodium phosphate, TCEP and guanidinium chloride, and a lower HFIP containing phase which included the peptide (figure **5.62a**). The binary system imminently formed an emulsion by agitation. The suspension was able to convert peptide **P23** to product **P25** within 6 h (figure **5.61b**). Both phases were easily separable by short centrifugation. Product **P25** was obtained with a nearly quantitative yield and purified by preparative RP-HPLC of the separated lower HFIP phase following instructions **11.1.2**.

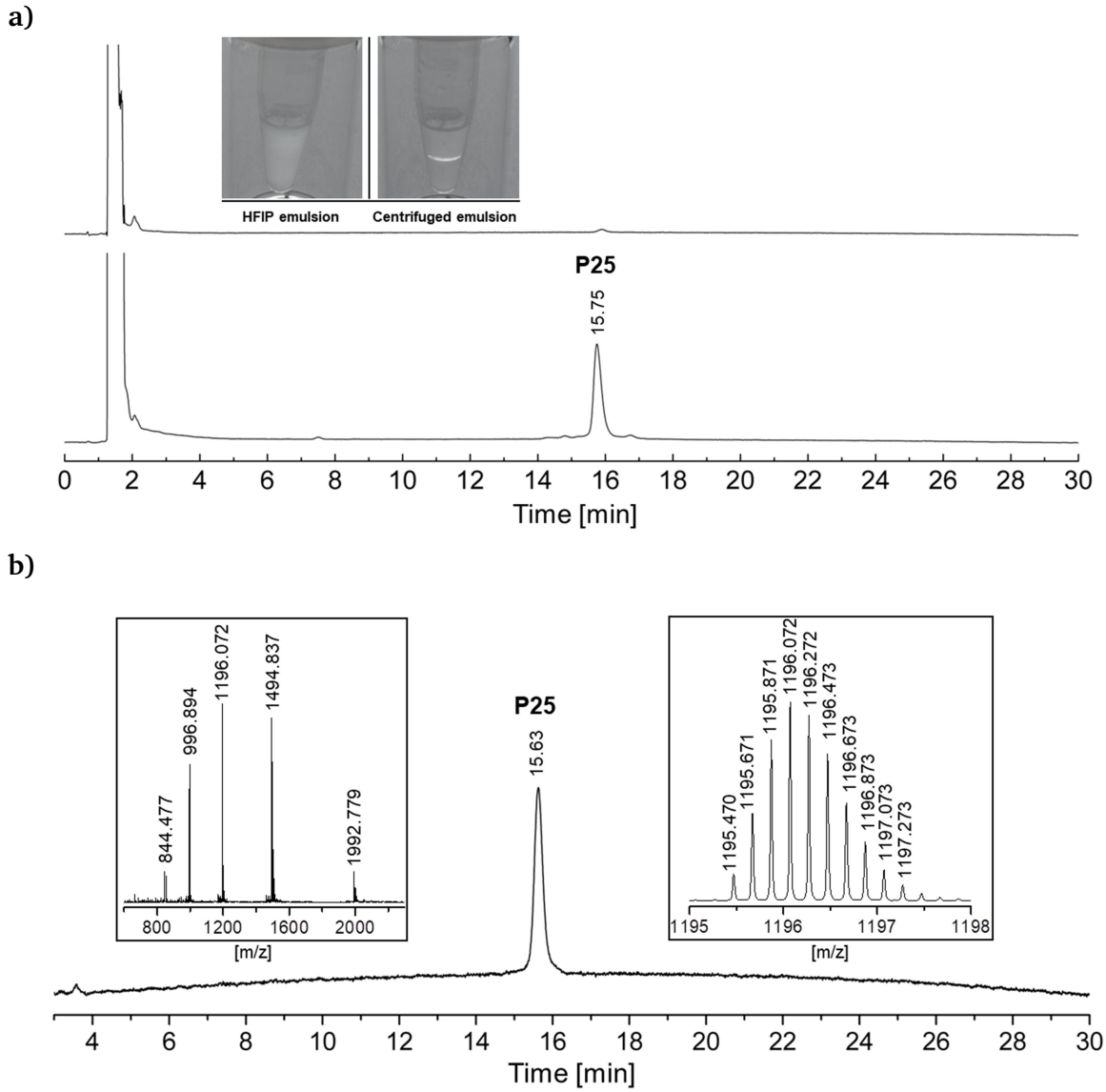

Figure 5.62: **a)** Comparison of the upper water containing phase and the lower HFIP phase. After centrifugation, the lower HFIP phase contains almost the entire product, **b)** RP-HPLC, ESI-MS and isotopic pattern ([M+5H]$^{5+}$) of the purified peptide **P25**. RP-HPLC conditions: C4 column (MultoHigh U C4, 100 x 4 mm), gradient 45 – 70% acetonitrile in 30 min, flow rate of 1 ml/min.

5.3.2. Acm deprotection using conventional procedures

One of the most utilized protecting groups for thiols is the acetaminomethyl (Acm) group. Acm is not cleavable under basic or acidic conditions and remains at cysteine during peptide cleavage from the solid support. This protecting group is also stable under radical conditions like described for the metal-free desulfurisation (chapter **5.3.1**). However, Acm is an unpopular protecting group due to its difficulties in removal. Over the time, many different methods were published with the aim of remove Acm efficiently from cysteine residues. Nevertheless, most of these methods require toxic chemicals such as heavy metal salts like mercury acetate. Alternative, elemental iodine can also be applied for Acm deprotection, however, with the risk of peptide oxidation. Acm deprotection by iodine is especially useful for peptides with multiple Acm protecting groups. Thereby, peptides with disulfide bonds are formed which are less sensitive to oxidation. However, for deprotection of a single Acm group within the peptide chain, heavy metal ions were described as more efficient (chapter **3.6.2**). Today, the use of silver salts is the most common way to remove Acm from cysteine. Interestingly, not all silver salts show the same efficiency for Acm deprotection. The anion of the silver salt seems to play an equally important role for an efficient cleavage. Silver trifluoromethanesulfonate (AgOTf) was found to be the most potent salt in previous studies.[187] However, silver ions sometimes create strong complexes with membrane peptides making AgOTf difficult for Acm deprotection.[219] Some studies even describe the usage of elemental iodine as the most efficient alternative to heavy metal ions without any oxidation observed by RP-HPLC and ESI-MS.[182a] In order to investigate the best method for Acm deprotection from peptide **P25** [Cys(Acm)^{11}][Leu^{21}]BM2(1-51) elemental iodine and AgOTf were tested and compared according to instructions **12.1.1** and **12.1.2** (figure **5.63**). As product **P26** [Leu^{21}]BM2(1-51) was acquired.

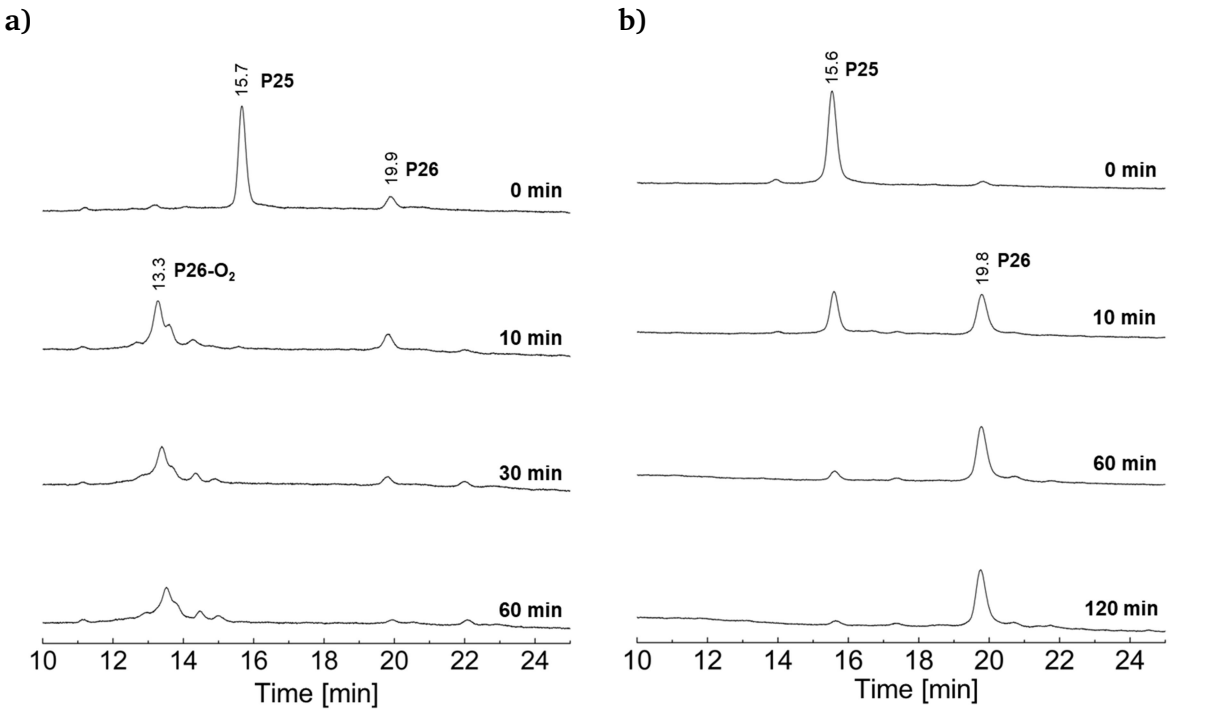

Figure 5.63: **a)** Acm deprotection of peptide **P25** with elemental iodine in concentrated acetic acid. **b)** Acm deprotection of peptide **P25** with AgOTf. HPLC conditions: C4 column (MultoHigh U C4, 100 x 4 mm), gradient 45–70% acetonitrile in 30 min, flow rate of 1 ml/min.

The Acm deprotection by elemental iodine resulted in several products with similar retention times of around 13.3 min. A further single product with a retention time of 19.9 min was already detected at the beginning of the reaction. The reaction was completed after 10 min since no traces of starting peptide **P25** [Cys(Acm)^{11}][Leu^{21}]BM2(1-51) were detectable by RP-HPLC.

ESI-MS analysis of all products revealed that the peaks at approximately 13.3 min were oxidized side products of product **P26** [Leu^{21}][BM2(1-51). The main signal in ESI-MS could be assigned to the two-fold oxidized side product **P26-O$_2$**. The product with the retention time of 19.9 min showed the exact mass and the correct isotopic pattern of final peptide product **P26** [Leu^{21}][BM2(1-51). According to RP-HPLC analysis Acm deprotection with elemental iodine reached a yield of 20%. The results of the ESI-MS analysis are depicted in figure **5.64**.

a) Isotopic pattern **P26-O$_2$** **b)** ESI-MS of **P26** **c)** Isotopic pattern **P26**

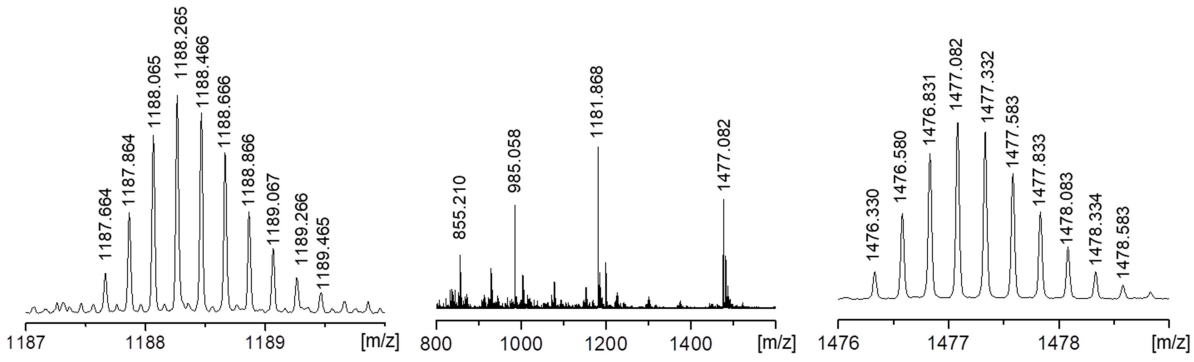

Theoretical monoisotopic mass
$C_{270}H_{442}N_{76}O_{68}S_3$
$[M+5H]^{5+}$ = 1187.660 m/z

Theoretical average masses
$C_{270}H_{442}N_{76}O_{66}S_3$
$[M+5H]^{5+}$ = 1182.023 m/z

Theoretical monoisotopic mass
$C_{270}H_{442}N_{76}O_{66}S_3$
$[M+4H]^{4+}$ = 1476.325 m/z

Figure 5.64: **a)** Isotopic pattern of product **P26-O$_2$** that was monitored in RP-HPLC at 13.3 min, **b)** Entire ESI-MS spectrum of product **P26** collected at a retention time of 19.9 min, **c)** isotopic pattern of peptide P**26**.

A further deprotection experiment tested silver trifluoromethanesulfonate (AgOTf) for cleavaging Acm from **P25**. Deprotection was carried out in concentrated TFA containing 0.2 M AgOTf following instruction **12.1.1**. According to RP-HPLC analysis, 50% of the starting peptide **P25** [Cys(Acm)^{11}][Leu^{21}]BM2(1-51) was deprotected after 10 min. Product **P26** [Leu^{21}]BM2(1-51) occurred at a retention time of 19.8 min similar to the deprotection product acquired by the oxidative deprotection with elemental iodine. The reaction was completed after 120 min. In table **5.30** the yields of the Acm deprotection by iodine and AgOTf are compared.

Table 5.30: Acquired yields of peptide **P26** by Acm deprotection using elemental iodine or AgOTf.

Peptide	Solution for Acm deprotection	Yield [%]
[Leu^{21}]BM2(1-51)	0.2 M AgOTf in TFA	66^a
[Leu^{21}]BM2(1-51)	0.2 M I_2 in AcOH	20^b

a Calculated by real obtained mass.

b Calculated by relative peak area analysis by RP-HPLC.

After successful Acm deprotection using AgOTf, product **P26** was purified by preparative RP-HPLC following procedure **8.1.7**. The final peptide **P26** [Leu^{21}]BM2(1-51) was analyzed by analytical RP-HPLC and ESI-MS. In figures **5.65** the reinjection of the purified peptide **P26** and the results of the mass spectrometry are illustrated.

a)

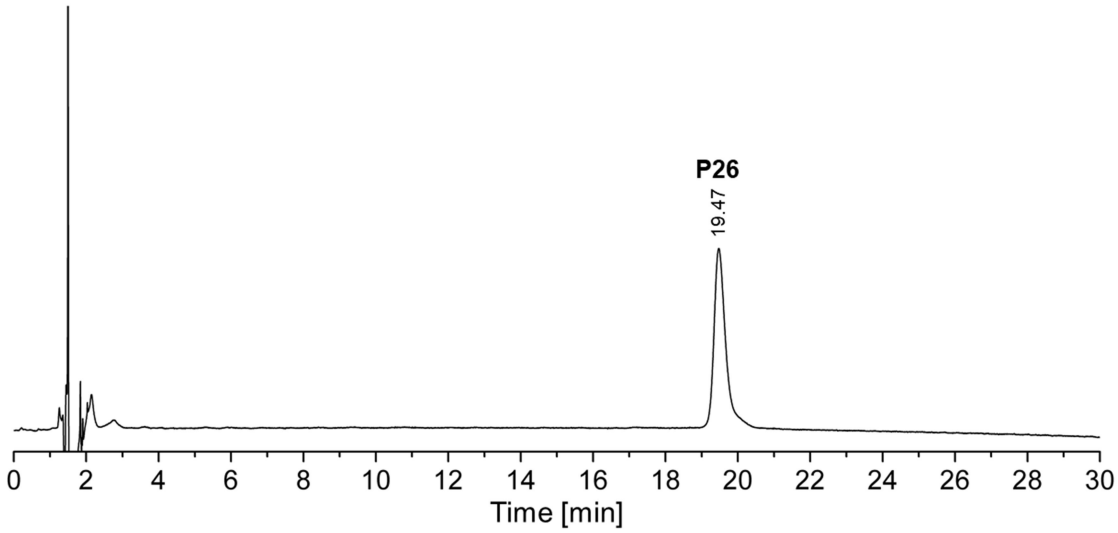

b) ESI-MS of **P26** [Leu^{21}]BM2(1-51)

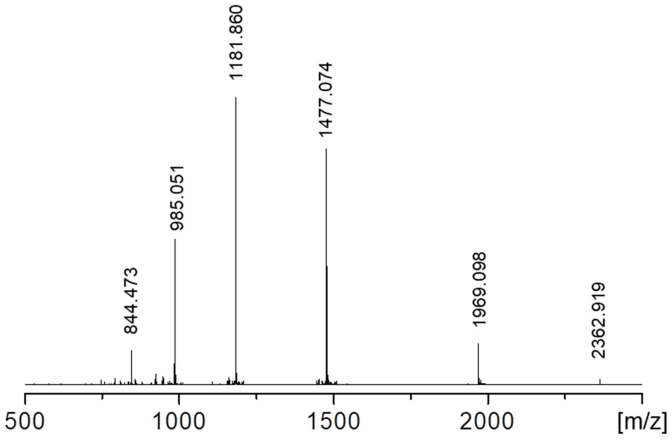

c) Isotopic pattern **P26**

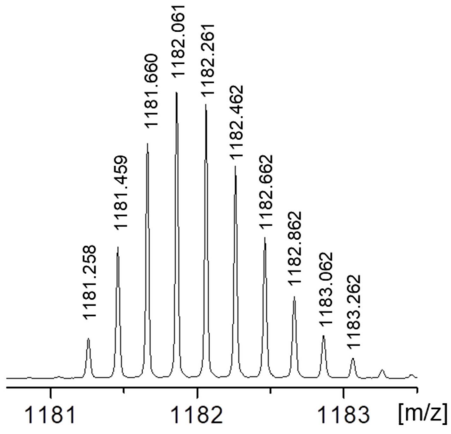

Theoretical average masses

$[M+6H]^{6+}$ = 985.187 m/z $[M+4H]^{4+}$ = 1477.277 m/z

$[M+5H]^{5+}$ = 1182.023 m/z $[M+3H]^{3+}$ = 1969.367 m/z

Theoretical monoisotopic mass

$C_{270}H_{442}N_{76}O_{66}S_3$

$[M+5H]^{5+}$ = 1181.262 m/z

Figure 5.65: **a)** Reinjection of the purified product **P26**. The RP-HPLC experiment was performed with a C4 column (MultoHigh U C4, 100 x 4 mm) using water as eluent A and acetonitrile as eluent B containing 0.1% TFA. Gradient: 45–70% acetonitrile in 30 min, with a flow rate of 1 ml/min, **b)** ESI-MS spectra of purified product **P26** obtained by Acm deprotection using AgOTf, **c)** Isotopic pattern of the $[M+5H]^{5+}$ signal of **P26**.

5.4. Predominate fold analysis of BM2 peptides by CD spectroscopy

After cleavage from the solid support, freeze drying and purification, most chemically synthesized peptides were obtained as an unstructured "random coil". Under physiological conditions and in the presence of folding inducing additives, defined secondary structures with the lowest energetic ground state are preferred. Fluorine containing solvents such as TFE possess folding promoting properties and facilitate the formation of secondary structures (chapter **3.5.2**).[126a, 126b] A simple method to determine the percentage of α-helices, β-turns and unstructured regions within a peptide chain is circular dichroism (CD) spectroscopy. This method relies on differential absorption of right- and left-handed circularly polarized light through chiral, optically active molecules such as peptides and proteins. Right-handed α-helical peptides provide a CD spectrum with a characteristic negative CD band at 209 nm and 222 nm.[220] The helical content of the synthesized BM2 fragments **P2** [Cys^{22}]BM2(22-51) and **P17** BM2(1-21)-NH_2 and final target peptides **P26** [Leu^{21}]BM2(1-51) and **P27** [Leu^{10}]BM2(1-51) were determined by CD spectroscopy according to instruction **8.1.9**. Previous NMR studies already provided some structural information on the BM2 channel sequence which is highlighted in figure **5.66**.[195] However, the structure between residues 36-44 is not fully clarified yet.

Figure 5.66: Available structural information of BM2(1-51) obtained from solution NMR and CD studies.[4, 195]

In order to gain more structural information's about the BM2(1-51) channel domain, CD spectroscopy of the BM2 fragments **P2** and **P17** and of the ligation products **P25**, **P26** and **P27** were performed. These measurements were carried out in a phosphate buffer, TFE or POPC lipid bilayers according to instructions **8.1.9** and **8.1.10**.

Circular dichroism in phosphate buffer and TFE

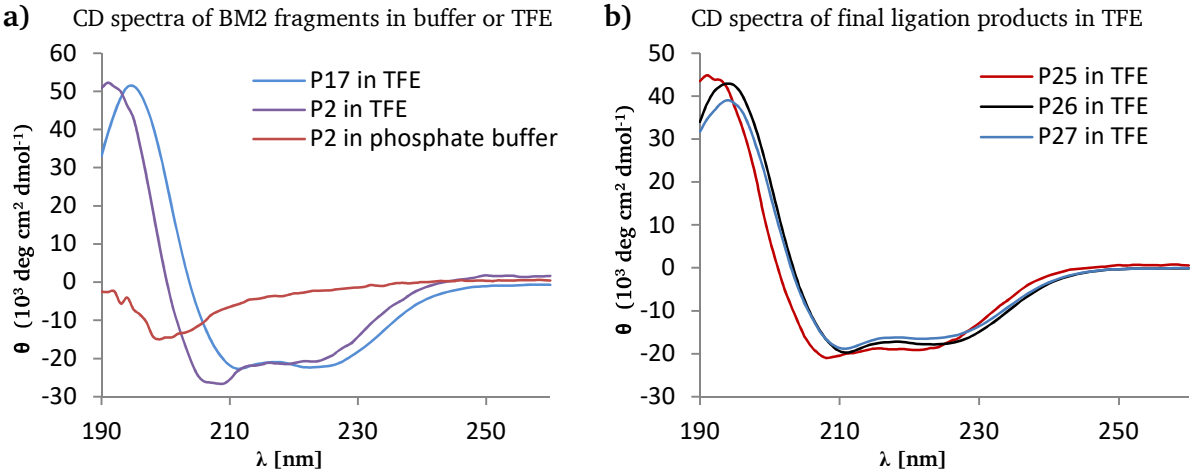

Figure 5.67: Far UV CD spectra between 190–260 nm, **a)** BM2(1-21) **P17** in TFE (blue), [Cys^{22}]BM2(22-51) **P2** in TFE (purple), [Cys^{22}]BM2(22-51) **P2** in 0.2 M Na_2HPO_4 buffer (red), **b)** [Cys(Acm)^{11}][Leu^{21}]BM2(1-51) **P25** (red), [Leu^{21}]BM2(1-51) **P26** (black) and [Leu^{10}]BM2(1-51) **P27** (blue).

CD spectroscopy of **P2** [Cys^{22}]BM2(1-51) in phosphate buffer showed a typical CD band for a random coil with an undefined secondary structure and a minimum at approximately 200 nm. The helical percentage of peptide **P2** in phosphate buffer was lower than 20%. This result confirmed that phosphate buffers, without addition of helix promoting additives, are not cable of inducing peptide folding efficiently. However, analysis of **P2** [Cys^{22}]BM2(1-51) and **P17** BM2(1-21)-NH_2 in TFE displayed characteristic spectra for an α-helix. Surprisingly, analysis of **P2** in TFE showed an unexpectedly high helical content of over 76.5% which was slightly higher than the α-helical content of peptide **P17** (72.7%) that carries the half of the proton conducting channel domain of BM2(1-51).

Deconvolution of CD spectra of **P25** [Cys(Acm)^{11}][Leu^{21}]BM2(1-51), **P26** [Leu^{21}]BM2(1-51) and **P27** [Leu^{10}]BM2(1-51) showed α-helical contents between 59-66% (table **5.31**). The additional Acm group at peptide **P25** had only a minor but rather helix promoting effect in TFE. The results of the final deprotected ligation products **P26** [Leu^{21}]BM2(1-51) and **P27** [Leu^{10}]BM2(1-51) were almost equal and reached α-helical contents of around 60%.

Table 5.31: Results of the deconvoluted CD spectra at a wavelength of 190-260 nm in TFE.

Peptide	P2[a]	P2	P17	P25	P26	P27
Helical	18.10 %	76.50 %	72.70 %	66.30 %	63.30 %	59.1 %
Antiparallel	55.30%	0.40%	0.20%	0.60%	0.50%	0.7%
Parallel	10.00%	2.20%	3.90%	3.50%	4.80%	5.1%
Beta-Turn	22.30 %	11.00 %	10.10 %	12.00 %	11.60 %	12.4 %
Rndm. Coil	29.40 %	6.70 %	17.60 %	13.00 %	21.10 %	22.1 %
Total Sum	135.10 %	96.70 %	104.50 %	95.50 %	101.30 %	99.4 %

a 0.2 M Na_2HPO_4 buffer

Circular dichroism in POPC liposomes

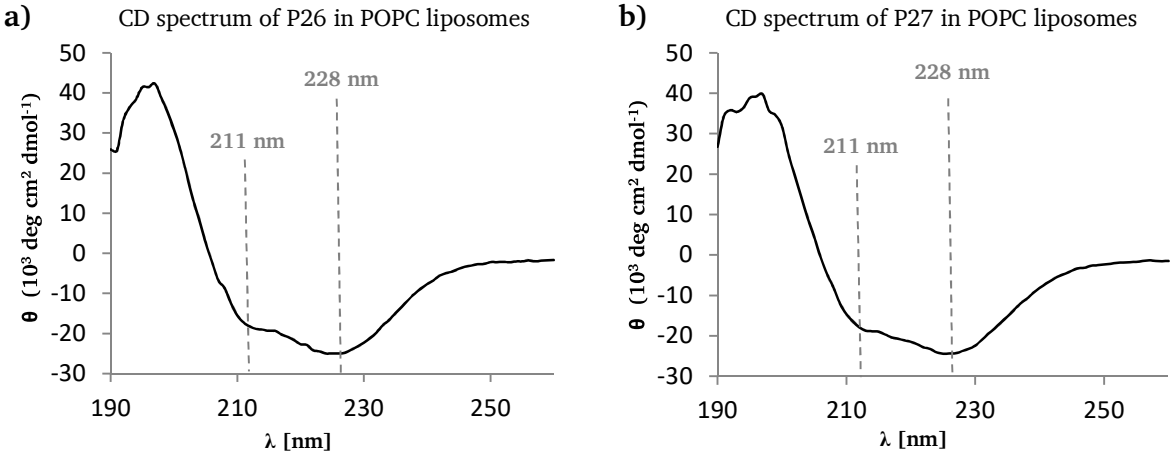

Figure 5.68: Far UV CD spectra between 190–260 nm of the final BM2 peptides in 0.65 mM POPC, Na_2HPO_4 buffer at a pH of 7.5. **a) P26** [Leu^{21}]BM2(1-51), **b) P27** [Leu^{10}]BM2(1-51).

Biological cell membranes are mainly composed of phospholipid bilayers in which transmembrane proteins are embedded. Commercially available phospholipids like 1-palmitoyl-2-oleoyl-sn-glycero-3-phosphocholine (POPC) are often applied to simulate the conditions in biological cell membranes due to their ability to form micelles or liposomes in

aqueous phosphate buffers. The lipophilic tails of phospholipids create a cell membrane similar liposome in which helical protein segments start to fold spontaneously.[221] In order to evaluate the secondary structure of the final peptides **P26** [Leu^{21}]BM2(1-51) and **P27** [Leu^{10}]BM2(1-51), in a cell membrane-like environment, CD spectroscopy was recorded in unilamellar POPC liposomes with low polydispersity. The liposomal suspension was prepared by extrusion using a membrane with a pore size of 1 μm according to instructions **8.1.9** and **8.1.10**. Figure **5.68** displays the CD spectra of **P26** [Leu^{21}]BM2(1-51) and **P27** [Leu^{10}]BM2(1-51) with the typical double minima at 211 nm and 228 nm.

The data confirmed that the final BM2 peptides **P26** [Leu^{21}]BM2(1-51) and **P27** [Leu^{10}]BM2(1-51) predominantly possess the characteristic folding of an α-helical structure in both POPC liposomes and TFE. Deconvolution of CD spectra revealed a predominant helical content of over 60% in POPC bilayers (table **5.32**) which is in line with CD spectra in TFE (table **5.31**).

Table 5.32: Results of the deconvoluted CD curves of peptides **P26** and **P27** at 200-260 nm in POPC/Na_2HPO_4 buffer.

Peptide	**P26** [Leu^{21}]BM2(1-51)	**P27** [Leu^{10}]BM2(1-51)
Helical	65.4 %	64.3 %
Antiparallel	2.40%	2.50%
Parallel	4.30%	4.60%
Beta-Turn	10.8 %	10.9 %
Rndm. Coil	24.4 %	25.5 %
Total Sum	107.3 %	107.7 %

Previous NMR studies demonstrated that the region of BM2(6–28) forms an α-helical structure while the rest of the peptide sequence was predicted to be structurally disordered.[4] In 2019, new NMR studies performed by Mei Hong *et al*. revealed that residues 1-5 and 29-35 display chemical shifts that belong to random coil or β-sheet conformation.[195] The CD studies in TFE and POPC, which were performed during this work, indicate that the region between residues 36-44 might also contain an α-helical section which concurs with recently published NMR studies.[195]

6. Conclusion

Advantages and disadvantages of Hmp-peptides

During this work, the Hmp group turned out to be highly useful for the preparation of peptide thioesters. Hmp-peptides provide several advantages over alternative thioester peptides such as a simple and fast synthesis and compatibility with Fmoc-based SPPS. Moreover, Hmp carries three functional groups which allow the attachment of C-terminal solubilizing tags or other functional groups. So far, the only alternative method which combines Fmoc-based SPPS with temporary bound solubilizing tags is the Dbz/MeDbz strategy developed by Dawson and co-workers.[40] However, in contrast to Dbz/MeDbz-peptides, Hmp-peptides are not prone to capping steps or over-acetylation and need no additional activation step by toxic chemicals such as 4-nitrophenyl chloroformate.[40a] During Fmoc-SPPS, Hmp is protected which reduces the risk of unexpected side reactions. Moreover, the thiol group of Hmp can be protected with different orthogonal protecting groups that enable one-pot ligations with multiple peptide segments. The only by-product that is formed during native chemical ligation is from hydrolysis of the Hmp-group under neutral or slightly basic conditions. This can decrease the ligation yield and needs to be kept into account while choosing Hmp-peptides.

However, all ligation methods investigated during this work were performed with reasonable ligation yields of approximately 90%. Although previous reports described the advantages of Hmp, this building block is not commercially available so far. Indeed, Hmp could be efficiently synthesized in two steps during this work starting from cheap and easily available precursors (chapter **5.1.1**).

Synthesis of Hmp-peptides

At the beginning of this thesis the production and properties of Hmp-peptides were intensively studied. The Mitsunobu reaction was found to be a decisive coupling step which was most efficient if performed as double coupling with a maximum coupling time of 2 h. Experiments with longer coupling times displayed no enhanced resin loadings. Racemisation of the Hmp coupled amino acid, induced by the Mitsunobu reaction, could be excluded as demonstrated by the synthesis and analysis of Phe-(L-Leu)-Hmp and Phe-(D-Leu)-Hmp (chapter **5.1.2**). However, the very different retention times in the chromatogram of the investigated dipeptide diastereomers were a surprising finding during these studies.

Model Hmp-peptides **P4**-**P12** could be easily synthesized by manual Fmoc-SPPS. Peptides **P4** [Ile^{21}]BM2(17-21)-Hmp, **P5** [Ile^{21}]BM2(17-21)-Hmp-ADO and **P6** [Ile^{21}]BM2(17-21)-Hmp-ADO$_2$ were synthesized with isoleucine at the ligation site while **P7** [Leu^{21}]BM2(17-21)-Hmp, **P8** [Leu^{21}]BM2(17-21)-Hmp-ADO and **P9** [Leu^{21}]BM2(17-21)-Hmp-ADO$_2$ were produced as leucine counterparts. Especially important was the production of model peptides **P10** [Leu^{21}]BM2(17-21)-Hmp-Lys$_5$, **P11** [Leu^{21}]BM2(17-21)-Hmp-ADO-Lys$_5$ and **P12** [Leu^{21}]BM2(17-21)-Hmp-ADO$_2$-Lys$_5$ which were assembled with C-terminal pentalysine tags. Thereby it was discovered that introduction of an ADO unit was necessary for a successful synthesis of Hmp-peptides with pentalysine tags. Peptide **P10** [Leu^{21}]BM2(17-21)-Hmp-Lys$_5$ without an additional spacer unit could not be obtained by Fmoc-SPPS. However, after preparative RP-HPLC, **P11** and **P12** were obtained with yields of 1.1% and 1.7%, respectively.

Model peptides **P13**-**P15** with C-terminal polyarginine tags could not be synthesized by Fmoc-SPPS even if ADO units were incorporated as spacer units. Synthesis of long Hmp-peptides **P16**-**P20** succeeded by automated, microwave-assisted Fmoc-SPPS. In order to prevent peptide cleavage from the solid support, 2-methylpiperidine was necessary for Fmoc deprotection steps. After purification, peptide **P16** [Leu^{10}]BM2(1-10)-Hmp was acquired with a yield of 2.9%. Peptides **P18** [Leu^{21}]BM2(1-21)-Hmp and **P19** [Leu^{21}]BM2(1-21)-Hmp-ADO_2 were obtained with 1.7% and 3.6% yield. Ingeniously, the synthesis of the long peptide **P20** [Leu^{21}]BM2(1-21)-Hmp-ADO-Lys_5 also succeeded and reached a yield of 0.56% after purification by preparative RP-HPLC. In conclusion all planned peptides could be synthesized successfully by manual or automated Fmoc-SPPS except for the arginine carrying model peptides **P13**-**P15**.

Solubilizing tag-assisted NCL

In a first set of ligation studies the influence of different solubilizing tags on ligation yields was studied. Therefore, model peptides **P4**, **P7**-**P9**, **P11**-**P12** were ligated using a conventional (aqueous) buffer solution (chapter **5.1.9**). **P22** [Leu^{21}]BM2(17-35) was acquired as product.

Initial ligation studies with **P4** [Ile^{21}]BM2(17-21)-Hmp and **P7** [Leu^{21}]BM2(17-21)-Hmp revealed ligation yields of only 3% for the isoleucine carrying peptide **P4** and 87% yield for the leucine counterpart **P7**. These results confirmed previous findings by Liu and co-workers.[60] Next, the influence of C-terminal ADO tags was tested by the ligation of **P8** [Leu^{21}]BM2(17-21)-Hmp-ADO and **P9** [Leu^{21}]BM2(17-21)-Hmp-ADO_2 which both reached yields of approximately 85%. These results showed that C-terminal ADO units possess only a small steric hindrance which could not reduce ligation efficiency. Especially interesting were ligation experiments with peptides with C-terminal pentalysine tags. These ligation experiments were also performed in aqueous ligation buffer **A**. The successful ligations of model peptides **P11** [Leu^{21}]BM2(17-21)-Hmp-ADO-Lys_5 and **P12** [Leu^{21}]BM2(17-21)-Hmp-ADO_2-Lys_5 proved the feasibility of the method. According to RP-HPLC analysis both ligations reached yields over 80% indicating only a small negative effect of the C-terminal pentalysine tag to the ligation yield.

A powerful demonstration of the solubilizing tag-assisted NCL was made by the successful ligation of **P23** [$Cys(Acm)^{11}$][Cys^{22}][Leu^{21}]BM2(1-51) in aqueous phosphate buffer **A**. This ligation could be achieved with a yield of 71%. Since organic co-solvents as additives were not necessary in buffer **A**, the solubilizing tag-assisted native chemical ligation strategy represents an environmentally friendly method for the production of hydrophobic peptides.

Investigation of the HFIP/TFE-assisted NCL

The usage of fluorinated alcohols as co-solvents for aqueous ligation buffers turned out to be another efficient method to ligate hydrophobic Hmp-peptides. However, TFE as an additive led to the formation of an unexpected side product **SP2** which was not capable of reacting during the ligation. ESI-MS revealed a mass increase of 26 Da which could be explained by carbamylation of the N-terminal cysteine residue of peptide **P2** [Cys^{22}]BM2(22-51). Possible peptide carbamylation is well described in the literature in the presence of cyanate. Different

studies investigated an equilibrium between urea and cyanate as well as cyclic modifications of cysteine side chains by cyanate.[213-214] However, this side reaction has never been described in the literature using TFE as a co-solvent for ligation buffers. Considering these results TFE was suspected to promote cyanate formation by deamination of urea. Successful ligation studies of the AM2 proton channel,[131] using TFE as a co-solvent, were performed in guanidinium chloride based buffers which tend not to *in situ* cyanate formation. In conclusion, it was found that TFE and urea cannot be used together for peptide buffers without the risk of unintended modifications. As a consequence HFIP was further investigated as a possible co-solvent for urea-based phosphate buffers. In the course of this work HFIP turned out to be an ideal co-solvent for Hmp-peptides. In contrast to TFE no peptide modifications were detectable in analytical RP-HPLC or ESI-MS using HFIP as co-solvent. All hydrophobic peptides **P16** [Leu^{10}]BM2(1-10)-Hmp, **P18** [Leu^{21}]BM2(1-21)-Hmp and **P19** [Leu^{21}]BM2(1-21)-Hmp-ADO$_2$ were entirely soluble in the HFIP buffer **C** and could be efficiently ligated. Moreover, the presence of HFIP seemed to reduce the formation of the hydrolysis product. As a result, ligation products **P23** [Cys(Acm)^{11}][Cys^{22}][Leu^{21}]BM2(1-51) and **P27** [Leu^{10}]BM2(1-51) were acquired with yields of 82-96%.

Investigation of N-heterocyclic carbenes (NHCs) in [C$_2$mim][OAc]

The detailed study of [C$_2$mim][OAc] during this thesis confirmed that imidazolium-based ionic liquids are able to chemically react with sulfur containing compounds and cysteine residues in peptides. For the first time reaction products of [C$_2$mim][OAc] and organic model compounds could be isolated and unambiguously identified by TLC, ESI-MS and solution NMR. All sulfur containing compounds (PhSH, PhSSPh, BzlSH and BzlSSBZl) were tested as thiols and disulfides. Surprisingly, both forms (disulfides and thiols) were always detectable right after dissolution in the ionic liquid independent of which form was used as starting compound. This observation suggests that reducing and oxidizing conditions exist simultaneously in [C$_2$mim][OAc]. The obtained RP-HPLC data confirmed the assumption that the *in situ* generated N-heterocyclic carbenes (NHCs) react primarily with disulfides (chapter **5.2.5** and **5.2.6**). This finding supports the hypothesis that thiols are oxidized first in [C$_2$mim][OAc] before they undergo chemical modifications by imidazolium carbenes. Furthermore, it was found that the presence of an adjacent methyl group at the sulfur containing compound led to cleavage of sulfur. However, in absence of an adjacent methyl group as in the case of diphenyl disulfide, the reaction stops after reaction of the imidazolium cation with sulfur.

In the further course of this work the cysteine containing peptide **P1** [Cys^{22}]BM2(22-35) was dissolved and analyzed in the neat ionic liquid [C$_2$mim][OAc]. It could be demonstrated that peptide **P1** was modified in a similar way as observed for the organic model compounds (PhSH, PhSSPh, BzlSH and BzlSSBZl). In neat [C$_2$mim][OAc] peptide **P1** was first oxidized to the disulfide before it was attacked by the imidazolium cation. Additionally, further oxidation of the cysteine residue was found by ESI-MS. An interesting side reaction was observed by desulfurization of cysteine to the corresponding alanine residue which provides a possible alterative way for a one-pot ligation-desulfurization strategy. However, this observed side reaction must first be investigated and improved in further studies before it can be used as an alternative synthetic pathway for hydrophobic peptides.

Ligation experiments in [C_2mim][OAc]

The native chemical ligation in the ionic liquid based buffers succeeded for short model Hmp-peptides as well as for long and hydrophobic BM2 fragments. The discovery that a water content of at least 30% was sufficient to prevent NHCs-induced modifications of peptide **P1** [Cys^{22}]BM2(22-35) was the fundament of the IL-based buffer solution (chapter **5.2.8**). The ideal water content for the native chemical ligation of Hmp-peptides was discovered by a series of ligation experiments using rising amounts of water from 0-50% (v/v). **P7** [Leu^{21}]BM2(17-21)-Hmp and **P1** [Cys^{22}]BM2(22-35) were applied as model peptides for these ligation studies (chapter **5.2.9**).

The IL-based ligation buffers **D1** (0% water, pH 11.4) and **D2** (10% water, pH 10.5) showed no product formation. These results were explained by the high pH values of the solutions which primarily hydrolysed the Hmp group. Buffer **D3** (20% water, pH 9.45) showed product formation, however, with a yield of only 10%. In buffer **D4** (30% water, pH 8.70) a ligation yield of 40.8% was achieved. Buffer **D5** (40% water, pH 7.5) turned out as most efficient ligation media. This buffer solution was composed of 60% [C_2mim][OAc] and 40% water containing 150 mM TCEP HCl and 150 mM thiophenol. In buffer **D5** ligation product **P22** [Leu^{21}]BM2(17-35) was obtained with a yield of 72%. Although buffer **D6** (50% water, pH 6.8) showed ligation yields of approximately 56%, a dramatic loss of peptide solubility began. In the further course of this work buffer **D5** was investigated for the ligation of long hydrophobic BM2 segments. The power of the this buffer solution was impressively demonstrated by the successful ligation of the final product **P27** [Leu^{10}]BM2(1-51) with yields between 73-76% (chapter **5.2.10**).

Desulfurization and Acm deprotection

The radical-based desulfurization of peptide **P23** [Cys(Acm)^{11}][Leu^{21}][Cys^{22}]BM2(1-51) to product **P25** [Cys(Acm)^{11}][Leu^{21}]BM2(1-51) was not possible in the commonly applied 6 M guanidinium chloride based (aqueous) desulfurization buffer which is usually described in literature. The poor solubility of peptide **P23** led to precipitation and poor cysteine conversion as shown in the desulfurization experiment using the standard, aqueous buffer solution (chapter **5.3.1**). Since HFIP was successfully applied in ligation experiments (chapter **5.2.3**), desulfurization buffers on the base of HFIP were tested. As result an HFIP/buffer based emulsion was discovered, which could be successfully applied for the desulfurization of peptide **P23** with a yield of 99%. The newly developed emulsion showed further advantages in comparison with “classical” buffer solutions. One major benefit was the significantly simplified product separation by centrifugation. After centrifugation almost all the peptide was left in the lower HFIP phase as shown in figure **5.62**. By separation of the upper aqueous phase all good water soluble impurities were removed immediately. The remaining lower HFIP phase could then be subjected to preparative RP-HPLC for purification of product **P25**.

Acm deprotection of peptide **P25** [Cys(Acm)^{11}][Leu^{21}]BM2(1-51) to the product **P26** [Leu^{21}]BM2(1-51) succeeded in two different ways. In a first experiment deprotection of Acm was possible by treatment with elementary iodine reaching 20% yield. However, massive amounts of oxidized side products were detected by ESI-MS and analytical RP-HPLC. Finally, the deprotection of Acm was achieved with a yield of 66% using silver trifluoromethanesulfonate (AgOTf).

Predominant fold analysis of the final target peptides by CD spectroscopy

Structural analysis of **P26** [Leu^{21}]BM2(1-51) and **P27** [Leu^{10}]BM2(1-51) displayed a characteristic spectra of an α-helix with double-minima at 209/223 nm in TFE and 211/228 nm in the POPC emulsion. The deconvolution of the CD spectra in TFE or POPC liposomes gave similar results. It was found that **P26** and **P27** exist predominantly in an α-helical form, containing around 60% α-helix which is in line with recent NMR studies.[195] These finding might indicate some ordered helical regions between the BM2 residues 36-44 which were predicted to be structurally disordered in former solution NMR studies of the BM2 channel.[4]

Comparison of the final target peptides with the native BM2(1-51) sequence

During this thesis the first total chemical synthesis of the two hydrophobic membrane peptide sequences **P26** [Leu^{21}]BM2(1-51) and **P27** [Leu^{10}]BM2(1-51) was achieved. Substitution of Ile10 or Ile21 by leucine was necessary for synthesis *via* NCL since isoleucine neighbouring ligation sites resulted in exceptionally low ligation yields (chapter **5.1.9**). These results confirmed previous studies with Hmp-peptides by F. Liu and co-workers.[60] According to the current state of knowledge, both mutation sites Leu21 and Leu10 are located outside of the channel pore, directed to the lipid bilayer membrane (figure **3.8**).[4] For this reason, it is reasonable to suppose that the mutations should not dramatically change the function and the proton flux rate compared to the native BM2(1-51) sequence.

7. Chemicals and Materials

7.1. Reagents and solvents for analytic methods

All reagents and solvents for analytical purposes were purchased from commercial sources and stored according to manufacturer recommendations.

Liquid chemicals for analytic: Acetonitrile HPLC grade (Sigma-Aldrich), water HPLC grade (VWR chemicals), trifluoroacetic acid for HPLC (Carl Roth), demethylsolfoxid-d_6 (DMSO-d_6) (Sigma Aldrich), chloroform-d_1 ($CDCl_3$) (Deutero), deuterium oxide (D_2O) (Deutero), cyclohexane-d12 (Deutero), 1,1,1,3,3,3-hexaflorpropan-2-ol (Carbolution Chemicals), 2,2,2-trifluorethanol (Carbolution Chemicals).

Solid chemicals for analytic: Sinapinic acid (Fluka analytical), cyano-4-hydroxycinnamic acid (Sigma-Aldrich), 5,5-dithiobis-2-nitrobenzoic acid (Ellman-reagent) (VWR Chemicals), 1-palmitoyl-2-oleoyl-sn-glycero-3-phosphocholine (POPC) (Avanti).

7.2. Reagents and solvents for synthetic methods

All purchased reagents and building blocks for the Fmoc-solid phase peptide synthesis (Fmoc-SPPS) were used without pre-purification and stored as recommended by the manufacturer. The Hmp(Trt) building block was synthesized according to procedure **9.1** and used without further purification steps.

Solvents and liquid reagents for synthesis: Anisole (Sigma-Aldrich), dichloromethane (Carl Roth), diethyl ether (Carl Roth), diisopopylcarbodiimide (Iris Biotech), N,N-dimethylformamide (Merck Millipore), hydrochloric acid (VWR Chemicals), N,N-diisopropylethylamine (Sigma-Aldrich), N-methyl-2-pyrrolidone (Carl Roth), piperidine (Carl Roth), tetrahydrofuran anhydrous (VWR Chemicals), trifluoroacetic acid (Carl Roth), triisoprpylsilane (Sigma-Aldrich), (Sigma-Aldrich), N,N-diisopropylethylamine (Carl Roth), acetic acid (Carl Roth), acetic acid anhydride (Carl Roth), 1,2-diemethoxyethane (Sigma-Aldrich), 1,1,1,3,3,3-hexaflorpropan-2-ol (Carbolution Chemicals), 2,2,2-trifluorethanol (Carbolution Chemicals), 2-methylpiperidine (Alfa Aesar), 3-chloro-1,2-propanediol (Sigma-Aldrich), hexane (Sigma-Aldrich), 1-ethyl-3-methylimidazolium acetate [C_2mim][AcO] (Iolitec), thiophenol (Sigma-Aldrich), benzyl mercaptan (Alfa Aesar), diphenyl sulfide (Sigma-Aldrich), diethyl azodicaboxylate solution in 40% toluene (Sigma-Aldrich), N,N,N,N-tetramethylethylenediamine (Sigma-Aldrich), nitric acid 68% (Carl Roth).

Solid reagents for synthesis: Guanidinium chloride (Carl Roth), O-(7-Azabenzotriazol-1-yl)-N,N,N′,N′-tetramethyluronium-hexafluorphosphat (HATU) (Carbolution Chemicals), monosodium phosphate (Carl Roth), sodium hydroxide (Carl Roth), tris-(2-carboxyethyl)-phosphine hydrochloride (TCEP ·HCl) (Iris Biotech), 4-mercatophenylacetic acid (Sigma-Aldrich), urea (Carl Roth), disodium phosphate (Carl Roth), glutathione (Sigma Aldrich), 2,2-dithiobis(5-nitropyridine) (Sigma Aldrich), 2,2-azobis[2-(2-imidazolin-2-yl)propane dihydrochloride (VA044) (TCI), sodium hydride 60% dispersion in mineral oil (Sigma-Aldrich).

Table 7.1: Solid supports for the Fmoc-solid phase peptide synthesis (Fmoc-SPPS).

Name	Loading [mmol/g]	Commercial source
AmphiSpheres 40 RAM	0.33 / 0.27	Agilent Technologies
TentaGel R RAM	0.18	RAPP Polymere
Rink Amide MBHA resin	0.40	Novabiochem

Table 7.2: Used Fmoc protected building blocks for the solid phase peptide synthesis (SPPS).

Building blocks for Fmoc-SPPS	Molecular weight [g/mol]	Commercial source
Fmoc-L-Ala-OH	311.3	Carbolution Chemicals
Fmoc-L-Arg(Pbf)-OH	648.8	Carbolution Chemicals
Fmoc-L-Asn(Trt)-OH	596.7	Carbolution Chemicals
Fmoc-L-Asp(OtBu)-OH	411.5	Carbolution Chemicals
Fmoc-L-Cys(Trt)-OH	585.7	Carbolution Chemicals
Fmoc-L-Gln(Trt)-OH	610.7	Carbolution Chemicals
Fmoc-L-Glu(OtBu)-OH	425.5	Carbolution Chemicals
Fmoc-L-Gly-OH	297.3	Carbolution Chemicals
Fmoc-L-His(Trt)-OH	619.7	Carbolution Chemicals
Fmoc-L-Ile-OH	353.4	Carbolution Chemicals
Fmoc-L-Leu-OH	353.4	Carbolution Chemicals
Fmoc-L-Lys(Boc)-OH	468.6	Carbolution Chemicals
Fmoc-L-Met-OH	371.5	Carbolution Chemicals
Fmoc-L-Phe-OH	387.4	Carbolution Chemicals
Fmoc-L-Pro-OH	337.3	Carbolution Chemicals
Fmoc-L-Ser(tBu)-OH	383.4	Carbolution Chemicals
Fmoc-L-Thr(tBu)-OH	397.5	Carbolution Chemicals
Fmoc-L-Trp(Boc)-OH	526.6	Carbolution Chemicals
Fmoc-L-Tyr(tBu)-OH	459.5	Carbolution Chemicals
Fmoc-L-Val-OH	339.4	Carbolution Chemicals
Fmoc-8-amino-3,6-dioxaoctanoiic acid (Fmoc-ADO-OH)	385.42	Ires Biotech
Hmp(Trt)-OH	332.0	Comm. not available
Fmoc-Cys(Acm)-OH	378.0	Ires Biotech
Fmoc-D-Leu-OH	353.4	Carbolution Chemicals

7.3. Laboratory equipment

Table 7.3: Instruments for analytical or synthetic methods used during this work.

Analytical/Synthetic method	Instrument Type	Manufacturer
Preparative RP-HPLC	996 Photodiode Array Detector (PAD) 600-MS system controller 600 Pump	Waters
Analytical RP-HPLC	2998 Photodiode Array Detector 2695 Separation Module	Waters
MALDI-TOF-MS	Autoflex speed TOF/TOF	Bruker Daltonik
Electrospray ionization (ESI) mass spectrometry	Impact II	Bruker Daltonik
LC-MS	HPLC 1200/Impact II	Agilent/Bruker
UV/Vis spectroscopy	UV-1600PC	VWR
pH measurement	716 DMS Titrino Five Easy F20	Metrohm Mettler Toledo
Peptide synthesis	Liberty	CEM
Circular dichroism (CD) spectroscopy	J-810 spectropolarimeter	Jasco
Nuclear Magnetic Resonance (NMR) spectroscopy	300 MHz Avance III 500 MHz DRX 500	Bruker BioSpin

Table 7.4: Analytical columns for reverse phase high-performance liquid chromatography (RP-HPLC).

Solid phase	Column specification
C4	MultoHigh Bio 300-5-C4, 125 x 4 mm, 300 Å pore diameter, 5 μm particle size
C4	MultoHigh U C4, 100 x 4 mm, 100 Å pore diameter, 5 μm particle size
C8	Prontosil 120-5 C8 SH, 125 x 4 mm, 120 Å pore diameters, 5 μm particle size
C18	MultoHigh 100 RP18 3μ, 150 x 4 mm, 100 Å pore diameter, 3 μm particle size

Table 7.5: Preparative columns for reverse phase high-performance liquid chromatography (RP-HPLC).

Solid phase	Column specification
C4	MultoHigh Bio300-5, 250 x 20 mm, 300 Å pore diameter, 5.0 μm particle size
C18	MultoKrom 100-5, 250 x 20 mm, 100 Å pore diameter, 5.0 μm particle size

8. Analytical Methods

8.1. Analytic methods

8.1.1. Analysis of thiols and disulfides in [C_2mim][OAc]

Reactions of sulfur-containing compounds in 1-ethyl-3-methyl-imidazolium acetate were studied by dissolving thiophenol (19.8 mg, 1.83 μl), diphenyl disulfide (39.3 mg), benzyl mercaptan (22.3 mg, 2.11 μl) and dibenzyl disulfide (44.4 mg) in 1.5 ml neat [C_2mim][OAc]. The mixtures were agitated at room temperature until reactions were completed according to RP-HPLC analysis. For reaction monitoring by RP-HPLC aliquots of the solutions (5 μl) were dissolved in 250 μl acetonitrile (0.1% TFA) and analyzed after 0, 1, 2, 4, 8, 12, 24, 48 and 72 h. Reaction products were purified by column chromatography using a mixture of acetonitrile/water (9:1) as an eluent. Product containing fractions were combined and evaporated under reduced pressure. For clear identification, all products were analyzed by TLC, ESI-MS and NMR spectroscopy.

8.1.2. Analysis of [Cys^{22}]BM2(22-35) in [C_2mim][OAc]

Model peptide [Cys^{22}]BM2(23-35) (0.825 mg, 12 mM) was dissolved in 43 μl neat [C_2mim][OAc] (molar ratio 1:500) and agitated at room temperature until no further reaction progress was detectable by RP-HPLC. The effect of the water content to possible peptide modifications was investigated by increasing the water content (10, 20, 30% (v/v). For sample preparation, aliquots of the reaction mixture (4 μl) were dissolved in 60 μl acetonitrile/water (0.4% TFA) and analyzed after 0, 0.5, 1, 2, 4, 8 and 24 h. All found products in the chromatogram were separated and analyzed by ESI-MS.

8.1.3. Thin-layer chromatography (TLC)

Thin-layer chromatography (TLC) was carried out on silica gel 60 F 254 coated glass plates. For hydrophobic samples pure n-hexane or a mixture of n-hexane/ethyl acetate (59:1, v/v) was prepared. For hydrophilic or ionic substances, a solvent system containing acetonitrile/water (9:1, v/v) was applied. All plates were analysed by UV irradiation with 254 nm and 366 nm. The results and retardation factors (R_F) of the TLC measurements are shown in the appendix (chapter **15.2.2**).

8.1.4. Nuclear magnetic resonance (NMR) spectroscopy

NMR spectroscopy was performed using a Bruker Avance III spectrometer with a frequency of 300 MHz for ^{1}H-NMR and 75 MHz for ^{13}C-NMR. Ionic liquids and hydrophilic compounds were dissolved in deuterium oxide (D_2O) or dimethyl sulfoxide-d6 (DMSO-d6). For hydrophobic compounds chloroform-d1 (Cl_3CD) or cyclohexane-d12 was used. Hydrophobic and volatile substances which could not be isolated from ionic liquids by column chromatography were directly extracted by cyclohexane-d12 and measured. All results were evaluated using MestReNova 11.0 software from Mestrelab Research.

8.1.5. Mass spectrometry LC-MS, ESI-MS and MALDI-TOF-MS

MALDI-TOF mass spectrometry was performed using an Autoflex speed TOF/TOF spectrometer from Bruker Daltonics. Sinapinic acid (SA) or α-cyano-4-hydroxycinnamic acid (HCCA) were applied as a matrix for the preparation of peptide samples. The samples were dissolved in a mixture of acetonitrile and water (80/20%, v/v) containing 0.1% TFA and mixed with a concentrated matrix solution (1:1). For sample preparation, 0.2 μl of the mixture was pipetted onto a MALDI-TOF target plate and dried at room temperature.

Liquid chromatography mass spectrometry (LC-MS) was carried out with an Impact II mass spectrometer from Bruker Daltonics. As ionization method, electrospray ionization (ESI) was applied. Good water soluble samples were dissolved in 0.1% TFA or in a mixture of acetonitrile and 0.1% TFA (1:1). Hydrophobic samples, especially hydrophobic peptides, were dissolved in a mixture of 70% TFE and 30% water containing 0.1% TFA.

8.1.6. Reverse-phase high performance liquid chromatography

Analytical reverse-phase high performance liquid chromatography (RP-HPLC) was carried out on a Waters HPLC System (2695 Separation Module, 2998 PAD). As eluent A, water (0.1% TFA) and as eluent B, acetonitrile (0.1% TFA) were applied. Analysis of short model peptides were performed on a C18 column (MultoHigh 100 RP18 3μ, 150 x 4 mm, 100 Å pore diameter, 3 μm particle size). Long, hydrophobic peptides were measured on one of two C4 columns (MultoHigh Bio 300-5-C4, 125 x 4 mm, 300 Å pore diameter, 5 μm particle size or MultoHigh U C4, 100 x 4 mm). HPLC studies with ionic liquids were performed with a C8 column (Prontosil 120-5 C8 SH, 125 x 4 mm, 120 Å pore diameters, 5 μm particle size). Strong hydrophobic and poorly soluble peptides were pre-dissolved with TFE or HFIP and diluted with a 0.2% TFA. The used columns, the gradient and the exact method of each measurement are described in the caption of each chromatogram.

8.1.7. Purification by preparative RP-HPLC

Short model peptides were purified by preparative RP-HPLC using a C18 column (MultoKrom 100-5, 250 x 20 mm, 100 Å pore diameter, 5.0 μm particle size) with water (0.1% TFA) and acetonitrile (0.1% TFA) as eluents. Longer, more hydrophobic peptides were purified with a C4 column (MultoHigh Bio300-5, 250 x 20 mm, 300 Å pore diameter, 5.0 μm particle size). Good soluble peptides were dissolved in the smallest possible amount of water/acetonitrile (0.2% TFA) (2:1). Hydrophobic peptides were pre-dissolved in TFE or HFIP and carefully diluted (without precipitation) using a mixture of water/acetonitrile (0.2% TFA) (1:1). Peptides obtained by ligation, desulfurization or Acm deprotection were directly separated from the reaction buffer. Therefore, the buffers were diluted with TFE/water (0.2% TFA) (1:1) and injected in the preparative HPLC. After purification, the separated fractions were frozen and lyophilized. The purified products were characterized by mass spectrometry (**8.1.5**) and analytical RP-HPLC (**8.1.6**).

8.1.8. UV/Vis spectroscopy

UV/Vis spectroscopy was primarily used to determine the number of Fmoc-groups on the resin support. To calculate the resin loading the method of Eissler and Samson was applied.[222] Fmoc cleavage was achieved by 20% piperidine in DMF. The piperidine solution was agitated with the resin twice (5 min, 15 min) and transferred into a 50 ml volumetric flask. Subsequently, the volumetric flask was filled up to 50 ml with 20% piperidine/DMF solution. The concentrated Fmoc deprotection solution from the flask was diluted (1:100, v/v) with 20% piperidine/DMF and transferred in a cuvette with 1 cm path length. The absorption of the diluted Fmoc deprotection solution was analysed at 289.8 nm. As reference (blank) sample served 20% piperidine solution in DMF. The calculation of the resin loading was carried out with formula **1**.

$$L_{resin} = \frac{\Delta A_{289.8} \cdot V \cdot d}{E_c \cdot w \cdot m_{resin}} \quad \textbf{(1)}$$

$L_{resin} = resin\ loading$
$A_{289.8} = absorbance\ at\ 289.8\ nm$
$V = volumen\ of\ cleavage\ soltion$
$d = dilution = 100$
$E_c = ext.coefficient = 6089ml/mmol \cdot cm$
$L_{resin} = width\ of\ the\ cuvette = 1cm$
$m_{resin} = weight\ of\ the\ resin$

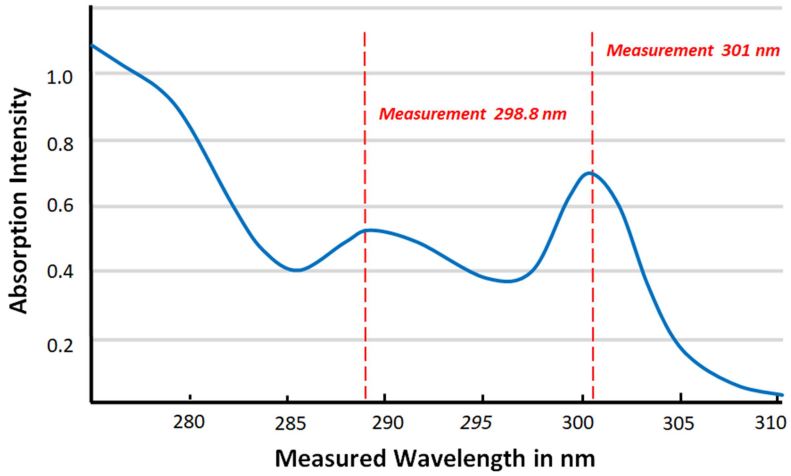

Figure 8.1 Absorption spectrum of the Fmoc deprotection product N-(9H-Fluoren-9-ylmethyl)-piperidine in 20% piperidine/DMF. The absorption maximum at 298.8 nm shows a broader signal compared to 301 nm which led to a more accurate calculation of the resin loading using formula **1**.[222]

8.1.9. Circular dichroism (CD)-spectroscopy

Circular dichroism (CD) was recorded with a Jasco J-810 spectropolarimeter using a wavelength range between 190 – 260 nm at 20 °C (0.1 cm path-length cuvette). CD spectroscopy in TFE or in phosphate buffer (0.2 M Na_2HPO_4, pH 7.0) was performed at a peptide concentration of 0.1 mg/ml. Peptides which were measured in 1-palmitoyl-2-oleoyl-sn-glycero-3-phosphocholine (POPC) liposomes were prepared as follows: 1 mM (1.0 equiv.) of the peptide and 15 mM (15.0 equiv.) POPC were dissolved in the smallest

possible amount of TFE. Subsequently, TFE was removed from the sample with nitrogen gas and the remaining residue was dried in vacuum for 24 h. The dried residue was suspended in degassed Na_2HPO_4 buffer (10 mM, pH 7.5) under argon atmosphere for 2 h at room temperature. The amount of degassed Na_2HPO_4 buffer was calculated to a final POPC concentration of 0.5 mg/ml. Finally, the sample was subjected to three freeze/thaw cycles and extruded 20 times through a polycarbonate membrane following instruction **8.1.10**. All data were acquired in [mdeg] and converted into molar ellipticity [deg x cm^2 x $dmol^{-1}$]. The obtained data were deconvoluted using the software CDNN.

Table 8.1: Amounts and peptides investigated by CD spectroscopy.

Entry	Type	Peptide	[mg]	Buffer / Solvent
P2	Fragments	[Cys^{22}]BM2(22-51)	0.02	phosphate buffer
P2		[Cys^{22}]BM2(22-51)	0.02	TFE
P17		BM2(1-21)-NH_2	0.02	TFE
P25	Ligation products	[Cys(Acm)^{11}][Leu^{21}]BM2(1-51)	0.02	TFE
P26		[Leu^{21}]BM2(1-51)	0.02	TFE
P27		[Leu^{10}]BM2(1-51)	0.02	TFE
P26	Ligation products	[Leu^{21}]BM2(1-51)	0.02	POPC buffer
P27		[Leu^{10}]BM2(1-51)	0.02	POPC buffer

Phosphate buffer: 0.2 M Na_2HPO_4 buffer, pH 7.0
POPC buffer: 0.65 mM POPC in 10 mM Na_2HPO_4, pH 7.5

UV -Range	Vol. [ml]	Conc. [mg/ml]	Cuvette length	Temp.
190 – 260 nm	0.2	0.1	0.1 cm	20 °C

8.1.10. Reconstitution of membrane peptides into lipid POPC vehicles

Liposomal POPC suspensions for CD spectroscopy were prepared by extrusion using a mini extruder with a polycarbonate membrane. The extrusion was performed over the transition temperature of POPC (Tm = -2 °C) at room temperature. The assembly of the mini extruder is illustrated in the three-dimensional exploded view drawing below.

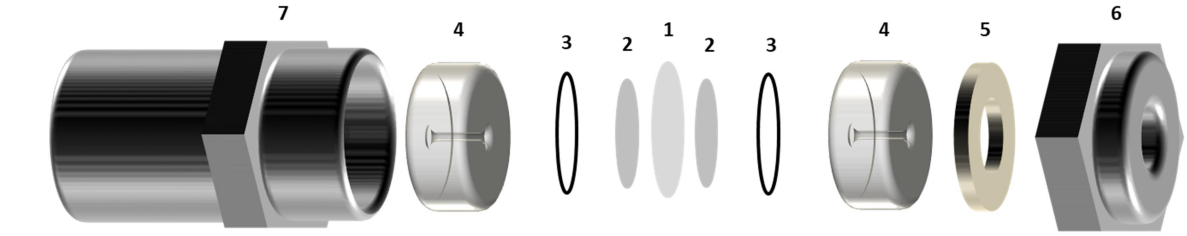

Figure 8.2: Assembly of the Extruder, 1) Polycarbonate Membrane, 2) Filter Supports, 3) O-Rings, 4) Membrane Supports, 5) Teflon Ring, 6) Retainer Nut, 7) Outer Casting.

Once the sample was subjected to three freeze-thaw cycles the solution was carefully loaded in a gas-tight syringe which was placed into the hole of retainer nut **6**. An empty second syringe was placed in the hole at the end of the outer casting **7**. The samples were extruded by transferring the solution through the polycarbonate membrane **1** (pore size: 1 μm) from the syringe at position **6** into the syringe at position **7**. This step was repeated 20 times to obtain unilamellar vesicles.

8.1.11. SDS-polyacrylamide gel electrophoresis (PAGE)

Preparation of the buffers and gels were performed as described in the literature.[223] Peptide samples were prepared in 20 μl of sample buffer by heating to 95 °C for 10 minutes. The electrophoresis was performed with an initial voltage of 30 V until the sample completely entered the stacking gel. Finally, the voltage was increased to 200 V until the run was over. Gels were stained after gel electrophoresis with 0.02% Coomassie stain solution and then destained by a fixing solution for 6 h at room temperature. Protein sizes were compared to a color-coded low range Protein Marker (1.7-42 kDa) as a reference.

9. Synthetic Methods

9.1. Synthesis of Hmp(Trt)

9.1.1. 3-Chloro-2-hydroxypropanoic acid

3-chloro-1, 2-propanediole (1 equiv., 10.0 g, 90.5 mmol) was carefully added to 30 ml conc. nitric acid and slowly heated to 80 °C until the release of brown nitrogen oxides started. The temperature was kept at 80 °C for 20 min and carefully increased to 100 °C for further 20 min. Afterwards, the reaction solution was cooled to room temperature and partially neutralized by slowly adding 7 g $NaHCO_3$. The product was extracted with diethyl ether (6 x 100 ml), the organic layer dried over Na_2SO_4 and the solvent removed under reduced pressure. At the end of the evaporation the temperature was carefully increased to 60 °C to remove any remaining nitric acid. In order to precipitate the product, the viscous residue was cooled to 5 °C and treated with ultrasonic. Finally, the crude product was washed three times with cold chloroform and filtered to obtain 7.4 g (66%) 3-chloro-2-hydroxypropanoic acid.

9.1.2. 2-Hydroxy-3-(triphenylmethyl)thio-propanoic acid (Hmp(Trt))

3-chloro-2-hydroxypropanoic acid (1 equiv., 5.92 g, 47.5 mmol) was dissolved in 50 ml dry-DME and cooled to 0 °C. Sodium hydride (60% oil dispersion) (1 equiv., 1.9 g, 47.5 mmol) was slowly added to the stirred solution in small portions. A second solution of triphenylmethyl thiol (1.05 equiv., 13.11 g, 49.8 mmol) and sodium hydride (1 equiv., 1.9 g, 47.5 mmol) was added dropwise within 30 min under stirring. After 4 h of stirring, the solvent was removed under reduced pressure. The remaining residue was dissolved in a mixture of 400 ml diethyl ether/water (1:1). Afterwards the aqueous phase was separated, washed with diethyl ether (2 x 100 ml) and acidified to a final pH of 3 using 1 M hydrochloric acid. The product was extracted with ethyl acetate (3 x 100 ml) and the organic layer dried over Na_2SO_4. Finally, the solvent was removed under reduced pressure until a highly viscous liquid was left. The viscous liquid was solidified in the refrigerator and the rest of the solvent was removed under reduced pressure at room temperature. The dry and yellow powder was directly used for Fmoc-SPPS. Yield: 11.08 g (98%).

9.2. Manual synthesis of model Hmp-peptides

Manual Fmoc-SPPS of Hmp-peptides was performed in a syringe with a filter inlet. The exact amounts of amino acids, activator and activator base as well as the coupling/deprotection conditions are presented for each peptide in the tables below. Peptides with a C-terminal solubilizing tag (Lys_5, ADO_2) were preloaded manually following a standard Fmoc-SPPS protocol using the respective amino acid building block (4 equiv., 0.2 M) with 1-[bis(dimethylamin)methylen]-1H-1,2,3-triazol[4,5-b]pyridinium-3-oxid-hexafluorophosphat (HATU, 0.2 M, 3.95 equiv.) as an activator and N,N-diisopropylethylamin (DIEA, 0.4 M, 8.00 equiv.) as an activator base. All coupling steps were performed twice at room temperature for 30 min. Fmoc cleavage was achieved by treating the resin for 5 min and 15 min with 20% piperidine/DMF solution at room temperature. Loading determination was performed using the method of Eissler and Samson according to instruction **8.1.8**.[222] All coupling and deprotection steps were followed by intense washing steps with DMF and DCM.

For the coupling of the Hmp rearrangement unit Hmp(Trt) (4.0 equiv., 0.2 M), HATU (3.95 equiv., 0.2 M) and DIEA (8.0 equiv., 0.4 M) were dissolved in DMF and agitated with the resin for 60 min at room temperature (double coupling). The first amino acid (Leu or Ile) at Hmp(Trt) was coupled by the Mitsunobu reaction. According to this procedure, amino acid coupling was achieved by agitating the solid support in a solution of the respective amino acid (0.2 M, 4 equiv.), triphenylphosphane (PPh_3, 0.2 M, 3.9 equiv.) and diethyl azodicarboxylate (DEAD, 40 wt% in toluene, 3.9 equiv.) in dry-THF (2 h, double coupling).

Peptide cleavage from the resin was achieved in a mixture of 90% TFA, 5% water, 2.5% TIPS and 2.5% anisole for 3 h at room temperature. For 100 mg of resin, 1 ml of cleavage solution was applied. The crude peptides were precipitated in cold diethyl ether, centrifuged, and washed with three times with cold diethyl ether.

Table 9.1: Types, amounts and loading capacities of resin supports for manual Fmoc-SPPS of Hmp-peptides.

Entry	Peptide	Resin Amount [g]	Loading [mmol/g]
P4	[Ile^{21}]BM2(17-21)-Hmp	0.30[a]	0.33
P5	[Ile^{21}]BM2(17-21)-Hmp-ADO	0.125[b]	0.18
P6	[Ile^{21}]BM2(17-21)-Hmp-ADO_2	0.125[b]	0.18
P7	[Leu^{21}]BM2(17-21)-Hmp	0.5[a]	0.33
P8	[Leu^{21}]BM2(17-21)-Hmp-ADO	0.25[a]	0.33
P9	[Leu^{21}]BM2(17-21)-Hmp-ADO_2	0.25[a]	0.33
P10	[Leu^{21}]BM2(17-21)-Hmp-Lys_5	0.25[a]	0.33
P11	[Leu^{21}]BM2(17-21)-Hmp-ADO-Lys_5	0.25[a]	0.33
P12	[Leu^{21}]BM2(17-21)-Hmp-ADO_2-Lys_5	0.25[a]	0.33
P13	[Leu^{21}]BM2(17-21)-Hmp-Arg_5	0.25[a]	0.33
P14	[Leu^{21}]BM2(17-21)-Hmp-ADO-Arg_5	0.25[a]	0.33
P15	[Leu^{21}]BM2(17-21)-Hmp-ADO_2-Arg_5	0.25[a]	0.33

a *AmphiSpheres RAM 40 resin*

b *Tentagel resin*

Synthesis of P4: [Ile^{21}]BM2(17-21)-Hmp

Table 9.2: Amino acids and coupling conditions for the manual Fmoc-SPPS of peptide P4.

Building block	Amount [mg]	DMF [ml]	Activator/Base and coupling conditions	Deprotection Base and conditions
Hmp	145	2	HATU/DIEA, 30 min (double coupling)	No deprotection
Ile	140	2.5 dry-THF	DEAD/PPh_3, 2 h (double coupling)	20% piperidine, double deprotection (5 min, 15 min)
Phe	155	2	HATU/DIEA, 30 min (double coupling)	
His	248	2		
Leu	140	2		
Ala	130	2		
Coupling with HATU/DIEA			149 mg HATU/138 μl DIEA	
Wash after coupling			1 min , 5 ml (3 times DMF)	
Fmoc-deprotection			5 ml (20% piperidine/DMF)	
Wash after Fmoc-deprotection			1 min, 5 ml (3 times DMF, 3 times DCM, 3 times DMF)	
Wash before Mitsunobu reaction			1 min , 5 ml (3 times DMF, 4 times dry-THF)	
Coupling with DEAD/PPh_3			225 μl DEAD (100%)/130 mg PPh_3	
Wash after Mitsunobu reaction			1 min , 5 ml (5 times DMF)	

Synthesis of P5: [Ile^{21}]BM2(17-21)-Hmp-ADO

Table 9.3: Amino acids and coupling conditions for the manual Fmoc-SPPS of peptide P5.

Building block	Amount [mg]	DMF [ml]	Activator/Base and coupling conditions	Deprotection Base and conditions
ADO	70	2.0	HATU/DIEA, 30 min (double coupling)	20% piperidine, double deprotection (5 min, 15 min)
Hmp	82	2.0		No deprotection
Ile	160	2.3 dry-THF	DEAD/PPh_3, 2 h (double coupling)	20% piperidine, double deprotection (5 min, 15 min)
Phe	70	2.0	HATU/DIEA, 30 min (double coupling)	
His	112	2.0		
Leu	64	2.0		
Ala	60	2.0		
Coupling with HATU/DIEA			67 mg HATU/63 μl DIEA	
Wash after coupling			1 min , 3 ml (3 times DMF)	
Fmoc-deprotection			3 ml (20% piperidine/DMF)	
Wash after Fmoc-deprotection			1 min, 3 ml (3 times DMF, 3 times DCM, 3 times DMF)	
Wash before Mitsunobu reaction			1 min , 3 ml (3 times DMF, 4 times dry-THF)	
Coupling with DEAD/PPh_3			70 μl DEAD (100%)/118 mg PPh_3	
Wash after Mitsunobu reaction			1 min , 3 ml (5 times DMF)	

Synthesis of P6: [Ile^{21}]BM2(17-21)-Hmp-ADO$_2$

Table 9.4: Amino acids and coupling conditions for the manual Fmoc-SPPS of peptide P6.

Building block	Amount [mg]	DMF [ml]	Activator/Base and coupling conditions	Deprotection Base and conditions
ADO	70	2.0	HATU/DIEA, 30 min (double coupling)	20% piperidine, double deprotection (5 min, 15 min)
ADO	70	2.0		
Hmp	82	2.0		No deprotection
Ile	160	2.3 dry-THF	DEAD/PPh$_3$, 2 h (double coupling)	20% piperidine, double deprotection (5 min, 15 min)
Phe	70	2.0	HATU/DIEA, 30 min (double coupling)	
His	112	2.0		
Leu	64	2.0		
Ala	60	2.0		
Coupling with HATU/DIEA			67 mg HATU/63 μl DIEA	
Wash after coupling			1 min , 3 ml (3 times DMF)	
Fmoc-deprotection			3 ml (20% piperidine/DMF)	
Wash after Fmoc-deprotection			1 min, 3 ml (3 times DMF, 3 times DCM, 3 times DMF)	
Wash before Mitsunobu reaction			1 min , 3 ml (3 times DMF, 4 times dry-THF)	
Coupling with DEAD/PPh$_3$			70 μl DEAD (100%)/118 mg PPh$_3$	
Wash after Mitsunobu reaction			1 min , 3 ml (5 times DMF)	

Synthesis of P7: [Leu^{21}]BM2(17-21)-Hmp

Table 9.5: Amino acids and coupling conditions for the manual Fmoc-SPPS of peptide P7.

Building block	Amount [mg]	DMF [ml]	Activator/Base and coupling conditions	Deprotection Base and conditions
Hmp	240	3.3	HATU/DIEA, 30 min (double coupling)	No deprotection
Leu	292	4.2 dry-THF	DEAD/PPh$_3$, 2 h (double coupling)	20% piperidine, double deprotection (5 min, 15 min)
Phe	256	3.3	HATU/DIEA, 30 min (double coupling)	
His	409	3.3		
Leu	234	3.3		
Ala	218	3.3		
Coupling with HATU/DIEA			248 mg HATU/230 μl DIEA	
Wash after coupling			1 min , 5 ml (3 times DMF)	
Fmoc-deprotection			5 ml (20% piperidine/DMF)	
Wash after Fmoc-deprotection			1 min, 5 ml (3 times DMF, 3 times DCM, 3 times DMF)	
Wash before Mitsunobu reaction			1 min , 5 ml (3 times DMF, 4 times dry-THF)	
Coupling with DEAD/PPh$_3$			375 μl DEAD (40% in toluene)/216 mg PPh$_3$	
Wash after Mitsunobu reaction			1 min , 5 ml (5 times DMF)	

Synthesis of P8: [Leu^{21}]BM2(17-21)-Hmp-ADO

Table 9.6: Amino acids and coupling conditions for the manual Fmoc-SPPS of peptide P8.

Building block	Amount [mg]	DMF [ml]	Activator/Base and coupling conditions	Deprotection Base and conditions
ADO	64	1	HATU/DIEA, 30 min (double coupling)	20% piperidine, double deprotection (5 min, 15 min)
Hmp	120	2		No deprotection
Leu	146	2 dry-THF	DEAD/PPh_3, 2 h (double coupling)	20% piperidine, double deprotection (5 min, 15 min)
Phe	128	2	HATU/DIEA, 30 min (double coupling)	
His	205	2		
Leu	117	2		
Ala	109	2		
Coupling with HATU/DIEA			124 mg HATU/115 μl DIEA	
Wash after coupling			1 min , 5 ml (3 times DMF)	
Fmoc-deprotection			5 ml (20% piperidine/DMF)	
Wash after Fmoc-deprotection			1 min, 5 ml (3 times DMF, 3 times DCM, 3 times DMF)	
Wash before Mitsunobu reaction			1 min , 5 ml (3 times DMF, 4 times dry-THF)	
Coupling with DEAD/PPh_3			187 μl DEAD (40% in toluene)/109 mg PPh_3	
Wash after Mitsunobu reaction			1 min , 5 ml (5 times DMF)	

Synthesis of P9: [Leu^{21}]BM2(17-21)-Hmp-ADO$_2$

Table 9.7: Amino acids and coupling conditions for the manual Fmoc-SPPS of peptide P9.

Building block	Amount [mg]	DMF [ml]	Activator/Base and coupling conditions	Deprotection Base and conditions
ADO	64	1	HATU/DIEA, 30 min (double coupling)	20% piperidine, double deprotection (5 min, 15 min)
ADO	64	1		
Hmp	120	2		No deprotection
Leu	146	2 dry-THF	DEAD/PPh_3, 2 h (double coupling)	20% piperidine, double deprotection (5 min, 15 min)
Phe	128	2	HATU/DIEA, 30 min (double coupling)	
His	205	2		
Leu	117	2		
Ala	109	2		
Coupling with HATU/DIEA			124 mg HATU/115 μl DIEA	
Wash after coupling			1 min , 5 ml (3 times DMF)	
Fmoc-deprotection			5 ml (20% piperidine/DMF)	
Wash after Fmoc-deprotection			1 min, 5 ml (3 times DMF, 3 times DCM, 3 times DMF)	
Wash before Mitsunobu reaction			1 min , 5 ml (3 times DMF, 4 times dry-THF)	
Coupling with DEAD/PPh_3			187 μl DEAD (40% in toluene)/109 mg PPh_3	
Wash after Mitsunobu reaction			1 min , 5 ml (5 times DMF)	

Synthesis of P10: [Leu^{21}]BM2(17-21)-Hmp-Lys$_5$

Table 9.8: Amino acids and coupling conditions for the manual Fmoc-SPPS of peptide P10.

Building block	Amount [mg]	DMF [ml]	Activator/Base and coupling conditions	Deprotection Base and conditions
Lys*	155	2	HATU/DIEA, 30 min (double coupling)	20% piperidine, double deprotection (5 min, 15 min)
Hmp	120	2		No deprotection
Leu	146	2 dry-THF	DEAD/PPh$_3$, 2 h (double coupling)	20% piperidine, double deprotection (5 min, 15 min)
Phe	128	2	HATU/DIEA, 30 min (double coupling)	
His	205	2		
Leu	117	2		
Ala	109	2		
Coupling with HATU/DIEA			124 mg HATU/115 μl DIEA	
Wash after coupling			1 min , 4 ml (3 times DMF)	
Fmoc-deprotection			4 ml (20% piperidine/DMF)	
Wash after Fmoc-deprotection			1 min, 4 ml (3 times DMF, 3 times DCM, 3 times DMF)	
Wash before Mitsunobu reaction			1 min , 4 ml (3 times DMF, 4 times dry-THF)	
Coupling with DEAD/PPh$_3$			187 μl DEAD (40% in toluene)/109 mg PPh$_3$	
Wash after Mitsunobu reaction			1 min , 4 ml (5 times DMF)	

* Repeated five times (synthesis of Lys$_5$ tag).

Synthesis of P11: [Leu^{21}]BM2(17-21)-Hmp-ADO-Lys$_5$

Table 9.9: Amino acids and coupling conditions for the manual Fmoc-SPPS of peptide P11.

Building block	Amount [mg]	DMF [ml]	Activator/Base and coupling conditions	Deprotection Base and conditions
Lys*	155	2	HATU/DIEA, 30 min (double coupling)	20% piperidine, double deprotection (5 min, 15 min)
ADO	64	2		
Hmp	120	2		No deprotection
Leu	146	2 dry-THF	DEAD/PPh$_3$, 2 h (double coupling)	20% piperidine, double deprotection (5 min, 15 min)
Phe	128	2	HATU/DIEA, 30 min (double coupling)	
His	205	2		
Leu	117	2		
Ala	109	2		
Coupling with HATU/DIEA			124 mg HATU/115 μl DIEA	
Wash after coupling			1 min , 4 ml (3 times DMF)	
Fmoc-deprotection			4 ml (20% piperidine/DMF)	
Wash after Fmoc-deprotection			1 min, 4 ml (3 times DMF, 3 times DCM, 3 times DMF)	
Wash before Mitsunobu reaction			1 min , 4 ml (3 times DMF, 4 times dry-THF)	
Coupling with DEAD/PPh$_3$			187 μl DEAD (40% in toluene)/109 mg PPh$_3$	
Wash after Mitsunobu reaction			1 min , 4 ml (5 times DMF)	

* Repeated five times (synthesis of Lys$_5$ tag).

Synthesis of P12: [Leu^{21}]BM2(17-21)-Hmp-ADO$_2$-Lys$_5$

Table 9.10: Amino acids and coupling conditions for the manual Fmoc-SPPS of peptide P12.

Building block	Amount [mg]	DMF [ml]	Activator/Base and coupling conditions	Deprotection Base and conditions
Lys*	155	2	HATU/DIEA, 30 min (double coupling)	20% piperidine, double deprotection (5 min, 15 min)
ADO	64	2		
ADO	64	2		
Hmp	120	2		No deprotection
Leu	146	2 dry-THF	DEAD/PPh$_3$, 2 h (double coupling)	20% piperidine, double deprotection (5 min, 15 min)
Phe	128	2	HATU/DIEA, 30 min (double coupling)	
His	205	2		
Leu	117	2		
Ala	109	2		
Coupling with HATU/DIEA			124 mg HATU/115 μl DIEA	
Wash after coupling			1 min , 4 ml (3 times DMF)	
Fmoc-deprotection			4 ml (20% piperidine/DMF)	
Wash after Fmoc-deprotection			1 min, 4 ml (3 times DMF, 3 times DCM, 3 times DMF)	
Wash before Mitsunobu reaction			1 min , 4 ml (3 times DMF, 4 times dry-THF)	
Coupling with DEAD/PPh$_3$			187 μl DEAD (40% in toluene)/109 mg PPh$_3$	
Wash after Mitsunobu reaction			1 min , 4 ml (5 times DMF)	

* Repeated five times (synthesis of Lys$_5$ tag).

Synthesis of P13: [Leu^{21}]BM2(17-21)-Hmp-Arg$_5$

Table 9.11: Amino acids and coupling conditions for the manual Fmoc-SPPS of peptide P13.

Building block	Amount [mg]	DMF [ml]	Activator/Base and coupling conditions	Deprotection Base and conditions
Arg*	215	2	HATU/DIEA, 30 min (double coupling)	20% piperidine, double deprotection (5 min, 15 min)
Hmp	120	2		No deprotection
Leu	146	2 dry-THF	DEAD/PPh$_3$, 2 h (double coupling)	20% piperidine, double deprotection (5 min, 15 min)
Phe	128	2	HATU/DIEA, 30 min (double coupling)	
His	205	2		
Leu	117	2		
Ala	109	2		
Coupling with HATU/DIEA			124 mg HATU/115 μl DIEA	
Wash after coupling			1 min , 4 ml (3 times DMF)	
Fmoc-deprotection			4 ml (20% piperidine/DMF)	
Wash after Fmoc-deprotection			1 min, 4 ml (3 times DMF, 3 times DCM, 3 times DMF)	
Wash before Mitsunobu reaction			1 min , 4 ml (3 times DMF, 4 times dry-THF)	
Coupling with DEAD/PPh$_3$			187 μl DEAD (40% in toluene)/109 mg PPh$_3$	
Wash after Mitsunobu reaction			1 min , 4 ml (5 times DMF)	

* Repeated five times (synthesis of Arg$_5$ tag).

Synthesis of P14: [Leu^{21}]BM2(17-21)-Hmp-ADO-Arg$_5$

Table 9.12: Amino acids and coupling conditions for the manual Fmoc-SPPS of peptide P14.

Building block	Amount [mg]	DMF [ml]	Activator/Base and coupling conditions	Deprotection Base and conditions
Arg*	215	2	HATU/DIEA, 30 min (double coupling)	20% piperidine, double deprotection (5 min, 15 min)
ADO	64	2		
Hmp	120	2		No deprotection
Leu	146	2 dry-THF	DEAD/PPh_3, 2 h (double coupling)	20% piperidine, double deprotection (5 min, 15 min)
Phe	128	2	HATU/DIEA, 30 min (double coupling)	
His	205	2		
Leu	117	2		
Ala	109	2		
Coupling with HATU/DIEA			124 mg HATU/115 μl DIEA	
Wash after coupling			1 min , 4 ml (3 times DMF)	
Fmoc-deprotection			4 ml (20% piperidine/DMF)	
Wash after Fmoc-deprotection			1 min, 4 ml (3 times DMF, 3 times DCM, 3 times DMF)	
Wash before Mitsunobu reaction			1 min , 4 ml (3 times DMF, 4 times dry-THF)	
Coupling with DEAD/PPh_3			187 μl DEAD (40% in toluene)/109 mg PPh_3	
Wash after Mitsunobu reaction			1 min , 4 ml (5 times DMF)	

* Repeated five times (synthesis of Arg_5 tag).

Synthesis of P15: [Leu^{21}]BM2(17-21)-Hmp-ADO$_2$-Arg$_5$

Table 9.13: Amino acids and coupling conditions for the manual Fmoc-SPPS of peptide P15.

Building block	Amount [mg]	DMF [ml]	Activator/Base and coupling conditions	Deprotection Base and conditions
Arg*	215	2	HATU/DIEA, 30 min (double coupling)	20% piperidine, double deprotection (5 min, 15 min)
ADO	64	2		
ADO	64	2		
Hmp	120	2		No deprotection
Leu	146	2 dry-THF	DEAD/PPh_3, 2 h (double coupling)	20% piperidine, double deprotection (5 min, 15 min)
Phe	128	2	HATU/DIEA, 30 min (double coupling)	
His	205	2		
Leu	117	2		
Ala	109	2		
Coupling with HATU/DIEA			124 mg HATU/115 μl DIEA	
Wash after coupling			1 min , 4 ml (3 times DMF)	
Fmoc-deprotection			4 ml (20% piperidine/DMF)	
Wash after Fmoc-deprotection			1 min, 4 ml (3 times DMF, 3 times DCM, 3 times DMF)	
Wash before Mitsunobu reaction			1 min , 4 ml (3 times DMF, 4 times dry-THF)	
Coupling with DEAD/PPh_3			187 μl DEAD (40% in toluene)/109 mg PPh_3	
Wash after Mitsunobu reaction			1 min , 4 ml (5 times DMF)	

* Repeated five times (synthesis of Arg_5 tag).

9.3. Automated microwave-assisted Fmoc-SPPS

Automated microwave-assisted Fmoc-SPPS was carried out on a Liberty peptide synthesizer (CEM) using a standard Fmoc protocol. Peptide sequences as well as the resin types, amounts and loading capacities are depicted in table **9.14**. The amount of the activator, activator base and amino acids for each peptide are presented in the following tables below. The coupling cycles for the automated Fmoc-SPPS are shown in the appendix (chapter **15.1.4**). The resins for the synthesis of Hmp-peptides **P16**, **P18**, **P19** and **P20** were manually preloaded with the solubilizing tag (Lys_5, ADO_2), spacer (ADO), Hmp and the first two amino acids following instruction **9.2**.

Coupling reactions (double coupling, 15min) were performed with Fmoc-amino acids (0.2 M, 4 equiv.), activated with 1-[bis(Dimethylamin)methylen]-1H-1,2,3-triazol[4,5-b]pyridinium-3-oxid-hexafluorophosphat (HATU, 0.2 M, 3.95 equiv.) and N,N-diisopropylethylamin (DIEA, 0.4 M, 8.00 equiv.) in N,N-Dimethylformamide (DMF) under microwave irradiation.[2] Fmoc deprotection from peptides **P1**, **P2**, **P3** and **P17** was achieved with 20% piperidine in DMF. Fmoc cleavage from Hmp-peptides **P16**, **P18**, **P19** and **P20** was performed with 20% 2-methylpiperidin in DMF.[60] All deprotection and coupling steps were followed by intensive washing steps with DMF and DCM according to the protocols in the appendix (chapter **15.1.4**).

Peptide cleavage from the resin was accomplished in a mixture of 90% TFA, 5% water, 2.5% TIPS and 2.5% anisole for 3 h at room temperature. For 100 mg of resin, 1 ml of cleavage solution was applied. The crude peptides were precipitated in cold diethyl ether, centrifuged, and washed three times with diethyl ether.

Table 9.14: Types, amounts and loading capacities of the resin supports used for the automated microwave-assisted Fmoc-SPPS of long BM2 peptides.

Entry	Peptide sequence	Resin Amount [g]	Loading [mmol/g]
P1	CWTIGHLNQIKRGI	0.5[b]	0.40
P2	CWTIGHLNQIKRGINMKIRIKGPNKETINR	0.68[a]	0.27
P3	CSFILSALHFLAWTIGHLNQIKRGINMKIRIKGPNKETINR	0.75[a]	0.33
P16	MLEPFQILSL-Hmp	0.76[a]	0.33
P17	MLEPFQILSICSFILSALHFL	0.27[a]	0.33
P18	MLEPFQILSIC(Acm)SFILSALHFL-Hmp	0.68[a]	0.33
P19	MLEPFQILSIC(Acm)SFILSALHFL-Hmp-ADO-ADO	0.27[a]	0.33
P20	MLEPFQILSIC(Acm)SFILSALHFL-Hmp-ADO-KKKKK	0.68[a]	0.33

a *AmphiSpheres RAM 40 resin.*

b *Rink Amide MBHA resin.*

Fmoc-SPPS of P1: [Cys^{22}]BM2(22-35)

Table 9.15: Amino acids and coupling conditions for the automated, microwave-assisted Fmoc-SPPS of peptide P1.

Amino acid	Weight [g]	DMF [ml]	Coupling Conditions	Fmoc-Deprotection
Ala	0.7	11	Double coupling 50 °C, 40 W, 12 min	Double deprotection 50 °C, 40 W, 320 sec
Arg	2.7	21		
Asn	2.5	21		
Cys	2.5	21		
Gln	1.35	11		
Gly	1.25	21		
His	1.37	11		
Ile	2.27	32		
Leu	0.78	11		
Lys	2.0	21		
Thr	0.9	11		
Trp	1.16	11		
Activator:	15.2 g HATU dissolved in 80 ml DMF			
Base:	14 ml DIEA diluted to 40 ml with NMP			
Deprotection:	42 ml piperidine and 168 ml DMF			
DMF:	560 ml			

Fmoc-SPPS of P2: [Cys^{22}]BM2(22-51)

Table 9.16: Amino acids and coupling conditions for the automated, microwave-assisted Fmoc-SPPS of peptide P2.

Amino acid	Weight [g]	DMF [ml]	Coupling Conditions	Fmoc-Deprotection
Arg	5.1	39	Double coupling 50°C , 35 W, 14 min	Double deprotection 30°C, 35 W, 40 sec 50°C, 35 W, 3min
Asn	6	50		
Cys	1.9	16		
Gln	2	16		
Glu	1.4	16		
Gly	2.3	39		
His	2	16		
Ile	5.16	73		
Leu	1.13	16		
Lys	4.7	50		
Met	1.2	16		
Pro	1.1	16		
Thr	2.5	27		
Trp	1.7	16		
Activator:	26.6 g HATU dissolved in 140 ml DMF			
Base:	25 ml DIEA diluted to 71 ml with NMP			
Deprotection:	136 ml piperidine and 544 ml DMF			
DMF:	6000 ml			

Fmoc-SPPS of P3: [Cys^{11}]BM2(11-51)

Table 9.17: Amino acids and coupling conditions for the automated, microwave-assisted Fmoc-SPPS of peptide P3.

Amino acid	Weight [g]	DMF [ml]	Coupling Conditions	Fmoc-Deprotection
Ala	1.62	26	Double coupling 60 °C, 33 W, 12 min	Double deprotection 50 °C, 40 W, 120 sec
Arg	4.93	38		
Asn	5.85	49		
Cys	1.73	15		
Gln	1.84	15		
Glu	1.28	15		
Gly	2.26	38		
His	3.22	26		
Ile	6.71	95		
Leu	2.68	38		
Lys	4.59	49		
Met	1.11	15		
Phe	2.01	26		
Pro	1.01	15		
Ser	1.99	26		
Thr	2.07	26		
Trp	1.58	26		
Activator:	35.15 g HATU dissolved in 185 ml DMF			
Base:	44.4 ml DIEA diluted to 40 ml with NMP			
Deprotection:	190 ml piperidine and 570 ml DMF			
DMF:	7300 ml			

Fmoc-SPPS of P16: [Leu^{10}]BM2(1-10)-Hmp

Table 9.18: Amino acids and coupling conditions for the automated, microwave-assisted Fmoc-SPPS of peptide P16.

Amino acid	Weight [g]	DMF [ml]	Coupling Conditions	Fmoc-Deprotection
Gln	1.84	15	Double coupling 60 °C, 33 W, 12 min	Double deprotection 50 °C, 40 W, 200 sec
Glu	1.28	15		
Ile	1.06	15		
Leu	1.84	26		
Met	1.11	15		
Phe	1.16	15		
Pro	1.01	15		
Activator:	7.6 g HATU dissolved in 40 ml DMF			
Base:	9.25 ml DIEA diluted to 25 ml with NMP			
Deprotection:	40 ml 2-methylpiperidine and 160 ml DMF			
DMF:	1400 ml			

Fmoc-SPPS of P17: [Ile^{21}]BM2(1-21)

Table 9.19: Amino acids and coupling conditions for the automated, microwave-assisted Fmoc-SPPS of peptide P17.

Amino acid	Weight [g]	DMF [ml]	Coupling Conditions	Fmoc-Deprotection
Ala	0.7	11	Double coupling 50 °C, 33 W, 12 min	Double deprotection 35 °C, 40 W, 60 sec 50 °C, 40 W, 360 sec
Cys	1.3	11		
Gln	1.35	11		
Glu	1.0	11		
His	1.4	11		
Ile	2.0	28		
Leu	2.0	28		
Met	0.82	11		
Phe	1.8	23		
Pro	0.75	11		
Ser	1.8	23		
Activator:	9.5 g HATU dissolved in 50 ml DMF			
Base:	10.5 ml DIEA diluted to 30 ml with NMP			
Deprotection:	70 ml piperidine and 280 ml DMF			
DMF:	3500 ml			

Fmoc-SPPS of P18: [Leu^{21}]BM2(1-21)-Hmp

Table 9.20: Amino acids and coupling conditions for the automated, microwave-assisted Fmoc-SPPS of peptide P18.

Amino acid	Weight [g]	DMF [ml]	Coupling Conditions	Fmoc-Deprotection
Ala	1.1	17	Double coupling 50 °C, 30 W, 14 min	Double deprotection 35 °C, 40 W, 60 sec 50 °C, 40 W, 3 min
Gln	2.1	17		
Glu	1.5	17		
His	2.1	17		
Ile	2.8	40		
Leu	3.6	51		
Met	1.3	17		
Phe	2.2	28		
Pro	1.15	17		
Ser	3.1	40		
Manual coupling of Fmoc-Cys(Acm)-OH			3.13 mg Fmoc-Cys(Acm), 282 mg HATU, 263 μl DIEA in 3.7 ml DMF (60 min, double coupling)	
Activator:	16.2 g HATU dissolved in 85 ml DMF			
Base:	15.7 ml DIEA diluted to 45 ml with NMP			
Deprotection:	70 ml 2-methylpiperidine and 280 ml DMF			
DMF:	3500 ml			

Fmoc-SPPS of P19: [Leu^{21}]BM2(1-21)-Hmp-ADO$_2$

Table 9.21: Amino acids and coupling conditions for the automated, microwave-assisted Fmoc-SPPS of peptide P19.

Amino acid	Weight [g]	DMF [ml]	Coupling Conditions	Fmoc-Deprotection
Ala	0.7	11	Double coupling 50 °C, 30 W, 14 min	Double deprotection 35 °C, 40 W, 60 sec 50 °C, 40 W, 3 min
Gln	1.34	11		
Glu	0.95	11		
His	1.4	11		
Ile	1.63	23		
Leu	2.0	28		
Met	0.82	11		
Phe	1.32	17		
Pro	0.75	11		
Ser	1.76	23		
Manual coupling of Fmoc-Cys(Acm)-OH			1.56 mg Fmoc-Cys(Acm), 141 mg HATU, 132 μl DIEA in 2.0 ml DMF (60 min, double coupling)	
Activator:	9.5 g HATU dissolved in 50 ml DMF			
Base:	10.50 ml DIEA diluted to 30 ml with NMP			
Deprotection:	60 ml 2-methylpiperidine and 240 ml DMF			
DMF:	3000 ml			

Fmoc-SPPS of P20: [Leu^{21}]BM2(1-21)-Hmp-ADO-Lys$_5$

Table 9.22: Amino acids and coupling conditions for the automated, microwave-assisted Fmoc-SPPS of peptide P20.

Amino acid	Weight [g]	DMF [ml]	Coupling Conditions	Fmoc-Deprotection
Ala	1.1	17	Double coupling 50 °C, 30 W, 14 min	Double deprotection 35 °C, 40 W, 60 sec 50 °C, 40 W, 3 min
Gln	2.1	17		
Glu	1.5	17		
His	2.1	17		
Ile	2.8	40		
Leu	3.6	51		
Met	1.3	17		
Phe	2.2	28		
Pro	1.15	17		
Ser	3.1	40		
Manual coupling of Fmoc-Cys(Acm)-OH			3.13 mg Fmoc-Cys(Acm), 282 mg HATU, 263 μl DIEA in 3.7 ml DMF (60 min, double coupling)	
Activator:	16.2 g HATU dissolved in 85 ml DMF			
Base:	15.7 ml DIEA diluted to 45 ml with NMP			
Deprotection:	70 ml 2-methylpiperidine and 280 ml DMF			
DMF:	3500 ml			

10. Development of Ligation Protocols

10.1. Summary of ligation experiments

Ligation yields, hydrolysis amounts and possible side reactions were investigated by detailed ligation studies using the model Hmp-peptides **P4**, **P7**-**P12**. These results were applied to optimise conditions for ligation experiments with long BM2 peptides. For the synthesis of the proton channel sequences **P26** [Leu^{21}]BM2(1-51) and **P27** [Leu^{10}]BM2(1-51), the Hmp-peptides **P16**, **P18**, **P19** and **P20** were ligated with the N-terminal cysteine peptides **P2** or **P3**. Dependent on the type of the C-terminal solubilizing tag four different ligation buffers **A**, **B**, **C** or **D** were tested. The compositions of these buffers are listed in table **10.2**. The good soluble Hmp-peptide **P20** was ligated in the water based standard buffer **A**. More hydrophobic peptides **P18** and **P19** were ligated in buffer **B** or **C**. For ligation experiments in the ionic liquid based buffers **D1**-**D6** model Hmp-peptide **P7** was applied. The ligation of the final product **P27** [Leu^{10}]BM2(1-51) was performed in the optimized ionic-liquid based buffer **D5**.

Table 10.1: Ligation experiments in ligation buffers **A**, **B**, **C** and **D**.

Entry	Ligation product	Cys-peptide	Hmp-peptide	Buffer
P21	[Ile^{21}]BM2(17-35)	P1	P4	A
P22	[Leu^{21}]BM2(17-35)	P1	P7	A
	[Leu^{21}]BM2(17-35)	P1	P7	D1-D6
	[Leu^{21}]BM2(17-35)	P1	P8	A
	[Leu^{21}]BM2(17-35)	P1	P9	A
	[Leu^{21}]BM2(17-35)	P1	P11	A
	[Leu^{21}]BM2(17-35)	P1	P12	A
P23	[Cys^{11}(Acm)][Leu^{21}]BM2(1-51)	P2	P18a	B, C
	[Cys^{11}(Acm)][Leu^{21}]BM2(1-51)	P2	P18b	C
	[Cys^{11}(Acm)][Leu^{21}]BM2(1-51)	P2	P19a	C
	[Cys^{11}(Acm)][Leu^{21}]BM2(1-51)	P2	P19b	C
	[Cys^{11}(Acm)][Leu^{21}]BM2(1-51)	P2	P20	A,C
P27	[Leu^{10}]BM2(1-51)	P3	P16a	C
P27	[Leu^{10}]BM2(1-51)	P3	P16b	C
P27	[Leu^{10}]BM2(1-51)	P3	P16a	D5
P27	[Leu^{10}]BM2(1-51)	P3	P16b	D5

a *Hmp peptide diastereomer 1.*

b *Hmp peptide diastereomer 2.*

Table 10.2: Compositions of the tested ligation buffers **A**, **B**, **C** and **D**.

Abbre.	Ligation conditions
Buffer A	8 M Urea + 0.2 M Na_2HPO_4 + 150 mM MPAA + 100 mM TCEP, pH 7.00
Buffer B	Buffer A / trifluoroethanol (TFE) (2:1), pH 7.00
Buffer C	Buffer A / hexafluoro-2-propanol (HFIP) (2:1), pH 7.50
Buffer D1	[C_2mim][OAc], 150 mM thiophenol, 150 mM TCEP
Buffer D2	[C_2mim][OAc]/water (90:10, v/v), 150 mM thiophenol, 150 mM TCEP
Buffer D3	[C_2mim][OAc]/water (80:20, v/v), 150 mM thiophenol, 150 mM TCEP
Buffer D4	[C_2mim][OAc]/water (70:30, v/v), 150 mM thiophenol, 150 mM TCEP
Buffer D5	[C_2mim][OAc]/water (60:40, v/v), 150 mM thiophenol, 150 mM TCEP
Buffer D6	[C_2mim][OAc]/water (50:50, v/v), 150 mM thiophenol, 150 mM TCEP

10.1.1. Native chemical ligation in buffer A

Ligation experiments in buffer **A** were performed in 500 μl of 8 M urea solution containing 14.14 mg (200 mM) disodium phosphate, 7.17 mg (50 mM, 50 equiv.) tris(2-carboxyethyl)phosphine hydrochloride (TCEP HCl) and 12.6 mg (150 mM, 150 equiv.) 4-mercaptophenylacetic acid (MPAA) as a catalyst. To dissolve MPAA, 10 M sodium hydroxide solution was added until a final pH of 6.0 was reached. In order to dissolve the peptides, 1.5 equiv. of the N-terminal cysteine peptide and 1.0 equiv. of the C-terminal Hmp-peptide were agitated in ligation buffer **A** for 5 min at room temperature. The reaction was started by adjusting the pH to 7.0 using a 2.5 M sodium hydroxide solution. Finally, the reaction mixture was agitated under a nitrogen atmosphere.

Reaction progress was monitored by RP-HPLC after 0 h, 0.5 h, 1 h and 2 h for short model Hmp-peptides **P1**, **P2**, **P4**, **P7**-**P12** and 0 h, 1 h, 2 h, 4 h, 8 h and 24 h for the long Hmp-peptide **P20**. Samples preparation: 5 μl of the ligation buffer was diluted with 60 μl acetonitrile/water (0.1% TFA) (1:1, v/v).

Table 10.3: Equivalents and amounts of cysteine and Hmp-peptides for 500 µl ligation buffer **A**.

Entry	Peptide	Mw [g/mol]	Equiv.	Amount [mg]
P1	[Cys^{22}]BM2(22-35)	1637.95	1.5	1.06
P2	[Cys^{22}]BM2(22-51)	3532.20	1.5	1.1[a]
P4	[Ile^{21}]BM2(17-35)-Hmp	702.86	1.0	0.35
P7	[Leu^{21}]BM2(17-35)-Hmp	702.86	1.0	0.35
P8	[Leu^{21}]BM2(17-35)-Hmp-ADO	848.02	1.0	0.43
P9	[Leu^{21}]BM2(17-35)-Hmp-ADO_2	993.18	1.0	0.50
P11	[Leu^{21}]BM2(17-35)-Hmp-ADO-Lys_5	1489.89	1.0	0.75
P12	[Leu^{21}]BM2(17-35)-Hmp-ADO_2-Lys_5	1635.02	1.0	0.82
P20	[Leu^{21}]BM2(1-21)-Hmp-ADO-Lys_5	3383.19	1.0	0.68[a]

a *Buffer volume 200 µl.*

10.1.2. Native chemical ligation in buffer B

Ligation experiments in buffer **B** were performed in 200 μl of a mixture containing ligation buffer **A** and TFE (2:1, v/v) at a pH of 7.00. For dissolution of hydrophobic peptides 1.0 equiv. Hmp-peptide and 1.5 equiv. of cysteine peptide were pre-dissolved in 66 μl TFE. The reaction was started by adding 134 μl of ligation buffer **A** and agitated for 24 h under a nitrogen atmosphere.

Reaction progress was monitored by RP-HPLC after 0 h, 1 h, 2 h, 4 h, 8 h and 24 h. Therefore, aliquots of 2.5 μl ligation buffer were mixed with 7 μl of TFE and dissolved in 30 μl water (0.1% TFA).

Table 10.4: Equivalents and amounts of cysteine and Hmp-peptides for 200 µl ligation buffer **B**.

Entry	Peptide	Mw [g/mol]	Equiv.	Amount [mg]
P2	[Cys^{22}]BM2(22-51)	3532.20	1.5	1.1
P18a	[Leu^{21}]BM2(1-21)-Hmp	2597.17	1.0	0.53

10.1.3. Native chemical ligation in buffer C

Ligation experiments in buffer **C** were performed in 200 μl of a mixture containing ligation buffer **A** and HFIP (2:1, v/v) at a pH of 7.50. For dissolution of hydrophobic peptides, 1.0 equiv. of the Hmp-peptide and 1.5 equiv. of the cysteine peptide were pre-dissolved in 66 μl HFIP. The reaction was started by adding 134 μl of ligation buffer **A**. If necessary small amounts of pure water were added to obtain a single phase. Finally, the reaction mixture was agitated for 24 h under a nitrogen atmosphere.

Reaction progress was monitored by RP-HPLC after 0 h, 1 h, 2 h, 4 h, 8 h and 24 h. Therefore aliquots of 2.5 μl sample solution were diluted with 7 μl HFIP and dissolved in 30 μl water (0.1% TFA). Subsequently the reaction product was purified by preparative RP-HPLC following procedure **8.1.7**.

Table 10.5: Equivalents and amounts of cysteine and Hmp-peptides for 200 µl ligation buffer **C**.

Entry	Peptide	Mw [g/mol]	Equiv.	Amount [mg]
P2	[Cys^{22}]BM2(22-51)	3532.20	1.5	1.1
P3	[Cys^{22}]BM2(11-51)	4732.64	1.1	1.136
P16a	[Leu^{21}]BM2(1-10)-Hmp	1293.59	1.0	0.278
P16b	[Leu^{10}]BM2(1-10)-Hmp	1293.59	1.0	0.278
P18a	[Leu^{21}]BM2(1-21)-Hmp Dia.1	2597.17	1.0	0.53
P18b	[Leu^{21}]BM2(1-21)-Hmp Dia. 2	2597.17	1.0	0.53
P19a	[Leu^{21}]BM2(1-21)-Hmp-ADO$_2$ Dia. 1	2887.48	1.0	0.61
P19b	[Leu^{21}]BM2(1-21)-Hmp-ADO$_2$ Dia. 2	2887.48	1.0	0.61

10.1.4. Native chemical ligation in buffer D (D1-D6)

For the preparation of the ionic liquid based buffers **D1**-**D6**, 8.55 mg (0.03 mmol, 150 mM TCEP HCl and 3.09 μl (0.03 mmol, 150 mM) thiophenol were dissolved in 200 μl [C_2mim][OAc] containing increasing amounts of water according to table **10.6**. The ligation of model peptides **P1** and **P7** was started by dissolving 0.36 mg (11 mM, 1.1 equiv.) of cysteine peptide [Cys^{22}]BM2(22-35) and 0.14 mg (10 mM, 1.0 equiv.) of ALHFL-Hmp in 20 μl ligation buffer **D**. The reaction mixture was agitated at room temperature under argon for 6 h.

For analytical RP-HPLC 2 μl of the reaction mixture were dissolved in 30 μl acetonitrile/water (60:40, v/v) with 0.8% TFA. The reaction progress was monitored after 0 min, 10 min, 30 min, 1 h, 2 h, 4 h and 6 h.

Table 10.6: Compositions of ligation buffers **D1**-**D6**.

Buffer	[C_2mim][OAc] [%]	Water content [%]
D1	100	0
D2	90	10
D3	80	20
D4	70	30
D5	60	40
D6	50	50

10.1.5. Native chemical ligation of P27 in buffer D5

For the preparation of ligation buffer **D5**, 8.55 mg (0.03 mmol, 150 mM) TCEP HCl and 3.09 μl (0.03 mmol, 150 mM) thiophenol were dissolved in a mixture of 200 μl [C_2mim][OAc] and water (60:40, v/v). In order to start the reaction 0.139 mg (1.1 x 10^{-4} mmol, 2.15 mM, 1.0 equiv.) of [Leu^{10}]BM2(1-10)-Hmp and 0.568 mg (1.2 x 10^{-4} mmol, 2.4 mM, 1.1 equiv.) of [Cys^{11}]BM2(11-51) were dissolved in 50 μl of the ligation solution. The final ligation solution was agitated for 24 h at room temperature under argon atmosphere.

Reaction progress was monitored by analytical RP-HPLC with acetonitrile (0.1% TFA) and water (0.1% TFA) as liquid phase. Therefore, 4 μl from the ligation solution was diluted with 40 μl acetonitrile/water (60:40, v/v) with 0.8 % TFA. The ligation product was purified and separated from the ligation solution by preparative RP-HPLC following the procedure described in section **8.1.7**.

Table 10.7: Equivalents and amounts of cysteine and Hmp-peptides for 50 µl ligation buffer **D**.

Entry	Peptide	Mw [g/mol]	Equiv.	Amount [mg]
P3	[Cys^{11}]BM2(11-51)	4732.64	1.1	0.568
P16a/P16b	[Leu^{10}]BM2(1-10)-Hmp	1293.59	1.0	0.139

11. Desulfurization Protocols

11.1. Conventional and HFIP-based desulfurization of BM2 peptides

11.1.1. Metal-free desulfurization in conventional buffer

The desulfurization experiment of the hydrophobic peptide **P23** (0.6 mg, 0.01 μmol) was carried out in 200 μl of 6 M guanidinium chloride (GdnHCl)/0.2 M disodium phosphate buffer containing 0.5 M TCEP HCl. After dissolution of TCEP HCl, the pH of the mixture was adjusted to 6.5 using a 5 M sodium hydroxide solution. In order to start the reaction 12.5 μl of 160 mM glutathione and 20 μl of 300 mM 2,2-azobis[2-(2-imidazolin-2-yl)propane dihydrochloride (VA044) solution were added. The reaction mixture was agitated (1000 rpm) under inert conditions (Ar, N_2) at room temperature. After complete conversion of the reactant by analytical HPLC, the reaction was stopped by adding aliquots of concentrated TFA until a final pH of 2 was reached. Reaction progress was followed by analytical RP-HPLC at 220 nm. For HPLC sample preparation, 10 μl of the reaction mixture was dissolved in 30 μl of water (0.1% TFA).

Table 11.1: Molecular weight and amount of peptide P23 for desulfurization in conventional buffer.

Entry	Peptide	Mw [g/mol]	Equiv.	Amount [mg]
P23	[Cys(Acm)^{11}][Cys^{22}]BM2(1-51)	6008.22	1.0	0.60

11.1.2. Metal-free desulfurization in HFIP containing buffer

Peptide **P23** (0.6 mg, 0.01 mmol) was dissolved in 320 μl of desulfurization emulsion containing one part HFIP (80 μl) and three parts (240 μl) 6 M guanidinium chloride (GdnHCl)/0.2 M disodium phosphate buffer with 0.5 M tris(2-carboxyethyl)phosphine hydrochloride (TCEP HCl) at a pH of 6.5. For pH adjustment, a 5 M sodium hydroxide solution was added. The reaction was started by adding 12.5 μl of 160 mM glutathione (GSH) and 20 μl of 300 mM 2,2-azobis[2-(2-imidazolin-2-yl)propane dihydrochloride (VA044) to the reaction mixture. The solution was agitated under argon at room temperature. After complete conversion of the reactant by RP-HPLC, concentrated TFA was added until a final pH of 2 was reached. In order to observe the reaction progress aliquots of 10 μl of the reaction mixture were dissolved in 30 μl water (0.1% TFA) and analyzed by RP-HPLC at 220 nm. After desulfurization product **P25** was purified by preparative RP-HPLC according to instruction **8.1.7**.

Table 11.2: Molecular weight and amount of peptide P23 for desulfurization in the HFIP-based buffer.

Entry	Peptide	Mw [g/mol]	Equiv.	Amount [mg]
P23	[Cys(Acm)^{11}][Cys^{22}]BM2(1-51)	6008.22	1.0	0.60

12. Acetaminomethyl (Acm) deprotection

12.1. Comparison between silver salts and elemental iodine

12.1.1. Acm deprotection using silver trifluoromethanesulfonate

The deprotection of the acetaminomethyl (Acm) group with silver ions was carried out by treating 0.6 mg of **P25** (0.1 μM, 1.0 equiv.) in 1 ml of concentrated trifluoroacetic acid (TFA) containing of 7.7 mg (30 mM, 300 equiv.) silver trifluoromethanesulfonate (AgOTf) and 1.6 μl (15 mM, 150 equiv.) anisole. During the Acm deprotection, the reaction was kept at 4 °C and agitated under an argon atmosphere (1000 rpm). In order to protect the silver ions from light, the deprotection was performed in a black, opaque reaction vessel. The reaction progress was monitored by analytical HPLC after 0, 10, 60 and 120 min. For analysis *via* RP-HPLC, 10 μl of the reaction solution was diluted with 40 μl of 6 M DTT solution in acetic acid/water (1:1, v/v). According to RP-HPLC analysis, the deprotection of Acm was finished after 120 min. In order to stop the reaction a two-fold excess (2 ml) of 6 M DTT solution in acetic acid/water (1:1, v/v) was added and the mixture was agitated (2000 rpm) for 2 h at room temperature. Finally, product **P26** was purified by preparative RP-HPLC following procedure **8.1.7**.

Table 12.1: Amounts and equivalents of peptide **P25**, AgOTf and anisole in 1 ml concentrated TFA.

Substance	Molecular weight	Equivalents	Amount [μmol]	Amount[mg]
P25	5976.16 g/mol	1.0	0.1	0.60
AgOTf	256.94 g/mol	300	30	7.70
Anisole	108.14 g/mol	150	15	1.59

12.1.2. Acm deprotection using elemental iodine

For the deprotection of the acetaminomethyl (Acm) group by elementary iodine, 0.6 mg (0,02 mM, 1.0 equiv.) of peptide **P25** was dissolved in 5 ml concentrated acetic acid containing 15.18 mg (12 mM, 600 equiv.) elemental iodine and 4.44 μl 37 % aqueous HCl solution. The solution was flushed with argon and agitated at room temperature for 60 min. Analytical HPLC was applied after 0, 10, 30 and 60 min by diluting 10 μl of the reaction solution with 50 μl of 0.1 M sodium ascorbate solution in TFE/water (1:1, v/v). After disappearance of the starting peptide by HPLC, the excess iodine was destroyed by the addition of 1 ml of 1 M sodium thiosulfate ($Na_2S_2O_3$) solution. In order to reduce disulfide bonds, 2 ml of 6 M DTT solution was mixed with the reaction solution and agitated at room temperature for 1 h.

Table 12.2: Amounts and equivalents of peptide **P25** and iodine in 5 ml concentrated acetic acid.

Substance	Molecular weight	Equivalents	Amount [μmol]	Amount[mg]
P25	6005.28 g/mol	1.0	0.1	0.60
Iodine	253.8 g/mol	600	60	15.2

13. List of Abbreviations

Abbreviation	Name
Aβ	Amyloid beta peptides
ACN	Acetonitrile
ACP	Acyl carrier protein
Acm	Acetaminomethyl
ADO	8-(9-Fluorenylmethyloxycarbonyl-amino)-3,6-dioxaoctanoic acid
$AgBF_4$	Silver tetrafluoroborate
AgOAc	Silver acetate
AgOTf	silver trifluoromethanesulfonate
AIBN	Azobisisobutyronitrile
AM2	Influenza A virus matrix 2 protein
AMP	2-Amino-2-methylpropane-1-thiol
APS	Ammonium persulfate
BM2	Influenza B virus matrix 2 protein
BMIM-PF6	1-Butyl-3-methylimidazolium hexafluorophosphate
Boc	tert-Butyloxycarbonyl
BPTI	Bovine pancreatic trypsin inhibitor
Bzl	Benzyl mercaptan
C1q	Complement component 1q protein complex
Cbz	Carbobenzoxy
CD	Circular dichroism
$[C_2mim][OAc]$	1-Ethyl-3-methylimidazolium acetate
CPB	Carboxypeptidase B
GPCR	G protein-coupled receptor
CP10	Chemotactic protein 10 kDa
3D	Three-Dimensional
DAGK	Escherichia coli diacylglycerol kinase
DBU	1,8-Diazabicyclo[5.4.0]undec-7ene
DCC	N,N'-Dicyclohexylcarbodiimide
DCM	Dichloromethane
Ddae	4,4-dimethyl-2,6-dioxocyclohexylidene-3-[2-(2-aminoethoxy) ethoxyl]-propan-1-ol
DEN2C	Dengue virus capsid protein 2
DGK	Diacylglycerol kinase
Dia.	Diastereomer
DIC	N,N'-Diisopropylcarbodiimide
DIEA	N,N-Diisopropylethylamine
DMAP	4-Dimethylaminopyridine
DMF	Dimethylformamide

Dmmb	2-Mercapto-4,5-dimethoxybenzyl
DMSO	Dimethyl sulfoxide
DNA	Deoxyribonucleic acid
DPC	Dodecylphosphocholine
DSC	N,N-Disuccinimidyl carbonate
DTNP	2,2′-Dithiobis(5-nitropyridine)
DTT	Dithiothreitol
EPO	Hormone erythropoietin
ESI	Electrospray ionization
EtOH	Ethanol
Fmoc	Fluorenylmethyloxycarbonyl
GnHCl	Guanidinium chloride
GroES	E. coli cochaperonin
GST	Glutathione-S-transferase
H4	Histone H4
HATU	O-(7-Azabenzotriazol-1-yl)-N,N,N′,N′-tetramethyluronium-hexafluorphosphat
HBTU	2-(1H-Benzotriazole-1-yl)-1,1,3,3-tetramethyluronium hexafluorophosphate
HCCA	α-Cyano-4-hydroxycinnamic acid
HCV p7	Hepatitis C virus ion channel p7
hEPO	Human erythropoietin
HPLC	High performance liquid chromatography
HF	Hydrofluoric acid
HFIP	Hexafluoroisopropanol
Histone H2B	Human histone protein of chromatin
Hiv	Human immunodeficiency viruses
4-Hmb	4-Hydroxymethyl benzoic acid
Hmp	2-hydroxy-3-mercaptopropanamide
HMSP	2-hydroxy-2-methyl-3-sulfanylpropanoic acid
HMPA	Hexamethylphosphoramide
HMPB resin	4-(4-Hydroxymethyl-3-methoxyphenoxy)-butanoyl amide resin
HOAt	1-Hydroxy-7-azabenzotriazol
HOBt	1-Hydroxybenzotriazole
IFITM3	Interferon-induced transmembrane protein 3
IGF1	Insulin-like growth factor 1
INT	Intermediate
KAHA ligation	α-Ketoacid-hydroxylamine ligation
KCL	Kinetically controlled ligation
KcsA	potassium channel of streptomyces A
Kir5.1	Potassium Voltage-Gated Channel Subfamily J Member 16
LC3-II	Autophagosomal Marker Protein

LCMS	Liquid chromatography mass spectroscopy
M1	Matrix protein 1
MALDI	Matrix-assisted laser desorption/ionization
MCoTI-II	Momordica cochinchinensis trypsin inhibitor-II
MeBzl	Methylbenzyl
MeNbz	Ortho-(N-methyl)aminoanilide
MeOH	Methanol
mKC	CXC chemokine from murine
MMPA	1-Mercapto-3-methoxypropan-2-yl acetate
Mmsb	2-methoxy-4-methylsulfinylbenzyl alcohol
MS	Mass spectroscopy
MO	1-Monooleoyl-rac-glycerol
3-MPA	3-Mercaptopropionic acid
MPAA	4-Mercatophenylacetic acid
MSP	1-methoxy-3-sulfanylpropan-2-ol
Nbz	N-acyl-benzimidazolinone
NCL	Native chemical ligation
NHC	N-heterocyclic carbenes
Nmbu	4-(N-methylamino)butanoyl
NMR	Nuclear magnetic resonance
Nmec	N-methyl-N-[2-(methylamino)ethyl]carbamoyl
NMP	N-Methyl-2-pyrrolidone
Ntl	N-terminal linker (2-[(2-Aminoethyl)sulfonyl]ethanol)
NY-ESO-1	New York esophageal squamous cell carcinoma-1
OG	Octylglycoside
oNb-OEG3	Ortho-nitrobenzyl-(oligoethylene glycol)$_3$
ORL1	Opioid receptor like 1
PEGA	Mono-2-acrylamidoprop-1-yl[2-aminoprop-1-yl] polyethylene glycol cross-linked with bis 2-acrylamidoprop-1-yl polyethyleneglycol
Phacm	phenylactamidomethyl
PBS	Phosphate-buffered saline
PEG	Polyethylene glycol
POPC	1-Palmitoyl-2-oleoylphosphatidylcholine
POPG	1-Palmitoyl-2-oleoyl-sn-glycero-3-phosphoglycerol
PPh_3	Triphenylphosphine
PSh	Thiophenol
PPO	Polyethylene glycol-polyamide
PPO_2	(Polyethylene glycol-polyamide)$_2$
PYY	Peptide tyrosine tyrosine
Q11	Amino acid sequence: Ac-Gln-Gln-Lys-Phe-Gln-Phe-Gln-Phe-Glu-Gln-Gln
RBM	Removable backbone modification

RNA	Ribonucleic acid
Rndm.	Random
RNP	Ribonucleoprotein
RP	Reverse phase
SA	Sinapinic acid
SDS	Sodium dodecyl sulfate
SDS PAGE	Sodium dodecyl sulfate polyacrylamide gel electrophoresis
SEA	Bis(2-sulfanylethyl)amido
SNUT	Solubility enhancing ubiquitous tags
SPPS	Solid phase peptide synthesis
SUMO-2	Small ubiquitin-related modifier 2
TBS	t-Butyldimethylsilyl
TCEP	Tris(2-carboxyethyl)phosphine
TEMED	Tetramethylethylendiamine
TEGBz	4-(3,6,9-Trioxadecyl)oxybenzyl alcohol
TEV cleavage site	Tobacco etch virus cleavage site
TLC	Thin-layer chromatography
TM	Trans membrane
TMD	Trans membrane domain
TMP	Trans membrane peptide
TMS-CHN_2	Trimethylsilyldiazomethane
TFA	Trifluoroacetic acid
TFE	Trifluoroethanol
THF	Tetrahydrofuran
Thz	Thiazolidine
TIS	Triisopropylsilane
TIPS	Triisopropylsilane
Tris	Tris(hydroxymethyl)aminomethane
TS	Transition state
UV/Vis	Ultraviolet / visible
VA-044	2,2'-Azobis[2-(2-imidazolin-2-yl)propane] dihydrochloride
Vpu	Viral Protein U (HIV virus)
vRNPs	Viral ribonucleoproteins

14. References

[1] A. C. Baumruck, D. Tietze, A. Stark, A. A. Tietze, *The Journal of organic chemistry* **2017**, *82*, 7538-7545.

[2] A. C. Baumruck, D. Tietze, L. K. Steinacker, A. A. Tietze, *Chemical Science* **2018**.

[3] Ü. Özdilek, *TU Darmstadt* **2015**, *Master Thesis, AK Tietze/Buntkowsky*.

[4] J. Wang, R. M. Pielak, M. A. McClintock, J. J. Chou, *Nature structural & molecular biology* **2009**, *16*, 1267.

[5] aT. Curtius, *J. Prakt. Chemie* **1882**, *26*, 45–208; bE. Fischer, Fourneau, E., *Ber. Dtsch. Chem. Ges.* **1901**, *34*, 2868-2879.

[6] aT. Curtius, *J. Prakt. Chemie* **1904**, *70*, 57–108; bT. Kimmerlin, D. Seebach, *The Journal of Peptide Research* **2005**, *65*, 229-260.

[7] T. Wieland, M. Bodanszky, in *The World of Peptides*, Springer, **1991**, pp. 44-76.

[8] aV. d. Vigneaud, C. Ressler, C. J. M. Swan, C. W. Roberts, P. G. Katsoyannis, S. Gordon, *Journal of the American Chemical Society* **1953**, *75*, 4879-4880; bV. d. Vigneaud, H. C. Lawler, E. A. Popenoe, *Journal of the American Chemical Society* **1953**, *75*, 4880-4881.

[9] L. A. Carpino, *Accounts of chemical research* **1973**, *6*, 191-198.

[10] aL. A. Carpino, G. Y. Han, *Journal of the American Chemical Society* **1970**, *92*, 5748-5749; bL. A. Carpino, G. Y. Han, *The Journal of organic chemistry* **1972**, *37*, 3404-3409.

[11] aY. S. KLAUSNER, M. BODANSZKY, *Synthesis* **1974**, *1974*, 549-559; bL. A. Carpino, M. Beyermann, H. Wenschuh, M. Bienert, *Accounts of chemical research* **1996**, *29*, 268-274; cG. W. Anderson, J. E. Zimmerman, F. M. Callahan, *Journal of the American Chemical Society* **1967**, *89*, 5012-5017.

[12] aJ. C. H. Sheehan, G.P, *J. Am. Chem. Soc.* **1955**, *77*, 1067–1068; bH. G. Khorana, *Chem. Ind. (London)* **1955**, *33*, 1087–1088.

[13] M. R. INFANTE, V. MOSES, *International journal of peptide and protein research* **1994**, *43*, 173-179.

[14] R. B. Merrifield, *Journal of the American Chemical Society* **1963**, *85*, 2149-2154.

[15] G. BARANY, N. KNEIB-CORDONIER, D. G. MULLEN, *International journal of peptide and protein research* **1987**, *30*, 705-739.

[16] R. Merrifield, in *Hypotensive Peptides*, Springer, **1966**, pp. 1-13.

[17] A. C. Conibear, E. E. Watson, R. J. Payne, C. F. Becker, *Chemical Society Reviews* **2018**, *47*, 9046-9068.

[18] V. K. Sarin, S. B. Kent, A. R. Mitchell, R. Merrifield, *Journal of the American Chemical Society* **1984**, *106*, 7845-7850.

[19] aE. Saxon, J. I. Armstrong, C. R. Bertozzi, *Organic letters* **2000**, *2*, 2141-2143; bB. L. Nilsson, L. L. Kiessling, R. T. Raines, *Organic letters* **2000**, *2*, 1939-1941; cM. Köhn, R.

Breinbauer, *Angewandte Chemie International Edition* **2004**, *43*, 3106-3116; dR. Franke, C. Doll, J. Eichler, *Tetrahedron letters* **2005**, *46*, 4479-4482; eJ. E. Moses, A. D. Moorhouse, *Chemical Society Reviews* **2007**, *36*, 1249-1262; fP. Botti, T. D. Pallin, J. P. Tam, *Journal of the American Chemical Society* **1996**, *118*, 10018-10024.

[20] aP. E. Dawson, T. W. Muir, I. Clark-Lewis, S. Kent, *Science* **1994**, *266*, 776-779; bP. Thapa, R.-Y. Zhang, V. Menon, J.-P. Bingham, *Molecules* **2014**, *19*, 14461-14483; cP. A. Cistrone, M. J. Bird, D. T. Flood, A. P. Silvestri, J. C. Hintzen, D. A. Thompson, P. E. Dawson, *Current protocols in chemical biology* **2019**, *11*, e61; dS. B. Kent, *Chemical Society Reviews* **2009**, *38*, 338-351.

[21] E. C. Johnson, S. B. Kent, *Journal of the American Chemical Society* **2006**, *128*, 6640-6646.

[22] W. Lu, M. Qasim, S. B. Kent, *Journal of the American Chemical Society* **1996**, *118*, 8518-8523.

[23] V. Agouridas, O. a. El Mahdi, V. Diemer, M. Cargoët, J.-C. M. Monbaliu, O. Melnyk, *Chemical reviews* **2019**.

[24] aL. Raibaut, N. Ollivier, O. Melnyk, *Chemical Society Reviews* **2012**, *41*, 7001-7015; bL. Raibaut, H. Adihou, R. Desmet, A. F. Delmas, V. Aucagne, O. Melnyk, *Chemical Science* **2013**, *4*, 4061-4066; cS. Tang, Y. Y. Si, Z. P. Wang, K. R. Mei, X. Chen, J. Y. Cheng, J. S. Zheng, L. Liu, *Angewandte Chemie International Edition* **2015**, *54*, 5713-5717.

[25] P. E. Dawson, M. J. Churchill, M. R. Ghadiri, S. B. Kent, *Journal of the American Chemical Society* **1997**, *119*, 4325-4329.

[26] aQ. Wan, J. Chen, Y. Yuan, S. J. Danishefsky, *Journal of the American Chemical Society* **2008**, *130*, 15814-15816; bW. Xu, W. Jiang, J. Wang, L. Yu, J. Chen, X. Liu, L. Liu, T. F. Zhu, *Cell Discovery* **2017**, *3*, 17008; cW. Hou, L. Liu, X. Zhang, C. Liu, *Royal Society open science* **2018**, *5*, 172455.

[27] aL. R. Malins, R. J. Payne, *Current opinion in chemical biology* **2014**, *22*, 70-78; bP. E. Dawson, *Israel Journal of Chemistry* **2011**, *51*, 862-867.

[28] R. Raz, F. Burlina, M. Ismail, J. Downward, J. Li, S. J. Smerdon, M. Quibell, P. D. White, J. Offer, *Angewandte Chemie International Edition* **2016**, *55*, 13174-13179.

[29] X. Li, T. Kawakami, S. Aimoto, *Tetrahedron letters* **1998**, *39*, 8669-8672.

[30] A. B. Clippingdale, C. J. Barrow, J. D. Wade, *Journal of Peptide Science* **2000**, *6*, 225-234.

[31] X. Z. Bu, G. Y. Xie, C. W. Law, Z. H. Guo, *Tetrahedron Letters* **2002**, *43*, 2419-2422.

[32] F. Mende, O. Seitz, *Angewandte Chemie International Edition* **2011**, *50*, 1232-1240.

[33] aH. Li, S. Dong, *Science China Chemistry* **2017**, *60*, 201-213; bI. Sharma, D. Crich, *The Journal of organic chemistry* **2011**, *76*, 6518-6524.

[34] aA. Ishii, H. Hojo, Y. Nakahara, Y. ITO, Y. NAKAHARA, *Bioscience, biotechnology, and biochemistry* **2002**, *66*, 225-232; bK. Nakamura, N. Hanai, M. Kanno, A. Kobayashi, Y. Ohnishi, Y. Ito, Y. Nakahara, *Tetrahedron letters* **1999**, *40*, 515-518.

[35] S. Ficht, R. J. Payne, R. T. Guy, C. H. Wong, *Chemistry* **2008**, *14*, 3620-3629.

[36] R. Ingenito, E. Bianchi, D. Fattori, A. Pessi, *Journal of the American Chemical Society* **1999**, *121*, 11369-11374.

[37] A. P. Tofteng, K. K. Sørensen, K. W. Conde-Frieboes, T. Hoeg-Jensen, K. J. Jensen, *Angewandte Chemie* **2009**, *121*, 7547-7550.

[38] H. E. Elashal, Y. E. Sim, M. Raj, *Chemical science* **2017**, *8*, 117-123.

[39] aT. Leta Aboye, R. J. Clark, D. J. Craik, U. Göransson, *Chembiochem : a European journal of chemical biology* **2008**, *9*, 103-113; bJ. Zhu, Q. Wan, G. Ragupathi, C. M. George, P. O. Livingston, S. J. Danishefsky, *Journal of the American Chemical Society* **2009**, *131*, 4151-4158.

[40] aJ. B. Blanco-Canosa, P. E. Dawson, *Angewandte Chemie* **2008**, *47*, 6851-6855; bJ. B. Blanco-Canosa, B. Nardone, F. Albericio, P. E. Dawson, *Journal of the American Chemical Society* **2015**, *137*, 7197-7209.

[41] J. X. Wang, G. M. Fang, Y. He, D. L. Qu, M. Yu, Z. Y. Hong, L. Liu, *Angewandte Chemie International Edition* **2015**, *54*, 2194-2198.

[42] G. M. Fang, Y. M. Li, F. Shen, Y. C. Huang, J. B. Li, Y. Lin, H. K. Cui, L. Liu, *Angewandte Chemie International Edition* **2011**, *50*, 7645-7649.

[43] J.-S. Zheng, Y. He, C. Zuo, X.-Y. Cai, S. Tang, Z. A. Wang, L.-H. Zhang, C.-L. Tian, L. Liu, *Journal of the American Chemical Society* **2016**, *138*, 3553-3561.

[44] aG. A. Acosta, M. Royo, G. Beatriz, F. Albericio, *Tetrahedron Letters* **2017**, *58*, 2788-2791; bB. H. Gless, C. A. Olsen, *The Journal of organic chemistry* **2018**, *83*, 10525-10534.

[45] M. Kikuchi, R. Kurotani, H. Konno, *Tetrahedron Letters* **2017**, *58*, 4145-4148.

[46] J. Sueiras-Diaz, Y. Zhang, A. Velentza, B. Santoso, S. Yang, *Tetrahedron Letters* **2017**, *58*, 2448-2455.

[47] J. Palà-Pujadas, F. Albericio, J. B. Blanco-Canosa, *Angewandte Chemie* **2018**, *130*, 16352-16357.

[48] S. Tsuda, H. Nishio, T. Yoshiya, *Chemical Communications* **2018**, *54*, 8861-8864.

[49] aA. R. Katritzky, P. Angrish, K. Suzuki, *Synthesis* **2006**, *2006*, 411-424; bA. R. Katritzky, N. E. Abo-Dya, S. R. Tala, Z. K. Abdel-Samii, *Organic & biomolecular chemistry* **2010**, *8*, 2316-2319.

[50] aJ.-S. Zheng, S. Tang, Y.-K. Qi, Z.-P. Wang, L. Liu, *Nature protocols* **2013**, *8*, 2483; bM. Pan, Y. He, M. Wen, F. Wu, D. Sun, S. Li, L. Zhang, Y. Li, C. Tian, *Chemical Communications* **2014**, *50*, 5837-5839.

[51] J. S. Zheng, M. Yu, Y. K. Qi, S. Tang, F. Shen, Z. P. Wang, L. Xiao, L. Zhang, C. L. Tian, L. Liu, *Journal of the American Chemical Society* **2014**, *136*, 3695-3704.

[52] aQ. He, J. Li, Y. Qi, Z. Wang, Y. Huang, L. Liu, *Science China Chemistry* **2017**, *60*, 621-627; bP. Siman, S. V. Karthikeyan, M. Nikolov, W. Fischle, A. Brik, *Angewandte Chemie International Edition* **2013**, *52*, 8059-8063.

[53] J. S. Zheng, S. Tang, Y. Guo, H. N. Chang, L. Liu, *Chembiochem : a European journal of chemical biology* **2012**, *13*, 542-546.

[54] aJ. Kang, J. P. Richardson, D. Macmillan, *Chemical Communications* **2009**, 407-409; bN. I. Topilina, K. V. Mills, *Mobile Dna* **2014**, *5*, 5.

[55] J. D. Warren, J. S. Miller, S. J. Keding, S. J. Danishefsky, *Journal of the American Chemical Society* **2004**, *126*, 6576-6578.

[56] D. Bang, B. L. Pentelute, S. B. Kent, *Angewandte Chemie International Edition* **2006**, *45*, 3985-3988.

[57] J. S. Zheng, H. K. Cui, G. M. Fang, W. X. Xi, L. Liu, *Chembiochem : a European journal of chemical biology* **2010**, *11*, 511-515.

[58] aG. Chen, J. D. Warren, J. Chen, B. Wu, Q. Wan, S. J. Danishefsky, *Journal of the American Chemical Society* **2006**, *128*, 7460-7462; bJ.-S. Zheng, H.-N. Chang, J. Shi, L. Liu, *Science China Chemistry* **2012**, *55*, 64-69; cA. P. Tofteng, K. J. Jensen, T. Hoeg-Jensen, *Tetrahedron letters* **2007**, *48*, 2105-2107.

[59] C. Wang, Q.-X. Guo, *Science China Chemistry* **2012**, *55*, 2075-2080.

[60] F. Liu, J. P. Mayer, *The Journal of organic chemistry* **2013**, *78*, 9848-9856.

[61] P. Botti, M. Villain, S. Manganiello, H. Gaertner, *Organic letters* **2004**, *6*, 4861-4864.

[62] aE. A. George, R. P. Novick, T. W. Muir, *Journal of the American Chemical Society* **2008**, *130*, 4914-4924; bK. P. Chiang, M. S. Jensen, R. K. McGinty, T. W. Muir, *Chembiochem : a European journal of chemical biology* **2009**, *10*, 2182-2187.

[63] K. Wisniewski, *Organic Preparations and Procedures International* **1999**, *31*, 211-214.

[64] J. Vizzavona, F. Dick, T. Vorherr, *Bioorganic & medicinal chemistry letters* **2002**, *12*, 1963-1965.

[65] T. Kawakami, M. Sumida, T. Vorherr, S. Aimoto, *Tetrahedron letters* **2005**, *46*, 8805-8807.

[66] aS. Tsuda, M. Mochizuki, K. Sakamoto, M. Denda, H. Nishio, A. Otaka, T. Yoshiya, *Organic letters* **2016**, *18*, 5940-5943; bJ. Tailhades, N. A. Patil, M. A. Hossain, J. D. Wade, *Journal of Peptide Science* **2015**, *21*, 139-147; cY. Asahina, K. Nabeshima, H. Hojo, *Tetrahedron letters* **2015**, *56*, 1370-1373; dH. Hojo, Y. Onuma, Y. Akimoto, Y. Nakahara, Y. Nakahara, *Tetrahedron Letters* **2007**, *48*, 25-28.

[67] J. S. Zheng, H. N. Chang, F. L. Wang, L. Liu, *Journal of the American Chemical Society* **2011**, *133*, 11080-11083.

[68] N. Ollivier, J. Dheur, R. Mhidia, A. Blanpain, O. Melnyk, *Organic letters* **2010**, *12*, 5238-5241.

[69] F. Burlina, G. Papageorgiou, C. Morris, P. D. White, J. Offer, *Chem. Sci.* **2014**, *5*, 766-770.

[70] N. Ollivier, L. Raibaut, A. Blanpain, R. Desmet, J. Dheur, R. Mhidia, E. Boll, H. Drobecq, S. L. Pira, O. Melnyk, *Journal of Peptide Science* **2014**, *20*, 92-97.

[71] W. Hou, X. Zhang, F. Li, C.-F. Liu, *Organic letters* **2010**, *13*, 386-389.

[72] aR. m. Desmet, M. Pauzuolis, E. Boll, H. Drobecq, L. Raibaut, O. Melnyk, *Organic letters* **2015**, *17*, 3354-3357; bO. Melnyk, J. Vicogne, *Tetrahedron Letters* **2016**, *57*, 4319-4324.

[73] M. E. Jung, G. Piizzi, *Chemical reviews* **2005**, *105*, 1735-1766.

[74] J.-B. Li, S. Tang, J.-S. Zheng, C.-L. Tian, L. Liu, *Accounts of chemical research* **2017**, *50*, 1143-1153.

[75] V. Paraskevopoulou, F. Falcone, *Microorganisms* **2018**, *6*, 47.

[76] Y. Asahina, S. Kamitori, T. Takao, N. Nishi, H. Hojo, *Angewandte Chemie International Edition* **2013**, *52*, 9733-9737.

[77] aH. Kawashima, T. Kuruma, M. Yamashita, Y. Sohma, K. Akaji, *Journal of Peptide Science* **2014**, *20*, 361-365; bL. A. Carpino, E. Krause, C. D. Sferdean, M. Schümann, H. Fabian, M. Bienert, M. Beyermann, *Tetrahedron letters* **2004**, *45*, 7519-7523; cH. Hojo, H. Katayama, C. Tano, Y. Nakahara, A. Yoneshige, J. Matsuda, Y. Sohma, Y. Kiso, Y. Nakahara, *Tetrahedron letters* **2011**, *52*, 635-639; dY. Sohma, M. Sasaki, Y. Hayashi, T. Kimura, Y. Kiso, *Chemical Communications* **2004**, 124-125.

[78] aC. F. Becker, M. Oblatt-Montal, G. G. Kochendoerfer, M. Montal, *The Journal of biological chemistry* **2004**, *279*, 17483-17489; bV. Castelletto, I. W. Hamley, J. Seitsonen, J. Ruokolainen, G. Harris, K. Bellmann-Sickert, A. G. Beck-Sickinger, *Biomacromolecules* **2018**, *19*, 4320-4332.

[79] A. Kato, K. Maki, T. Ebina, K. Kuwajima, K. Soda, Y. Kuroda, *Biopolymers: Original Research on Biomolecules* **2007**, *85*, 12-18.

[80] M. Paradís-Bas, M. Albert-Soriano, J. Tulla-Puche, F. Albericio, *Organic & biomolecular chemistry* **2014**, *12*, 7194-7196.

[81] K. Wahlström, O. Planstedt, A. Undén, *Tetrahedron letters* **2008**, *49*, 3779-3781.

[82] L. Kocsis, T. Bruckdorfer, G. Orosz, *Tetrahedron Letters* **2008**, *49*, 7015-7017.

[83] K. Wahlström, A. Undén, *Tetrahedron Letters* **2009**, *50*, 2976-2978.

[84] Z. Tan, S. Shang, S. J. Danishefsky, *Proceedings of the National Academy of Sciences* **2011**, *108*, 4297-4302.

[85] Y. C. Huang, Y. M. Li, Y. Chen, M. Pan, Y. T. Li, L. Yu, Q. X. Guo, L. Liu, *Angewandte Chemie International Edition* **2013**, *52*, 4858-4862.

[86] S. K. Maity, G. Mann, M. Jbara, S. Laps, G. Kamnesky, A. Brik, *Organic letters* **2016**, *18*, 3026-3029.

[87] C. Zuo, S. Tang, Y.-Y. Si, Z. A. Wang, C.-L. Tian, J.-S. Zheng, *Organic & biomolecular chemistry* **2016**, *14*, 5012-5018.

[88] M. T. Jacobsen, M. E. Petersen, X. Ye, M. Galibert, G. H. Lorimer, V. Aucagne, M. S. Kay, *Journal of the American Chemical Society* **2016**, *138*, 11775-11782.

[89] J. A. Karas, A. Noor, C. Schieber, T. U. Connell, F. Separovic, P. S. Donnelly, *Chemical Communications* **2017**, *53*, 6903-6905.

[90] S. Tang, C. Zuo, D.-L. Huang, X.-Y. Cai, L.-H. Zhang, C.-L. Tian, J.-S. Zheng, L. Liu, *nature protocols* **2017**, *12*, 2554.

[91] S. Tsuda, M. Mochizuki, H. Ishiba, K. Yoshizawa-Kumagaye, H. Nishio, S. Oishi, T. Yoshiya, *Angewandte Chemie* **2018**, *130*, 2127-2131.

[92] S. Tsuda, S. Masuda, T. Yoshiya, *Organic & biomolecular chemistry* **2019**.

[93] T. Yoshiya, S. Tsuda, S. Masuda, *Chembiochem : a European journal of chemical biology* **2019**.

[94] F. Shen, S. Tang, L. Liu, *Science China Chemistry* **2011**, *54*, 110-116.

[95] M. Mochizuki, H. Hibino, Y. Nishiuchi, *Organic letters* **2014**, *16*, 5740-5743.

[96] A. P. Tofteng, K. J. Jensen, L. Schäffer, T. Hoeg-Jensen, *Chembiochem : a European journal of chemical biology* **2008**, *9*, 2989-2996.

[97] D. R. Englebretsen, G. T. Robillard, *Tetrahedron* **1999**, *55*, 6623-6634.

[98] M. M. Disotuar, M. E. Petersen, J. M. Nogueira, M. S. Kay, D. H.-C. Chou, *Organic & biomolecular chemistry* **2019**, *17*, 1703-1708.

[99] D. R. Englebretsen, P. F. Alewood, *Tetrahedron letters* **1996**, *37*, 8431-8434.

[100] aC. T. Choma, G. T. Robillard, D. R. Englebretsen, *Tetrahedron Letters* **1998**, *39*, 2417-2420; bD. R. Englebretsen, C. T. Choma, G. T. Robillard, *Tetrahedron letters* **1998**, *39*, 4929-4932.

[101] T. Sato, Y. Saito, S. Aimoto, *Journal of peptide science: an official publication of the European Peptide Society* **2005**, *11*, 410-416.

[102] E. C. Johnson, S. B. Kent, *Tetrahedron Lett* **2007**, *48*, 1795-1799.

[103] D. J. Boerema, V. A. Tereshko, S. B. Kent, *Peptide Science* **2008**, *90*, 278-286.

[104] E. C. Johnson, E. Malito, Y. Shen, D. Rich, W.-J. Tang, S. B. Kent, *Journal of the American Chemical Society* **2007**, *129*, 11480-11490.

[105] Y. Sohma, B. L. Pentelute, J. Whittaker, Q. x. Hua, L. J. Whittaker, M. A. Weiss, S. B. Kent, *Angewandte Chemie International Edition* **2008**, *47*, 1102-1106.

[106] M. A. Hossain, A. Belgi, F. Lin, S. Zhang, F. Shabanpoor, L. Chan, C. Belyea, H.-T. Truong, A. R. Blair, S. Andrikopoulos, *Bioconjugate chemistry* **2009**, *20*, 1390-1396.

[107] aP. W. Harris, M. A. Brimble, *Synthesis* **2009**, *2009*, 3460-3466; bP. W. Harris, M. A. Brimble, *Peptide Science* **2010**, *94*, 542-550.

[108] A. Belgi, M. A. Hossain, F. Shabanpoor, L. Chan, S. Zhang, R. A. Bathgate, G. W. Tregear, J. D. Wade, *Biochemistry* **2011**, *50*, 8352-8361.

[109] S. Lahiri, M. Brehs, D. Olschewski, C. F. Becker, *Angewandte Chemie International Edition* **2011**, *50*, 3988-3992.

[110] S.-H. Yang, J. M. Wojnar, P. W. Harris, A. L. DeVries, C. W. Evans, M. A. Brimble, *Organic & biomolecular chemistry* **2013**, *11*, 4935-4942.

[111] C. Zhan, L. Zhao, X. Chen, W.-Y. Lu, W. Lu, *Bioorganic & medicinal chemistry* **2013**, *21*, 3443-3449.

[112] S. Peigneur, M. Paolini-Bertrand, H. Gaertner, D. Biass, A. Violette, R. Stöcklin, P. Favreau, J. Tytgat, O. Hartley, *Journal of Biological Chemistry* **2014**, *289*, 35341-35350.

[113] M. Paradís-Bas, J. Tulla-Puche, F. Albericio, *Organic letters* **2014**, *17*, 294-297.

[114] S. Chemuru, R. Kodali, R. Wetzel, *Peptide Science* **2014**, *102*, 206-221.

[115] T. J. Harmand, V. R. Pattabiraman, J. W. Bode, *Angewandte Chemie International Edition* **2017**, *56*, 12639-12643.

[116] S. Bondalapati, E. Eid, S. M. Mali, C. Wolberger, A. Brik, *Chemical science* **2017**, *8*, 4027-4034.

[117] aE. Bianchi, R. Ingenito, R. J. Simon, A. Pessi, *Journal of the American Chemical Society* **1999**, *121*, 7698-7699; bC. Zuo, S. Tang, J. S. Zheng, *Journal of Peptide Science* **2015**, *21*, 540-549.

[118] A. Otaka, S. Ueda, K. Tomita, Y. Yano, H. Tamamura, K. Matsuzaki, N. Fujii, *Chemical Communications* **2004**, 1722-1723.

[119] C. L. Hunter, G. G. Kochendoerfer, *Bioconjugate chemistry* **2004**, *15*, 437-440.

[120] M. Dittmann, J. Sauermann, R. Seidel, W. Zimmermann, M. Engelhard, *Journal of Peptide Science* **2010**, *16*, 558-562.

[121] aM. Dittmann, M. Sadek, R. Seidel, M. Engelhard, *Journal of Peptide Science* **2012**, *18*, 312-316; bS. Kitzig, K. Rück-Braun, *Journal of Peptide Science* **2017**, *23*, 567-573; cM. Dittmann, R. Seidel, I. Chizhov, M. Engelhard, *Journal of Peptide Science* **2014**, *20*, 137-144.

[122] S. Khaksar, *Journal of Fluorine Chemistry* **2015**, *172*, 51-61.

[123] aN. Nishino, H. Mihara, Y. Makinose, T. Fujimoto, *Tetrahedron letters* **1992**, *33*, 7007-7010; bH. KURODA, Y. N. CHEN, T. KIMURA, S. SAKAKIBARA, *International journal of peptide and protein research* **1992**, *40*, 294-299.

[124] aS. C. MILTON, R. d. L. Milton, *International journal of peptide and protein research* **1990**, *36*, 193-196; bD. Yamashiro, J. Blake, C. H. Li, *Tetrahedron Letters* **1976**, *17*, 1469-1472.

[125] A. Bossi, P. G. Righetti, *Journal of Chromatography A* **1999**, *840*, 117-129.

[126] aF. Sönnichsen, J. E. Van, R. Hodges, B. Sykes, *Biochemistry* **1992**, *31*, 8790-8798; bT. P. Pitner, D. Urry, *Journal of the American Chemical Society* **1972**, *94*, 1399-1400; cP. Luo, R. L. Baldwin, *Biochemistry* **1997**, *36*, 8413-8421.

[127] R. Rajan, P. Balaram, *International journal of peptide and protein research* **1996**, *48*, 328-336.

[128] D. Roccatano, G. Colombo, M. Fioroni, A. E. Mark, *Proceedings of the National Academy of Sciences of the United States of America* **2002**, *99*, 12179.

[129] M. Narita, S. Honda, H. Umeyama, S. Obana, *Bulletin of the Chemical Society of Japan* **1988**, *61*, 281-284.

[130] G. G. Kochendoerfer, D. Salom, J. D. Lear, R. Wilk-Orescan, S. B. Kent, W. F. DeGrado, *Biochemistry* **1999**, *38*, 11905-11913.

[131] B. Kwon, D. Tietze, P. B. White, S. Y. Liao, M. Hong, *Protein science : a publication of the Protein Society* **2015**, *24*, 1087-1099.

[132] J.-P. Begue, D. Bonnet-Delpon, B. Crousse, *Synlett* **2004**, *2004*, 18-29.

[133] T. Welton, *Chemical reviews* **1999**, *99*, 2071-2084.

[134] T. Welton, *Biophysical reviews* **2018**, *10*, 691-706.

[135] A. A. Tietze, P. Heimer, A. Stark, D. Imhof, *Molecules* **2012**, *17*, 4158-4185.

[136] R. V. Hangarge, D. V. Jarikote, M. S. Shingare, *Green Chemistry* **2002**, *4*, 266-268.

[137] D. W. Morrison, D. C. Forbes, J. H. Davis Jr, *Tetrahedron Letters* **2001**, *42*, 6053-6055.

[138] T. Fischer, A. Sethi, T. Welton, J. Woolf, *Tetrahedron Letters* **1999**, *40*, 793-796.

[139] R. L. Vekariya, *Journal of Molecular Liquids* **2017**, *227*, 44-60.

[140] K. D. Clark, O. Nacham, H. Yu, T. Li, M. M. Yamsek, D. R. Ronning, J. L. Anderson, *Analytical chemistry* **2015**, *87*, 1552-1559.

[141] R. R. Mazid, U. Divisekera, W. Yang, V. Ranganathan, D. R. MacFarlane, C. Cortez-Jugo, W. Cheng, *Chemical Communications* **2014**, *50*, 13457-13460.

[142] aU. Kragl, M. Eckstein, N. Kaftzik, *Current Opinion in Biotechnology* **2002**, *13*, 565-571; bM. Moniruzzaman, K. Nakashima, N. Kamiya, M. Goto, *Biochemical Engineering Journal* **2010**, *48*, 295-314.

[143] A. Benedetto, P. Ballone, *ACS Sustainable Chemistry & Engineering* **2015**, *4*, 392-412.

[144] aA. Miloslavina, C. Ebert, D. Tietze, O. Ohlenschläger, C. Englert, M. Görlach, D. Imhof, *Peptides* **2010**, *31*, 1292-1300; bA. A. Miloslavina, E. Leipold, M. Kijas, A. Stark, S. H. Heinemann, D. Imhof, *Journal of peptide science: an official publication of the European Peptide Society* **2009**, *15*, 72-77.

[145] aA. A. Tietze, F. Bordusa, R. Giernoth, D. Imhof, T. Lenzer, A. Maaß, C. Mrestani-Klaus, I. Neundorf, K. Oum, D. Reith, *ChemPhysChem* **2013**, *14*, 4044-4064; bH. Weingärtner, C. Cabrele, C. Herrmann, *Physical Chemistry Chemical Physics* **2012**, *14*, 415-426.

[146] aH. Zhao, *Journal of Chemical Technology & Biotechnology* **2016**, *91*, 25-50; bM. Naushad, Z. A. ALOthman, A. B. Khan, M. Ali, *International journal of biological macromolecules* **2012**, *51*, 555-560.

[147] N. Gunasekaran, *Advanced Synthesis & Catalysis* **2015**, *357*, 1990-2010.

[148] P. Heimer, A. A. Tietze, M. Böhm, R. Giernoth, A. Kuchenbuch, A. Stark, E. Leipold, S. H. Heinemann, C. Kandt, D. Imhof, *Chembiochem : a European journal of chemical biology* **2014**, *15*, 2754-2765.

[149] G. Tabarelli, E. E. Alberto, A. M. Deobald, G. Marin, O. E. Rodrigues, L. Dornelles, A. L. Braga, *Tetrahedron Letters* **2010**, *51*, 5728-5731.

[150] aM. Chen, P. Heimer, D. Imhof, *Amino Acids* **2015**, *47*, 1283-1299; bM. Konwar, N. D. Khupse, P. J. Saikia, D. Sarma, *Journal of Chemical Sciences* **2018**, *130*, 53.

[151] M. Böhm, T. Kühl, K. Hardes, R. Coch, C. Arkona, B. Schlott, T. Steinmetzer, D. Imhof, *ChemMedChem* **2012**, *7*, 326-333.

[152] T. Kühl, M. Chen, K. Teichmann, A. Stark, D. Imhof, *Tetrahedron letters* **2014**, *55*, 3658-3662.

[153] aS. Wellens, N. R. Brooks, B. Thijs, L. Van Meervelt, K. Binnemans, *Dalton Transactions* **2014**, *43*, 3443-3452; bS. Wang, X. Wang, *Angewandte Chemie International Edition* **2016**, *55*, 2308-2320; cD. D. Liu, Y. Zhang, E. Y.-X. Chen, *Green Chemistry* **2012**, *14*, 2738-2746.

[154] R. Olofson, W. Thompson, J. Michelman, *Journal of the American Chemical Society* **1964**, *86*, 1865-1866.

[155] A. J. Arduengo, *Accounts of chemical research* **1999**, *32*, 913-921.

[156] S. Chowdhury, R. S. Mohan, J. L. Scott, *Tetrahedron* **2007**, *63*, 2363-2389.

[157] aZ. Kelemen, O. Hollóczki, J. Nagy, L. Nyulászi, *Organic & biomolecular chemistry* **2011**, *9*, 5362-5364; bO. Hollóczki, D. Gerhard, K. Massone, L. Szarvas, B. Németh, T. Veszprémi, L. Nyulászi, *New Journal of Chemistry* **2010**, *34*, 3004-3009.

[158] V. K. Aggarwal, I. Emme, A. Mereu, *Chemical Communications* **2002**, 1612-1613.

[159] H. Chen, D. R. Justes, R. G. Cooks, *Organic letters* **2005**, *7*, 3949-3952.

[160] G. Gurau, H. Rodríguez, S. P. Kelley, P. Janiczek, R. S. Kalb, R. D. Rogers, *Angewandte Chemie International Edition* **2011**, *50*, 12024-12026.

[161] H. Rodríguez, G. Gurau, J. D. Holbrey, R. D. Rogers, *Chemical Communications* **2011**, *47*, 3222-3224.

[162] S. L. Cooley, J. L. Wood, *Archives of biochemistry and biophysics* **1951**, *34*, 372-377.

[163] M. Perlstein, M. Atassi, S. Cheng, *Biochimica et Biophysica Acta (BBA)-Protein Structure* **1971**, *236*, 174-182.

[164] L. Z. Yan, P. E. Dawson, *Journal of the American Chemical Society* **2001**, *123*, 526-533.

[165] B. L. Pentelute, S. B. Kent, *Organic letters* **2007**, *9*, 687-690.

[166] Q.-Q. He, G.-M. Fang, L. Liu, *Chinese Chemical Letters* **2013**, *24*, 265-269.

[167] aK. Jin, X. Li, *Chemistry–A European Journal* **2018**, *24*, 17397-17404; bZ. Harpaz, P. Siman, K. A. Kumar, A. Brik, *Chembiochem : a European journal of chemical biology* **2010**, *11*, 1232-1235; cC. Haase, H. Rohde, O. Seitz, *Angewandte Chemie International Edition* **2008**, *47*, 6807-6810; dL. R. Malins, K. M. Cergol, R. J. Payne, *Chembiochem : a European journal of chemical biology* **2013**, *14*, 559-563; eP. Siman, S. V. Karthikeyan, A. Brik, *Organic letters* **2012**, *14*, 1520-1523; fS. Dery, P. S. Reddy, L. Dery, R. Mousa, R. N. Dardashti, N. Metanis, *Chemical science* **2015**, *6*, 6207-6212.

[168] H. Rohde, O. Seitz, *Peptide Science* **2010**, *94*, 551-559.

[169] F. W. Hoffmann, R. J. Ess, T. C. Simmons, R. S. Hanzel, *Journal of the American Chemical Society* **1956**, *78*, 6414-6414.

[170] aC. Walling, R. Rabinowitz, *Journal of the American Chemical Society* **1957**, *79*, 5326-5326; bC. Walling, R. Rabinowitz, *Journal of the American Chemical Society* **1959**, *81*, 1243-1249; cC. Walling, O. H. Basedow, E. S. Savas, *Journal of the American Chemical Society* **1960**, *82*, 2181-2184; dC. Walling, M. S. Pearson, *Journal of the American Chemical Society* **1964**, *86*, 2262-2266.

[171] A. González, G. Valencia, *Tetrahedron: Asymmetry* **1998**, *9*, 2761-2764.

[172] Q. Wan, S. J. Danishefsky, *Angewandte Chemie International Edition* **2007**, *46*, 9248-9252.

[173] O. Reimann, C. Smet-Nocca, C. P. Hackenberger, *Angewandte Chemie International Edition* **2015**, *54*, 306-310.

[174] Y. Tian, L. Wang, J. Shi, H.-z. Yu, *Chinese Journal of Chemical Physics* **2015**, *28*, 269.

[175] aA. Ansaloni, Z. M. Wang, J. S. Jeong, F. S. Ruggeri, G. Dietler, H. A. Lashuel, *Angewandte Chemie International Edition* **2014**, *53*, 1928-1933; bJ. Li, S. Dong, S. D. Townsend, T. Dean, T. J. Gardella, S. J. Danishefsky, *Angewandte Chemie International Edition* **2012**, *51*, 12263-12267; cP. Siman, O. Blatt, T. Moyal, T. Danieli, M. Lebendiker, H. A. Lashuel, A. Friedler, A. Brik, *Chembiochem : a European journal of chemical biology* **2011**, *12*, 1097-1104.

[176] K. Jin, T. Li, H. Y. Chow, H. Liu, X. Li, *Angewandte Chemie International Edition* **2017**, *56*, 14607-14611.

[177] aD. D. Martin, M.-Q. Xu, T. C. Evans, *Biochemistry* **2001**, *40*, 1393-1402; bN. H. Shah, G. P. Dann, M. Vila-Perelló, Z. Liu, T. W. Muir, *Journal of the American Chemical Society* **2012**, *134*, 11338-11341.

[178] W. F. HEATH, J. P. TAM, R. Merrifield, *International Journal of Peptide and Protein Research* **1986**, *28*, 498-507.

[179] aH. TAMAMURA, R. IKOMA, M. NIWA, S. FUNAKOSHI, T. MURAKAMI, N. FUJII, *Chemical and pharmaceutical bulletin* **1993**, *41*, 978-980; bY.-K. Qi, Q.-Q. He, H.-S. Ai, J.-B. Li, J.-S. Zheng, *Synlett* **2017**, *28*, 1907-1912; cG. N. Boross, D. Schauenburg, J. W. Bode, *Helvetica Chimica Acta* **2019**, *102*, e1800214.

[180] D. Veber, J. Milkowski, S. Varga, R. Denkewalter, R. Hirschmann, *Journal of the American Chemical Society* **1972**, *94*, 5456-5461.

[181] aD. Andreu, F. Albericio, N. A. Solé, M. C. Munson, M. Ferrer, G. Barany, in *Peptide synthesis protocols*, Springer, **1994**, pp. 91-169; bI. Vetter, Z. Dekan, O. Knapp, D. J. Adams, P. F. Alewood, R. J. Lewis, *Biochemical pharmacology* **2012**, *84*, 540-548.

[182] aP. M. Moyle, C. Olive, M. F. Good, I. Toth, *Journal of peptide science: an official publication of the European Peptide Society* **2006**, *12*, 800-807; bS. Zhang, F. Lin, M. A. Hossain, F. Shabanpoor, G. W. Tregear, J. D. Wade, *International Journal of Peptide Research and Therapeutics* **2008**, *14*, 301-305; cI. Friligou, E. Papadimitriou, D. Gatos, J. Matsoukas, T. Tselios, *Amino acids* **2011**, *40*, 1431-1440; dP. M. Moyle, C. Olive, M.-F. Ho, M. F. Good, I. Toth, *Journal of medicinal chemistry* **2006**, *49*, 6364-6370.

[183] J. V. Castell, A. Tun-Kyi, *Helvetica Chimica Acta* **1979**, *62*, 2507-2510.

[184] aK. M. Harris, S. Flemer Jr, R. J. Hondal, *Journal of peptide science: an official publication of the European Peptide Society* **2007**, *13*, 81-93; bE. J. Ste. Marie, E. L. Ruggles, R. J. Hondal, *Journal of Peptide Science* **2016**, *22*, 571-576; cA. L. Schroll, R. J. Hondal, S. Flemer Jr, *Journal of Peptide Science* **2012**, *18*, 1-9.

[185] M. YOSHIDA, K. AKAJI, T. TATSUMI, S. IINUMA, Y. FUJIWARA, T. KIMURA, Y. KISO, *Chemical and Pharmaceutical Bulletin* **1990**, *38*, 273-275.

[186] C. Li, Z. Wu, M. Liu, M. Pazgier, W. Lu, *Protein Science* **2008**, *17*, 1624-1629.

[187] N. Fujii, A. Otaka, T. Watanabe, A. Okamachi, H. Tamamura, H. Yajima, Y. Inagaki, M. Nomizu, K. Asano, *Journal of the Chemical Society, Chemical Communications* **1989**, 283-284.

[188] aS. Andrew, *Journal of the Chemical Society, Perkin Transactions 1* **1993**, 1947-1952; bK. Sato, K. Kitakaze, T. Nakamura, N. Naruse, K. Aihara, A. Shigenaga, T. Inokuma, D. Tsuji, K. Itoh, A. Otaka, *Chemical Communications* **2015**, *51*, 9946-9948.

[189] aY. Zhang, H. Zhang, Q. Zheng, *Physical Chemistry Chemical Physics* **2019**, *21*, 2984-2991; bP. Santner, J. o. M. d. S. Martins, J. S. Laursen, L. Behrendt, L. Riber, C. A. Olsen, I. T. Arkin, J. R. Winther, M. Willemoës, K. Lindorff-Larsen, *Biochemistry* **2018**, *57*, 5949-5956.

[190] C. Ma, J. Wang, *Biochimica et Biophysica Acta (BBA)-Biomembranes* **2018**, *1860*, 272-280.

[191] L. H. Pinto, R. A. Lamb, *Molecular bioSystems* **2007**, *3*, 18-23.

[192] A. Wanitchang, P. Wongthida, A. Jongkaewwattana, *Virology* **2016**, *498*, 99-108.

[193] L. H. Pinto, R. A. Lamb, *Journal of Biological Chemistry* **2006**, *281*, 8997-9000.

[194] S. Caini, Q. S. Huang, M. A. Ciblak, G. Kusznierz, R. Owen, S. Wangchuk, C. M. Henriques, R. Njouom, R. A. Fasce, H. Yu, *Influenza and other respiratory viruses* **2015**, *9*, 3-12.

[195] V. S. Mandala, S.-Y. Liao, M. D. Gelenter, M. Hong, *Scientific reports* **2019**, *9*, 3725.

[196] aJ. K. Williams, D. Tietze, M. Lee, J. Wang, M. Hong, *Journal of the American Chemical Society* **2016**, *138*, 8143-8155; bJ. K. Williams, A. A. Shcherbakov, J. Wang, M. Hong, *Journal of Biological Chemistry* **2017**, *292*, 17876-17884.

[197] R. M. Pielak, J. J. Chou, *Biochimica et Biophysica Acta (BBA)-Biomembranes* **2011**, *1808*, 522-529.

[198] K. Otomo, A. Toyama, T. Miura, H. Takeuchi, *Journal of biochemistry* **2009**, *145*, 543-554.

[199] aN. Sunstrom, L. Premkumar, A. Premkumar, G. Ewart, G. Cox, P. Gage, *The Journal of membrane biology* **1996**, *150*, 127-132; bJ. A. Mould, R. G. Paterson, M. Takeda, Y. Ohigashi, P. Venkataraman, R. A. Lamb, L. H. Pinto, *Developmental cell* **2003**, *5*, 175-184.

[200] G. G. Kochendoerfer, D. Clayton, C. Becker, *Protein and peptide letters* **2005**, *12*, 737-741.

[201] aH. Yin, A. D. Flynn, *Annual review of biomedical engineering* **2016**, *18*, 51-76; bM. S. Almén, K. J. Nordström, R. Fredriksson, H. B. Schiöth, *BMC biology* **2009**, *7*, 50.

[202] J. P. Overington, B. Al-Lazikani, A. L. Hopkins, *Nature reviews Drug discovery* **2006**, *5*, 993.

[203] Y. Jin, H. Zhong, J. R. Omnaas, R. Neubig, H. I. Mosberg, *The Journal of peptide research* **2004**, *63*, 141-146.

[204] aQ.-S. Du, R.-B. Huang, S.-Q. Wang, K.-C. Chou, *PloS one* **2010**, *5*, e9388; bN. Tran, L. Tran, L. Le, *Medicinal Chemistry Research* **2013**, *22*, 6078-6088.

[205] S. K. Bagal, B. E. Marron, R. M. Owen, R. I. Storer, N. A. Swain, *Channels* **2015**, *9*, 360-366.

[206] aJ. Du, T. A. Cross, H.-X. Zhou, *Drug discovery today* **2012**, *17*, 1111-1120; bS. Z. Grinter, X. Zou, *Molecules* **2014**, *19*, 10150-10176.

[207] A. Kopp, *TU Darmstadt* **2018**, *Bachelor Thesis, AK Tietze*.

[208] K. K. Swamy, N. B. Kumar, E. Balaraman, K. P. Kumar, *Chemical reviews* **2009**, *109*, 2551-2651.

[209] P. P. de Laureto, M. Donadi, E. Scaramella, E. Frare, A. Fontana, *Biochimica et Biophysica Acta (BBA)-Protein Structure and Molecular Enzymology* **2001**, *1548*, 29-37.

[210] C. K. Lee, J. M. Manning, *Journal of Biological Chemistry* **1973**, *248*, 5861-5865.

[211] J. Lippincott, I. Apostol, *Analytical biochemistry* **1999**, *267*, 57-64.

[212] P. Dirnhuber, F. Schütz, *Biochemical Journal* **1948**, *42*, 628.

[213] P. Hagel, J. Gerding, W. Fieggen, H. Bloemendal, *Biochimica et Biophysica Acta (BBA)-Protein Structure* **1971**, *243*, 366-373.

[214] G. R. Stark, *Biochemistry* **1965**, *4*, 2363-2367.

[215] G. R. Stark, in *Methods in enzymology, Vol. 11*, Elsevier, **1967**, pp. 590-594.

[216] A. J. Arduengo III, R. L. Harlow, M. Kline, *Journal of the American Chemical Society* **1991**, *113*, 361-363.

[217] aT. L. Amyes, S. T. Diver, J. P. Richard, F. M. Rivas, K. Toth, *Journal of the American Chemical Society* **2004**, *126*, 4366-4374; bY. Chu, H. Deng, J.-P. Cheng, *The Journal of organic chemistry* **2007**, *72*, 7790-7793.

[218] G.-F. Thomas, *TU Darmstadt* **2018**, *Bachelor Thesis, AK Tietze*.

[219] aG. Drochioiu, M. Manea, M. Dragusanu, M. Murariu, E. S. Dragan, B. A. Petre, G. Mezo, M. Przybylski, *Biophysical chemistry* **2009**, *144*, 9-20; bH. Li, K. Michael Siu, R. Guevremont, J. Yves Le Blanc, *Journal of the American Society for Mass Spectrometry* **1997**, *8*, 781-792.

[220] W. C. Johnson Jr, *Proteins: Structure, Function, and Bioinformatics* **1990**, *7*, 205-214.

[221] aD. Engelman, T. Steitz, *Cell* **1981**, *23*, 411-422; bR. Renthal, *Cellular and molecular life sciences* **2010**, *67*, 1077-1088; cA. S. Ladokhin, M. Fernández-Vidal, S. H. White, *The Journal of membrane biology* **2010**, *236*, 247-253; dS. O. Smith, R. Jonas, M. Braiman, B. J. Bormann, *Biochemistry* **1994**, *33*, 6334-6341.

[222] S. Eissler, M. Kley, D. Bächle, G. Loidl, T. Meier, D. Samson, *Journal of Peptide Science* **2017**, *23*, 757-762.

[223] H. Schägger, *Nature protocols* **2006**, *1*, 16.

References from internet sources

[A] https://www.aphorismen.de/zitat/84782, retrieved at **03.06.2018**.

[B] From RCSB PDB: https://www.rcsb.org/3d-view/2kix, retrieved at **15.05.2019**. Channel domain of BM2 protein from influenza B virus. Image of 2KIX (J. Wang, R. M. Pielak, M. A. McClintock, J. J. Chou, Nature structural & molecular biology **2009**, 16, 1267.) created with NGL (A.S. Rose, A.R. Bradley, Y. Valasatava, J.D. Duarte, A. Prlić, P.W. Rose (**2018**) NGL viewer: web-based molecular graphics for large complexes. Bioinformatics 34: 3755–3758).

15. Appendix

15.1. Supporting information for internal modifications

15.1.1. Synthesis of model Hmp-peptides (chapter 5.1.5)

ESI-MS of P4 [Ile^{21}]BM2(17-21)-Hmp

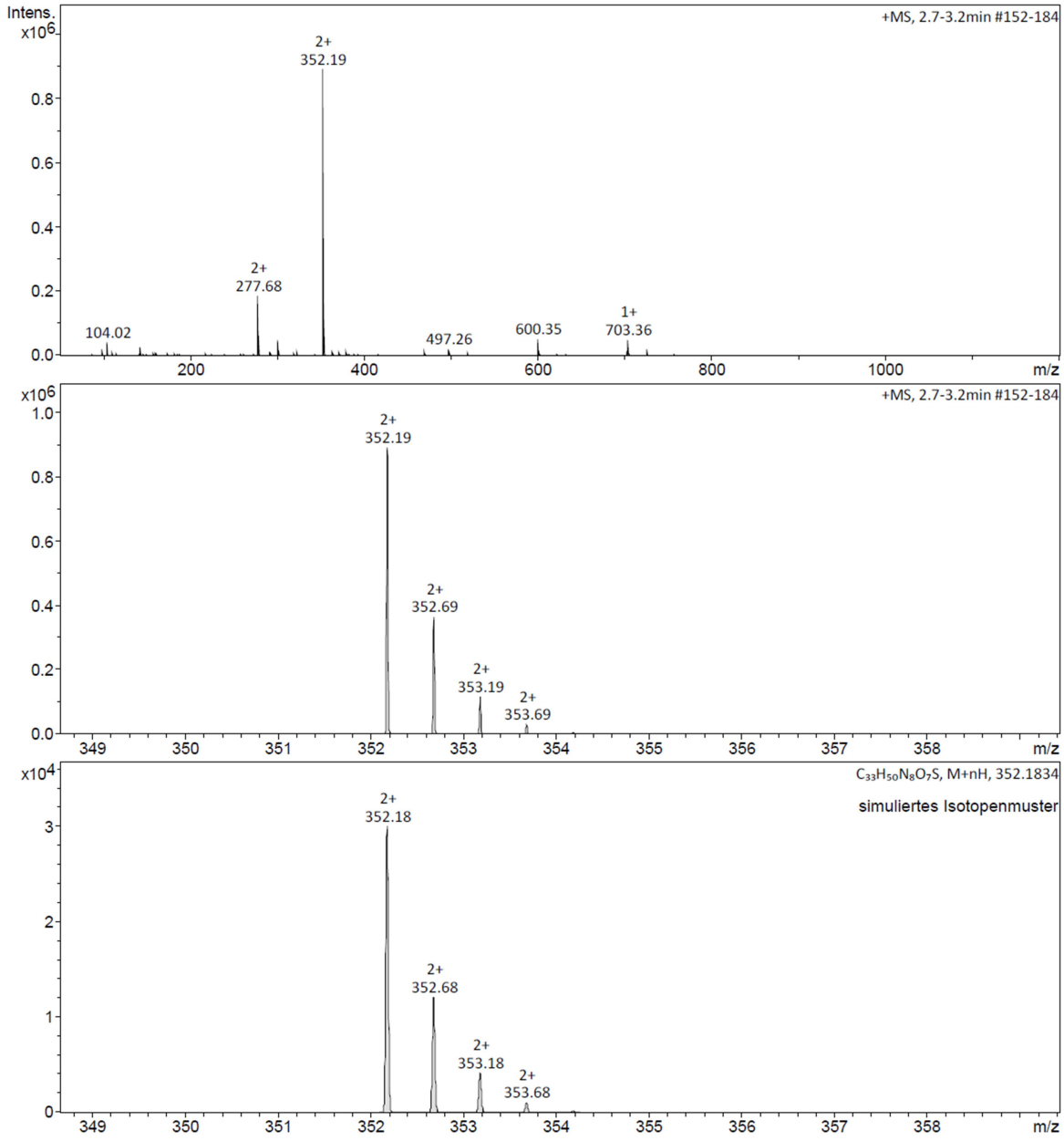

Figure 15.1: Experimental and simulated isotopic pattern of model peptide P4.

ESI-MS of P5 [Ile^{21}]BM2(17-21)-Hmp-ADO

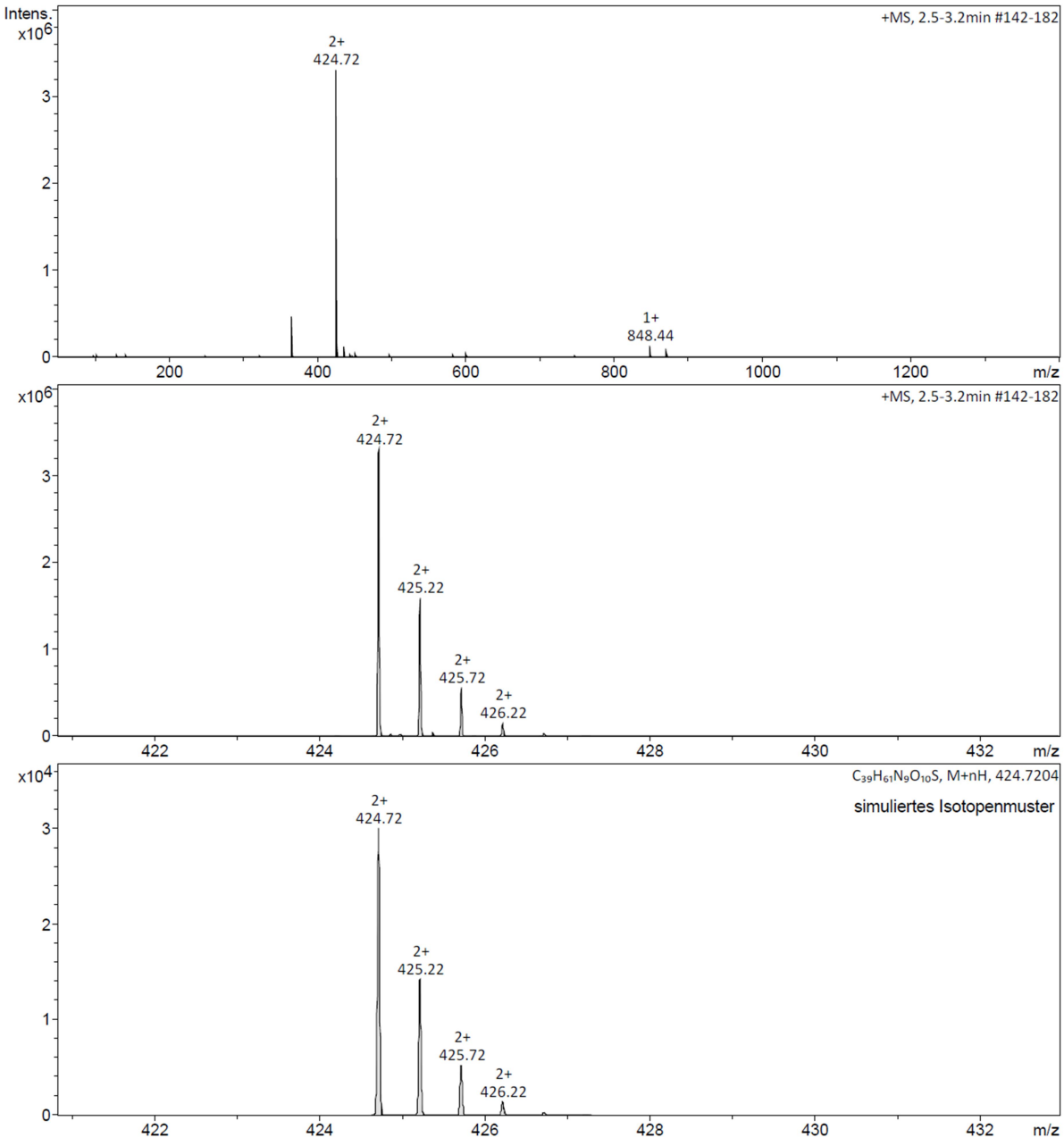

Figure 15.2: Experimental and simulated isotopic pattern of model peptide P5.

ESI-MS of P6 [Ile^{21}]BM2(17-21)-Hmp-ADO$_2$

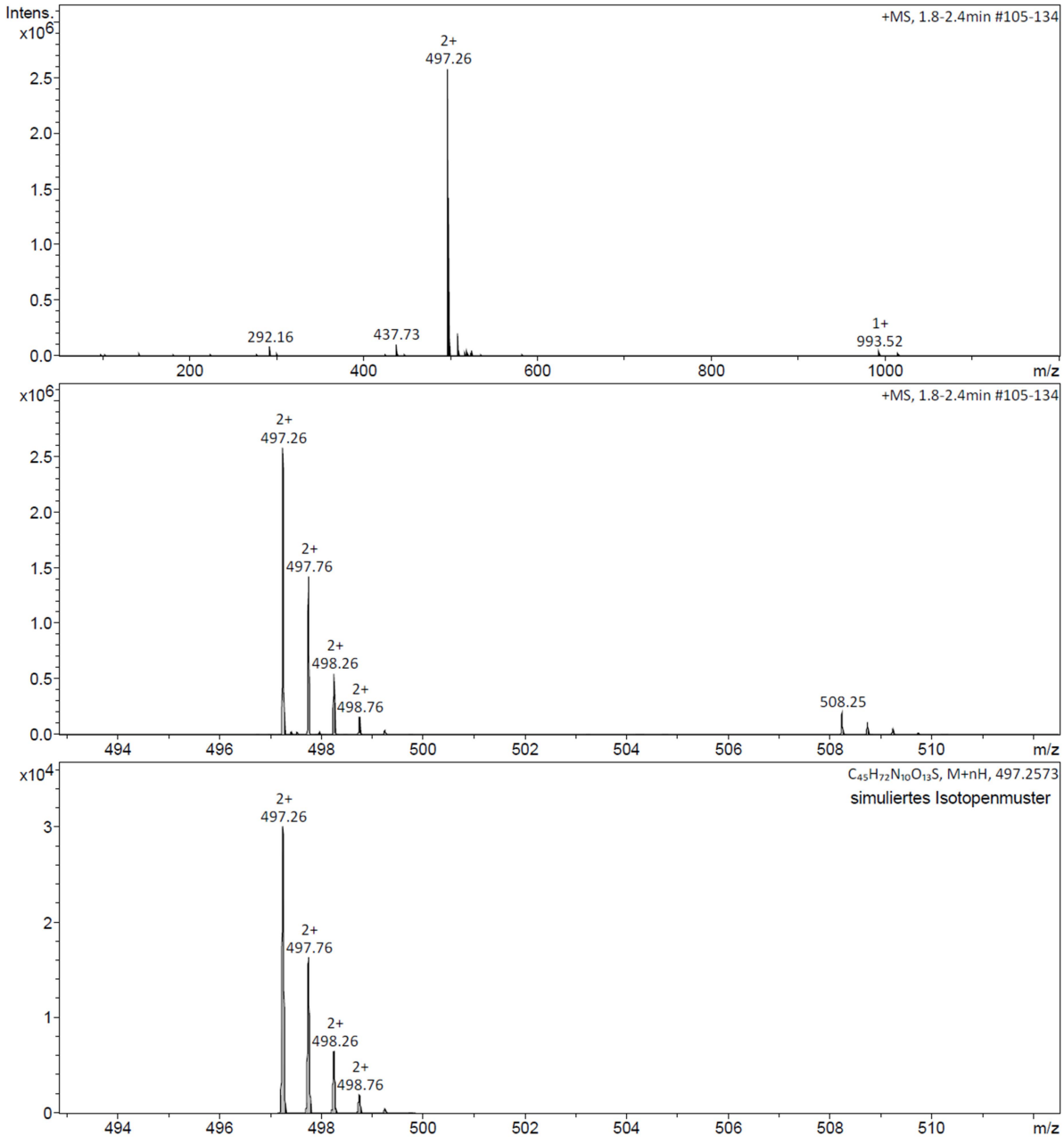

Figure 15.3: Experimental and simulated isotopic pattern of model peptide P6.

ESI-MS of P7 [Leu^{21}]BM2(17-21)-Hmp

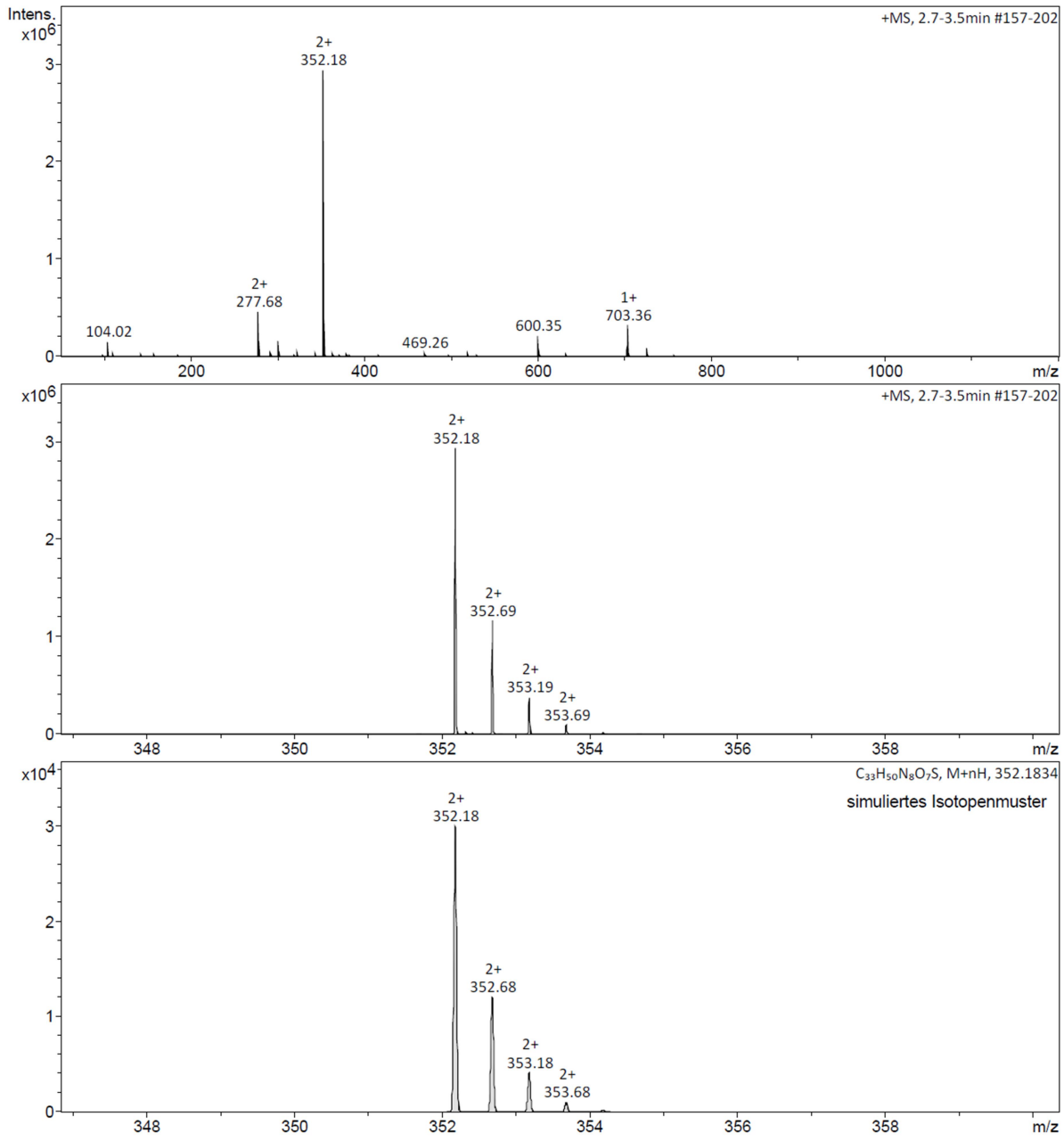

Figure 15.4: Experimental and simulated isotopic pattern of model peptide P7.

ESI-MS of P8 [Leu^{21}]BM2(17-21)-Hmp-ADO

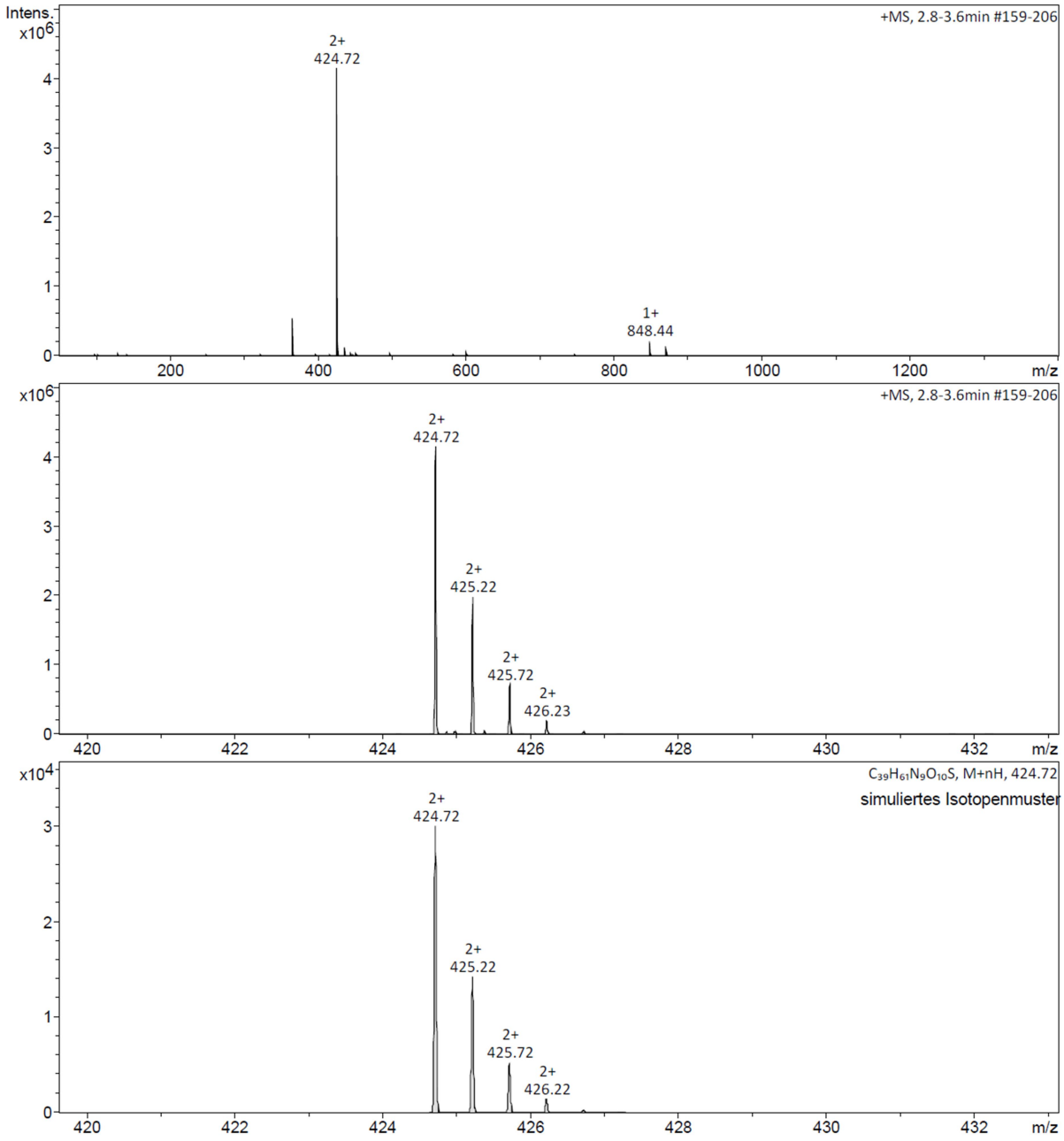

Figure 15.5: Experimental and simulated isotopic pattern of model peptide P8.

ESI-MS of P9 [Leu^{21}]BM2(17-21)-Hmp-ADO$_2$

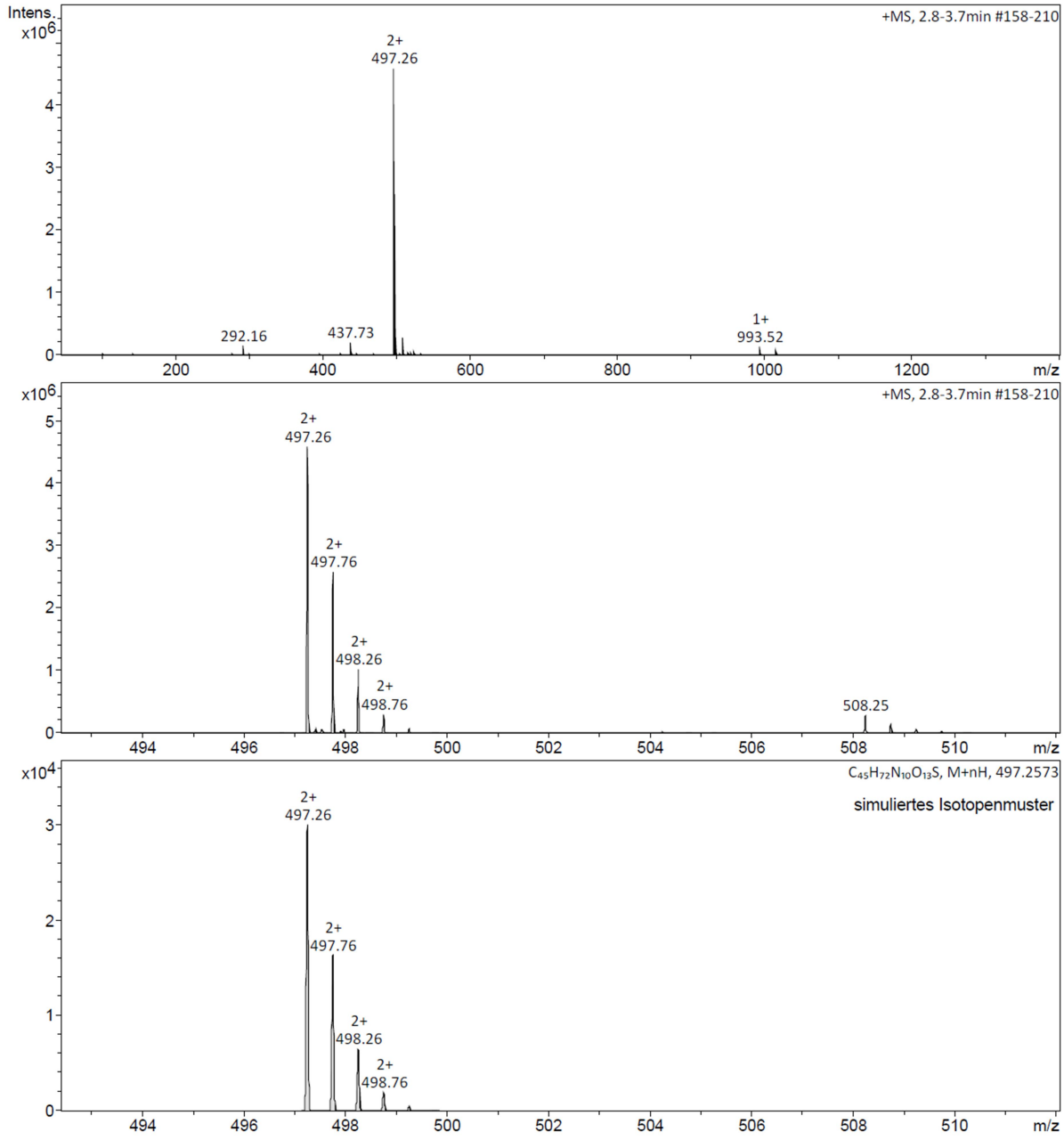

Figure 15.6: Experimental and simulated isotopic pattern of model peptide P9.

15.1.2. Test cleavage after ADO, Hmp and Leu coupling

Table 15.1: Found molecular masses and possible products after test cleavage.

Entry	Test cleavage	Found [m/z]	Found product
a)	ADO-Lys_5	803.66^{1+}	ADO-Lys_5
b)	Hmp-ADO-Lys_5	907.67^{1+}	Hmp-ADO-Lys_5
c)	Leu-Hmp-ADO-Lys_5	1132.81^{1+}	$(Leu)_2$-Hmp-ADO-Lys_5

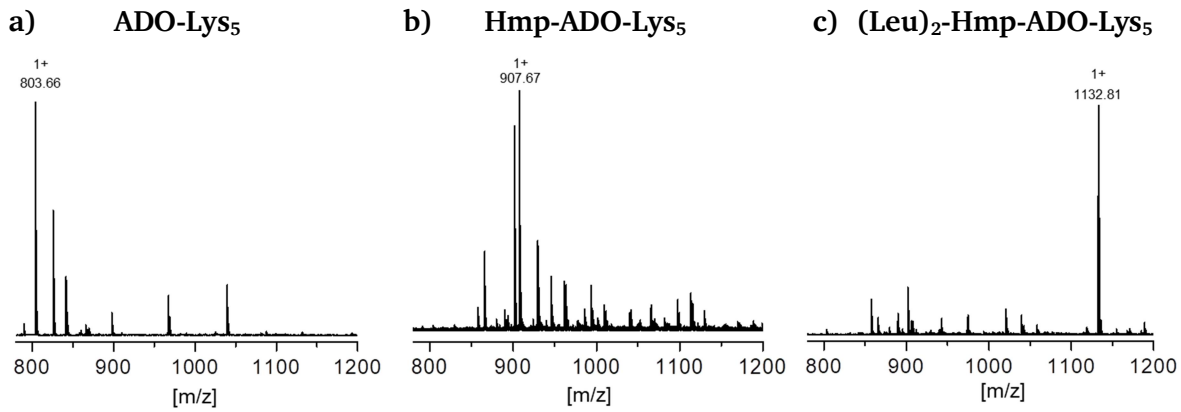

Figure 15.7: Spectra for table 16.1. Test cleavage of peptide **P11** [Leu^{21}]BM2(17-21)-Hmp-ADO-Lys_5. This experiment proved that the main side product $(Leu)_2$-Hmp-ADO-Lys_5 was the result of the Mitsunobu reaction.

15.1.3.Solubility test of the penta-lysine tag

P18: [Leu^{21}]BM2(1-21)-Hmp
MLEPFQILSIC(Acm)SFILSALHFL-Hmp

P20: [Leu^{21}]BM2(1-21)-Hmp-ADO-Lys_5
MLEPFQILSIC(Acm)SFILSALHFL-Hmp-ADO-KKKKK

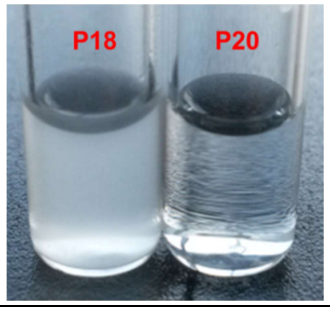

Figure 15.8: Comparison of the solubility of peptide **P18** [Leu^{21}]BM2(1-21)-Hmp without a C-terminal solubilizing tag (left, 0.5 mg/ml) and peptide **P20** [Leu^{21}]BM2(1-21)-Hmp-ADO-Lys_5 with a penta-lysine tag (right, 0.5 mg/ml) in water containing 0.1% TFA.

15.1.4. Synthesis of complete BM2 peptides (chapter 5.1.6)

Coupling cycles for N-terminal cysteine peptides

Table 15.2: Standard coupling cycle for the synthesis of the N-terminal cysteine peptides **P1** [Cys^{22}]BM2(22-35) and **P2** [Cys^{22}]BM2(22-51) using automated microwave assisted Fmoc-SPPS with a scale of 0.25 mmol.

Operation	Solvent	Volume [ml]
Swell Resin	DMF	10.0

Operation	Solvent	Volume [ml]
Wash-Top	DMF	10.0
Fmoc-Deprotection	20 % Piperidine/DMF	10.0
Fmoc-Deprotection	20 % Piperidine/DMF	10.0
Wash-Top	DMF	10.0
Wash-Bottom	DMF	10.0
Wash-Top	DMF	10.0
Wash-Top	DMF	10.0
Add Amino Acid	0.2 M DMF	5.0
Add Activator	0.5 M DMF	2.0
Add Activator Base	2.0 M NMP	1.0
Microwave Method	-	-
Add Amino Acid	0.2 M DMF	5.0
Add Activator	0.5 M DMF	2.0
Add Activator Base	2.0 M NMP	1.0
Microwave Method	-	-
Wash-Top	DMF	10.0
Wash-Bottom	DMF	10.0
Wash-Top	DMF	10.0

Operation	Solvent	Volume [ml]
No final deprotection	-	-
Wash-Top	DMF	10.0
Wash-Top	DMF	10.0
Wash-Top	DMF	10.0

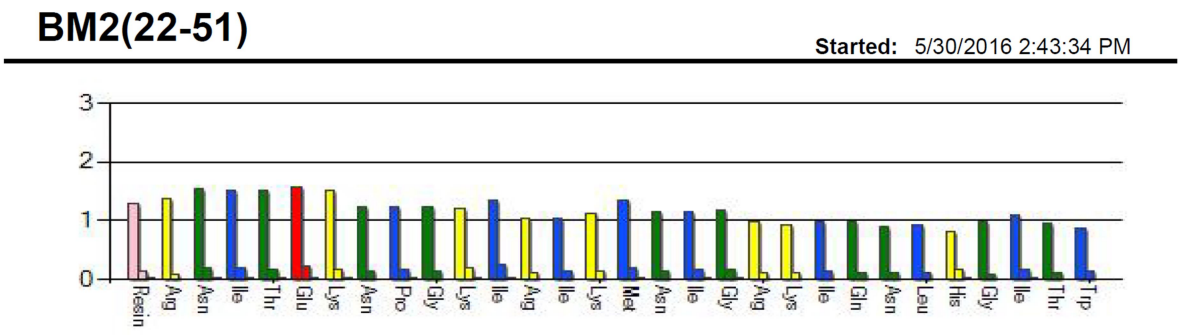

Figure 15.9: UV Report of N-terminal cysteine peptide P2 [Cys^{22}]BM2(22-51).

Table 15.3: Coupling cycle with additional washing steps for the synthesis of the N-terminal cysteine peptides **P3** [Cys[11]]BM2(11-51) using automated microwave assisted Fmoc-SPPS with a scale of 0.25 mmol.[207]

Operation	Solvent	Volume [ml]
Swell Resin	DMF	10.0

Operation	Solvent	Volume [ml]
Wash-Top	DMF	10.0
Fmoc-Deprotection	20 % Piperidine/DMF	10.0
Wash-Top	DMF	
Fmoc-Deprotection	20 % Piperidine/DMF	10.0
Wash-Top	DMF	10.0
Wash-Bottom	DCM	10.0
Wash-Top	DCM	10.0
Wash-Top	DMF	10.0
Wash-Top	DMF	10.0
Add Amino Acid	0.2 M DMF	5.0
Add Activator	0.5 M DMF	2.0
Add Activator Base	2.0 M NMP	1.0
Microwave Method	-	-
Add Amino Acid	0.2 M DMF	5.0
Add Activator	0.5 M DMF	2.0
Add Activator Base	2.0 M NMP	1.0
Microwave Method	-	-
Wash-Top	DMF	10.0
Wash-Bottom	DCM	10.0
Wash-Top	DMF	10.0

Operation	Solvent	Volume [ml]
No final deprotection	-	-
Wash-Top	DCM	10.0
Wash-Top	DCM	10.0

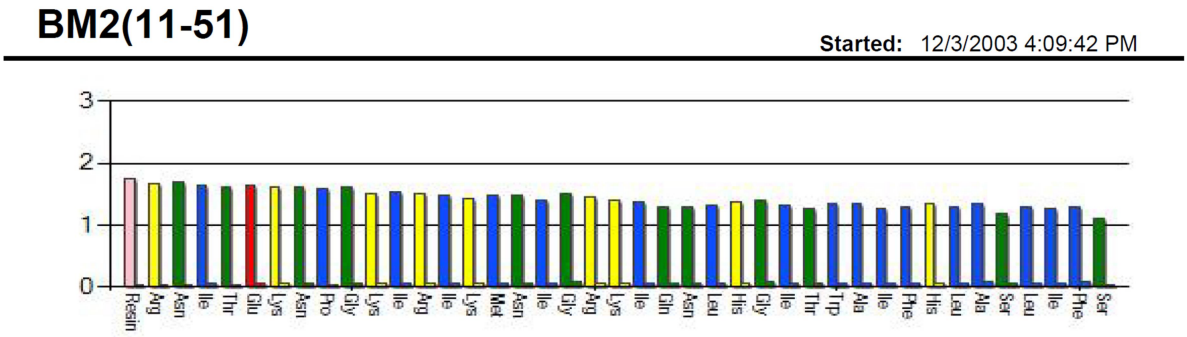

Figure 15.10: UV Report of N-terminal cysteine peptide P3 [Cys[11]]BM2(11-51) using an improved coupling cycle.[207]

Coupling cycle for C-terminal Hmp-peptides

Table 15.4: Coupling cycle for Hmp-peptides using automated, microwave-assisted Fmoc-SPPS for a scale of 0.25 mmol.

Operation	Solvent	Volume [ml]
Swell Resin	DMF	10.0

Operation	Solvent	Volume [ml]
Wash-Top	DMF	10.0
Fmoc-Deprotection	20 % 2-Methylpiperidine/DMF	10.0
Wash-Top	DMF	
Fmoc-Deprotection	20 % 2-Methylpiperidine/DMF	10.0
Wash-Top	DMF	10.0
Wash-Bottom	DCM	10.0
Wash-Top	DCM	10.0
Wash-Top	DMF	10.0
Wash-Top	DMF	10.0
Add Amino Acid	0.2 M DMF	5.0
Add Activator	0.5 M DMF	2.0
Add Activator Base	2.0 M NMP	1.0
Microwave Method	-	-
Add Amino Acid	0.2 M DMF	5.0
Add Activator	0.5 M DMF	2.0
Add Activator Base	2.0 M NMP	1.0
Microwave Method	-	-
Wash-Top	DMF	10.0
Wash-Bottom	DCM	10.0
Wash-Top	DMF	10.0

Operation	Solvent	Volume [ml]
No final deprotection	-	-
Wash-Top	DCM	10.0
Wash-Top	DCM	10.0

15.1.5. Analytical RP-HPLC of P22 [Leu^{21}]BM2(17-35) (chapter 5.1.9)

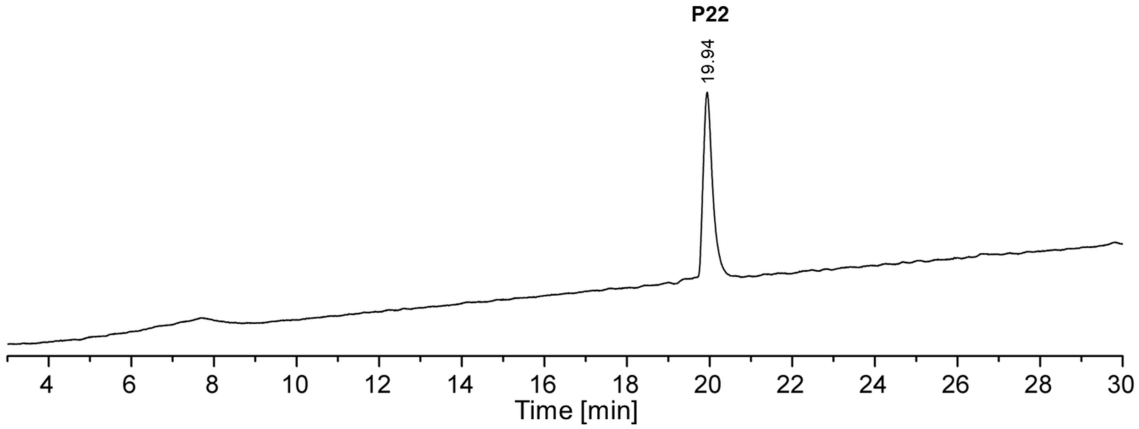

Figure 15.11: Reinjection of **P22**. HPLC conditions: C18 column (150 x 4 mm, 100 Å pore diameter, 3 µm particle size). Gradient: 15 – 45% acetonitrile in 30 min, flow rate of 1 ml/min.

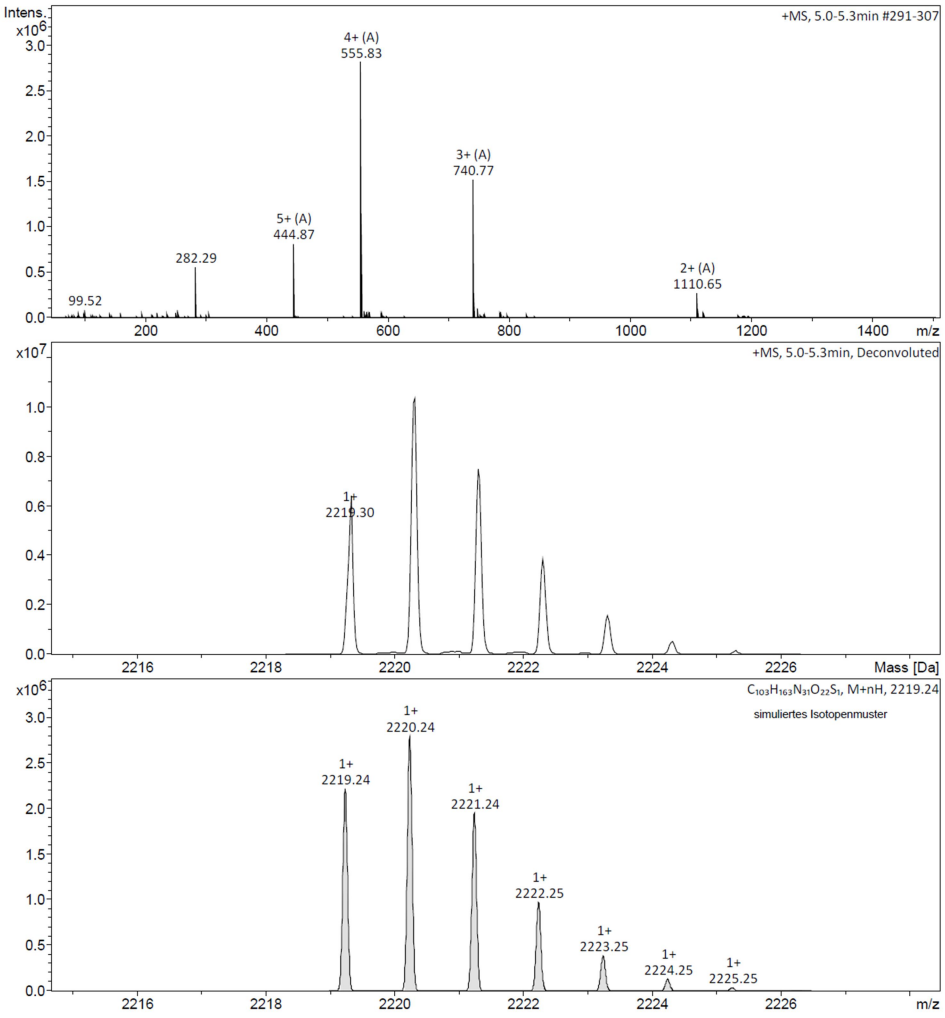

Figure 15.12: ESI-MS of ligation product P22 [Leu^{21}]BM2(17-35) synthesized in conventional ligation buffer A.

15.2. Supporting information for external conditions

15.2.1. HFIP-assisted NCL: ESI-MS of ligation product P23 (chapter 5.2.3)

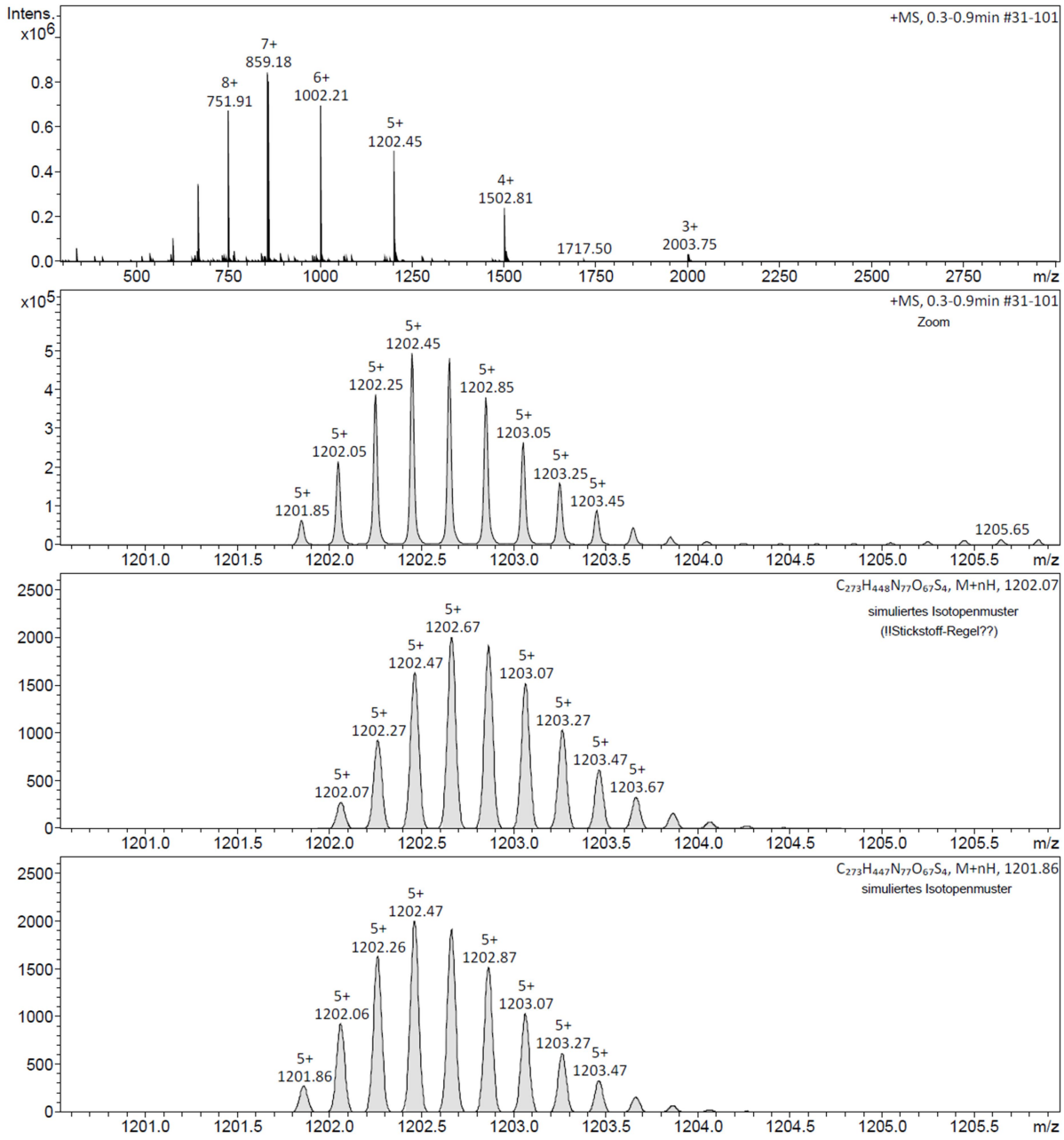

Figure 15.13: ESI-MS of ligation product P23 synthesised in the HFIP-based buffer C.

15.2.2. TLCs of sulfur compounds in [C_2mim][OAc] (chapter 5.2.5 and 5.2.6)

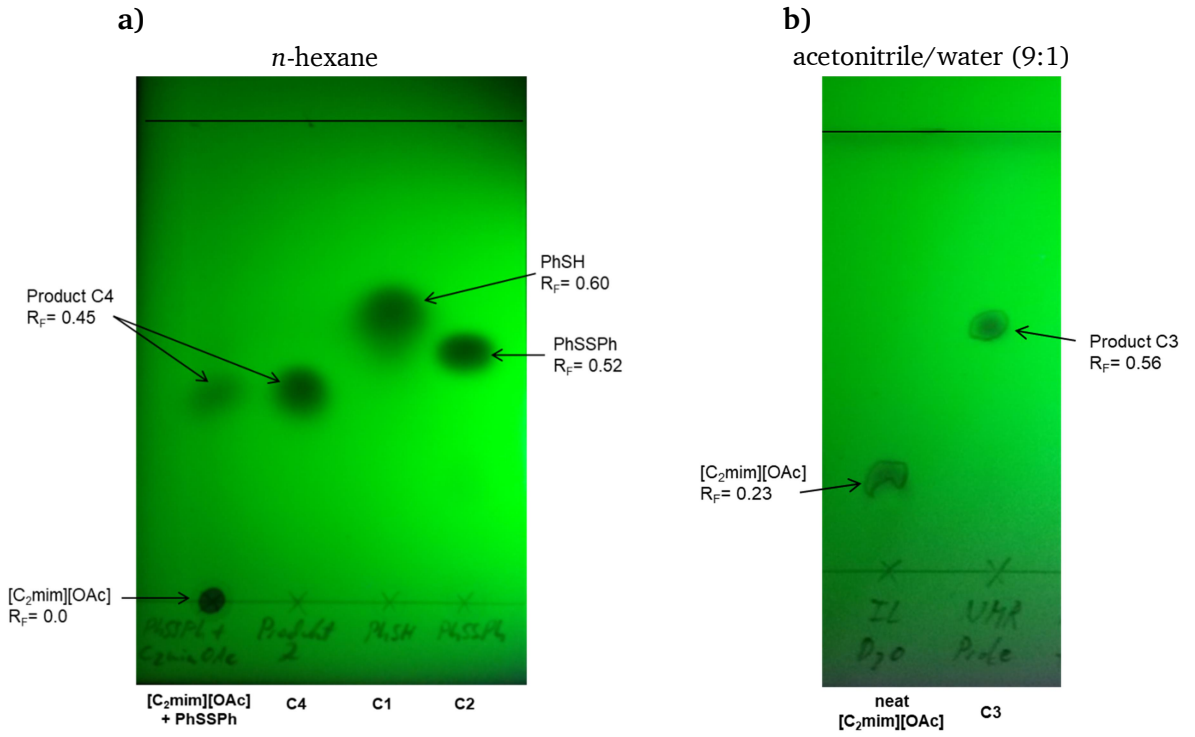

Figure 15.14: TLC of diphenyl disulfide in [C_2mim][OAc] with **a)** *n*-hexane as eluent and **b)** acetonitrile/water (9:1).

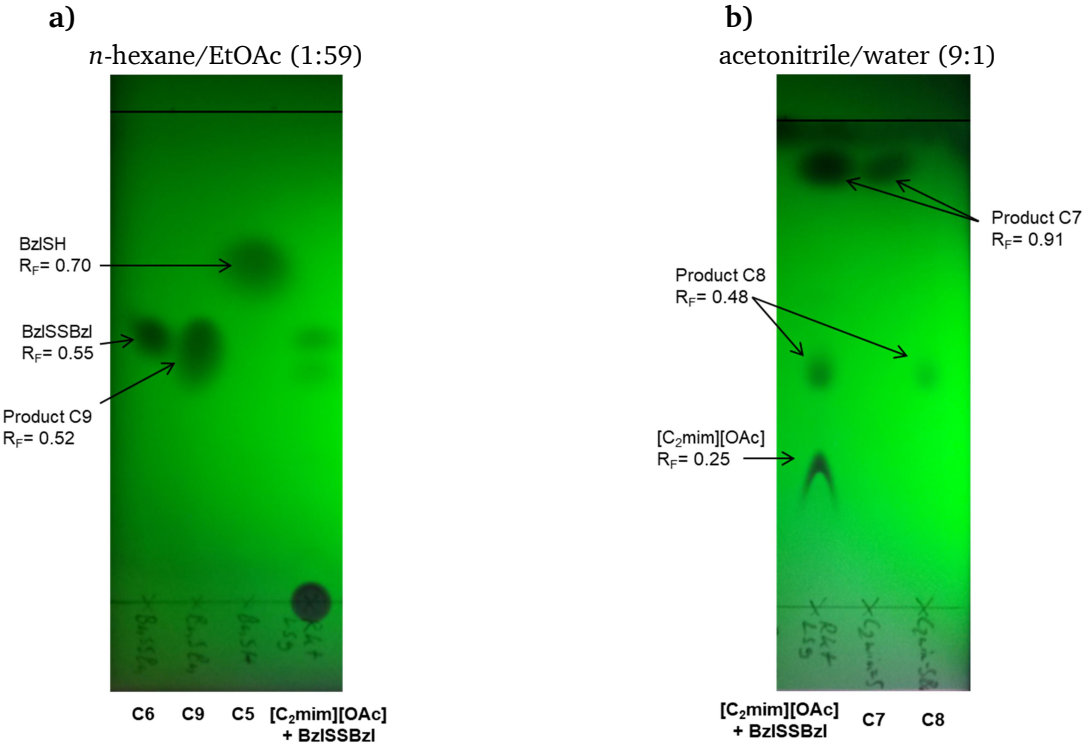

Figure 15.15: TLC of dibenzyl disulfide in [C_2mim][OAc] with **a)** *n*-hexane/EtOAc (1:59) as eluent and **b)** acetonitrile/water (9:1).

15.2.3. Ionic liquid-mediated NCL: ESI-MS P22 (chapter 5.2.9)

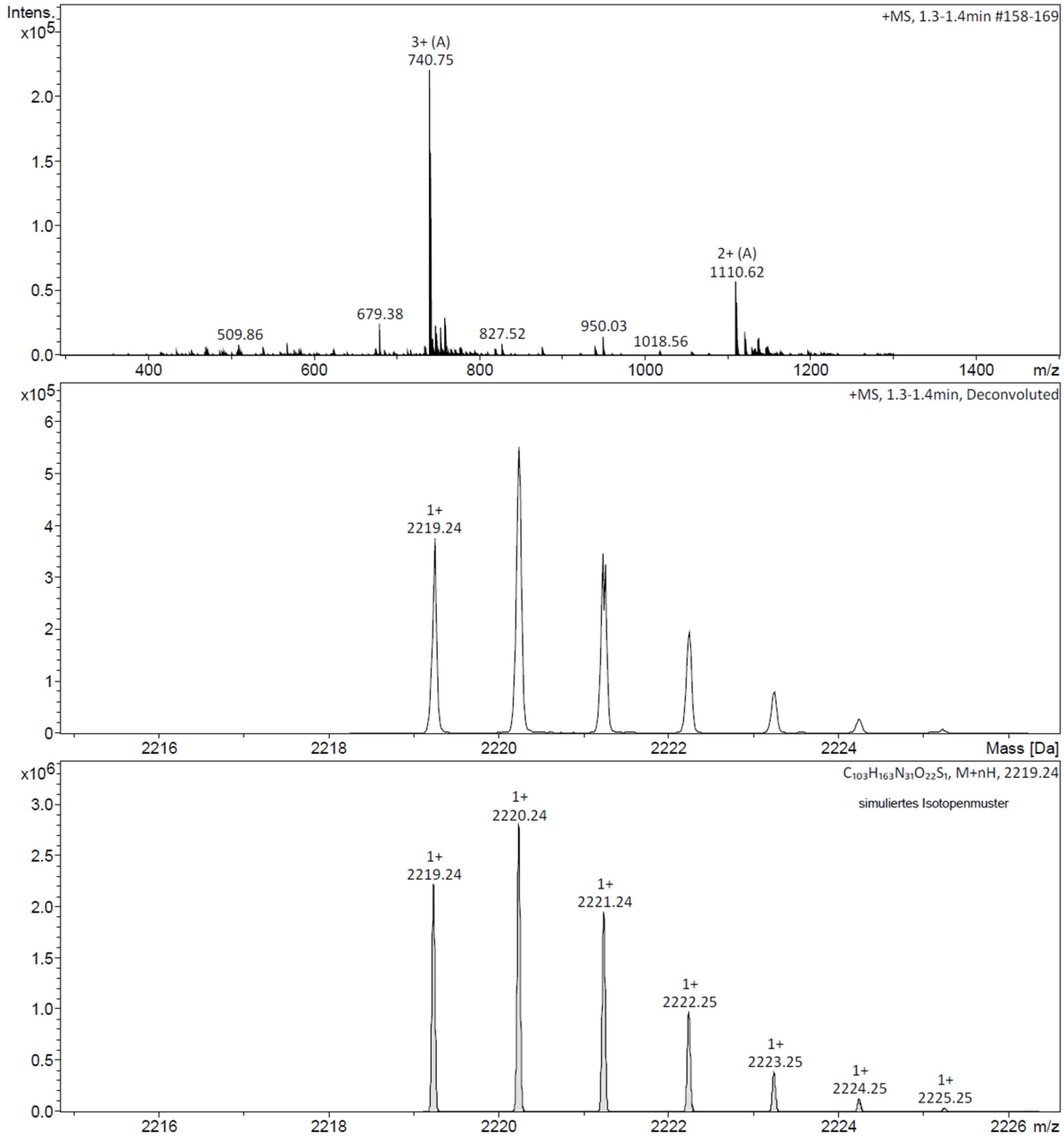

Figure 15.16: ESI-MS of ligation product P22 [Leu21]BM2(17-35) synthesised in the ionic liquid based buffer D5.

15.2.4. Ionic liquid-mediated NCL: ESI-MS of P27 (chapter 5.2.10)

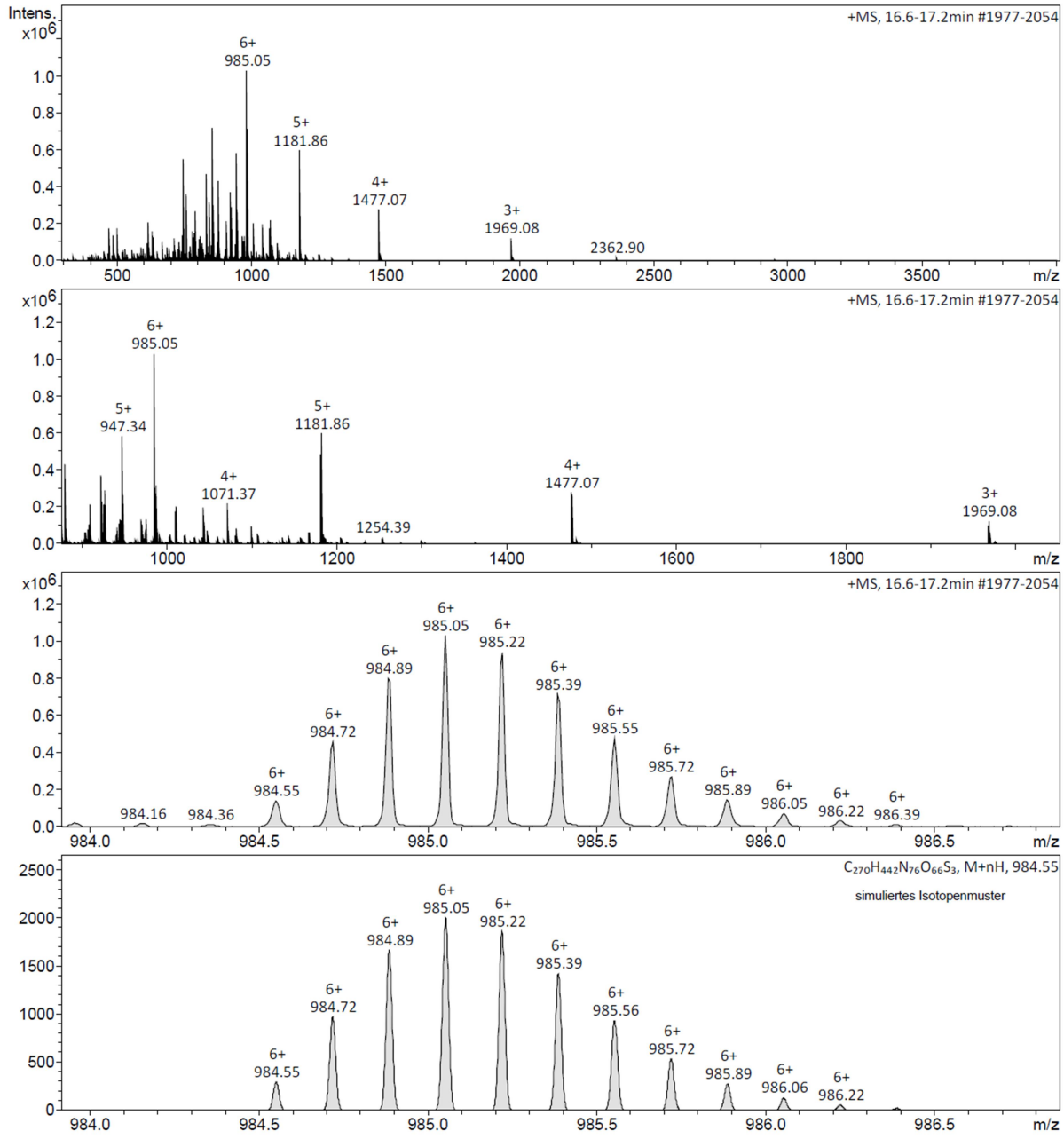

Figure 15.17: ESI-MS of ligation product P27 [Leu[10]]BM2(1-51) synthesised in the ionic liquid based buffer D5.

15.3. Supporting information for follow-up protocols

15.3.1. Desulfurization: ESI-MS of product P25 (chapter 5.3.1)

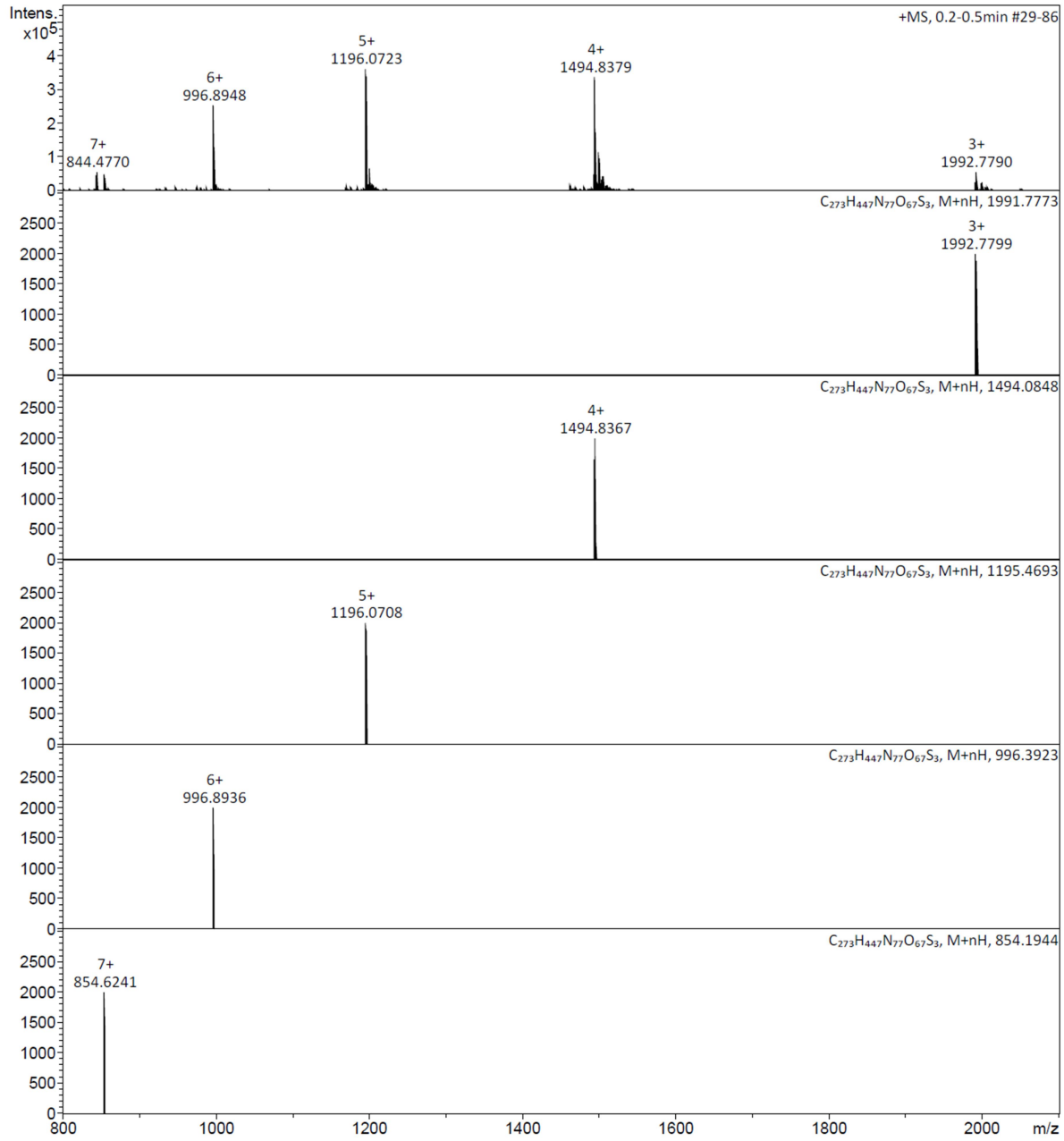

Figure 15.18: Experimental and simulated ESI mass spectrum of P25.

15.3.2. Acm deprotection: ESI-MS of product P26 (chapter 5.3.2)

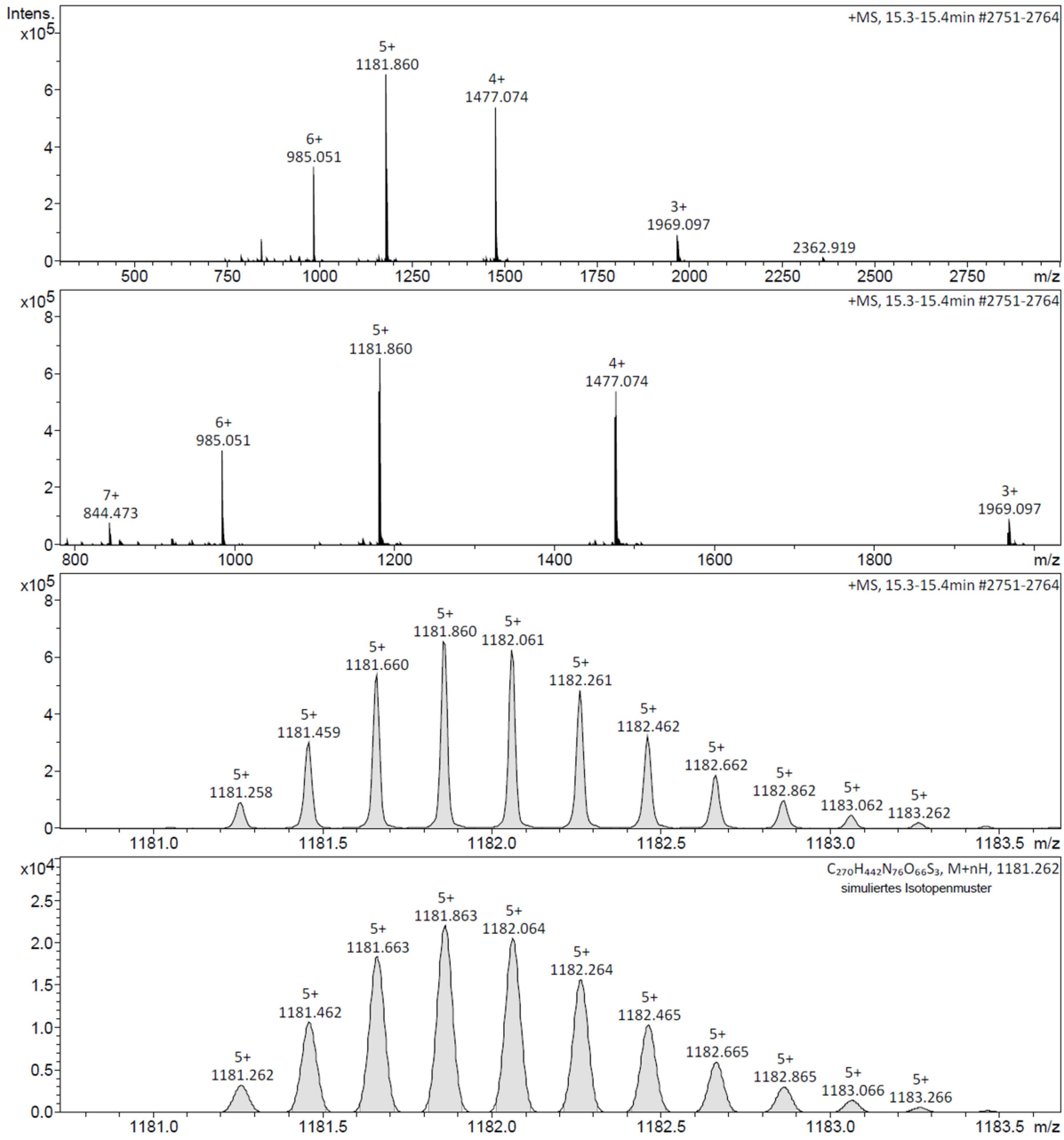

Figure 15.19: Experimental and simulated ESI mass spectrum of P26.

15.4. Circular dichroism spectroscopy

15.4.1. CD spectroscopy in TFE and phosphate buffer (chapter 5.4)

Table 15.5: Results of the deconvoluted CD curve of peptide **P17** analyzed in TFE.

Wavelength	190 - 260 nm	195 – 260 nm	200 – 260 nm	205 – 260 nm	210 – 260 nm
Helix	72.70 %	74.20 %	74.60 %	69.60 %	72.60 %
Antiparallel	0.20 %	0.70 %	1.90 %	2.90 %	2.30 %
Parallel	3.90 %	3.10 %	2.90 %	2.90 %	3.10 %
Beta-Turn	10.10 %	10.20 %	10.30 %	11.70 %	11.00 %
Rndm. Coil	17.60 %	17.50 %	15.30 %	14.60 %	13.80 %
Total Sum	104.50 %	105.60 %	104.90 %	101.70 %	102.90 %

Table 15.6: Results of the deconvoluted CD curve of peptide **P2** analyzed in TFE.

Wavelength	190 - 260 nm	195 – 260 nm	200 – 260 nm	205 – 260 nm	210 – 260 nm
Helix	76.50 %	75.10 %	73.70 %	78.90 %	74.70 %
Antiparallel	0.40 %	1.20 %	2.40 %	2.20 %	2.20 %
Parallel	2.20 %	2.20 %	2.30 %	2.00 %	2.90 %
Beta-Turn	11.00 %	11.00 %	11.40 %	10.60 %	10.80 %
Rndm. Coil	6.70 %	8.30 %	10.00 %	10.30 %	12.90 %
Total Sum	96.70 %	97.70 %	99.80 %	104.00 %	103.50 %

Table 15.7: Results of the deconvoluted CD curve of peptide **P2** in 0.2 M Na_2HPO_4 buffer.

Wavelength	190 - 260 nm	195 – 260 nm	200 – 260 nm	205 – 260 nm	210 – 260 nm
Helix	18.10 %	16.90 %	16.50 %	20.00 %	17.30 %
Antiparallel	55.30 %	32.50 %	17.90 %	12.10 %	15.20 %
Parallel	10.00 %	12.80 %	14.30 %	14.50 %	14.50 %
Beta-Turn	22.30 %	21.60 %	21.70 %	19.50 %	20.80 %
Rndm. Coil	29.40 %	35.50 %	41.70 %	44.70 %	47.10 %
Total Sum	135.10 %	119.40 %	112.20 %	110.90 %	114.80 %

Table 15.8: Results of the deconvoluted CD curve of peptide **P25** in TFE.

Wavelength	190 - 260 nm	195 – 260 nm	200 – 260 nm	205 – 260 nm	210 – 260 nm
Helix	66.30 %	64.70 %	64.40 %	67.70 %	65.50 %
Antiparallel	0.60 %	1.90 %	3.20 %	3.10 %	3.00 %
Parallel	3.50 %	3.40 %	3.50 %	3.10 %	3.80 %
Beta-Turn	12.00 %	12.20 %	12.40 %	12.10 %	12.10 %
Rndm. Coil	13.00 %	14.50 %	15.30 %	15.00 %	16.70 %
Total Sum	95.50 %	96.70 %	98.70 %	101.10 %	101.10 %

Table 15.9: Results of the deconvoluted CD curve of peptide **P26** in TFE.

Wavelength	190 - 260 nm	195 – 260 nm	200 – 260 nm	205 – 260 nm	210 – 260 nm
Helix	63.30 %	63.50 %	63.00 %	58.90 %	60.50 %
Antiparallel	0.50 %	1.50 %	3.10 %	4.00 %	3.60 %
Parallel	4.80 %	4.20 %	4.10 %	4.20 %	4.40 %
Beta-Turn	11.60 %	11.90 %	12.10 %	13.10 %	12.70 %
Rndm. Coil	21.10 %	21.10 %	19.40 %	19.10 %	18.90 %
Total Sum	101.30 %	102.20 %	101.60 %	99.30 %	100.00 %

Table 15.10: Results of the deconvoluted CD curve of peptide **P27** in TFE.

Wavelength	190 - 260 nm	195 – 260 nm	200 – 260 nm	205 – 260 nm	210 – 260 nm
Helix	59.1 %	59.6 %	59.2 %	55.9 %	56.6 %
Antiparallel	0.7 %	1.9 %	3.6 %	4.3 %	4.0 %
Parallel	5.1 %	4.6 %	4.5 %	4.6 %	4.8 %
Beta-Turn	12.4 %	12.5 %	12.7 %	13.5 %	13.3 %
Rndm. Coil	22.1 %	21.8 %	20.5 %	20.4 %	20.6 %
Total Sum	99.4 %	100.4 %	100.4 %	98.8 %	99.3 %

15.4.2. CD spectroscopy in POPC liposomes (chapter 5.4)

Table 15.11: Results of the deconvoluted CD curves of peptide **P26** in POPC/Na_2HPO_4 buffer.

Wavelength	190 - 260 nm	195 – 260 nm	200 – 260 nm	205 – 260 nm	210 – 260 nm
Helix	59.20 %	61.90 %	65.40 %	57.70 %	66.30 %
Antiparallel	0.30 %	1.10 %	2.40 %	4.00 %	2.90 %
Parallel	6.80 %	5.30 %	4.30 %	4.40 %	3.70 %
Beta-Turn	11.00 %	11.30 %	10.80 %	12.90 %	11.80 %
Rndm. Coil	35.40 %	31.50 %	24.40 %	20.50 %	16.50 %
Total Sum	112.70 %	111.10 %	107.30 %	99.30 %	101.20 %

Table 15.12: Results of the deconvoluted CD curves of peptide **P27** in POPC/Na_2HPO_4 buffer.

Wavelength	190 - 260 nm	195 – 260 nm	200 – 260 nm	205 – 260 nm	210 – 260 nm
Helix	62.1 %	62.4 %	64.3 %	55.5 %	64.6 %
Antiparallel	0.2 %	1.0 %	2.5 %	4.2 %	3.0 %
Parallel	6.4 %	5.3 %	4.6 %	4.7 %	3.8 %
Beta-Turn	10.5 %	11.2 %	10.9 %	13.1 %	12.1 %
Rndm. Coil	34.4 %	32.3 %	25.5 %	21.5 %	17.2 %
Total Sum	113.6 %	112.2 %	107.7 %	99.0 %	100.8 %

Curriculum Vitae

Persönliche Daten

Name	Andreas Christopher Baumruck
Geburtsdatum	29. Juli 1984
Geburtsort	Fulda in Hessen
Staatsangehörigkeit	deutsch
Familienstand	verheiratet

Schul- und Berufsausbildung

08/1991 – 07/1995	Landgräfin-Anna-Grundschule, Bronnzell
08/1995 – 07/2001	Konrad-Adenauer-Schule, Realschule Abschluss: Mittlere Reife
08/2001 – 01/2005	Ferdinand-Braun Schule, Berufsschule Ausbildung zum Zerspanungsmechaniker Fachrichtung Drehtechnik, *Emod-Motoren*, Fulda
02/2005 – 07/2007	Zerspanungsmechaniker, *Emod-Motoren*, Fulda
08/2007 – 06/2008	Ferdinand-Braun-Schule, Fachoberschule Abschluss: Fachhochschulreife

Akademischer Werdegang

10/2008 – 09/2012	Studium der Chemie B. Sc. an der TU-Darmstadt **Bachelor Thesis**: Clemens-Schöpf Institut für Organische Chemie und Biochemie, *AK Prof. Dr. W. D. Fessner* **Titel:** Synthese von 1-Alkoxy-3-hydroxypropan-2-onen
10/2012 – 03/2015	Studium der Chemie M. Sc. an der TU-Darmstadt **Master Thesis:** Clemens-Schöpf Institut für Organische Chemie und Biochemie, *AK A. A. Tietze* **Titel:** Synthesis and characterisation of sodium channel Nav1.7 voltage sensor supported by native chemical ligation
06/2015 – heute	Promotion im Fachbereich Chemie der Technischen Universität Darmstadt

Ort, Datum

Andreas Baumruck

Andreas Baumruck
Karlstraße 65
64285 Darmstadt

Erklärung

Ich erkläre hiermit, dass ich meine Dissertation selbständig und nur mit den angegebenen Hilfsmitteln angefertigt und noch keinen Promotionsversuch unternommen habe.

Andreas Baumruck

Andreas Baumruck
Karlstraße 65
64285 Darmstadt

Erklärung der Übereinstimmung

Ich erkläre hiermit, dass die elektronische Version der Doktorarbeit mit der schriftlichen Version übereinstimmt. Die elektronische Version liegt dem Prüfungssekretariat vor.

Andreas Baumruck